

# OASIS 9

## *International Conference & Exhibition on Optics & Electro-Optics*

**10-11 March, 2025** | David InterContinental Hotel, Tel-Aviv, Israel

# Digital Abstract Book



**Scan me to view the conference program**

## Table of Contents

ULTRAFAST PHENOMENA SESSION	4
SPECTROSCOPY AND OPTICAL SENSINGS SESSION	26
QUANTUM COMPUTERS SESSION	46
OPTICS IN MEDICINE AND BIOLOGY SESSION	52
OPTICAL ENGINEERING Session	70
NONLINEAR OPTICS SESSION	86
MICRO AND NANO-OPTICS SESSION	112
LASERS AND APPLICATIONS SESSION	154
ELECTRO-OPTICS IN INDUSTRY SESSION	173
ARTIFICIAL INTELLIGENCE IN OPTICS SESSION	184
ATOMIC AND QUANTUM OPTICS Session	197
ELECTRO-OPTICS DEVICES SESSION	219
ELECTRO-OPTICS IN DEFENSE SESSION	240

**Dear Colleagues and Friends,**

I would like to invite you to the OASIS9 conference that will be held on **10-11 March 2025** at the David International Hotel, on the beautiful beach of Tel Aviv, a vibrant city, welcoming more than one million visitors a year.



OASIS9 is the ninth in the highly successful series of OASIS (Optical Engineering and Science in Israel) bi-annual conferences.

These conferences bring together scientists and engineers from academia, industry and research institutions, who discuss the most recent advances in optics and photonics, both globally and in Israel. The OASIS conferences are renowned for their very high scientific standards, and have fostered numerous cross-disciplinary collaborations.

Israel has been at war for more than a year. Yet, even in these difficult times, advanced research and development continues in all disciplines of science and engineering. In particular, the Israeli optics and electro-optics community is strong and very active. It is important to hold the high level OASIS9 conference to support this community.

You may visit the OASIS8 website [www.oasis8.org](http://www.oasis8.org) to see the scope and the impact of the OASIS conferences.

OASIS8 hosted 1400 participants, including 200 from abroad, featured more than 100 lectures in 15 sessions (one on hi-tech) and showcased 60 exhibitors, representing 100 Israeli and international companies. We believe that OASIS9 will surpass these achievements.

I look forward to welcoming you to the inspiring OASIS9 conference in March.

**Prof. Abraham Katzir**

*Tel Aviv University, ISRAEL*

*OASIS9 Conference Chair*

## ULTRAFAST PHENOMENA SESSION

### Oral presentations Abstracts:

#### Laser wakefield acceleration with an axiparabola and spatiotemporal couplings

Mr. Aaron Liberman

Weizmann Institute of Science

#### Authors:

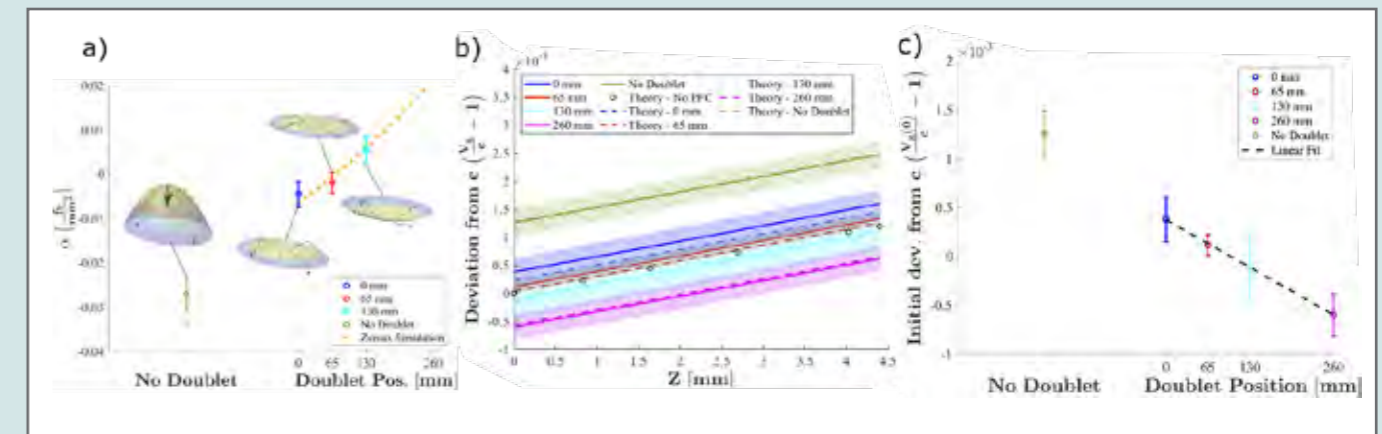
Aaron Liberman, Weizmann Institute of Science, Rehovot, Israel; Slava Smartsev, LOA, CNRS, Ecole Polytechnique, ENSTA Paris, Institut Polytechnique de Paris, Palaiseau, France; Anton Golovanov, Weizmann Institute of Science, Rehovot, Israel; Sheroy Tata Weizmann Institute of Science, Rehovot, Israel; Ronan Lahaye, LOA, CNRS, Ecole Polytechnique, ENSTA Paris, Institut Polytechnique de Paris, Palaiseau, France; Eitan Levine, Weizmann Institute of Science, Rehovot, Israel; Salome Benracassa, Weizmann Institute of Science, Rehovot, Israel; Igor Andriyash, LOA, CNRS, Ecole Polytechnique, ENSTA Paris, Institut Polytechnique de Paris, Palaiseau, France; Eyal Kroupp, Weizmann Institute of Science, Rehovot, Israel; Cedric Theory, LOA, CNRS, Ecole Polytechnique, ENSTA Paris, Institut Polytechnique de Paris, Palaiseau, France; Victor Malka, Weizmann Institute of Science, Rehovot, Israel

#### Abstract:

The axiparabola, a long-focal-depth reflective optical element that produces a quasi-Bessel beam, has generated significant interest for its potential to overcome both the laser diffraction and electron dephasing limitations of laser-wakefield acceleration. It thus promises to enable a much more favorable scaling of maximum electron energy with laser energy as well as with accelerator length.

By inducing a controlled amount of spherical aberrations in the beam, the axiparabola modifies the velocity with which intensity is focused on the optical axis. Since the wakefield is generated by the laser focus, this effectively modifies the propagation velocity of the wakefield itself. By combining the axiparabola with a manipulation of the pulse-front's propagation in space and time, via the introduction of spatiotemporal couplings, the velocity of the wakefield can be tuned to be in phase with the injected electron bunch, thus mitigating dephasing. Furthermore, the extended focal depth of the axiparabola-focused beam allows for a longer acceleration length.

We present a measurement of the modified, superluminal, velocity of focusing induced by the axiparabola. Furthermore, tunable spatiotemporal couplings are introduced into the pulse front via a specially designed refractive doublet and the subsequent changes to the velocity profile are also measured. We also present the first electrons directly accelerated with an axiparabola focused laser pulse. These electrons, while not yet achieving dephasingless acceleration, show the ability of the axiparabola-focused wakefield to successfully accelerate electrons to high energies. The electron results are also compared with PIC simulations. Finally, we show the first direct images of the wakefield generated by an axiparabola-focused laser pulse, taken using the femtosecond relativistic electron microscopy technique. These images yield insights into the novel regime of the axiparabola wakefield and are also back up by PIC simulations.



## Temporal chirpless microscope

**Ms. Or Refaeli**

*Bar Ilan University*

### Authors:

Or Refaely, Hamootal Duadi and Moti Fridman, Bar Ilan university, Ramat-Gan Israel

### Abstract:

Any imaging system with a lens imposes a quadratic phase on the image. When we measure the intensity – this phase does not affect the results. However, for certain applications, especially in quantum optics in the nanoscale regime – this phase can reduce the coherence of correlated photons.

In our lab, we developed a temporal imaging system which images signals in time, similar to a lens in space. Therefore, this imaging system also exhibits a quadratic phase on the output signal.

To cancel this quadratic phase, we designed a double-lens microscopy system without the additional quadratic phase leading to a magnified chirpless image of the input signal at the output. This system is ideal for imaging indistinguishable photons while preserving their entangled state.

## ◆ Invited speakers Abstracts:

### Ultrafast magnetism: novel control schemes and probes

**Dr. Ofer Neufeld**

*Technion- Israel institute of Technology*

### Abstract:

It is commonly established that by irradiating intense laser pulses onto magnets, their magnetization can be manipulated on ultrafast timescales, e.g. causing magnetization flip or demagnetization. Our recent predictions even establish a highly nonlinear optical regime where attosecond magnetization dynamics can occur via strong-field driving. However, measuring such fast magnetic phenomena remains elusive. Currently, no sources of intense attosecond magnetic pulses exist, and generating circularly polarized attosecond pulses for circular dichroism measurements is highly challenging (and will also only probe a specific energy window typically far from the Fermi energy). In this talk I'll present two recent approaches that we developed to probe ultrafast magnetism. The first relies on strong-field excitation of atomic ring currents, which are gated by two counter rotating circular laser pulses. Our ab-initio simulations revealed that this scheme has potential to generate Tesla-scale magnetic fields with down to ~800 (as) durations, marking the first scheme for magnetic attopulse generation. The second approach relies on symmetry-breaking spectroscopy of ultrafast photocurrent measurements. By engineering tailored driving fields that break, or exhibit, time-reversal symmetry, and using them to drive photogalvanic currents, we can sense magnetism – photocurrents can only be generated if the sample breaks time-reversal symmetry, which generates a background free signal. We demonstrate this scheme with ab-initio simulations and show that it should also apply to other phases with broken time-reversal symmetry such as Chern insulators. This is the first scheme capable of probing magnetism in the absence of magnetic fields and circularly-polarized electric fields.



## Widely Wavelength-Tunable Amplified All-Normal-Dispersion Laser aimed to excite Thorium-229 VUV transition

Dr. Yariv Shamir

Soreq NRC

### Authors:

Yariv Shamir<sup>1\*</sup>, Zaharit Refaeli<sup>1</sup>, Marcelo Wyszkin<sup>1</sup>, Moshe Koren<sup>1</sup>, Nitzan Haviv<sup>2</sup> and Pavel Sidorenko<sup>2</sup>

1 Soreq NRC, Yavne 8180000, Rd 4111, Israel

2 Department of Electrical and Computer Engineering and Solid-State Institute, Technion – Israel Institute of Technology, 32000 Haifa, Israel

### Abstract:

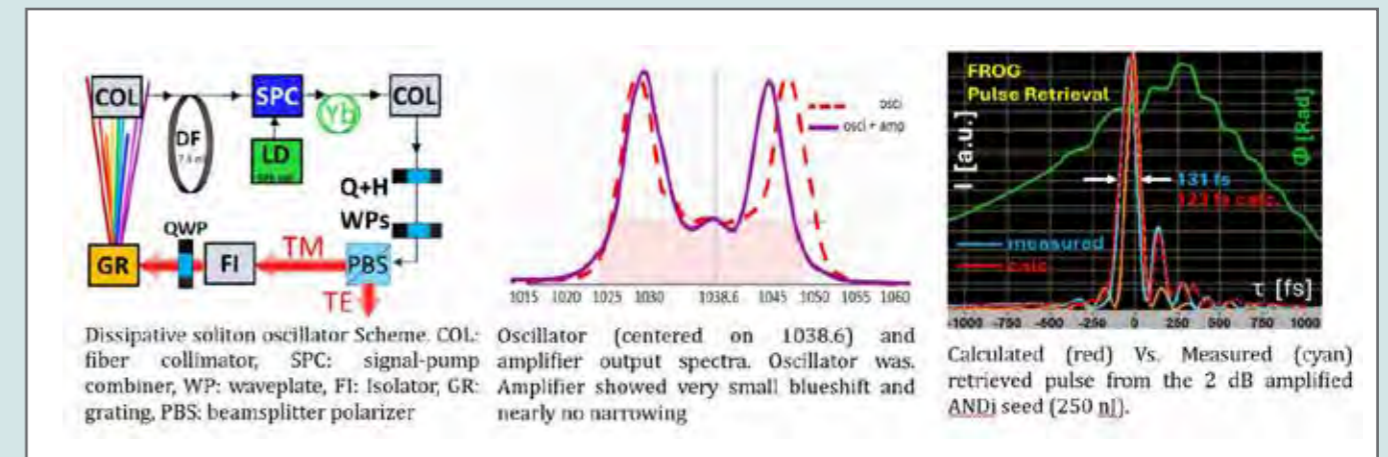
**Background:** The race for ever-better timepieces has recently peaked with advancements regarding future nuclear-clocks, based on Thorium 229 ( $\text{Th}^{229}$ ) laser excitation [1]. Tremendous improvements pinpointed its emission-line to vacuum-UV: 148.3821(5) nm [1], however necessitated complicated lasers and upconversion setups, e.g. CPA [2], or combined-CW lasers [1] and various nonlinear processes.

**Objective:** Developing a simple, compact, fiber-integrated laser-source that can excite  $\text{Th}^{229}$ -isomer via its 7th harmonic is highly-desirable for practical nuclear-clock. Here, we demonstrate the front-end of such a source, which is constructed from an All-Normal-Dispersion (ANDi) oscillator and amplifier.

**Method:** Here we propose applying a dissipative soliton ANDi femtosecond fiber oscillator [3] coupled to an amplifier, avoiding traditional chirped-pulse-amplifier. Being readily tunable between 1025 to 1065 nm, operation around 1038.6 nm was chosen, so its 7th harmonic is compatible to  $\text{Th}^{229}$  transition, establishing an attractive track for 1- $\mu\text{m}$  ultrashort-laser study. Pulse dynamics of ANDi was well described by the Complex-Ginzburg-Landau equation [4], with one realized solution of “Batman-like” spectrum. Here we used a large-mode-area fiber, with sufficient dispersion-accumulating length, a matching Yb-amplifier segment, waveplates and a polarizer, altogether stabilizing 20 MHz roundtrip pulses. The positive chirping allows for energies exceeding traditional fiber-oscillators, proven for many-tens of nanoJoules [3,5].

**Results:** An internal grating served twofold Objectives: both spectral-filtration, and provided tenability. The center-wave operation was tunable between 1025 to 1065 nm. First Energy boost was achieved with large Photonic-Crystal-Fiber Yb-amplifier, yielded potential for <120 fs pulse-time and for obtaining the desired-VUV harmonics. RF-spectrum pulsetrain showed no noticeable satellites. Amplification to 250 nJ and compression, yielded ~130 fs FROG trace, possibly a result of some nonlinearities.

**Conclusion:** a CPA-free ANDi and amplifier system provides compact stable low maintenance system, here aimed to generate high UV-harmonics. Further upgrade of ultra-large core amplifier is underway, aimed to achieve ~3  $\mu\text{J}$  ( $\sim 1.6 \times 10^{11} \text{ W/cm}^2$ ).



## Intense laser interaction with micro-bars

Ms. Michal Elkind

Tel Aviv university

### Authors:

M. Elkind<sup>1</sup>, I. Cohen<sup>1</sup>, N. Popper<sup>1</sup>, D. Balckman<sup>2</sup>, T. Meir<sup>1</sup>, A. Levanon<sup>1</sup>, S.H. Glenzer<sup>3</sup>, A. Arefiev<sup>2</sup>, and I. Pomerantz<sup>1</sup>

<sup>1</sup> The School of Physics and Astronomy, Tel Aviv University, Israel

<sup>2</sup> Department of Mechanical and Aerospace Engineering, University of California San Diego, USA

<sup>3</sup> SLAC National Accelerator Laboratory, USA

### Abstract:

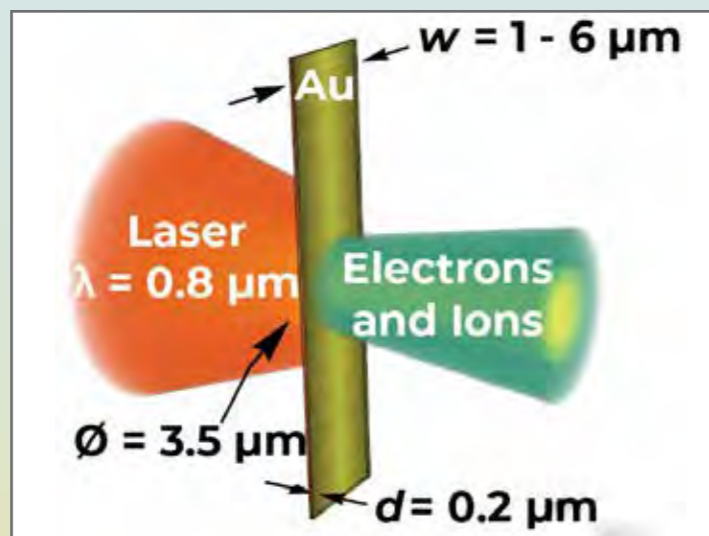
The interaction of an intense laser pulse with matter results in the emission of high-energy radiation in the form of MeV electrons, ions, and hard x-rays.

Many experiments showed that when the target surface is rough on the scale of the laser wavelength, the coupling of laser energy to high-energy particles increases.

To understand this phenomenon I irradiated isolated wavelength scale targets in the form of micrometric Au bars. My results showed two forward-directed electron jets with a small opening angle, having a narrow energy spectrum in the MeV range, and a positive correlation between angle and energy, as well as proton beams with energies exceeding 6 MeV. The latter result exceeds the proton energies emitted from flat foils when irradiated at the same conditions by a factor of three.

Simulations show that following ionization electrons near the target's edge stay in phase with the laser pulse, allowing the Lorentz force to guide them around the target's edge. These electrons form attosecond duration bunches while interacting with the laser field over long distances in vacuum and accelerating to within a narrow momentum range. The simulations also revealed that energy transfer from diffracted laser fields to the electrons on both sides of the target, combined with the reduced surface area of the structure, results in a thicker electron sheath and higher ion acceleration gradients.

Beyond understanding this basic aspect of how intense light interacts with matter, I will discuss how this new methodology can lead to the possibility of laser-ion acceleration in a cascaded manner from multiple irradiated targets, allowing manipulation of the ion spectrum by optical means.



## Quantum paths interference signatures in trARPES

Ms. Shiri Gvishi

Tel Aviv university

### Authors:

Shiri Gvishi, Raymond and Beverly Sackler School of Physics & Astronomy, Tel-Aviv University, Tel-Aviv 6779801, Israel. Ittai Sidilkover, Raymond and Beverly Sackler School of Physics & Astronomy, Tel-Aviv University, Tel-Aviv 6779801, Israel. Shaked Rosenstein, Raymond and Beverly Sackler School of Physics & Astronomy, Tel-Aviv University, Tel-Aviv 6779801, Israel. Adi Peled, Raymond and Beverly Sackler School of Physics & Astronomy, Tel-Aviv University, Tel-Aviv 6779801, Israel. Omer Pasternak, Raymond and Beverly Sackler School of Physics & Astronomy, Tel-Aviv University, Tel-Aviv 6779801, Israel. Nir Levin, Raymond and Beverly Sackler School of Physics & Astronomy, Tel-Aviv University, Tel-Aviv 6779801, Israel. Naaman Amer, Raymond and Beverly Sackler School of Physics & Astronomy, Tel-Aviv University, Tel-Aviv 6779801, Israel. Hadas Soifer, Raymond and Beverly Sackler School of Physics & Astronomy, Tel-Aviv University, Tel-Aviv 6779801, Israel.

### Abstract:

Interference is a fundamental phenomenon in physics that can be a basis for understanding quantum phenomena. Quantum-paths interference in two-photon absorption has been widely observed in atoms and molecules and used to study phases of intermediate states. However, this is an elusive task in solid-state physics. Here we resolve quantum-paths interference in a solid – the topological insulator Bi<sub>2</sub>Se<sub>3</sub> – by utilizing the helicity-dependence in photoemission of this spin-orbit coupled material.

We use time and angle-resolved photoemission spectroscopy (trARPES), which relies on two-photon photoemission using two femtosecond pulses. The visible light pulse (pump) excites the electrons to unoccupied states, probed with a UV pulse (probe). The probe leads to electron photoemission, enabling us to image the material band structure. When the pulses arrive simultaneously, the pump and probe can switch roles, resulting in two available quantum-paths.

Here, we show that helicity-dependence gives us great sensitivity to the interference of the two quantum-paths. Both images (Fig.1A-B) show the spectrum excited with a left-circularly polarized VIS pulse subtracted from the spectrum excited with a right-circularly polarized pulse. One of the 2-photon paths (purple) is only possible when the UV is p-polarized, giving us a control knob on the interference. When only one quantum-path is available (teal in Fig.1C), the peak intensities are observed on the band lines (Fig.1A). When both quantum-paths are allowed (teal and purple in Fig.1C), an interference pattern appears on the band line (Fig.1B). The change in the spectrum with the higher intensity below and above the band line indicates a phase shift and the existence of a Fano-like resonance. This interference signature shifts with the VIS photon energy, which shows that we can control the interference by polarization and wavelength. Understanding this mechanism will allow for better control of the photoemission process and its phase dependence.

## Coherent control of phonon anharmonicity

Ms. Gili Scharf

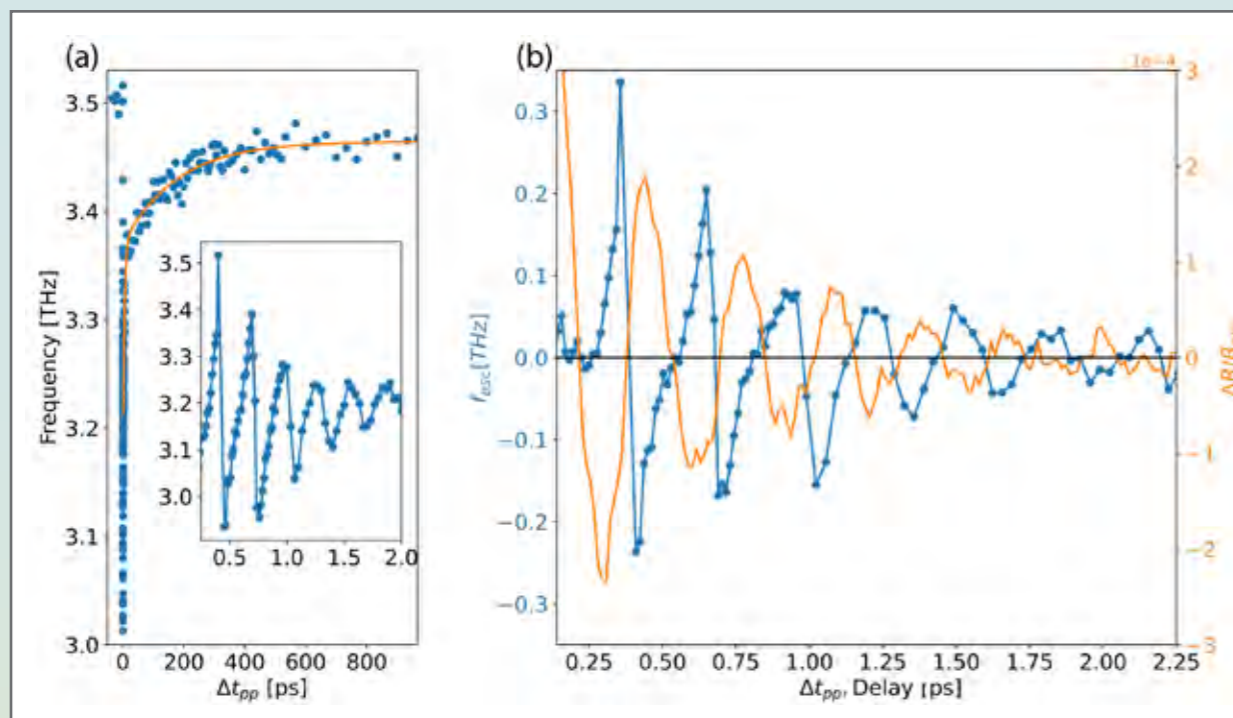
Tel Aviv university

### Authors:

Gili Scharf, Tomer Hasharoni, Lara Donval, Leah Ben Gur, Alon Ron

### Abstract:

Anharmonic lattice vibrations play a key role in many physical phenomena. They govern the heat conductivity of solids, strongly affect the phonon spectra, play a prominent role in soft mode phase transitions, allow ultrafast engineering of material properties and more. The most direct evidence for anharmonicity is to measure the oscillation frequency changing as a function of the oscillation amplitude. For lattice vibrations, this is not a trivial task, and anharmonicity is probed indirectly through its effects on thermodynamic properties and spectral features or through coherent decay of one mode to another. However, measurement of the anharmonicity of a single Raman mode is still lacking. We show that ultrafast double pump-probe spectroscopy could be used to directly observe frequency shifts of Raman phonons as a function of the oscillation amplitude and disentangle the coherent contributions from quasi-harmonic sources such as temperature and changes to the carrier density in the thermoelectric material SnTe. Our results have dramatic implications for the material engineering of future thermoelectrics. Moreover, our methodology could be used to isolate the basic mechanisms driving optically induced phase transitions and other nonlinear phenomena.



## Shaping exciton polarization dynamics in 2D semiconductors by tailored ultrafast pulses

Mr. Omri Meron

Tel Aviv university

### Authors:

Omri Meron, Uri Arieli, Eyal Bahar, Swarup Deb, Moshe Ben Shalom, Haim Suchowski

### Abstract:

**Objectives:** We aim to demonstrate precise control over resonant polarization dynamics in condensed matter systems through ultrafast pulse shaping, enabling enhanced nonlinear optical responses and selective state manipulation.

**Methods:** We employed a spatial light modulator-based pulse shaping apparatus with sub-10 fs pulses to study four-wave mixing (FWM) generation in monolayer WSe<sub>2</sub> under ambient conditions. By applying arctangent spectral phase functions, we studied the temporal dynamics of coherent exciton polarization. The experimental results were analyzed using TMD Bloch equations of motion, incorporating both Pauli blocking (PB) and exciton-exciton (X-X) interaction effects.

**Results:** Through tailored multiphoton pathway interference, we achieved a 2.6-fold enhancement in FWM generation compared to transform-limited pulses. Our analysis revealed that exciton-exciton interactions dominate the nonlinear response, contributing over 14 orders of magnitude more than Pauli blocking effects. Additionally, we demonstrated selective control over both 1s and 2s excitonic states, with the ability to manipulate their individual contributions to the overall nonlinear response.

**Conclusions:** This work establishes a novel method for controlling exciton coherence in 2D semiconductors using spectral phase manipulation. The demonstrated enhancement in nonlinear optical response and selective state control opens new possibilities for quantum state manipulation and advanced optoelectronic devices. The technique's effectiveness in ambient conditions suggests practical applications in future ultrafast optical technologies.



## Saturation Model for Photonic Time Crystals

Mr. Michael Tulchinsky

Technion– Israel institute of Technology

### Authors:

Michael Tulchinsky, Yonatan Plotnick, Oded Schiller, Mordehai Segev

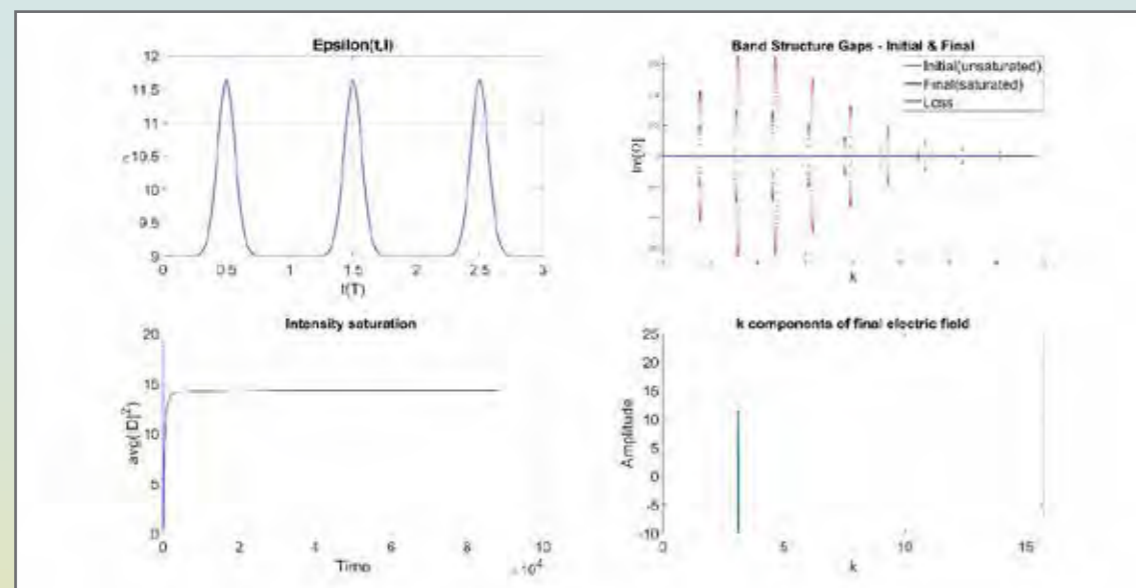
### Abstract:

A Photonic time crystal (PTC) is a medium homogeneous in space which changes its index of refraction periodically in time (Fig1). The sharp changes in the refractive index result in time-refracted and time-reflected waves. When these waves interfere, they create bands and gaps. Because of the temporal variations, energy is not conserved and plane waves whose  $k$ -vectors reside within the band gaps experience gain. It has been suggested that this gain can be harnessed to create a novel type of laser [1].

In this work, we study a more realistic model than in previous works, where the amplitude of the refractive index modulations saturates at large fields, while the refractive index remains homogeneous. We use numerical simulations to calculate the propagation of the EM waves in the PTC. The refractive index profile is modeled with a Gaussian pulse-train, with a simple linear loss mechanism which the material exhibits. As initial conditions, we populate all spatial frequencies of the EM field with a small, random amplitude. We model a saturation mechanism in the material based on phenomenological reasoning. Moreover, we calculate the initial (unsaturated) band structure and the final (saturated) band structure (fig2). Our main finding is that after a long enough propagation time, as we reach saturation (fig3) only the center frequency of the largest gap remains (fig4). This reminds us of a laser with homogeneous broadening.

In conclusion, we study a saturable photonic time crystal and find that it can be used as a laser, stabilizing on a single frequency. In future work the emphases will be on the exact nature of such saturation mechanisms, exploring more physical and local saturation. This work paves the way for new tunable laser devices in yet unattained frequencies such as THz.

[1] M.Lyubarov, "Amplified emission and lasing in photonic time crystals," Science



## Ultrafast Dynamics of Correlated Optical Singularities

Mr. Tomer Bucher

Technion–Israel Institute of Technology

### Authors:

T. Bucher<sup>1</sup>, A. Gorlach<sup>1</sup>, A. Niedermayr<sup>1</sup>, Q. Yan<sup>1</sup>, H. Nahari<sup>1</sup>, K. Wang<sup>2</sup>, R. Ruimy<sup>1</sup>, Y. Adiv<sup>1</sup>, M. Yannai<sup>1</sup>, T. L. Abudi<sup>1</sup>, E. Janzen<sup>3</sup>, C. Spaegele<sup>4</sup>, C. Roques-Carmes<sup>5</sup>, J. H. Edgar<sup>3</sup>, F. H. L. Koppens<sup>6,7</sup>, G. M. Vanacore<sup>8</sup>, H. Sheinfux<sup>9</sup>, S. Tsesses<sup>10</sup>, I. Kaminer<sup>1</sup> 1. Andrea & Erna Viterbi Dep. of ECE., Technion–Israel Institute of Technology, Haifa, Israel. 2. Shanghai Institute of Optics and Fine Mechanics, 899 Huiwang E Rd, Shanghai, China. 3. Tim Taylor Dep. of Chemical Eng., Kansas State Uni., Manhattan, KS, USA. 4. School of Eng. and App. Sci., Harvard University, Cambridge, MA, USA. 5. Edward L. Ginzton Laboratory, Stanford University, Stanford, CA, USA. 7. ICFO–Inst. de Ciències Fòniques, The Barcelona Inst. of Sci. & Tech., Castelldefels, Spain. 7. ICREA–Institutio Catalana de Recerca i Estudis Avanats, Barcelona, Spain. 8. Department of Materials Science, University of Milano–Bicocca, Milano, Italy. 9. Department of Physics, Bar Ilan University, Ramat–Gan, Israel. 10. Department of Physics, MIT, Cambri

### Abstract:

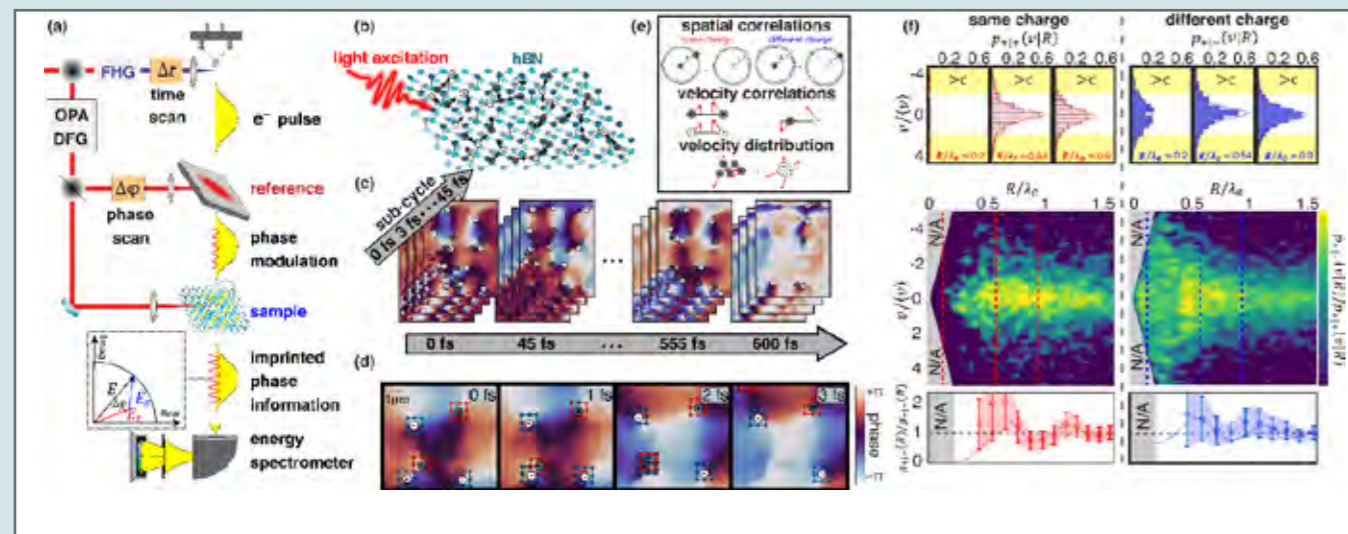
Singularities, points with nonzero topological charge [1], are ubiquitous in physics. Recent research has focused on their topological properties and their influence on global system behavior. Singularities can also be viewed as particle-like excitations, as they remain stable throughout their dynamics, annihilating only when meeting oppositely charged counterparts. In systems with many singularities, collective dynamics and large-scale statistical correlations become crucial. In 2000, Berry explored singularities–correlations in Gaussian random fields [2]. However, the dynamical correlations, such as multi-singularity velocity statistics predicted in [2], remain inaccessible in experiments. Studying the dynamics of optical singularities is challenging due to their rapid movement, requiring ultrafast nearfield imaging.

Here we use ultrafast phase-resolved electron microscopy [4,5] (Fig. a), to observe the dynamics of optical singularities ensembles in hexagonal boron nitride (Fig. b). We show that they follow the prediction in [5] and go further, measuring the first spatiotemporal correlations of singularities, revealing distance-dependent velocity correlations that emerge only for opposite-charge singularity pairs. To access these statistics, we capture long-time (600 fs) group dynamics with sub-cycle (single fs) temporal resolution (Fig. c). The dynamics of singularities ensembles reveal superluminal velocities of the singularities, and sub-cycle annihilation events (Fig. d). Comparing our experimental results with a random-wave model uncovers universal features of singularities' dynamics and correlations (Fig. e). Although singularities are not physical particles, they exhibit particle-like interactions: same-charges repel, and opposite-charges attract. Whereas spatial singularities correlations resemble those of 2D liquids, the velocity correlations are unique (Fig. f). Our work bridges topological perspectives of optical singularities with many-body spatiotemporal wave correlations, revealing when singularities can be treated as interacting particles, and what aspects are unique.

### References:

- [1] Nye, J.F. and Berry, M.V., P.R.S.London.336.165(1974)
- [2] Berry, M.V., and M.R. Dennis. P.R.S.London.456.2001(2000)
- [4] Barwick, B., et al. Nature.462,902–906(2009)
- [5] Bucher, T., et al. Nat. Photon.18,809–815(2024)





### Mechanism of resonant enhancement in HHG

Mr. Yoad Aharon

Hebrew University of Jerusalem

**Authors:**

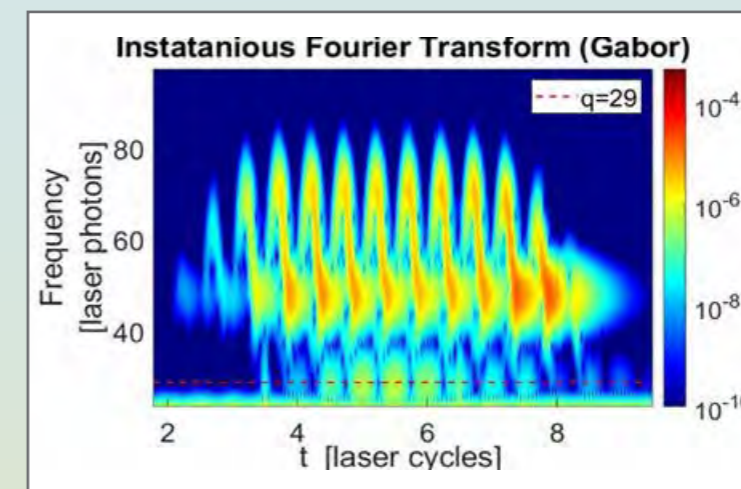
Hebrew University: Yoad Aharon, Adi Pick, Gilad Marcus. Technion: Ofer Neufeld

**Abstract:**

In high-harmonic generation (HHG), a characteristic plateau appears in the harmonic spectrum, commonly explained by the 3-step model [1]: (1) the strong laser field ionizes a valence electron, which is then (2) driven away and back toward the ion as the field oscillates, and (3) recombines into the ground-state, emitting its kinetic energy in the form of a high-energy photon. However, experiments with laser-ablated plasma have broadened the range of target materials, leading to the observation of a resonant effect, where a single harmonic order is significantly enhanced [2, 3]. This phenomenon occurs if the absorption spectrum of the ablated species includes an autoionizing (AI) state—a metastable state within the continuum. For enhancement to occur, the resonance condition must be satisfied:  $q\omega = E_{AI} - E_g$ , where  $E_{AI}$  is the energy of the AI state,  $E_g$  is the ground-state energy, and  $q$  is the order of the enhanced harmonic. To explain this observation, Strelkov proposed a 4-step model [4] that extends the conventional 3-step model by adding a step, whereby recombination occurs into the AI state and is then followed by a radiative transition back to the ground state.

In this work we study the enhancement mechanism. We solve the time-dependent Schrödinger equation of an atom containing a single electron by means of finite-difference methods. To incorporate a metastable state, we introduce potential barriers to create a shape resonance, following Strelkov’s approach.

We observe the enhancement of a single harmonic and investigate this effect by analyzing the solution in the temporal and frequency domains, employing Hermitian and non-Hermitian techniques. We also observe enhancement for ostensibly dipole-forbidden transition between same-parity states (Fig. 1 left), suggesting that the four-step model might not account for all aspects of the phenomenon.



**E posters Abstracts:****Tomographic Diffractometry of Laser Induced Plasma****Mr. Ivan Ostrovsky***Tel Aviv University***Authors:**

I. Ostrovsky, G. Hurvitz, E. Bograd, E. Flaxer, S. Hazra, and S. Fleischer

**Abstract:**

**Objectives:** Laser-induced air plasma has gained vast scientific interest over the last decades, fueled by a variety of prospected applications [1] as well as the pure scientific richness of this highly non-linear optical phenomenon [2]. In this work we study the spatial evolution of laser-induced plasma throughout the propagation direction of the plasma-generating laser pulse.

**Methods:** We utilize a transverse optical diffractometry setup that provides unprecedented sensitivity and spatial resolution of  $\sim 20\mu\text{m}$ . We introduce a novel Supergaussian (SG) plasma density distribution model and extract the key parameters of the plasma: the plasma density, its radial spread (width), and most importantly – the shape of the plasma distribution given by the SG order parameter ‘Gamma’. The latter is found pivotal for understanding the intricate laser-plasma effects that govern the entire laser-induced plasma evolution [3].

**Results:**

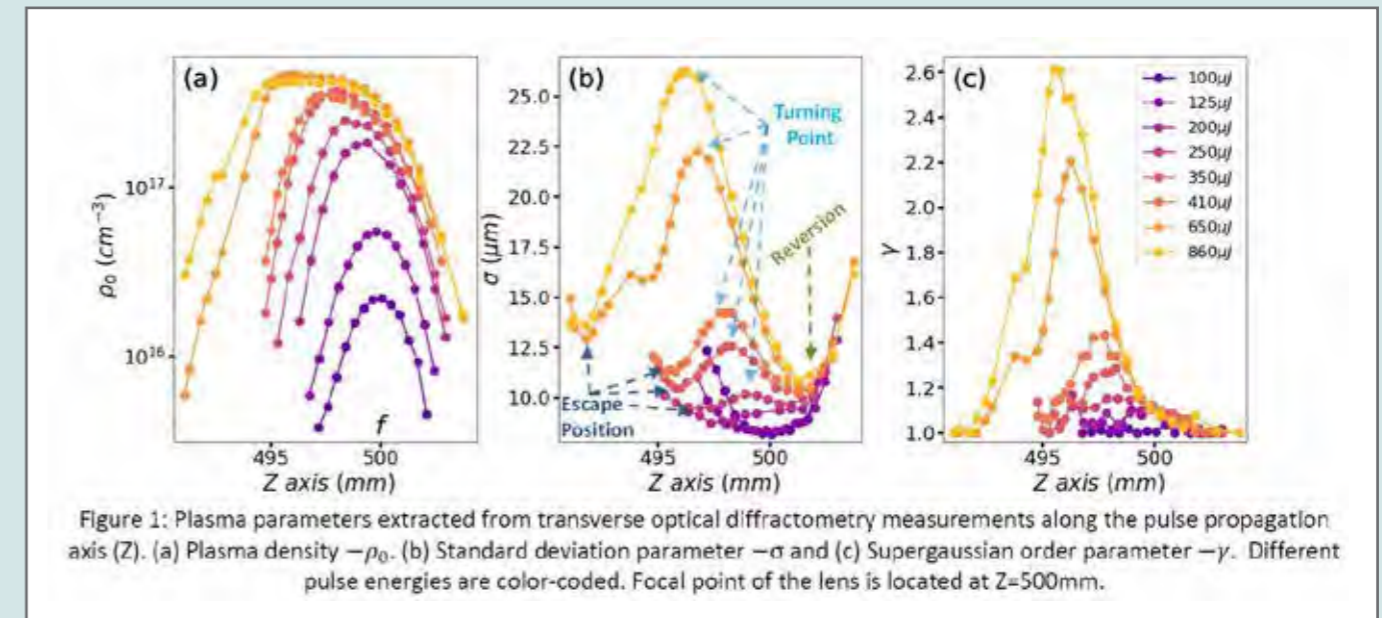
Our experimental and theoretical results unveil several key features in the evolution of the plasma:

- ‘Escape position’ – the position at which the beam defocuses from its lens-imposed geometry.
- ‘Turning point’ – the position at which defocusing ceases and the plasma reaches its maximal width.
- The ‘diffractive reversion’ of the SG beam back to Gaussian ‘effective lens’ propagation.

The attached figure depicts the position-dependent parameters of plasma entities induced by fs pulses with different energies (color-coded), starting from the effective ‘birth’ of the plasma (purple, 100microJ) and far beyond into the intensity clamping region (yellow, 860microJ). Note that the reversion position shared by all of the plasma entities – resulting from the SG diffraction and balanced by plasma defocusing. The experimental results are in very good agreement with our theoretical calculations (not shown here).

**References:**

- [1] J. Kasparian and J.-P. Wolf, Physics and Applications of Atmospheric Nonlinear Optics and Filamentation, Opt. Express 16, 466 (2008).
- [2] A. Couairon, A. Mysyrowicz, Femtosecond Filamentation in Transparent Media, Phys. Rep. 441, 47 (2007).
- [3] I. Ostrovsky, G. Hurvitz, E. Bograd, E. Flaxer, S. Hazra, and S. Fleischer, Tomographic Diffractometry of Laser-Induced Plasma Formations, ArXiv 2408.02772 (2024).



## Temporal cavity dynamics

Ms. Yuval Tamir

Bar Ilan University

### Authors:

Yuval Tamir, Dr. Hamootal Duadi, prof. Moti Fridman

### Abstract:

Temporal optics arises from the duality between the diffraction of beams in space and the dispersion of pulses in time. From this equivalence, we design and realize various spatial schemes in the time domain, such as time-lenses. Time-lenses impose a quadratic phase in time, similar to spatial lenses that impose a quadratic phase in space.

Optical cavities have many applications such as lasers, filtering specific wavelengths and enhancing light-matter interactions in quantum system.

A temporal cavity is the temporal adaptation of the spatial cavity, namely, it confines light in the time domain. During the resonance of the cavity, temporal solitons are generated and interact with each other.

In this research, we study the dynamics of the temporal cavity. We analyze the way soliton-molecules are formed, and the effect of normal and anomalous dispersion in the cavity on the dynamics of such solitons.

## Novel Method for Enhancing Ultra-Short Pulse Contrast via Transient Grating Based YVO<sub>4</sub>

Dr. Zaharit Refaeli

Soreq Nuclear Research Center

### Authors:

Zaharit Refaeli, Yariv Shamir, Eyal Lebiush, Asaf Levanon, Haim Suchowski, Gilad Marcus

### Abstract:

**Background:** Short laser pulses are widely used in light-material interactions, such as material processing, high-field atom physics (e.g., proton acceleration), and dense plasma experiments. Pulse contrast refers to the ratio between the peak intensity of a laser pulse and the surrounding pedestal intensity caused by imperfections in optical systems, including gratings, back reflections, nonlinearities, dispersion, and amplifier noise. Maintaining high temporal pulse contrast is essential to limit unwanted pre-pulse interaction, inhibiting the desired experiment by target evaporating. To address this challenge, various pulse-cleaning techniques are being employed in chirped pulse amplifier systems. Methods such as cross-polarized waves, second-harmonic generation, self-focusing, and optical parametric amplification can significantly improve contrast levels. However, these approaches often require supplementary filtration components, which may restrict their overall effectiveness.

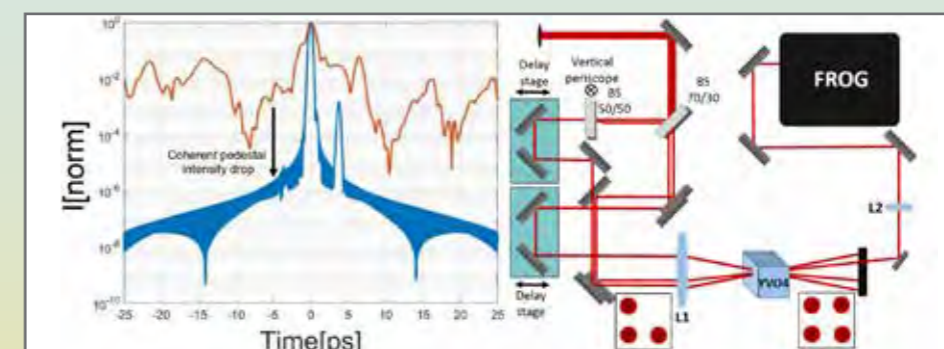
**Method:** This study employs transient grating (TG) as a nonlinear process to enhance pulse contrast [1]. When two pulses overlap at a specific angle ( $\theta$ ) within a  $\chi(3)$  nonlinear medium, a transient grating is formed. A third beam then interacts with this grating and is diffracted by it. While TG has traditionally been employed in spectroscopic studies or FROG configurations, we have employed its inherent intensity-sensitive efficiency for contrast enhancement purposes. TG inherently separates the clean beam from the generating beams, eliminating the need for additional filters.

**Results:** By utilizing a YVO<sub>4</sub> crystal, which is known for its enhanced nonlinearity, we achieved efficient TG generation with lower intensity requirements compared to fused silica. Our results demonstrated a contrast enhancement of up to 40 dB, with an absolute peak-to-noise contrast of 80 dB at approximately 1  $\mu$ J energy [2].

Setup modifications for higher pulse energies and corresponding higher efficiencies are underway.

### References:

- [1] Jun Liu et al. "Femtosecond pulses cleaning by transient-grating process in Kerr-optical media". In: Chinese Optics Letters 9.5 (2011), p. 051903.
- [2] Refaeli, Z., Shamir, Y., Lebiush, E., Levanon, A., Suchowski, H., & Marcus, G. (2025). Enhancement of 1  $\mu$ m laser pulse contrast using Transient Grating in YVO<sub>4</sub> crystal. Optics & Laser Technology, 180, 111494.





## Attosecond Waveform Control of Scanning Tunneling Microscopy

Mr. Daniel Davidovich

Technion– Israel institute of Technology

### Authors:

Daniel Davidovich Technion Israel, Adi Goldner Technion Israel, Boyang Ma Technion Israel, Michael Kruger Technion Israel

### Abstract:

**Objectives:** Reaching attosecond-nanometer resolution microscopy can enable observations of ultrafast electronic processes [1,2]. Here we combine an scanning tunneling microscope (STM) with an ultrashort laser pulse to achieve both resolution scales. However, in an STM environment, static tunneling induced by a bias voltage is needed to stabilize the tip distance from the sample, which obscures the laser-induced attosecond currents. By devising a new approach to measure the laser-induced currents alone, we demonstrate attosecond waveform current control in the STM.

**Methods:** We use a 1.8 um femtosecond laser and combine it with its second harmonic with a controllable delay to induce currents in a conventional STM junction. The delay allows us to create different waveforms which are not symmetrical, each of which generates a different tunneling current in the junction. Modulating the delay gives a modulated signal in the current, which can be detected using a lock-in amplifier at the given frequency. Furthermore, by momentarily freezing the tip in place, we can disable the bias and measure only the laser-induced tunneling currents.

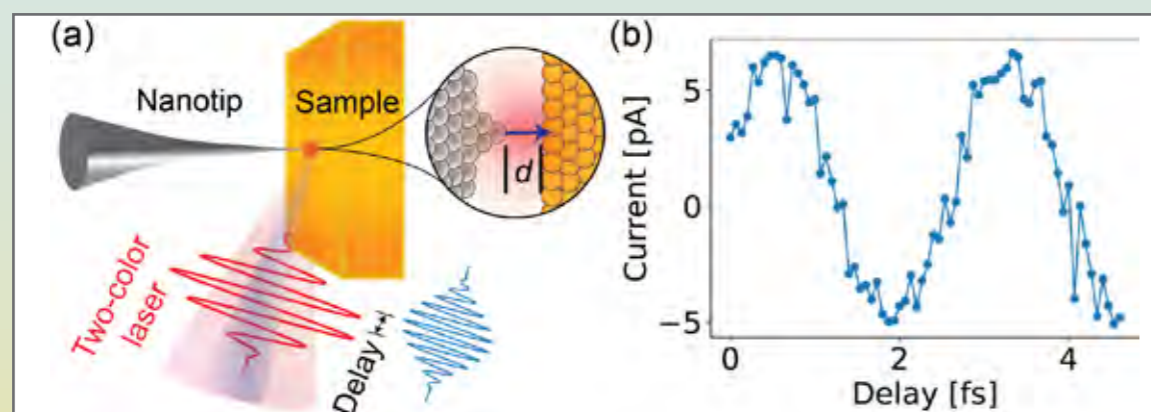
**Results:** We observe a clear signature of the laser-induced currents using both approaches. Using tip freezing we measure the dependence of the laser-induced tunneling currents on the delay without any background. We observe that the current oscillates as a function of the delay and changes direction according to the waveform of the two color field (see figure).

### Conclusions:

Our work shows for the first time that attosecond field waveforms can directly control the direction of the tunneling through an STM junction. With this advance, and the ability to resolve atomic scale structures, we can study the electron dynamics of molecules and nanostructures at the frontier of ultrafast microscopy.

### References:

- [1] Garg & Kern, Science 367, 411 (2020)  
[2] Ma & Kruger, PRL 133, 236901 (2024)



## Fabrication and Optical Characterization of Ultra-Fast YBCO Photon Detectors

Dr. Ankit Kumar

Technion– Israel institute of Technology

### Authors:

Ankit Kumar<sup>1</sup>, Dmitry Panna<sup>1</sup>, Shlomi Bouscher<sup>1</sup>, Avi Koriat<sup>1</sup>, Yuval Nitzav<sup>2</sup>, Gabriel Natale<sup>3</sup>, Vincent Plisson<sup>3</sup>, Kenneth S. Burch<sup>3</sup>, Ronen, Jacovi<sup>1</sup>, Amit Kanigel<sup>2</sup>, Alex Hayat<sup>1</sup>

<sup>1</sup> Department of Electrical Engineering, Technion Israel Institute of Technology, Haifa 3200003, Israel

<sup>2</sup> Department of Physics, Technion Israel Institute of Technology, Haifa 3200003, Israel

<sup>3</sup> Department of Physics, Boston College, Chestnut Hill 02467, USA

### Abstract:

**Objective:** High-temperature superconductors enable superconducting nanowire single photon detection (SNSPD) operation at significantly higher temperatures (above 77 K), facilitating the use of liquid nitrogen cooling. This significantly reduces the complexity and cost of the cryogenic system, leading to smaller, more portable, and more energy-efficient detection systems.

**Method:** We have fabricated a high-T<sub>c</sub> superconducting (YBa<sub>2</sub>Cu<sub>3</sub>O<sub>7-δ</sub>, YBCO) photodetector using our approach, which leverages an Al<sub>2</sub>O<sub>3</sub> mask and SEG-YBCO growth for device realization.

**Results:** In this work we demonstrate ultrafast optical response in high-T<sub>c</sub> superconductor (YBCO) wires operating at temperatures above 77 K [1]. We find rise time ~ 850 ps and the fall time ~ 1250 ps and an upper limit of timing jitter of ~ 100 ps, using twice the standard deviation of the fitted data. Using advanced nanofabrication techniques [2], we achieved miniaturized YBCO wires with widths approaching 100 nm. We observed a strong correlation between optical response and critical superconducting parameters, with peak response near critical temperature and current density. We have achieved the photoresponse of microwire to radiation in the mid-infrared spectrum at wavelengths 3.25 and 4.25 μm, at temperatures nearly ten times higher than those of existing low-temperature superconducting detectors. We showed a clear correlation between the photoresponse magnitude and the critical parameters of the superconductor, showcasing peak optical responses near the critical temperature and bias current density. Furthermore, our comprehensive electrical transport measurements conducted at various temperatures align closely with our optical response data.

**Conclusions:** This work demonstrates ultrafast optical response in high-temperature superconducting YBCO nanowires operating above liquid nitrogen. We achieved rise times ~850 ps, fall times ~1250 ps, and low jitter (<100 ps). We extended operation to the mid-infrared and observed peak response near critical parameters. Scalable fabrication using high-temperature masks enables practical implementation of these high-performance detectors for various applications.

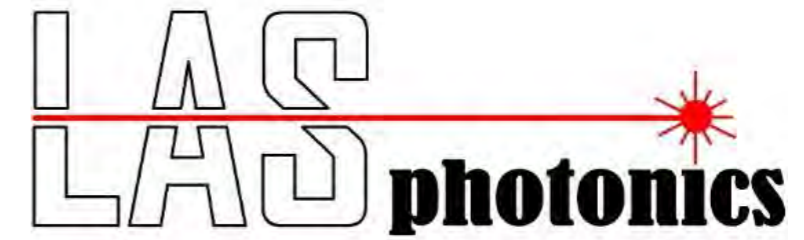
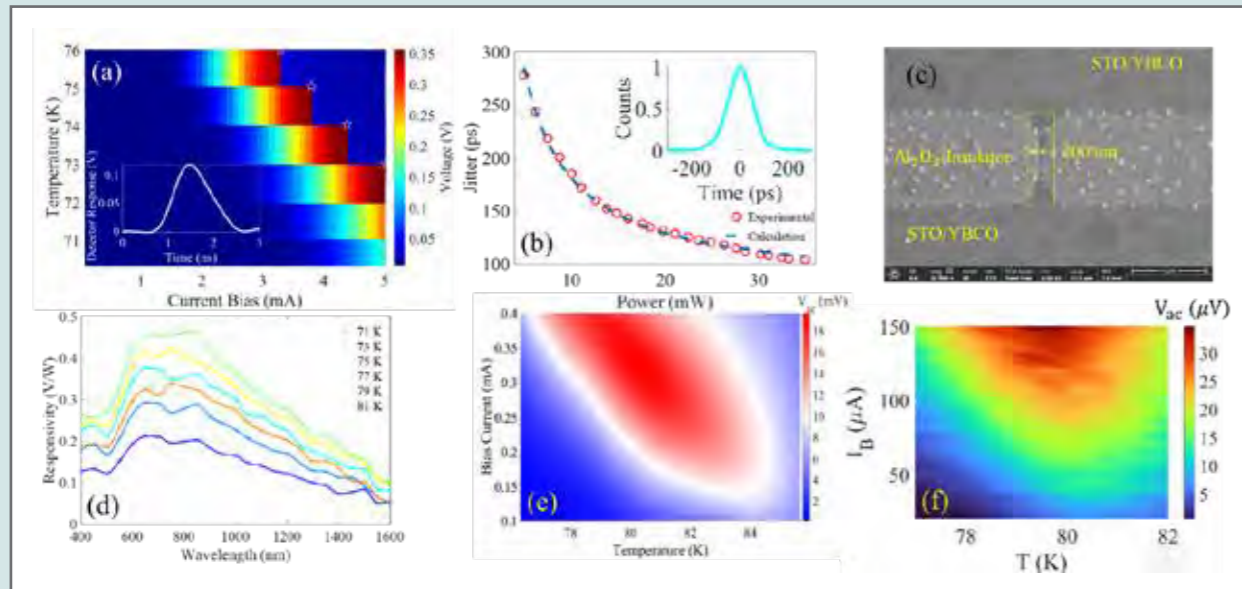
Fig. 1. (a) Surface plot of voltage vs current at different temperatures. shaped data points are critical currents obtained from I(V) measurement. The inset shows the transient photoresponse of the detector recorded using a 1 GHz sampling oscilloscope when the wire was biased at 2.1 mA at 76 K and illuminated with 4 ps-wide, 82-MHz-repetition-rate pulses at 810 nm wavelength from a mode-lock titanium-sapphire laser. (b) Main panel shows the measured jitter plot vs average laser power at a 1.7 mA bias current and the temperature was 76 K. The dashed curve is calculated dependence showing 1/Power behavior. The inset



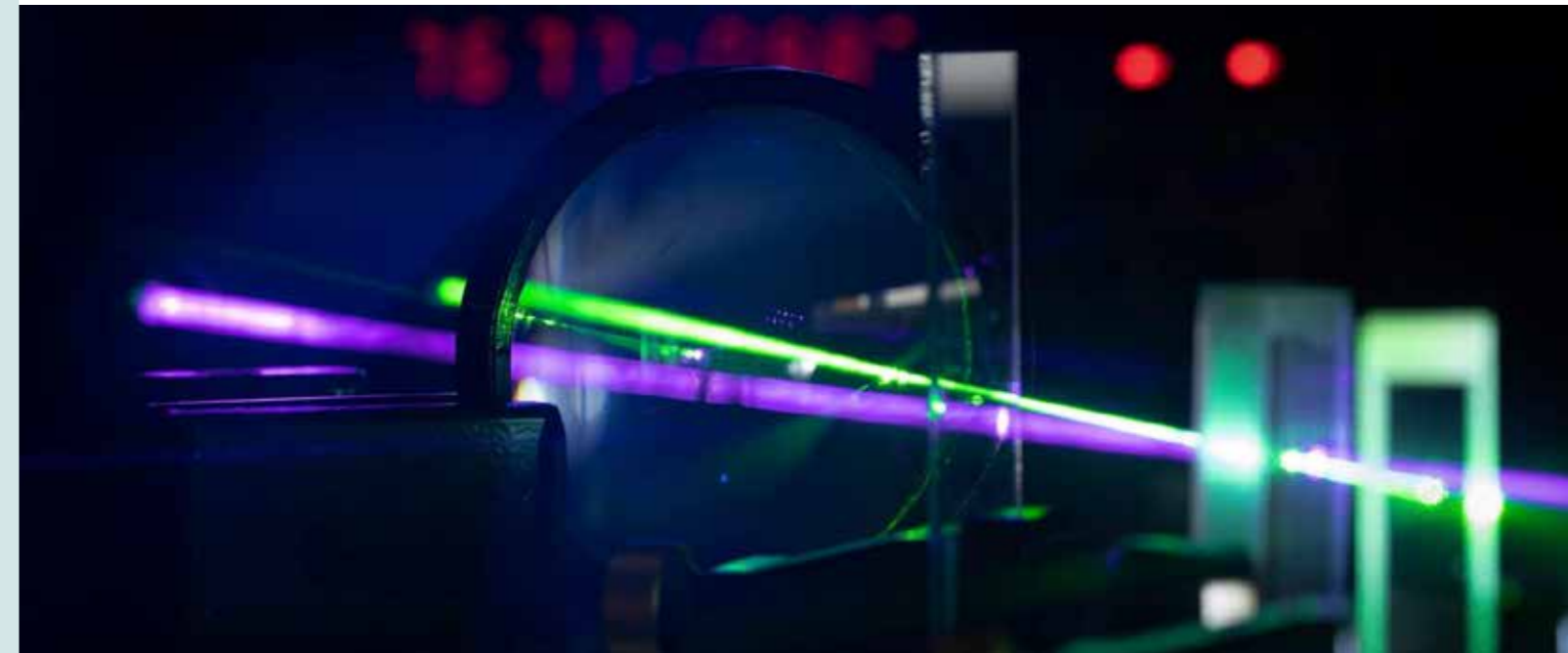
shows the histogram of the timing jitter of our device at a 1.7 mA bias current, 76 K temperature, and at 35 mW applied power. Twice the standard deviation obtained by fitting the measured data are 100 ps. (c) SEM images of 200 nm wide and 5 μm long (inside yellow dashed rectangle) and  $T_c = 84$  K. (d) Spectrally resolved responsivity for 750 nm wide meander structure at different temperatures. Lines are a guide to the eye. (e) Photoresponse vs bias current at different temperatures for 450 nm wide and 10 μm long wire. (f) Photoresponse vs bias current of the wire at different temperatures using  $4.25 \pm 0.25$  bandpass filter.

**References:**

- [1] A. Kumar, D. Panna, S. Bouscher, et al., "Ultrafast low-jitter optical response in high-temperature superconducting microwires," Appl. Phys. Lett. 122, 19 (2023).
- [2] A. Kumar, D. Panna, S. Bouscher, et al., "Optical response in a high- $T_c$  YBCO nanowire," Appl. Phys. Lett. 125, 022602 (2024).



**EXPERT IN INNOVATIVE PHOTONIC SOLUTIONS**



Laser and Light sources  
 Laser Material Processing solutions  
 Fiber-optics, Electro-optics and Laser components  
 Instruments and Systems  
 Imaging and Detection modules

**Booth#  
50**

## SPECTROSCOPY AND OPTICAL SENSINGS SESSION

### Oral presentations Abstracts:

#### Image-guided computational holographic wavefront shaping

Mr. Omri Haim

The Hebrew University of Jerusalem

##### Authors:

Omri Haim, Jeremy Boger-Lombard and Ori Katz. The Hebrew University of Jerusalem, Jerusalem, Israel

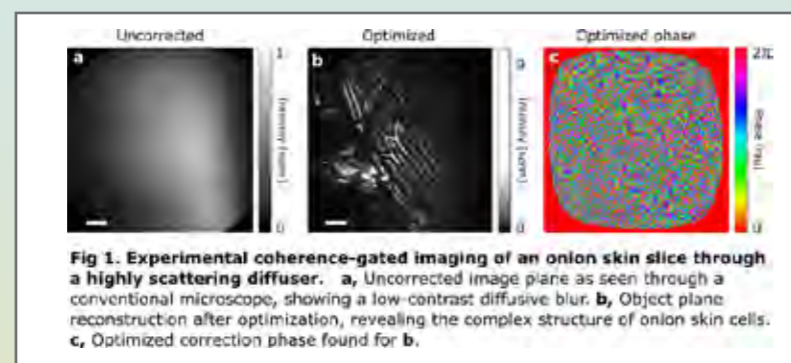
##### Abstract:

Optical imaging through scattering media is important in a variety of fields ranging from microscopy to autonomous vehicles. Although advanced wavefront shaping techniques have offered several breakthroughs in the past decade, current techniques still require a known guide star and a high-resolution spatial light modulator or a very large number of measurements and are limited in their correction field of view.

Here we introduce a guide-star-free, non-invasive approach that can correct more than 190,000 scattered modes using only 25 incoherently compounded, holographically measured, scattered light fields, obtained under unknown random illuminations. This is achieved by computationally emulating an image-guided wavefront shaping experiment, where several virtual spatial light modulators are simultaneously optimized to maximize the reconstructed image quality. Our method shifts the burden from the physical hardware to a digital, naturally parallelizable computational optimization, leveraging state-of-the-art automatic differentiation tools. We demonstrate the flexibility and generality of this framework by applying it to imaging through various complex samples and imaging modalities, including epi-illumination, anisoplanatic multi-conjugate correction of highly scattering layers, lensless endoscopy in multicore fibres and acousto-optic tomography.

The presented approach offers high versatility, effectiveness and generality for fast, non-invasive imaging in diverse applications.

Haim, O., Boger-Lombard, J. & Katz, O. Image-guided computational holographic wavefront shaping. Nature Photonics (2024) doi:10.1038/s41566-024-01544-6.



#### Non-destructive opto-mechanical analysis of fiber coating layers

Mr. Ori Pearl

Bar Ilan university

##### Authors:

A. Bernstein, E. Zehavi, S. Noimark, O. Pearl, Y. London, M. Hen, A. A. Stolov, and A. Zadok

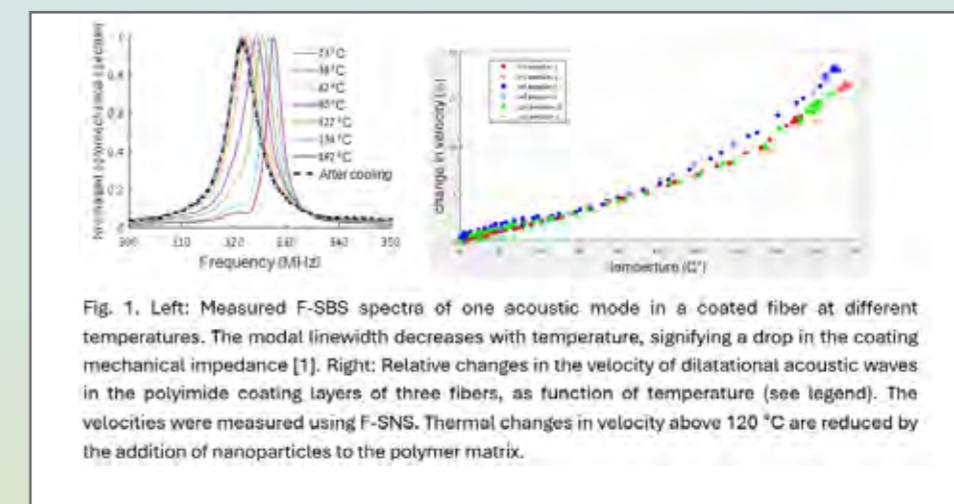
##### Abstract:

Polymer coating layers are essential for the handling and function of optical fibers. Monitoring the elastic properties of coatings is important for maintenance, quality control, and materials research. However, standard techniques of polymer analysis are destructive and unsuitable for working fiber.

Here we report the non-destructive monitoring of elastic coating parameters over working fiber, using forward stimulated Brillouin scattering (F-SBS) [1]. Pump pulses in the core of standard fiber launch packets of guided acoustic modes which span the entire cross-section of the coated fiber. The acoustic wave packet is affected by the elastic boundary conditions at the outer edge of the cladding and reaches into the coating. The decay rates and spectra of the acoustic waves are detected through photo-elastic modulation of co-propagating probe light. The protocol enables the analysis of conditions outside the fiber core, where guided light cannot reach.

In one example, the glass transition temperature ( $T_g$ ) of a coating layer is identified through a sharp drop in its mechanical impedance [2]. In another measurement, the velocities of dilatational acoustic waves in a polyimide coating layer are measured with 1% precision, in a temperature range of 20–220 °C. The addition of nano-particles into the polymer matrix reduces the thermal variations in the acoustic velocity.

Fig. 1. Left: Measured F-SBS spectra of one acoustic mode in a coated fiber at different temperatures. The modal linewidth decreases with temperature, signifying a drop in the coating mechanical impedance [1]. Right: Relative changes in the velocity of dilatational acoustic waves in the polyimide coating layers of three fibers, as function of temperature (see legend). The velocities were measured using F-SNS. Thermal changes in velocity above 120 °C are reduced by the addition of nanoparticles to the polymer matrix.





## Tips vs. Holes: $\times 10$ Higher Scattering in FIB-made Plasmonic Nanoscale Arrays for Spectral Imaging

Mr. Ya'akov Mandelbaum

Bar-Ilan U./Lev Academic Center

### Authors:

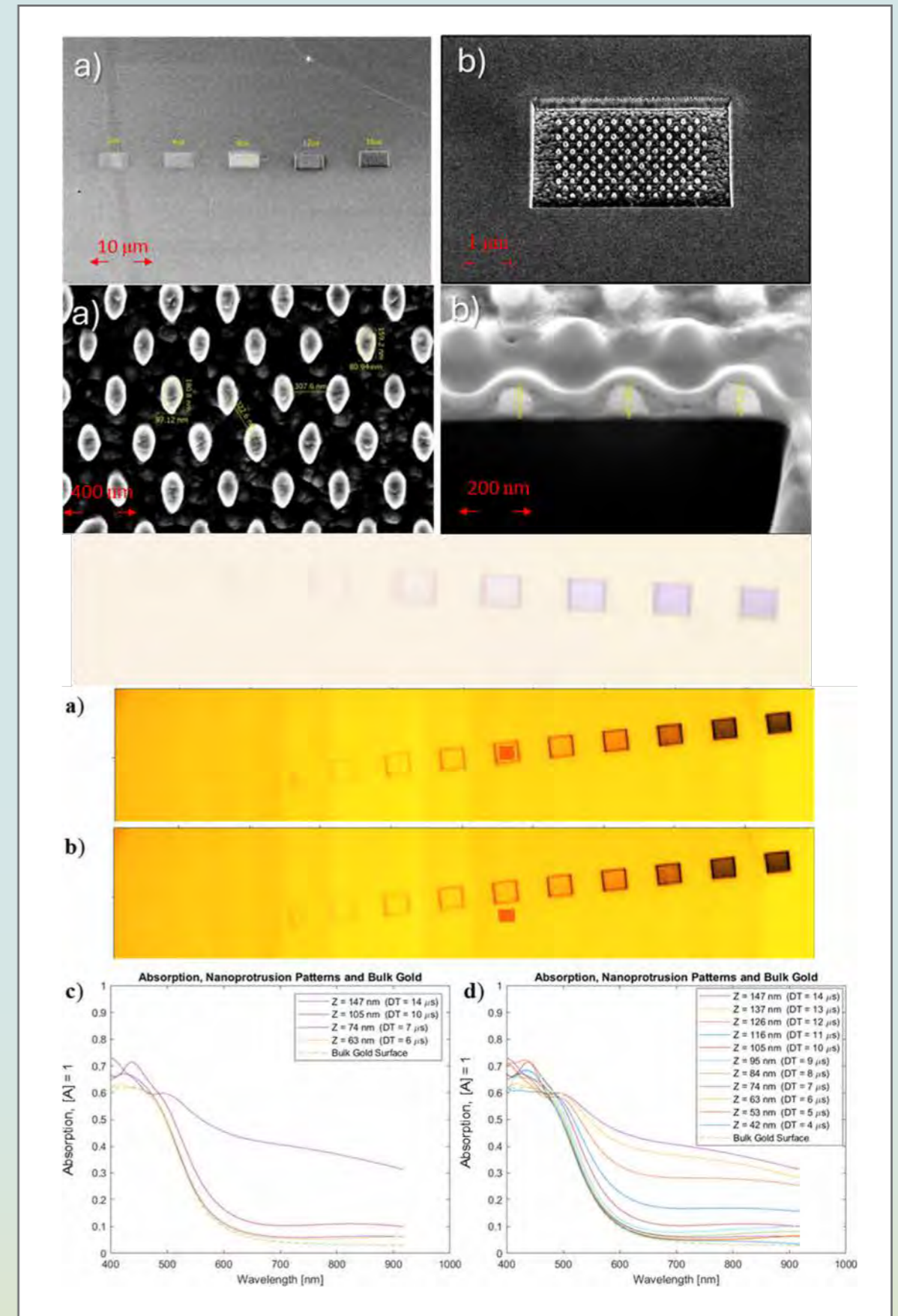
Mandelbaum, Ya'akov, Bar-Ilan U., Ramat-Gan/Lev Academic Center, Jerusalem, Israel; Tkachev, Maria, Bar-Ilan U., Ramat-Gan, Israel; Sanjeev, Abhijit, Bar-Ilan U., Ramat-Gan, Israel; Zalevsky, Zeev, Bar-Ilan U., Ramat-Gan, Israel; Zitoun, David, Bar-Ilan U., Ramat-Gan, Israel; Bar-Ilan U., Ramat-Gan, Israel; Karsenty, Avi, Lev Academic Center, Jerusalem/ Bar-Ilan U., Ramat-Gan, Israel

### Abstract:

The development of real-time sensors that can monitor continuous flow reactions is needed for investigation in many fields—environmental analysis, pharmaceuticals, material sciences, art and archeological research, forensic science, drug and explosives detection, food quality analysis, and single-algal cell detection. Therefore, imaging sensors, capable of recording and reporting spatial variations in real time, are desirable.

Plasmonic nano-structure arrays, designed for performance as pixels in an advanced SERS imaging device, were fabricated by gallium Focused Ion Beam (FIB). Though the FIB is best suited for etching holes and negative structures, our previously reported simulations favor protrusions. Herein, we report on the FIB methodology to 'sculpt' positive structures by 'ion-blasting' away the surrounding material. Nano-protrusions and nano-holes with different aspect ratios are compared experimentally with depth and height controlled by the dwell time. The amplitude and spectra of optical absorption and scattering from the two species are compared as a function of structure height. Measurements were performed using ASI's model Rainbow hyperspectral camera, demonstrating the utility of hyperspectral microscopy for plasmonic imaging applications. Both the scattered and absorbed radiation display the broad peak qualitatively similar to the localized surface plasmon (LSP) scattering spectrum of gold nano-spheroids. The intensity of the scattered light from the protrusions - measured in dark-field - was observed to be an order of magnitude higher than that from the nano-holes, consistent with simulation predictions. Poor contrast against bright background specular reflection is inherent in bright-field reflection mode; image-processing succeeded in detecting patterns indiscernible to the eye. To extract the absorption the full hyperspectral image field was exploited, allowing the sample to serve as its own reference. The resulting spectra display a plasmonic resonance which grows stronger and increasingly red-shifted at increasing heights, corroborating visual observations of changes in sample hue.

ACS Omega 2024, 9, 47, 46796–46812



## Generation of Non-Classical Light in an All-Fiber SU1,1 Interferometer

Mr. Elad Zehavi

Bar-Ilan University

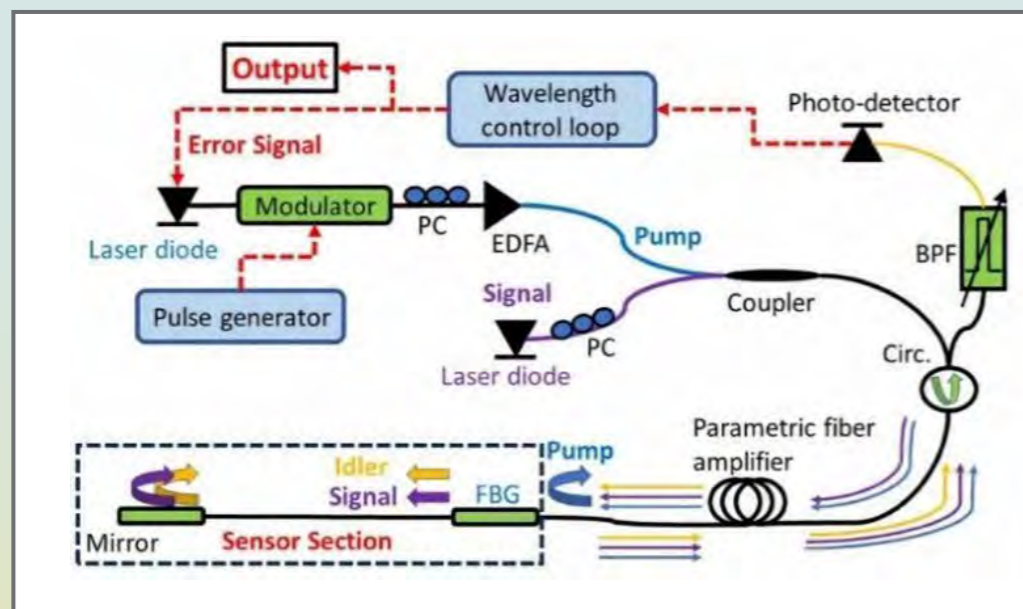
### Authors:

Elad Zehavi, Alon Bernstein, Michal Natan, Yosef London, Shahaf Noimark, Avi Zadok, and Avi Pe'er

### Abstract:

The sensitivity of interferometers may be enhanced beyond the shot-noise limit (SNL) using squeezed states of light. SU2 interferometers, such as Mach-Zehnder or Michelson configurations, enhance sensitivity by injecting squeezed vacuum into the unused input port, as in LIGO. In SU2, the sensitivity enhancement requires near-perfect detectors, which are technically demanding, difficult to scale and not available in all wavelengths. Alternatively, an SU1,1 interferometer with two optical parametric amplifiers (OPAs) in series may surpass the SNL, lifting the detectors limitation. We demonstrate a scalable SU1,1 design using all-fiber OPAs, standard components, and noisy detectors.

Periodic pump pulses of  $\sim 1$  W peak power and 40 ns duration are launched along the slow principal axis of a 100 m long dispersion shifted, polarization maintaining fiber. A continuous signal wave is co-aligned with the pump pulses. The fiber serves as an OPA, with parametric gain of 1.5. Idler wave pulses are generated at the OPA output. The pump wave is reflected at the far end of the fiber by a Bragg grating, whereas the signal and idler waves are transmitted to a meter-long sensing section of standard fiber. The signal and idler are reflected from a mirror at the end of the sensing fiber and rejoin the pump pulses for a second path through the fiber OPA. A feedback loop adjusts the frequency of the pump wave and locks three waves to a differential phase of  $\pi$ . The polarizations of all three waves are re-aligned with the slow axis prior to backpropagation. The idler wave is detected by a photo-receiver after the second path through the OPA. Small-scale perturbations to the differential phase induce variations to the detected idler power. Our interferometer implementation will allow to measure these variations with sensitivity of 3.5 dB beyond the SNL. Experimental characterization of sensitivity enhancement is under way.



## Stacking-Dependent Photoluminescence Modulation in Bilayer and Trilayer 3R-MoS2 via Asymmetric Dielectric Environments

Mr. Idan Kizel

Tel Aviv University

### Authors:

Omri Meron, Idan Kizel, Dror Hershkovitz, Maayan Vizner, Moshe Ben Shalom, Haim Suchowski. Condensed Matter Physics Department, School of Physics and Astronomy, Faculty of Exact Sciences, Tel Aviv University, Tel Aviv, Israel

### Abstract:

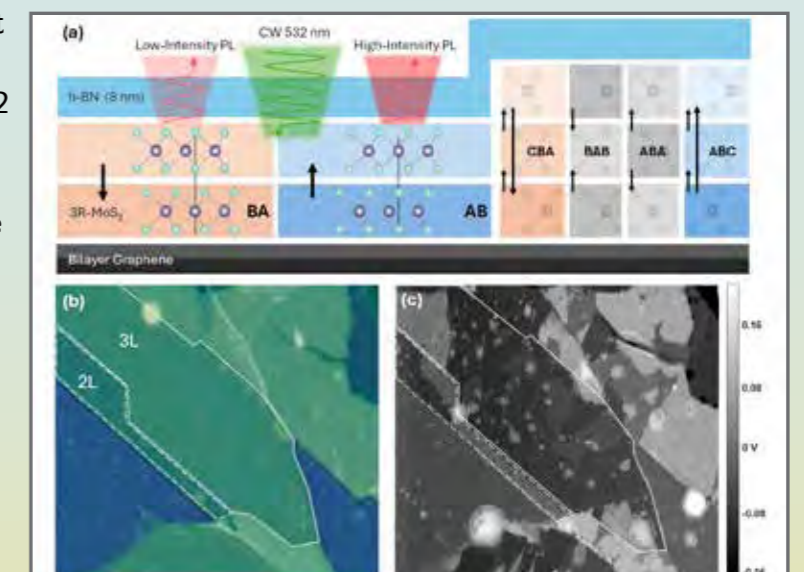
**Background and Motivation:** Rhombohedral transition metal dichalcogenides represent an emerging class of two-dimensional ferroelectric materials where lateral shifts between layers induce reversible polarization. While promising for next-generation electronics, identifying polarization domains remains challenging in device-ready architectures where conventional probing methods are impractical.

**Objectives:** To develop a non-invasive optical method for identifying ferroelectric domains in few-layer 3R-MoS2 by exploiting the interaction between intrinsic polarization and asymmetric dielectric environments, addressing the challenge of characterizing polarization domains in encapsulated architectures.

**Methods:** We investigated bilayer and trilayer 3R-MoS2 samples encapsulated between bilayer graphene substrate and h-BN capping layer. Using photoluminescence spectroscopy with 532 nm excitation, we characterized the optical response of different stacking configurations from 4K to 295K, with Kelvin probe microscopy serving as ground-truth reference.

**Results:** We observed pronounced differences in PL intensity between stacking configurations. In bilayer regions, AB-stacked (upward polarized) domains exhibited 300% stronger emission compared to BA-stacked (downward polarized) regions. Similar enhancement appeared in trilayer domains, with ABC stacking showing higher PL intensity than CBA and ABA/BAB configurations. These differences arise from polarization-induced modulation of the exciton-to-trion population balance.

**Conclusions:** Our findings demonstrate that engineered dielectric asymmetry can distinguish ferroelectric domains in 3R-MoS2 through PL spectroscopy. This non-invasive technique enables reliable domain mapping in fully encapsulated device architectures, advancing both fundamental understanding of polarization-dependent excitonic phenomena and development of polarization-sensitive devices.





## On the Optical Modeling of Excitons in 2D Semiconductors

Ms. Anabel Atash Kahlon

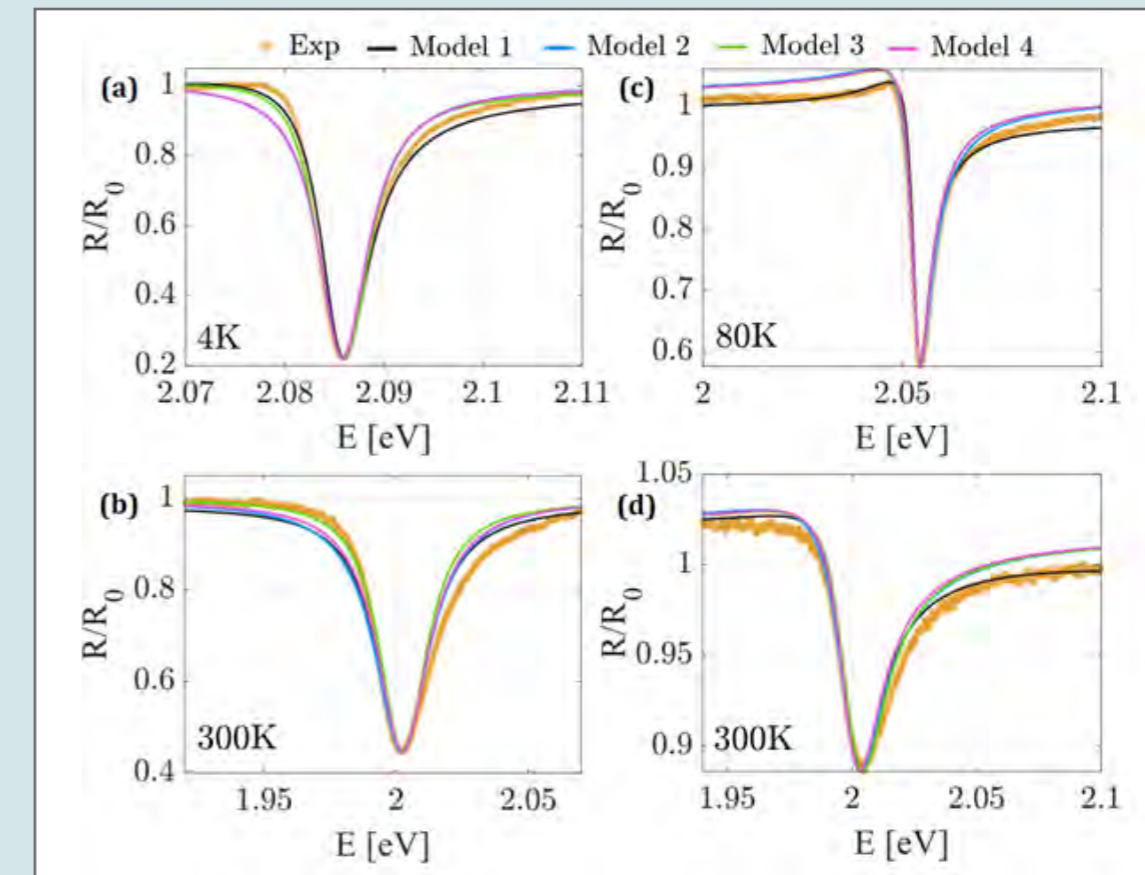
Tel Aviv University

### Authors:

Anabel Atash Kahlon, Tel Aviv University, Israel; Matan Meshulam, Tel Aviv University, Israel; Tomer Eini, Tel Aviv University, Israel; James H. Edgar, Kansas State University, Manhattan, KS, USA; Sefaattin Tongay, Lawrence Berkeley National Laboratory, Berkeley, 94720, California, USA, University of California, Berkeley, 94720-1760, California, USA, Arizona State University, Tempe, Arizona 85287, USA; Itai Epstein, Tel Aviv University, Tel Aviv, Israel

### Abstract:

Excitons in monolayer transition metal dichalcogenides (TMDs) dominate their optical response. Understanding their physical behavior and accurately modeling their response is crucial for both fundamental research and development of TMD-based optoelectronic devices. Several theoretical models have been proposed to describe this excitonic behavior; however, it remains unclear which model most accurately captures the underlying physical properties. Each model presents a distinct perspective on exciton dynamics, emphasizing different physical constituents and employing unique mathematical approaches to describe the optical response of a material. While some models characterize the optical response using only two parameters (radiative and non-radiative decay rates), others incorporate additional parameters such as pure dephasing or inhomogeneous broadening to capture more subtle quantum mechanical effects. In this study, we experimentally measure the optical response of high-quality monolayer TMD heterostructures in two common configurations (hBN/WS<sub>2</sub>/hBN/gold mirror and hBN/WS<sub>2</sub>/hBN/SiO<sub>2</sub>) across temperatures 5K–300K and compare the results with four different theoretical models to address this uncertainty. The figure shows experimental measurements and models fitting of the reflection contrast at different temperatures: (a–b) sample A (c–d) sample B. These curves reveal exciton energy shifts, linewidth changes, and the emergence of different spectral profiles as functions of the sample configuration and temperature. We employ a minimization technique to determine the various physical components of each model by comparing our experimentally obtained reflection data with analytically calculated models. Our analysis reveals that a three-independent parameter model incorporating quantum mechanical effects in the form of a quantum pure dephasing rate consistently outperforms the conventional two-parameter approaches, consisting of only radiative and non-radiative decay rates. The superior accuracy of the model stems from its explicit treatment of pure dephasing processes, providing crucial insights into the fundamental physics governing exciton dynamics. These findings establish a robust framework for understanding and predicting the optical properties of TMD-based devices.



## New Single-Particle TOF Mass Spectrometer coupled with Deep Learning for On-site Classification of Aerosol Particles

Dr. Heinrich Ruser

*Institute for Applied Physics and Measurement Technology, University of the Bundeswehr Munich*

### Authors:

Heinrich Ruser, Guanzhong Wang, Seongho Jeong, Thomas Adam: University of the Bundeswehr Munich, Germany; Andreas Walte: Photonion GmbH, Schwerin, Germany; Johannes Passig, Ralf Zimmermann: Joint Mass Spectrometry Centre, University of Rostock, Germany

### Abstract:

**Objectives:** The ability to rapidly detect and classify pollutant aerosol particles on-site is crucial for many security and health-relevant applications. Single-particle laser-based time-of-flight mass spectrometry (TOF-SPMS) is a unique measurement tool to reveal the chemical fingerprint of particle matter (PM) air-transported over distances from a few centimeters up to dozens of kilometers. Our new general evaluation method adaptively identifies unique and stable signatures in PM mass spectra and classifies the particles on-site in real-time, based on supervised deep learning.

**Methods:** The novel SPMS device applies a unique multi-step laser excitation for soft and hard ionization: Individual particles, singled out by an atmospheric lens in the range of 100 nm to 2.5  $\mu\text{m}$ , are exposed to a tailored combination IR and UV laser pulses (10.6  $\mu\text{m}$  CO<sub>2</sub> laser and 248 nm KrF excimer laser) for laser desorption/ionization (LDI) as well as for ultra-sensitive resonance-enhanced multiphoton ionization (REMPI) of organic compounds like carcinogenic Polycyclic Aromatic Hydrocarbons. Positive and negative ions are detected in a bipolar MS, revealing the chemical composition of every single particle by displaying the intensity distribution of mass-to-charge ratios ( $m/z$ ). Specific ion marker signatures in the MS patterns reveal plausible emission sources in real-time.

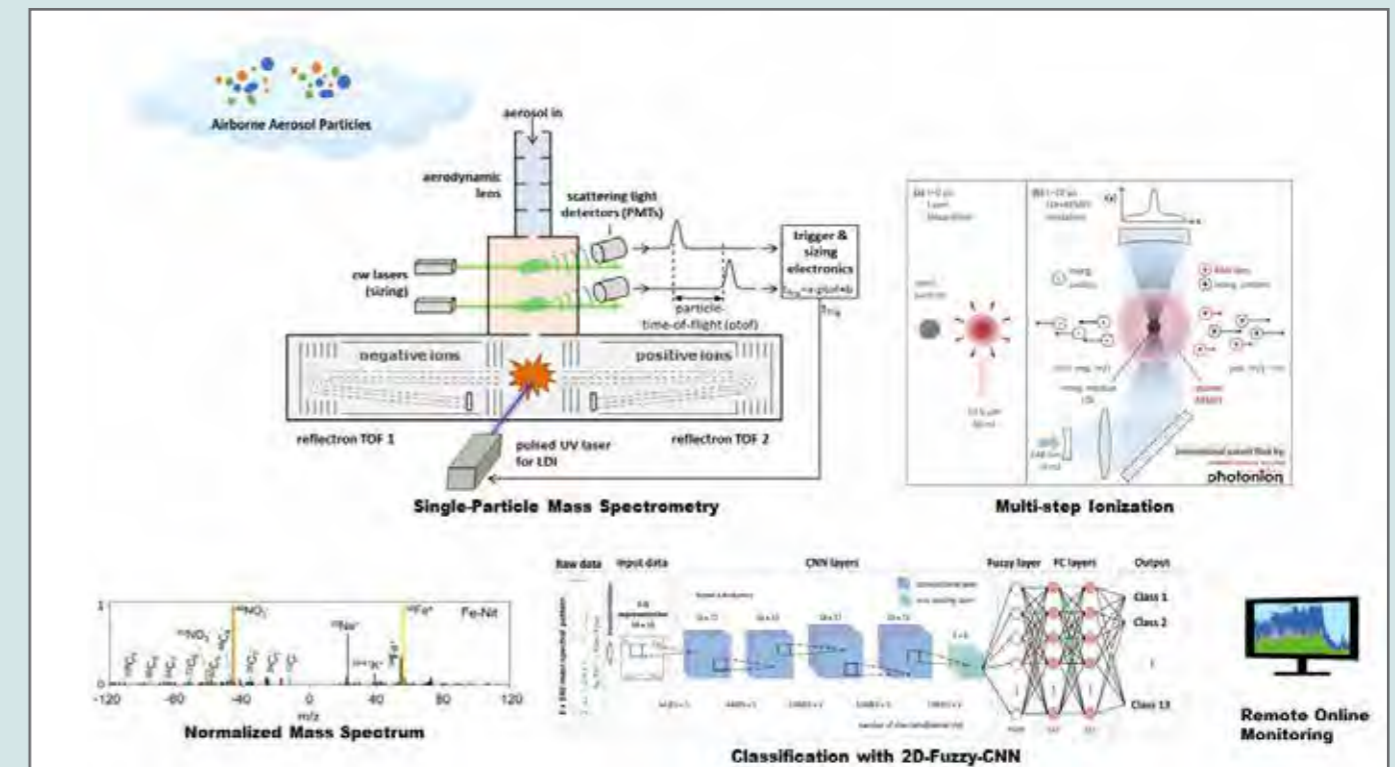
**Results:** Mobile measuring stations have been built-up and exploited in field campaigns. For SPMS on-site classification, we developed a hybrid 2D Fuzzy CNN architecture (FCNN) able to extract characteristic features in the data self-dependently during training. Trained with ~30,000 mass spectra labeled in 13 classes of airborne particles, high classification rates of > 92 % were achieved. Moreover, the MS of over 40 different explosive compounds were analyzed.

**Conclusions:** A large variety of fine and ultra-fine particles in the ambient air can be comprehensively analyzed in real-time for the first time. Potential applications go well beyond air quality monitoring, up to the identification of hazardous substances from warfare agents, explosives, narcotics and drugs. (304)

### References:

- J. Passig, R. Zimmermann (2021): Laser Ionization in Single-Particle Mass Spectrometry, in: Photoionization and Photo-Induced Processes in Mass Spectrometry, Wiley, pp. 359-411. DOI: 10.1002/9783527682201.ch11.
- G. Wang, H. Ruser et al. (2024). A Fuzzy Convolutional Neural Network for the Classification of Aerosol Particle Mass Spectral Patterns Generated by Single-Particle Mass Spectrometry, IEEE World Congress on Computational Intelligence (WCCI). DOI: 10.1109/IJCNN60899.2024.10650883
- H. Ruser, J. Schade et al. (2024). Real-time particle analysis of explosives compounds using single-particle mass spectrometry, SPIE Defense + Commercial Sensing, Next-Generation Spectroscopic Technologies

XVI; 130260J. DOI: 10.1117/12.3017532



## 4D Near-Field Electron Tomography

Mr. Tamir Shpiro

Technion – Israel Institute of Technology

### Authors:

Tamir Shpiro, Ron Ruimy, Kaizad Rustomji, Ido Kaminer

Solid State Institute, Technion – Israel Institute of Technology, Haifa 32000, Israel

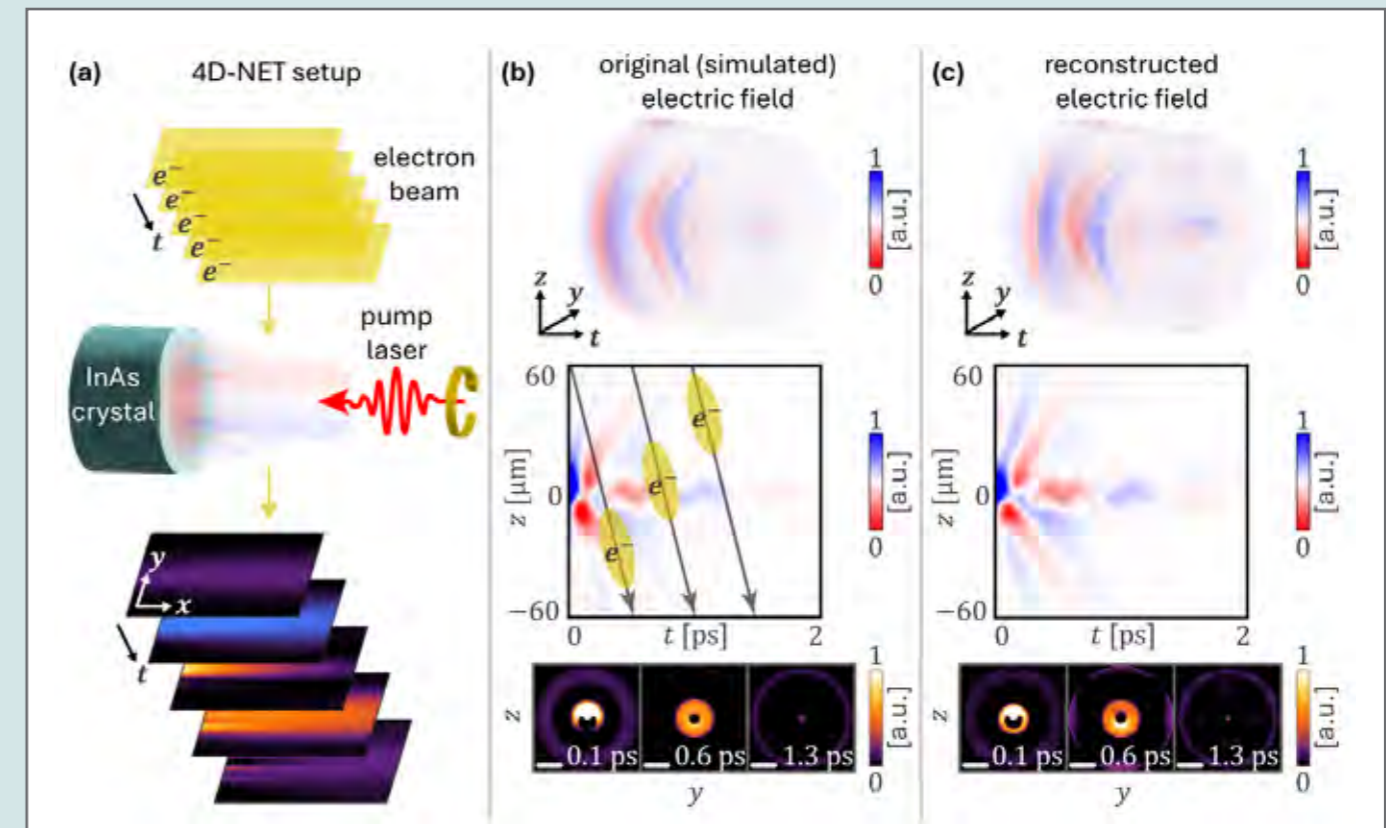
### Abstract:

New techniques for imaging electromagnetic near-fields have great importance in life science, material science, and nanotechnology [1]. Prominently, ultrafast imaging in electron microscopy has seen a surge of interest with the development of photon-induced nearfield electron microscopy (PINEM) [2]. This capability and its generalizations [3,4] provide unprecedented spatio-temporal resolutions, applicable to broad regimes of the electromagnetic spectrum, from THz [3] to optical [2] frequencies. However, all works so far only provided a 2D projection of the near-field, determined by the electron transmitted through the sample.

Drawing inspiration from the field of computed tomography (CT), we present a novel technique for 3+1D reconstruction of the near-field profiles, achieved by collecting time-resolved field measurements from multiple angles (Fig.a). Unlike reconstructed objects in conventional CT, near-fields oscillate rapidly and change during the electron transmission time (especially in THz frequencies and above). Consequently, each electron interacts with multiple time-frames of the near-field, mixing them together. We develop a technique that disentangles the mixed projections and reconstructs the full space and time (3+1D) information of the near-field, including its vector nature. We apply this technique on a simulated THz field mixing photo-Dember [5] and optical rectification [6] created by a laser pulse (800nm, 200fs pulse duration,  $10\mu\text{m}$  spot, 10nJ) illuminating an InAs crystal, showing a good fit of the electron-beam (velocity 0.7c) tomographic reconstruction, distinguishing the contributions of the mixed nonlinearities (Fig.b,c, white bars denote  $50\mu\text{m}$ ).

### References:

- [1] L. Novotny et al. Principles of Nano-Optics (Cambridge UP, 2012)
- [2] B. Barwick, et al., Nature. 462, 902-906 (2009)
- [3] M. Yannai, et al., ACS Nano 17, 3645-3656 (2023)
- [4] Bucher, T., et al. Nat. Photon. 18, 809-815 (2024)
- [5] G. Klatt et al., Opt. Express 18, 4939-4947 (2010)
- [6] S. Chuang et al., Phys. Rev. Lett. 68, 102 (1992)





**E posters Abstracts:****Enhancing Detection Sensitivity of Contaminants in Water by The Full Scattering Profile Within the Single Scattering Regime****Mr. Bar Atuar***Bar-Ilan University***Authors:**

Bar Atuar, Alon Tzroya, Dr. Hamootal Duadi and Prof. Dror Fixler

The Faculty of Engineering and the Institute of Nanotechnology and Advanced Materials, Bar Ilan University, Ramat Gan 5290000, Israel

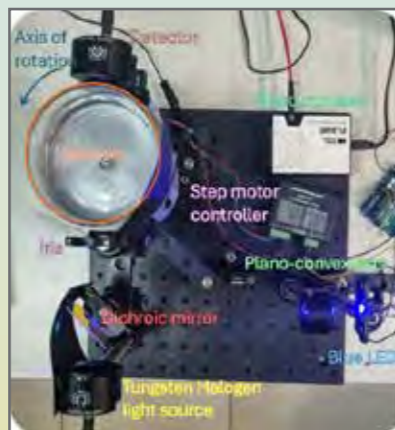
**Abstract:**

**Objectives:** The work aimed to enhance the capabilities of the existing iso-pathlength (IPL) system, which uses the full scattering profile of a sample to monitor water quality. The first phase focused on assessing the system's limitations, while the second phase aimed to improve its performance by adding a blue light source alongside the existing white light source using a dichroic mirror. This upgrade was intended to improve the system's ability to detect bacterial and heavy metal contaminants.

**Methods:** The IPL system utilizes the FSP, which represents the angular distribution of reemitted light from a cylindrical sample. A key feature is the IPL point, which maintains consistent light intensity, independent of the reduced scattering coefficient, and is determined by the sample's structure and geometry. This allows the IPL point to serve as a self-calibration reference, improving accuracy and aiding contaminant detection.

**Results:** Optimal calibration settings were identified, including a 10mm input beam diameter and a 90mm sample diameter, producing a clear IPL point. The integration of a blue LED with the Tungsten Halogen light source successfully enabled the detection of Cyanobacteria and CuCl<sub>2</sub>, increasing the system's sensitivity. The upgraded system also demonstrated higher resolution than a UV-VIS spectrophotometer. However, due to the unavailability of the ideal dichroic mirror, a suboptimal mirror was used, limiting part of the white light source. Additionally, the DPF for Cyanobacteria was not determined.

**Conclusions:** The project successfully optimized the IPL system by refining calibration settings and adding a blue LED light source, which enabled the detection of previously undetectable substances like Cyanobacteria and CuCl<sub>2</sub>. The system's resolution and sensitivity were significantly improved. However, further work is required, including acquiring a suitable dichroic mirror and conducting additional experiments to test the system's ability to differentiate multiple contaminants in a single measurement.

**Lead Halide Perovskite and PVC Subwavelength Gratings in Guided Mode Resonance (GMR) Sensor for Medical Applications****Dr. Moshe Zohar***Sami Shamoon College of Engineering***Authors:**

Zeev Fradkin, Maxim Pisklich, Moshe Zohar, and Mark Auslender

**Abstract:**

**Objective:** The GMR effect has great potential in different applications, such as sensors [1], optical filters [2], and solar cells [3]. A basic GMR structure includes diffraction grating and a dielectric waveguide. At resonance conditions, a sharp reflection peak is monitored on the wavelength axis due to the excitation of waveguide leaky mode by diffraction of incident light [4].

This work presents a GMR sensor for medical applications at normal and oblique incidence (based on lead halide perovskite and polymer subwavelength grating). These sensors allow low-cost soft lithography fabrication methods (such as imprint nanolithography, dip dep nanolithography [5], and others) without expensive photolithography equipment and fabrication.

**Methods:** The reflection of the sensor versus wavelength was investigated for different geometry parameters: grating pitch, angle of incidence, polarization (TE & TM), 1D & 2D optical grating. The sensitivity, Q-factor, and figure of merit (FOM) are analyzed. The optical simulations are based on rigorous coupled modes analysis (RCWA).

**Results:** Characteristics of sensor structures with different gratings materials (PVC, perovskite, and silicon nitride) on a silicon nitride waveguide were compared.

Most published research presents GMR sensors with their characteristics at normal incidence, where the Q-factor parameter range is between 100 and 300 [1]. Only a few works were published on GMR sensors under oblique incidence [6–8]. Guo et al. [6] tested photoresist grating (photolithography fabrication) on Ta<sub>2</sub>O<sub>3</sub> waveguide at oblique incidence; however, systematic testing of the Q-factor is not presented in these works.

According to Table 1 for TM polarization, the sensitivity and the Q-factor are increased with the incidence angle (in the presented angle range). Here, we present CsPbBr<sub>3</sub>-grating on silicon nitride waveguide 276nm/RIU at 30 degrees of incidence and 440 nm/RIU at 60 degrees of incidence, where the grating fabrication does not need to use photolithography. We also present a 1D PVC-grating sensor with a Q-factor of 40100 at an incidence angle of 60 degrees. So, the unique FOM of this sensor at TM polarization is significantly (order of magnitude) larger than those previously published [9]:

$$FOM=S \cdot Q=338 \cdot 40095=13.55 \cdot 10^6 \text{ [nm/RIU]}$$

**Conclusions:** A novel GMR sensor design for glucose and hemoglobin concentration is presented at normal and oblique incidence. In this design, polymer and perovskite allow flexible, low-cost fabrication by soft-lithography/imprint-lithography methods. The sensitivity, figure of merit (FOM), and Q-factor are presented for 1D and 2D optical grating structures.

A Q-factor of 50000 is achieved for 1D PVC grating on silicon nitride waveguide at TM polarization and 75 degrees obliqued incidence, which is about one order of magnitude larger relative to the Q factor value at normal incidence.



**References:**

- [1] Y. Zhou, Z. Guo, W. Zhou, S. Li, Z. Liu, X. Zhao, and X. Wu, "High-Q guided mode resonance sensors based on shallow sub-wavelength grating structures" *Nanotechnology* 31 (2020) 325501
- [2] G. Quaranta, G. Basset, O. J. F. Martin, and B. Gallinet, *Recent Advances in Resonant Waveguide Gratings*, *Laser Photonics Rev.* 2018, 12, 1800017
- [3] T. Khaleque, R. Magnusson *Journal of Nanophotonics*, Vol. 8, Issue 1, 083995 (March 2014).
- [4] R. Magnusson and Y. H. Ko "Guided-mode resonance nanophotonics: fundamentals and applications," *Proc. SPIE 9927, Nanoengineering: Fabrication, Properties, Optics, and Devices XIII*, 992702 (15 September 2016);
- [5] H. Lan and Y. Ding, "Nanoimprint Lithography" in *Lithography*, ed. By M. Wang, 2010 DOI10.5772/45639
- [6] L. Guo, L. Xu, L. Liu, "Sensitivity enhancement of guided mode resonance sensors under oblique incidence," *Photonics Research* Vol. 12 2327–9125/24/112667–09 Chinese Laser Press, Vol. 12
- [7] Yi Zhou, Bowen Wang, Zhihe Guo, and Xiang Wu, "Guided Mode Resonance Sensors with Optimized Figure of Merit," *Nanomaterials* 2019, 9, 837; doi:10.3390/nano9060837
- [8] L. Qian, K. Wang, 2 D. A. Bykov, 3 Y. Xu, 2 Li Zhu, and C. Yan," Improving the sensitivity of guided-mode resonance sensors under oblique incidence condition," *Optics Express*, Vol. 27, No. 21 / 14 October 2019, doi.org/10.1364/OE.27.030563
- [9] A. Drayton, I. Barth, T. F. Krauss "Guided mode resonances and photonic crystals for biosensing and imaging" In *Semiconductors and Semimetals*, Elsevier, Volume 100, p.115–148, Elsevier.

**Table 1: Influence of 1D-grating material on sensor characteristics at TM polarization**

Grating material	Q-factor			Figure of Merit $\left[\frac{nm}{RIU}\right]$		
	0°	30°	60°	0°	30°	60°
Silicon nitride	0.64x10 <sup>3</sup>	4.7x10 <sup>3</sup>	1.6x10 <sup>4</sup>	5.5x10 <sup>4</sup>	1.3x10 <sup>6</sup>	6.5x10 <sup>6</sup>
PVC	5.6x10 <sup>3</sup>	2.6x10 <sup>4</sup>	4x10 <sup>4</sup>	3x10 <sup>5</sup>	5.8x10 <sup>6</sup>	13.6x10 <sup>6</sup>
CsPbBr <sub>3</sub>	0.55x10 <sup>3</sup>	0.4x10 <sup>4</sup>	1.4x10 <sup>4</sup>	4.8x10 <sup>4</sup>	1.2x10 <sup>6</sup>	5.8x10 <sup>6</sup>

**Polarized object detection in glinted marine environment**

**Dr. Benny Milgrom**

*Jerusalem College of Technology*

**Authors:**

Yosef Golovachev, Benny Milgrom, Roy Avrahamy

**Abstract:**

When observing seawater, specular reflections of light sources, known as glints, can appear as transient bright points. These glints can merge to create a continuous, glittering pathway when viewed from a distance. In detection and observation systems, glints may cause severe saturation in image regions, resulting in blinding glares and observer fatigue, complicating marine remote sensing and target detection. Various mitigation techniques have been developed, but no universally accepted method has emerged. The polarization-based method for glint reduction, proposed long ago, remains a promising candidate for real-time coastal or onboard sensor systems. However, its effects have not been thoroughly reported. Recent numerical progress in studying polarization patterns of sea-reflected radiation motivates further experimental analysis of this method.

This research offers a comprehensive examination of the polarization method's effects on imaging and target detection in modern remote sensing systems. We established a dedicated setup on the Red Sea shore to conduct several experiments. Based on the simulated degree and angle of linear polarization parameters, we selected experimental conditions to match a theoretically optimal vertical polarizer angle. Qualitative discussions, histogram analysis, and additional quantitative evaluation tools demonstrated the beneficial impact of the polarization method on sea imaging and imaging parameters, as well as its effects on imaging other elements. Extensive contrast analysis revealed the method's advantages for object imaging and bright object detection, resulting from improved imaging parameters and image quality (Fig. 1). Additionally, we conducted an operators' survey, which corroborated our findings for human-controlled and observed systems.

This approach can substantially alleviate the challenges posed by glints, leading to more accurate and efficient marine observations and target detections. This advancement represents a significant step forward in the field of optoelectronics for defense applications, offering a promising solution for various oceanographic and remote sensing endeavors.

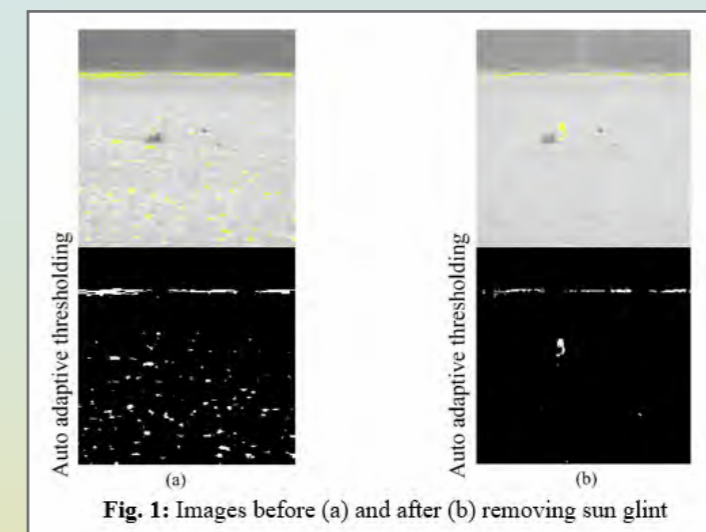


**Fig. 1:** Images before (a) and after (b) removing sun glint

## Virtual Reconstruction of s-SNOM from AFM Results

Mr. Binyamin Kusnetz

Jerusalem College of Technology

### Authors:

Binyamin Kusnetz [1,2], Avi Karsenty [1,2] [1] Advanced Laboratory of Electro-Optics, Jerusalem College of Technology, Jerusalem, Israel [2] Nanotechnology Center for Research & Education, Jerusalem College of Technology, Jerusalem, Israel

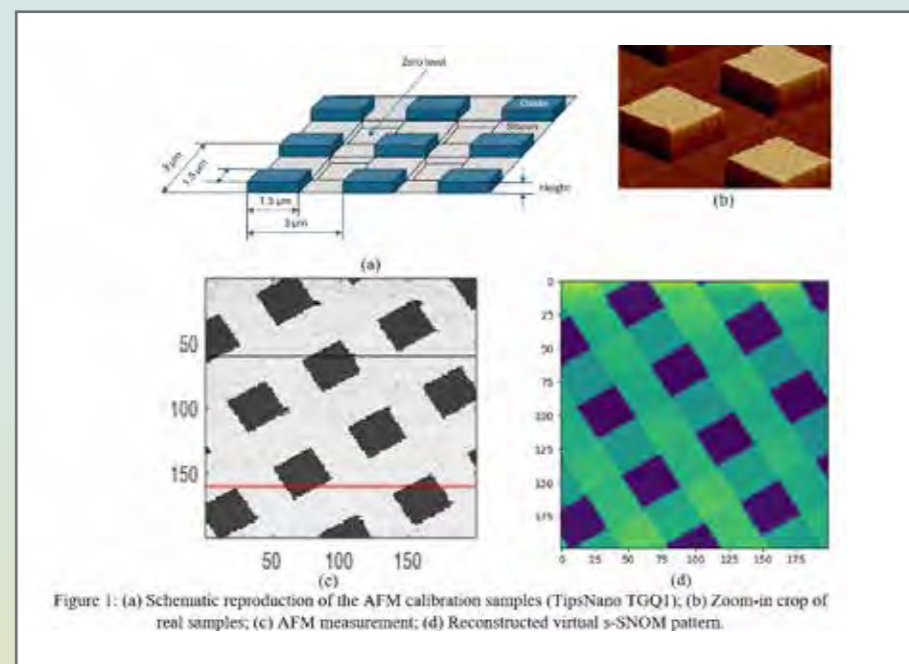
### Abstract:

**Objectives:** In this work, we apply the well-known Point Dipole Model (PDM) for simulating scattering-type scanning near field optical microscopy (s-SNOM) results. In contrast to previous simulation efforts, which employed simple pre-defined shapes, our method was used to replicate experimentally obtained AFM images with complex geometries.

**Methods:** A  $10\ \mu\text{m} \times 10\ \mu\text{m}$  area of a commercial AFM calibration grating was scanned, and the resulting topography values were used as inputs for a simulation model in COMSOL Multiphysics. The research consisted of simulated raster-scanning of the sample and calculating the effective tip-sample polarizability at each sampled point, a quantity proportional to the s-SNOM signal received at the far-field detector.

**Results:** The experimental, analytical and numerical approaches matched well for s-SNOM signals demodulated at the higher AFM tapping frequency harmonics, which are the ones typically selected for analysis.

**Conclusions:** By showing that accurate s-SNOM simulation is possible even for arbitrary, complex samples, this approach can serve as a basis for obtaining s-SNOM results without the need for actual measurements, enabling access to pseudo s-SNOM data for all AFM practitioners worldwide.



## Optical Racetrack Resonator Coupled to a Side Polished Fiber

Mr. Abhishek Singh Rathore

The Hebrew University Of Jerusalem

### Authors:

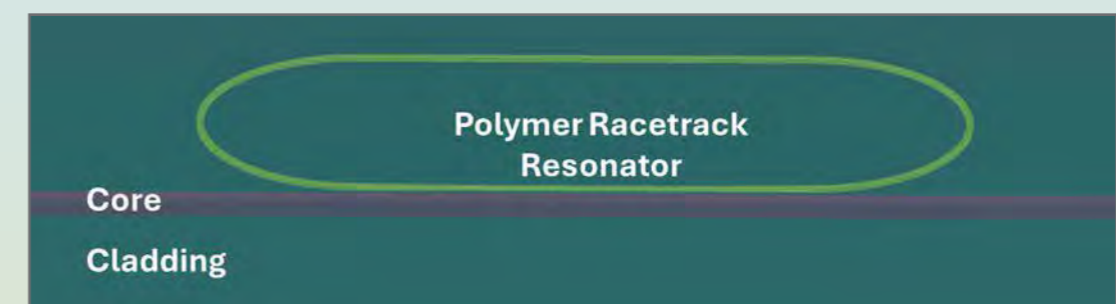
Abhishek Singh Rathore and Prof. Dan M. Marom Institute of Applied Physics, Hebrew University of Jerusalem, Jerusalem, Israel

### Abstract:

Optical fiber sensors provide a robust platform for monitoring the surrounding environment, yet the interaction is indirect as the guided light is shielded by the fiber's cladding layer. The common mechanisms of scattering (Rayleigh and Brillouin) or reflections from written Bragg gratings inside the core are influenced by outside factors as temperature and pressure that extend towards the core, but the signature is weak which necessitates sensitive readout modalities. In contrast, alternative optical sensing schemes (e.g. resonators) offer huge sensitivity, yet require other platforms for their implementation. Here we present their merging, by placement of an optical waveguide resonator directly adjacent to the fiber core, accessed by side polishing the fiber.

Consider the side-polished fiber (also referred to as D-shaped fiber) as an integration platform. Utilizing direct laser write (DLW) structures based on two-photon polymerization, we can write optical waveguides onto the fiber-polished surface and shape them as a racetrack resonator, with one straight segment placed over the core and parallel to it to induce evanescent coupling between them. The transmission spectrum of the fiber, with a resonator coupled at a discrete position, exhibits resonance dips whose sharpness depends on the resonator's quality factor (improves as losses are reduced) and depth on the coupling strength (which should match the losses).

To achieve the desired coupling and low-loss resonator, we meticulously optimized the structures using FDTD simulations to find key design parameters, including the polymer waveguide's height, width, resonator bend radius, coupling gaps, and material properties, under the constraints of the DLW system (feature size and writing range). Simulation results show that the optimized design achieves critical coupling to the low-loss resonator, having a circumference of  $680\ \mu\text{m}$  and resonance dips every  $324.7\ \text{GHz}$ , with a projected Q-factor of  $1.6 \times 10^4$ . This design enables sensing applications that monitor effects registered by the resonator.



## Simple chromatic shearing by PSF engineering

Mr. Ori Cohen

Tel Aviv University

### Authors:

Ori Cohen<sup>1</sup>, Reut Orange-Kedem<sup>1</sup>, Jonathan Jeffet<sup>2</sup>, Nadav Tenenboim<sup>2</sup>, Yuval Ebenstein<sup>2</sup> and Yoav Shechtman<sup>1</sup>

1 Technion – Israel Institute of Technology

2 Tel Aviv University

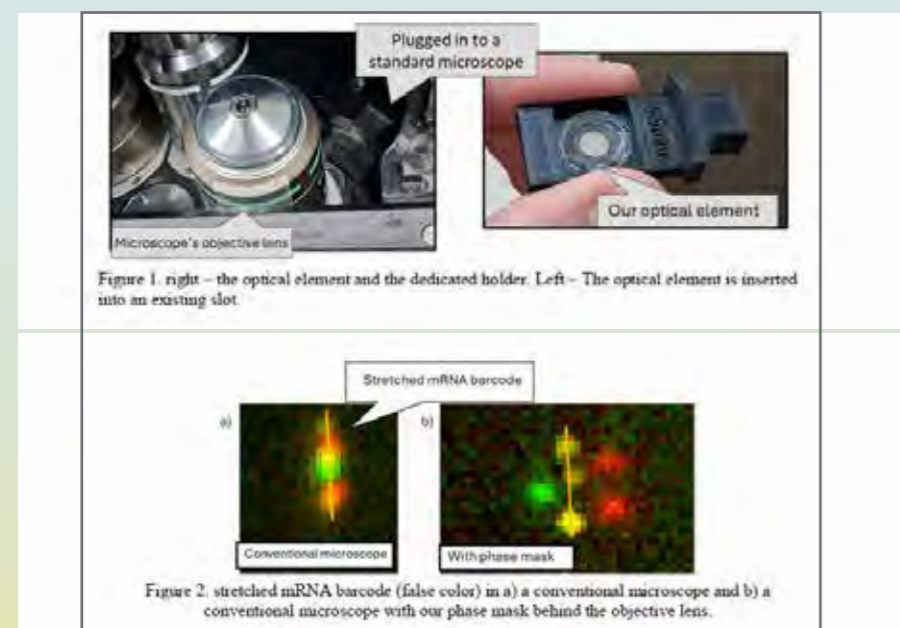
### Abstract:

**Objective:** Many biological imaging tasks take advantage of multi-colored emitters. The spectral axis provides additional useful information about sample composition, labeling, and more. The common techniques for multispectral imaging in microscopy require sequential imaging, multiple cameras along with channel splitting, or spectral splitting of the field of view. This necessitates additional components for channel splitting, decreased throughput for sequential imaging, or compromising the field of view. This project suggests a simple, low-cost implementation of chromatic shearing, for snapshot spectroscopy.

**Methods:** We designed and 3D-printed a blazed grating-based phase mask, based on a near-index-matching concept recently developed in the lab, that shifts the emitted color in the acquired image by a specified amount, as needed. The phase mask is then inserted into a standard microscope using a dedicated holder into an existing slot behind the objective lens (figure 1). Ultimately, by localizing the single emitters and analyzing the shifts, we decode the molecule's color.

**Results:** By using the phase mask in a standard Nikon microscope, an image of a stretched RNA barcode was acquired (fig 2.) and molecules with different colors experienced different shearing. Further image processing techniques can be implemented to determine the emitter's color.

**Conclusions:** The proposed method can provide a simple solution for easily designable chromatic shearing in a microscope, reducing system cost, throughput time and complexity. The 3D printing of the gratingbased phase mask can provide flexibility, resulting in a robust method for spectral separation.



## Spectroscopy and optical sensing

Mr. Saar Shaek

Department of Materials Science and Engineering, Technion, and The Solid-state institute, Technion – Israel Institute of Technology

### Authors:

Saar Shaek<sup>1,2</sup>, Boaz Pokroy<sup>1</sup>, Ivano E. Castelli<sup>3</sup>, Yehonadav Bekenstein<sup>1,2</sup>

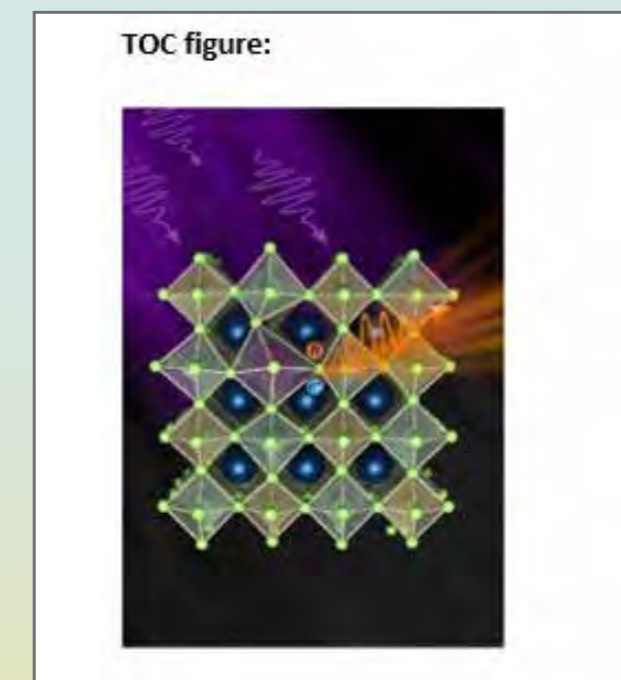
1 Department of Materials Science and Engineering, Technion, Israel Institute of Technology, 32000 Haifa, Israel

2 The Solid-state institute, Technion – Israel Institute of Technology, 32000 Haifa, Israel

3 Department of Energy Conversion and Storage (DTU Energy), Technical University of Denmark, Anker Engeldunds Vej 301, 2800 Kongens Lyngby, Denmark

### Abstract:

Lead-free perovskite nanocrystals are of interest due to their nontoxicity and potential application in the display industry. However, engineering their optical properties is nontrivial and demands an understanding of emission from both self-trapped and free excitons. Here, we focus on tuning silver-based double perovskite nanocrystals' optical properties via two iso-valent dopants, Bi and Sb. The photoluminescence quantum yield of the intrinsic Cs<sub>2</sub>Ag<sub>1-y</sub>NayInCl<sub>6</sub> perovskite increases dramatically upon doping. However, the two dopants affect the optical properties very differently. We hypothesize that the differences arise from their differences in electronic level contributions and ionic sizes. This hypothesis is validated through absorption and temperature dependence photoluminescence measurements, namely by employing the Haug-Rhys factor, which indicates the coupling of the exciton to the lattice environment. Synchrotron measurements reveal the microstaining different effects of the two sizes of dopants, demonstrating that the octahedral tilting is larger in the case of Bi due to its size. These differences make Sb more sensitive to doping concentration (optimum ~10%) and sodium allowing (optimum ~100%). Such understanding is important for the engineering of optical properties in double perovskite, especially in light of recent achievements in boosting the photoluminescence quantum yield.





## QUANTUM COMPUTERS SESSION

### Oral presentations Abstracts:

#### Hybrid quantum annealing algorithms for combinatorial optimization with Rydberg qubits

**Dr. Adi Pick**

*The Hebrew University Of Jerusalem*

##### Authors:

Adi Pick, Hebrew University, Jerusalem, Israel; Guy Karni, Hebrew University, Jerusalem, Israel; Noam Cohen, Hebrew University, Jerusalem, Israel

##### Abstract:

Following breakthroughs in quantum simulation, optimization, and error correction, current efforts focus on scaling quantum computers to tackle computationally challenging and practical problems. Hybrid algorithms, combining classical and quantum computing, offer a promising path forward. This talk will present two novel hybrid algorithms for the Maximum Independent Set (MIS) problem, using adiabatic quantum annealing with neutral atoms. The first algorithm implements an efficient shortcut to adiabaticity to address the slowing of traditional adiabatic algorithms as problem size increases. The second leverages Luby's classical parallel algorithm to enhance adiabatic MIS solutions. In both algorithms, there exists a tradeoff between the classical computation effort required to engineer the Hamiltonian and the quantum simulation time required to carry out the annealing process. Our calculations reveal strategies to divide time between classical and quantum computing to achieve top performance, based on the technology available. We run numerical simulations of our algorithms on systems with fewer than 15 qubits and analyze their complexity for larger systems using analytical methods. Our algorithms can run on cloud-available quantum annealers (e.g., QuEra or DWAVE platforms).

#### Quantum Error Correction with Adiabatic Quantum Computation

**Mr. Chen Scheim**

*The Hebrew University of Jerusalem*

##### Authors:

Chen Scheim, Applied Physics, Hebrew University of Jerusalem, Jerusalem, Israel. Adi Pick, Applied Physics, Hebrew University of Jerusalem, Jerusalem, Israel

##### Abstract:

One of the main reasons why a quantum computer is not yet a commercially available product is computational errors caused by noise. Methods for addressing such errors can be divided into two approaches: developing noise-resistant computation protocols, such as adiabatic quantum computation (AQC), and error correction techniques (such as stabilizer-based quantum error correction codes), assuming errors have occurred. In this work, we combine both approaches and propose a method for correcting errors that occur during adiabatic computation. We focus on two error correction protocols: the 4-qubit code by Jordan et al. and the repetition code. In both types of encoding, multiple physical qubits are used to encode a logical qubit in a subspace protected from errors. Error protection is achieved by ensuring that noise-induced errors take the system out of the logical subspace. In both protocols, the Hamiltonian required to encode in the logical subspace contains non-local interactions. To implement such a Hamiltonian on existing computational platforms, we engineer an effective Hamiltonian, using a common tool for AQC called perturbative gadgets. The effective Hamiltonian is constructed with only two-body interaction terms that approximately simulates the logical non-local Hamiltonian. We numerically demonstrate an adiabatic protocol in an error-protected space that performs a Rapid Adiabatic Passage (RAP). To this end, we simulated the dynamics of 15 qubits (effective space for 4-qubit code effective Hamiltonian) to achieve an adiabatic protocol for a single logical qubit. Our calculations allow us to predict the required parameters (intensities and frequencies of controlling lasers and interactions between qubits) to overcome errors and how these parameters depend on different noise processes and noise intensities. After numerically validating the results, we plan to run our protocols on cloud-based AQC platforms.



## Tomography of Hyperentangled Single Photon States with a Single Measurement Setup

Mr. Roey Shafran

*Technion – Israel Institute of Technology, Haifa, Israel*

### Authors:

Roey Shafran, Ron Ziv, Mordechai Segev

### Abstract:

The full quantum state tomography of a single-photon hyperentangled state, entangled between its multiple degrees of freedom (DoF), is a tedious procedure requiring the realization of different measurements and setup configurations. Moreover, as the state dimension increases, full tomography is often impractical due to scaling of the different measurements required for full characterization.

Motivated by the above, we introduce a new method for reconstructing the density matrix of a single photon state using only a single intensity measurement. We propose a system that couples the photonic DoFs to higher order spatial DoF, using them as ancillas to spatially encode the state's information, allowing for a single intensity image to contain the full state information, even for DoFs a traditional camera is blind to such as polarization.

We show how the photon density matrix can be recovered by solving a simple convex optimization problem and present theoretical requirements for a successful reconstruction. Additionally, we present two physical realizations for a coupling system to recover photon states entangled between their orbital angular momentum (OAM) and polarization, and OAM and a set of discrete frequency bins. We numerically showcase how the intrinsic coupling between spatial and polarization modes inside a multimode fiber (MMF) allows for reconstructing OAM-polarization modes, and how harnessing the cross-phase modulation effect inside a MMF allows for reconstructing OAM-frequency states. We show how these coupling systems can be modeled as a linear process thus allowing an efficient computational forward process reducing computational requirements in solving the inverse optimization problem.

Our method greatly simplifies the measurement of single-photon hyperentangled states, requiring a single setup configuration and a single intensity measurement, and has potential applications in quantum communication. Furthermore, this framework easily extends to states entangled between more than two DoFs, such as OAM-polarization-frequency.

## E posters Abstracts:

### Hybrid adiabatic algorithms for solving combinatorial optimization problems

Mr. Guy Karni

*Hebrew University of Jerusalem*

### Authors:

Adi Pick-HUJI-Jerusalem-Israel, Guy Karni-HUJI-Jerusalem-Israel, Noam Cohen-HUJI-Jerusalem-Israel

### Abstract:

Adiabatic quantum computation slows down for large problems as the energy gap decreases with problem size. If the gap shrinks too quickly, quantum computation offers no advantage. To address this, we use classical computational resources to identify Hamiltonians with better scaling, and then apply quantum computation to solve the problem. In this poster, we present two algorithms for maximum independent set (MIS) – a prototypical combinatorial optimization graph problem.

The first algorithm uses a shortcut-to-adiabaticity approach to accelerate existing adiabatic algorithms [3,4]. It is based on introducing “counter-diabatic” (CD) controls, which oppose diabatic errors [5]. As a result, the dynamics follows exactly the ground state of the original Hamiltonian for any protocol duration. The challenge lies in the significant classical computational effort required to determine the CD term. To address this issue, one can approximate the CD term using the Lanczos algorithm [1,2]. We construct an approximate CD Hamiltonian for solving MIS. We simulate intermediate-scale systems and derive analytic bounds on the complexity in the large-system size limit.

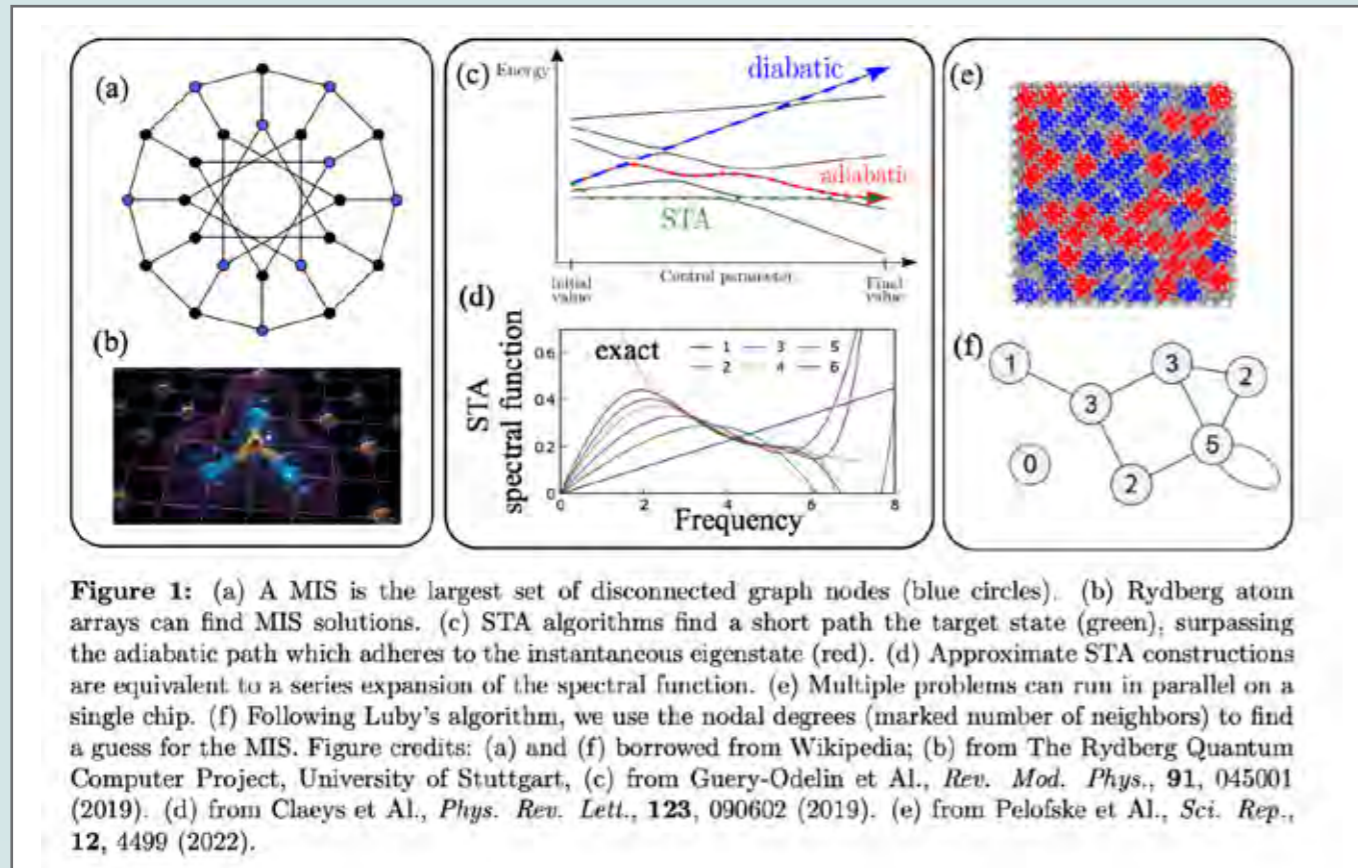
The second algorithm is a quantum analog of the classical parallel Luby algorithm [6], which efficiently identifies a MIS by iteratively selecting and removing nodes in a probabilistic manner based on their degree. We take inspiration from Luby's algorithm to generate an initial state, which is statistically closer to the solution. To have the required flexibility to prepare the initial state, we use three-level atoms containing a ground-, intermediate-, and a Rydberg state. The initial guess is prepared as a superposition of the ground and intermediate states, with superposition coefficients determined by the nodal degree. The Rydberg state is only utilized in a later stage of the algorithm, where its interactions become critical for finding the MIS. Simulation results have shown this solution improves minimum energy gaps, enabling more efficient computation.

### References:

- [1] Takahashi, Kazutaka, and Adolfo del Campo. “Shortcuts to adiabaticity in Krylov space.” *Physical Review X* 14.1 (2024): 011032.
- [2] Bhattacharjee, Budhaditya. “A Lanczos approach to the adiabatic gauge potential.” *arXiv preprint arXiv:2302.07228* (2023).
- [3] Pichler, Hannes, et al. “Quantum optimization for maximum independent set using Rydberg atom arrays.” *arXiv preprint arXiv:1808.10816* (2018).
- [4] Ebadi, Seppehr, et al. “Quantum optimization of maximum independent set using Rydberg atom arrays.” *Science* 376.6598 (2022): 1209–1215.



- [5] Berry, Michael Victor. "Transitionless quantum driving." *Journal of Physics A: Mathematical and Theoretical* 42.36 (2009): 365303.
- [6] Luby, Michael. "A simple parallel algorithm for the maximal independent set problem." *Proceedings of the seventeenth annual ACM symposium on Theory of computing*. 1985.



# PROLOG optics

PROLOG OPTICS - FOCUSED ON EXCELLENCE





## OPTICS IN MEDICINE AND BIOLOGY SESSION

### Oral Presentation Abstracts:

#### All-Optical Approach to Ultrasound Transmission Matrix Measurement

**Mr. Ron Moisseev**

*Technion – Israel Institute of Technology*

#### Authors:

Ron Moisseev and Amir Rosenthal, Technion – Israel Institute of Technology, Haifa, Israel

#### Abstract:

The acoustic characterization of objects using piezoelectric ultrasound transducers is limited by their size, bandwidth, and angular response. To address these limitations, this study proposes a modular all-optical platform that enables wideband operation (>50 MHz), omnidirectional sensitivity, and high signal fidelity. Ultrasound is generated via the optoacoustic effect by illuminating an optically absorbing coating with spatially modulated pulsed light, while detection utilizes a silicon-photonics acoustic detector. By employing basis-spanning illumination patterns and scanning the detector, the platform measures the full transmission matrix—capturing acoustic waveforms for all transmitter–receiver pairs in the setup—with an enhanced signal-to-noise ratio. Experimental validation in transmission mode confirmed its capabilities for beam steering, beam focusing, and imaging, yielding results in excellent agreement with theoretical models.

#### Large-field-of-view optical-resolution optoacoustic microscopy using silicon photonics acoustic detector

**Mrs. Tamar Harary**

*Technion\Electrical engineering\ Laboratory for Biomedical Imaging and Sensing*

#### Authors:

Tamar Harary<sup>1</sup>, Michael Nagli<sup>1</sup>, Nathan Suleymanov<sup>1</sup>, Ilya Goykhman<sup>1</sup> and Amir Rosenthal<sup>1</sup>

<sup>1</sup> Andrew and Erna Viterbi Faculty of Electrical & Computer Engineering, Technion – Israel Institute of Technology, Technion City, Haifa, 32000, Israel

#### Abstract:

**Significance:** Optical-resolution optoacoustic microscopy (OR-OAM) enables label-free imaging of microvasculature by leveraging optical pulse excitation and subsequent acoustic wave detection. This process typically employs a focused optical beam and ultrasound transducer, necessitating a coaxial configuration where the optical and acoustic paths are aligned. However, this setup often leads to a bulky setup that requires physically scanning the ultrasound transducer to achieve a large field of view (FOV).

**Aim:** The aim of this work is to develop a novel OR-OAM configuration that circumvents the need for physically scanning the ultrasound transducer or the acoustic beam path.

**Approach:** Our system adopts a non-coaxial configuration, utilizing a silicon photonics acoustic detector (SPADE) featuring semi-isotropic sensitivity. SPADE, based on a micro-ring resonator, fabricated in silicon nitride with a 30  $\mu\text{m}$  diameter, provides a bandwidth of 120 MHz and a noise-equivalent pressure of 7 mPa/ $\sqrt{\text{Hz}}$ , enabling detection from multiple directions and facilitating static detection during imaging. This innovative setup allows the optical beam alone to be scanned across the sample.

The system functions in both epi-illumination and trans-illumination configurations. In epi-illumination, SPADE and the optical elements are co-located on the same side of the sample, while in trans-illumination, they are positioned on opposite sides. In both setups, SPADE remains stationary throughout the imaging process, with only the optical excitation beam being scanned.

**Results:** The system demonstrated its capabilities through imaging resolution targets and in vivo visualization of microvasculature in a mouse ear. Optoacoustic imaging achieved focal spot sizes as small as 1.3  $\mu\text{m}$ , a lateral resolution of 4  $\mu\text{m}$ , and a field of view exceeding 4 mm in both lateral dimensions.

**Conclusion:** Our new OR-OAM design enables relatively large fields of view without scanning the acoustic detector or acoustic beam path. Furthermore, it offers the potential for high-speed imaging within compact, miniature probe and could potentially facilitate the clinical translation of OR-OAM technology.



## Novel Ablative Tm :YAP Pulsed Laser for Dermatology Applications

**Prof. Salman Noach**

*Jerusalem College of Technology*

### Authors:

Rotem Nahear, Neria Suliman, David J Friedman, Salman Noach

### Abstract:

Dermatological lasers are broadly classified as ablative or non-ablative, with tissue absorbance being a key consideration. The primary target in the Infrared (IR) spectrum is water, owing to its high absorption and its high concentration in tissues. Ablative lasers at 10 and 3  $\mu\text{m}$ , CO<sub>2</sub> and Er:YAG lasers, respectively, leverage this characteristic effectively.

Conversely, non-ablative lasers at 1.5–2  $\mu\text{m}$  primarily coagulate tissues without achieving the ablation threshold. Thulium lasers are positioned around a local peak of water absorption at 1.94  $\mu\text{m}$ , and exhibits approximately six times lower absorption than CO<sub>2</sub> (10.6  $\mu\text{m}$ ) and significantly higher absorption than the 1.5  $\mu\text{m}$  wavelength. They are employed as more superficial non-ablative lasers but not achieving the ablation threshold.

This study presents the first ablative Tm:YAP laser at 1.94  $\mu\text{m}$ . Employing high-energy, passively Q-switched pulses, the nanosecond pulse duration enables a lower ablation threshold by minimizing heat transfer to surrounding tissues. The intermediate absorption characteristics at 1.94  $\mu\text{m}$  ensure the laser surpasses the lowered ablation threshold successfully.

Experimental demonstrations on porcine skin using a fractional method showcased the creation of clean ablation micro-cavities. Micro-cavities with a remarkable thinness of up to 60 micrometers was demonstrated. Deep penetration of up to 2 mm was also observed.

The 1.94  $\mu\text{m}$  Tm:YAP laser, as an innovative addition to the arsenal of ablative lasers, has the potential to revolutionize dermatological practices, providing a safe and reliable solution for diverse skin ailments. Further refinement and development could open new avenues for enhancing patient care in dermatology.

## Label-free imaging flow cytometry using a motion sensitive camera for rare cell detection

**Ms. Eden Dotan**

*Tel Aviv University*

### Authors:

Eden Dotan, Itay Barnea, Dana Aharoni, Natan T. Shaked  
Department of Biomedical Engineering, Tel Aviv University, Tel Aviv, Israel

### Abstract:

**Objective:** This research integrates an event-based vision sensor (EVS) into a flow cytometry system to enhance cellular analysis. The system reconstructs intensity information and optical path delay (OPD) maps of flowing microparticles, enabling rapid detection of rare cells like circulating tumor cells in blood.

The key objectives include leveraging EVS for high-speed data acquisition, employing a flipping interferometer for label-free refractive index (RI) measurements, and advancing diagnostics and therapeutic development.

**Methods:** Integration of the event-based vision sensor with a flipping interferometer and a microfluidic system was conducted to enable high-speed, label-free cellular analysis. The EVS detects luminance changes asynchronously, outputting differential data for efficient processing. The CMOS camera records off-axis interferograms for OPD reconstruction, triggered by EVs.

Calibration was conducted to align data from the EVS and CMOS cameras, ensuring precise correlation between the two systems. This integration leverages the strengths of event-based detection and holographic imaging to enable rapid and accurate cellular analysis.

**Results:** Asynchronous data acquisition reduced processing time compared to frame-based methods. Hologram data grading enhanced precision, enabling accurate and sensitive detection of CTCs in blood samples.

**Conclusions:** This study demonstrates a high-speed system for reconstructing intensity and OPD maps of flowing cells. By integrating EVS with interferometric phase microscopy, the approach enables label-free, efficient detection of rare cells, advancing disease diagnostics and therapeutic development.

## Multi-Color Super-Resolution Imaging Using Spectral Confocal Spinning Disk Image Scanning Microscopy

Mr. Jonathan Jeffet

*School of Physics and Astronomy, Tel Aviv University*

### Authors:

Lanna Bram, Eli Flaxer, Yael Roichman, Yuval Ebenstein  
Tel Aviv University, Tel Aviv, Israel

### Abstract:

**Objectives:** This study aimed to extend confocal spinning disk-image scanning microscopy (CSD-ISM) capabilities by introducing a novel method to encode and resolve spectral information with improved temporal resolution. Our objective was to develop a system capable of achieving super-resolution imaging, doubling the optical diffraction-limited resolution, while simultaneously resolving multiple fluorescence colors in a single acquisition.

**Methods:** Using a custom-built, low-cost, open-source hardware synchronization chip, we converted a commercial CSD into CSD-ISM. To achieve spectral multiplexing, we designed and integrated a custom amici prism with linear dispersion into the emission path of the CSD setup. This modification allowed spectral information to be encoded as spatial translations on the camera chip for each point-spread-function of the confocal disk. The encoded data was computationally processed to differentiate multiple fluorophores in a single acquisition. Validation was conducted using multi-color fluorescent beads and four-color labeled biological cell samples, with imaging parameters optimized for accuracy and resolution.

**Results:** The modified system demonstrated robust performance, achieving precise spectral multiplexing and super-resolution imaging. Multi-color fluorescent beads were resolved with double the optical resolution of traditional CSD. In four-color labeled cell samples, distinct fluorophores were simultaneously visualized, revealing sub-cellular structures with enhanced resolution and spectral discrimination. Furthermore, our method significantly reduced acquisition time compared to conventional filter-based multi-color CSD-ISM approaches, allowing improved temporal resolution for dynamic imaging applications.

**Conclusions:** This innovative extension of CSD-ISM with a custom amici prism represents a major advancement in super-resolution microscopy. It enables efficient, high-throughput multi-color imaging with enhanced spatial and spectral resolution, offering a versatile tool for applications in cell biology, molecular imaging, and other fields requiring detailed nanoscale visualization.

## Advanced Optical Analysis of Focal-Point Divergence Between Surgical Neodymium-Doped Yttrium Aluminum Garnet (Nd:YAG) and Aiming-Beam Lasers

Mr. Ya'akov Mandelbaum

*Jerusalem College of Technology (JCT) – Lev Academic Center*

### Authors:

Averbukh, Edward, Hadassah University Medical Center, Hebrew University, Jerusalem, Israel; Slushetz, Yaakov, Jerusalem College of Technology–Lev AC, Jerusalem, Israel; Levy, Jaime, Hadassah University Medical Center, Hebrew University, Jerusalem, Israel; Patal, Rani, Hadassah University Medical Center, Hebrew University, Jerusalem, Israel; Mandelbaum, Yaakov, Jerusalem College of Technology–Lev AC, Jerusalem, Israel; Arieli, Yoel, Jerusalem College of Technology–Lev AC, Jerusalem, Israel

Ophthalmology Science

Volume 4, Issue 5, September–October 2024, 100512

[//doi.org/10.1016/j.xops.2024.100512](https://doi.org/10.1016/j.xops.2024.100512)

### Abstract:

**Background:** The 1064 nm Nd:YAG laser that is routinely used in ophthalmology for intraocular surgery is in fact invisible. Typically, a pair of intersecting auxiliary diode-lasers with a visible wavelength of 635 nm, are used for aiming. Ideally their intersection coincides with the waist of the Nd:YAG laser. However, due to dispersion in the ocular tissue – and in the high-power diverging lens placed adjacent to the eye – the differing wavelengths result in progressive deviation between the two focal points. This problem becomes especially significant for posterior segment laser treatments, threatening the success rate and the safety.

**Objectives:** This work set out to evaluate the divergence between the surgical laser and the aiming diode laser beams foci.

**Methods:** Hospital and laboratory studies were performed to characterize the Nidek – YC–1800 Nd:YAG laser apparatus together with the Volk–Goldman Goniofundus lens. A computerized ray-tracing model was then created to simulate optics in the eye and assess the difference between the focal points of the two beams. Analysis of ocular (sphero-)chromatic aberration was key. A calibration calculator was developed for the surgeons' use which computes the focal deviation in each region interior to the eye.

The aforementioned lens's high negative optical power, poses a challenge for common laboratory equipment and commercial devices. A novel method was developed to directly measure the focal length of a highly negative lens; it simultaneously renders the index of refraction.

**Results:** Focal points of the two laser beams converge 8 mm behind the cornea. Posterior to this point, the intersection of the diode laser aiming beams lies in front of the focal point of the Nd:YAG treatment laser, with distance between the 2 foci progressively increasing up to 305 microns at 24 mm behind the cornea.

**Conclusions:** To our knowledge this is the first study evaluating the deviation between the target predicted by the guidance beams and the actual focus of the surgical Nd:YAG laser due to chromatic

aberration of ocular tissue. These results can be immediately applied in clinical practice to increasing the accuracy and safety of Nd:YAG laser treatment, particularly in the posterior segment.

//ars.els-cdn.com/content/image/1-s2.0-S2666914524000484-mmc1.pdf

Y. Slushtetz, R. Patal, Y. Arieli, Y.M. Mandelbaum

yaaqovm/Advanced-Optical-Analysis-of-Divergence-Between-the-Foci-of-the-Nd-YAG-and-Aiming-Beam-Laser: Additional Material

Zenodo (2024), 10.5281/zenodo.10832421



## Planar objective design for multiphoton mouse brain imaging

**Dr. David Sinefeld**

*Jerusalem College of Technology*

### Authors:

Jacob Engelberg, Jonathan Weissfisch, Eliran Cohen, David Sinefeld

Dept. of Applied Physics & Electro-optical Eng., Jerusalem College of Technology, 21 Havaad Haleumi St., Jerusalem, Israel 9103501 \*sinefeld@gmail.com

### Abstract:

**Objective:** Achieving sub-cellular imaging of the entire mouse brain is a pivotal challenge in modern neuroscience, as it holds the potential to revolutionize our understanding of neural circuits and their spatiotemporal activity patterns. Current deep-tissue imaging techniques, such as two-photon microscopy (2PM) and three-photon microscopy (3PM), offer high-resolution imaging capabilities. While 2PM excels at imaging superficial brain layers, 3PM allows for deeper imaging with reduced background noise. However, both methods require large, bulky microscope objectives that hinder in-vivo imaging in freely moving animals, limiting behavioral research. Our objective is to overcome this limitation.

**Methods:** This paper proposes a novel imaging system that replaces the traditional high-NA objective with a lightweight, compact metalens plate serving as a planar cranial window. The system leverages a metalens doublet design to achieve high numerical aperture (NA 0.6) and a 0.5 mm field of view, enabling high-resolution imaging with a simplified setup. The metalens concept integrates metasurfaces for aberration correction and allows multi-diffraction order operation, which is particularly beneficial for 2PM using second harmonic generation.

**Results:** The results demonstrate that the primary challenge in designing a planar objective is addressing chromatic aberration caused by the short-pulsed laser's spectral width. The proposed solution involves a hybrid lens element that combines a negative metalens with a ZnSe plano-convex lens, introducing pre-compensation for chromatic aberration without increasing the system's size. The imaging system includes a remote focusing scheme, with lateral scanning achieved through mirrors and axial scanning using a Z-scanning system. To further minimize chromatic aberration, an afocal relay system is used to image the corrector on the objective.

**Conclusions:** The final system achieves near-diffraction-limited performance over a 0.5 mm field of view. This innovative approach promises to facilitate large-scale brain imaging in freely moving animals, providing valuable insights into neural mechanisms and advancing neuroscience research.



**E posters Abstracts:****Adaptive segmentation of DAPI-stained, C-banded, aggregated and overlapping chromosomes for the Dicentric Chromosome Assay****Dr. Max Platkov***NRCN***Authors:**

Max Platkov, Ziv J. Gardos, Lena Gurevich, Inna Levitsky, Ariela Burg, Shirly Amar, Aryeh Weiss, Raphael Gonen

**Abstract:**

Condensed, C-banded and DAPI stained chromosomes and centromeres are a new contrast mechanism for utilization in the Dicentric Chromosome Assay (DCA). C-banding brightens centromeres vs. the rest of the chromosome, yielding a better signal-to-noise. This calls for a redesign on the common DCA image processing algorithms, especially when applied in mass radiological events.

DAPI & C-Banding-stained centromeres on chromosomes were imaged through an epifluorescent microscope. Matlab and ImageJ were used for algorithm coding and analysis.

Our algorithms are adaptable: To perform an operation, e.g. enhancement, object separation etc. the best algorithm among several options is automatically chosen based on predefined figures of merit. Each algorithm is also automatically optimized by relying on a binary search to deliver Results: a filter/procedure parameter is repeatedly changed via binary search to optimize a feature in the image to comply with some threshold.

The algorithms separate mildly or moderately aggregated chromosomal clusters. The clusters are segmented by skeleton junctions, by narrowing of the overall object thickness and the watershed algorithm. The chromosomes are characterized by rules on geometrical shapes and vector directions of their skeletons, using minimal assumptions. Centromeres are detected by quantifying bright spots on the surface of the chromosomes, selecting which to analyze via cluster analysis and setting rules on their shape and intensity profiles.

High sensitivity and specificity for chromosome and centromere detection were achieved with the algorithms presented here. These algorithms, when used in future DCA-analysis software packages, will improve reliability and accuracy.

**Label-free 3D refractive-index mapping of freely swimming human sperm cells****Ms. Lydia Sokolovski***Department of Biomedical Engineering, Tel Aviv University, Tel Aviv, Israel***Authors:**

Lydia Sokolovski Tel Aviv Univ. (Tel Aviv, Israel), Itay Barnea Tel Aviv Univ. (Tel Aviv, Israel), Natan T. Shaked Tel Aviv Univ. (Tel Aviv, Israel)

**Abstract:**

**Objectives:** This study aims to develop and demonstrate a method for refractive index (RI) mapping of freely swimming human sperm cells by combining rapid tomographic phase microscopy with fluorescence imaging. A key objective is to decouple the refractive index and thickness of sperm cells using digital holographic microscopy in two different mediums. We offer detailed, label-free visualization of sperm morphology and movement, with potential applications in improving sperm selection during intracytoplasmic sperm injection (ICSI).

**Methods:** Sperm cells were first imaged using shearing interferometry in two mediums: phosphate-buffered saline (PBS) and air. Fixated sperm cells were analyzed to produce 2D phase images, which were used to calculate the RI of the sperm head, focusing on the nucleus and acrosome. To precisely delineate the nucleus and acrosome boundaries, fluorescence staining with Hoechst dye was employed. Fluorescence images were registered with the phase images, enabling accurate segmentation of the nucleus and subsequent RI mapping.

**Results:** The RI mapping revealed distinct values for the nucleus and acrosome within the sperm head enabling to distinguish between the different organelles of the sperm head.

**Conclusions:** The combination of quantitative phase interferometry and fluorescence imaging provides a powerful tool for label-free RI mapping of human sperm cells. This technique enables detailed visualization and analysis of sperm morphology and biophysical properties, which could significantly improve the sperm selection process in ICSI procedures. Future work will focus on extending this method to live, freely swimming sperm cells, further advancing its applicability in clinical and research settings.

## Yellow LASER (577nm) for Diabetic Retinopathy Treatment

Dr. Irit Juwiler

Shamoon College of Engineering

### Authors:

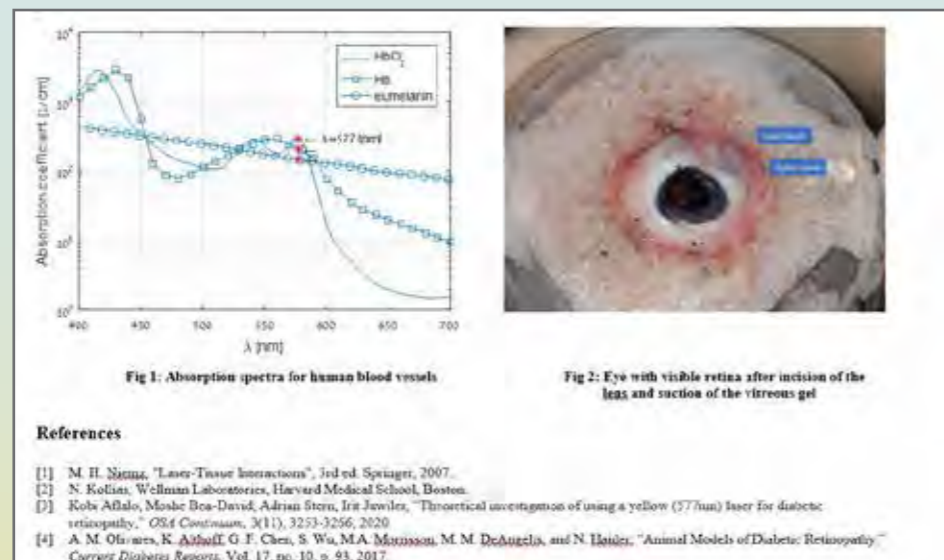
Moshe Ben-David, Shlomit Bar Kochva, Evyatar Mesika, and Irit Juwiler\*

Center for E.O, Development of LASER Technologies and their Applications, Shamoon College of Engineering, Ashdod 77245, Israel

### Abstract:

LASER radiation is widely used for eye surgery. The type of LASER wavelength and operation mode depends on the ophthalmic procedure. For example, vision correction uses ultra-short-pulsed LASERs, usually in the UV, while longer pulses (msec) and wavelength (near IR) are used for leaky blood vessel sealing. Diabetic retinopathy is a chronic metabolic disease in the blood vessels; some forms inside the retina, while most are in the choroid. To treat non-proliferative diabetic retinopathy, a procedure called pan-retinal photocoagulation (PRP) is needed. During the treatment, the damaged blood vessels are coagulated using a laser. Coagulation is achieved at about 60–70 [°C] [1]. Heating the tissue to the desired temperature range is done by a laser with high absorption at those tissues. To heat only the blood vessels and minimize the damage to the surrounding tissue, we choose a laser wavelength with a high absorption coefficient in blood vessels (hemoglobin as blood and melanin as vascular walls). We found that peak absorption occurs at 577 [nm]. The spectra of the blood are shown in Fig 1, and it is clear that there is a peak absorption in this specific wavelength [2].

In a previous paper [3], we examined theoretically the possibility of using a yellow wavelength (577 [nm]) laser for diabetic retinopathy eye surgery procedures and its advantages over the conventional green laser (532 [nm]). The main advantage of this wavelength is higher absorption in hemoglobin, which enables lower LASER power usage. This paper compares the theoretical results [3] to experimental results obtained with a yellow laser. Recent findings [4] show that pigs have vasculature and retinal structures similar to those of humans. Therefore, they can be used as a relatively decent model for DR under laser radiation, even though they lack some pathophysiology of neuronal and vascular changes at each stage of DR. Preliminary results show that using a yellow laser (577 [nm]) with a power of 50 [mW], a beam diameter of 500 [ $\mu$ m], and a pulse duration of 150 [msec] with a treatment time of 30 seconds, photocoagulation can be achieved. Due to the heat diffusion and using more than one pulse, the laser burn was measured to be  $1\pm 0.01$  [mm], see Fig.2.



## Q-sensing Method For Superficial Scattering Extraction

Mr. Alon Tzroya

Bar-Ilan university

### Authors:

Alon Tzroya, Hamootal Duadi, Dror Fixler

Faculty of Engineering and the Institute of Nanotechnology and Advanced Materials, Bar Ilan University, Israel

### Abstract:

**Objectives/Introduction:** Understanding the interaction between light and biological tissues is critical for advancing medical imaging and diagnostics. These interactions are governed by the tissue's optical properties, including scattering and absorption. However, conventional methods often face challenges in distinguishing the contributions from superficial and deeper tissue layers, which complicates accurate analysis. To overcome this limitation, our research utilizes the Q-Sensing Technique to harness light polarization, enabling differentiation between ballistic and scattered photons. By measuring co-polarized ( $I_{\parallel}$ ) and cross-polarized ( $I_{\perp}$ ) signals, we can probe tissue layers. The rapid depolarization of light caused by the complex structure of tissues highlights the importance of identifying depolarization locations, which can aid in detecting abnormalities.

**Methods:** To achieve this, we employ tissue-mimicking phantoms with varying thicknesses to replicate the optical properties of biological tissues and measure depolarization effects. The experimental results are further validated using Monte Carlo simulations, which model the behavior of polarized light in polydisperse (varying particle size) media, offering theoretical insights.

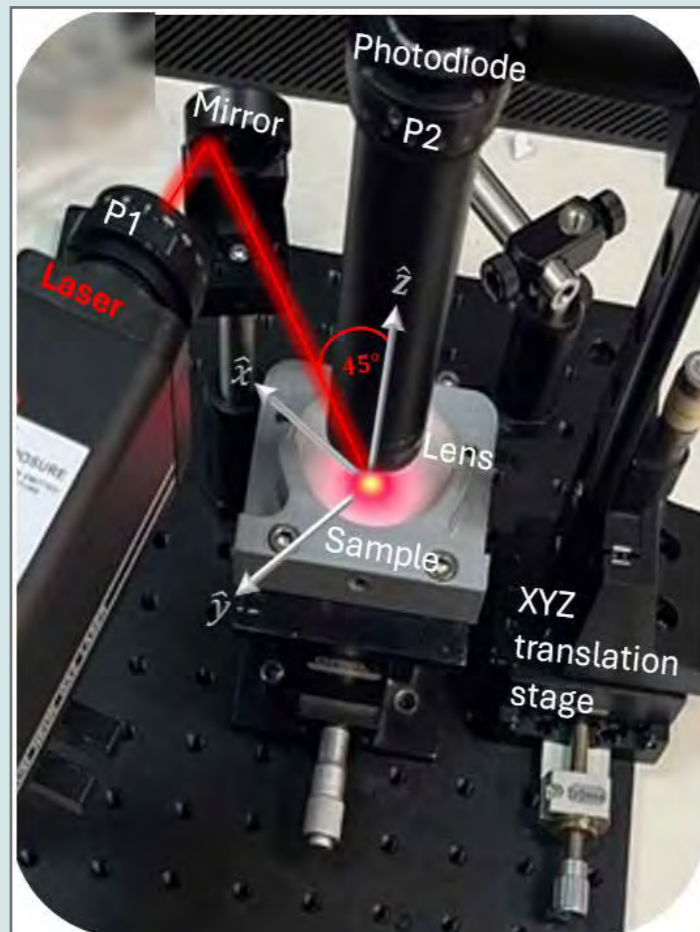
**Results:** Our results demonstrate that polarized light effectively distinguishes tissue layers based on thickness. The findings reveal the depth of superficial scattering, and the transition point where reflected photons originate solely from deeper layers. Phantoms with specific optical properties show sensitivity to changes up to 2 mm deep, while others are limited to 0.8 mm. Additionally, the technique enables the extraction of optical properties from both phantoms and biological tissues.

**Conclusions:** This research provides valuable insights into light-tissue interactions and establishes polarized light as a powerful tool for studying tissue structure and its optical properties. The ability to detect and analyze abnormalities based on polarization changes holds significant potential for improving diagnostic techniques in medical applications.

### References:

- Jacques, S.L., J.C. Ramella-Roman, and K. Lee, Imaging skin pathology with polarized light. *Journal of biomedical optics*, 2002. 7(3): p. 329-340.
- Fixler, D., et al., Depolarization of light in biological tissues. *Optics and Lasers in Engineering*, 2012. 50(6): p. 850-854.
- Jacques, S.L., J.R. Roman, and K. Lee, Imaging superficial tissues with polarized light. *Lasers in Surgery and Medicine: The Official Journal of the American Society for Laser Medicine and Surgery*, 2000. 26(2): p. 119-129.
- Tzroya, A., H. Duadi, and D. Fixler, Extracting Superficial Scattering by Q-Sensing Technique. *Journal of Biophotonics*, 2024: p. e202400262.

- 5 Tzroya, A., et al., Detecting Contaminants in Water Based on Full Scattering Profiles within the Single Scattering Regime. ACS omega, 2023. 8(26): p. 23733–23738.
- 6 Tzroya, A., H. Duadi, and D. Fixler, Optical Method for Detection and Classification of Heavy Metal Contaminants in Water Using Iso-pathlength Point Characterization. ACS omega, 2024. 9(6): p. 6986–6993.
- 7 Ramella-Roman, J.C., S.A. Prahl, and S.L. Jacques, Three Monte Carlo programs of polarized light transport into scattering media: part I. Optics Express, 2005. 13(12): p. 4420–4438.
- 8 Ramella-Roman, J.C. and T. Novikova, Polarized-Sensitive Monte Carlo, in Polarized Light in Biomedical Imaging and Sensing: Clinical and Preclinical Applications. 2022, Springer Nature. p. 105–132.



## A self-calibrated single-wavelength biosensor for measuring SpO2

Ms. Michal Katan

Bar Ilan University

### Authors:

Michal Katan, Dr. Hamootal Duadi and Prof. Dror Fixler

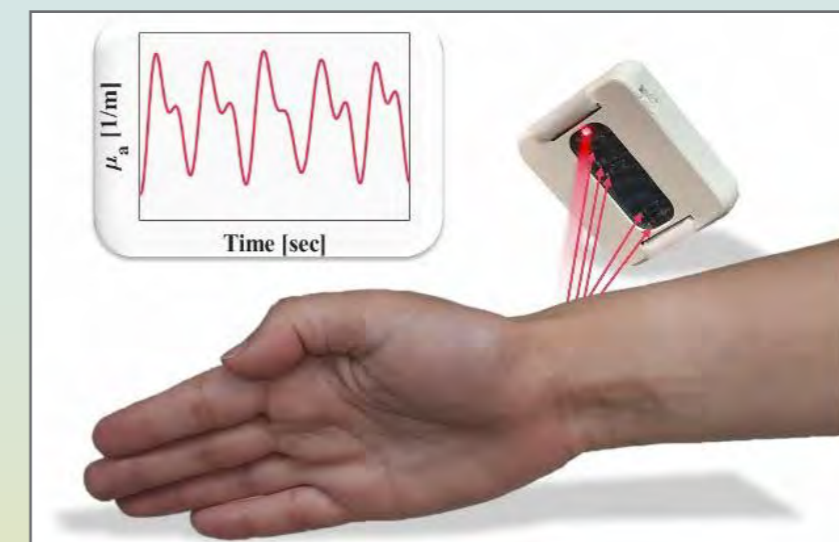
### Abstract:

**Objectives:** Optical techniques for diagnosis of a physiological tissue state are useful due to their noninvasive nature. Yet, light reflectance from a tissue is determined by the medium optical properties, absorption and scattering. Therefore, evaluating physiological parameters that correlate with absorption exclusively, requires calibration of the scattering. While extracting pulse rate is possible in a single wavelength, other parameters, such as oxygen saturation (SpO2), require more than one light source and ratiometric measurements. As a result, the differences in the optical pathlength of the different wavelengths produce an inherent error.

**Methods:** We have discovered the iso-path length (IPL) point, a specific position around a cylindrical media where the light intensity is not affected by the scattering. It was found by measuring the full scattering profile (FSP), meaning the angular distribution of light intensity of cylindrical tissues. Therefore, when measuring in this IPL point, the absorption can be isolated from the scattering. This allows extracting physiological parameters such as SpO2 from a single wavelength measurement. In this research we designed and built an optical biosensor for measuring the scattered light from the tissue, constructed with a single light source and several photodetectors, as one of them is in the IPL point's location.

**Results:** We conducted several experiments for measuring the oxygen saturation in ordinary conditions. In addition, we conducted experiments in a hypoxic chamber for simulating extreme conditions of lack of oxygen, at which we measured SpO2 values of 70–100% with an error of 0.4%.

**Conclusions:** The IPL point enables the isolation of absorption from scattering, allowing SpO2 to be measured using a single wavelength. Our biosensor demonstrates high accuracy and versatility, paving the way for further experiments to measure additional physiological parameters.





## AI-Driven Optical Analysis of Renal Obstruction: Deep Learning Segmentation with Fluoroscopic Tissue Quantification

**Dr. Talia Yeshua**

*Department of Electro-Optical Engineering and Applied Physics, Jerusalem College of Technology (JCT), Lev Academic Center*

### Authors:

Talia Yeshua, Jerusalem College of Technology, Jerusalem, Israel; Oriel Shitrit, Jerusalem College of Technology, Jerusalem, Israel; Mordechai Duvdevani, Hadassah Medical Center, Jerusalem, Israel; Jacob Sosna, Hadassah Medical Center, Jerusalem, Israel;

### Abstract:

**Objectives:** This study aims to develop and validate an innovative AI-driven pipeline that integrates Mask R-CNN deep learning segmentation with fluoroscopic imaging for automated, quantitative assessment of renal pelvis drainage. The goal is to enable the detection of partial renal obstructions through dynamic contrast material quantification, ultimately enhancing diagnostic capabilities in urology.

**Methods:** A dual-phase approach was employed: (1) Segmentation: A Mask R-CNN model was trained on 295 fluoroscopic images from 46 clinical cases and validated on 68 images from 10 independent cases. The model was optimized for accurate delineation of the renal collecting system, ensuring the exclusion of non-relevant radiopaque regions. Then, a post-segmentation algorithm was implemented to comprehensively include all contrast material regions. (2) Quantitative Analysis: A novel tissue absorption correction method was developed to quantify contrast material dynamics. Temporal analysis of sequential fluoroscopic images allowed for evaluating urinary tract patency by calculating the drainage time ( $t_{1/2}$ ), representing the time in which half of the contrast material drains from the renal pelvis.

**Results:** The deep learning model initially achieved a DICE coefficient of 0.86, sensitivity of 82%, and specificity of 94% in renal pelvis segmentation. The subsequent application of the post-segmentation algorithm significantly improved the sensitivity to 98%, ensuring the comprehensive inclusion of contrast material in the analysis. Temporal analysis of contrast material decay revealed distinct exponential patterns, enabling clear differentiation between normal and obstructed renal systems ( $p < 0.001$ ). A significantly higher  $t_{1/2}$  was observed in dilated cases, strongly correlating with clinical diagnoses and demonstrating the potential for automated obstruction detection.

**Conclusions:** This AI-driven, end-to-end pipeline represents a significant advancement in optical-based diagnostic imaging. The system's ability to quantitatively analyze contrast material dynamics provides an objective, reproducible method for assessing upper urinary tract drainage, with substantial potential to improve clinical decision-making and treatment planning for renal obstructions.

## Noninvasive optical technique for sensing nanoparticles permeation profile among skin layers

**Mr. Channa Shapira**

*Bar Ilan University*

### Authors:

Channa Shapira (1,2) (1)Faculty of Engineering and the Institute of Nanotechnology and Advanced Materials, Bar Ilan University, Ramat Gan 5290002, Israel (2)The Institute of Nanotechnology and Advanced Materials, Bar Ilan University, Ramat Gan 5290002, Israel Rawan Salami(2,3), Yifat Harel(2,3), Esthy Levy-Eitan(2,3) Department of Chemistry, Bar Ilan University, Ramat Gan 5290002, Israel The Institute of Nanotechnology and Advanced Materials, Bar Ilan University, Ramat Gan 5290002, Israel Leah Armon (4) Faculty of Life Science Bar Ilan University, Israel Hamootal Duadi(1,2), Dror Fixler(1,2) (1)Faculty of Engineering and the Institute of Nanotechnology and Advanced Materials, Bar Ilan University, Ramat Gan 5290002, Israel (2)The Institute of Nanotechnology and Advanced Materials, Bar Ilan University, Ramat Gan 5290002, Israel

### Abstract:

**Objectives:** A main challenge in designing nanoparticles (NPs) as nanocarriers for drug in topical treatment is detecting NPs permeation through the skin. NPs are typically too small to be detected by regular noninvasive imaging techniques due to their size and depth. Thus, the research proposes the use of the iterative multi-plane optical properties extraction (IMOPE) technique.

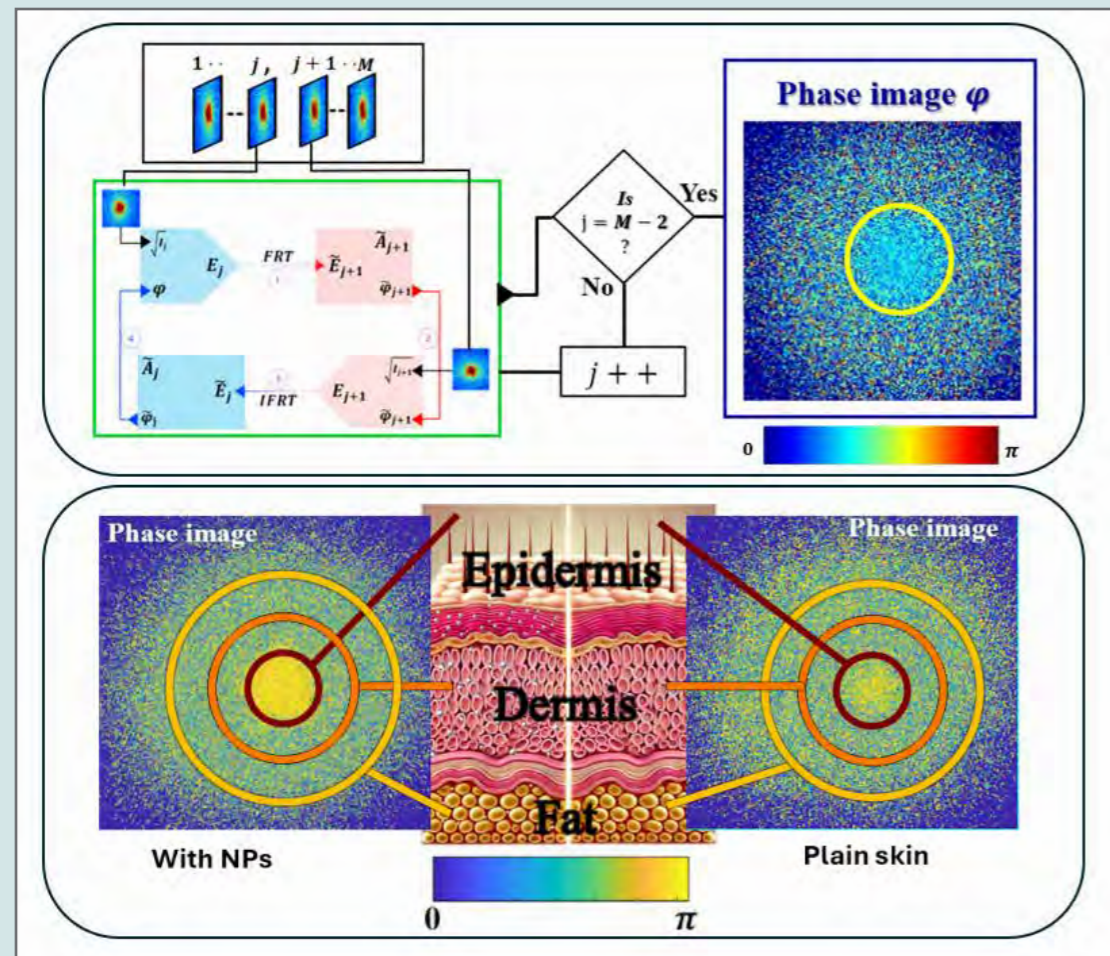
**Methods:** The proposed technique is a non-invasive method for estimating optical properties of opaque media based on a phase image reconstruction and analysis. The technique is based on a multi-plane version of the Gerchberg-Saxton phase retrieval algorithm and a theoretical model composed of an intensity model- based on dual source configuration of the method of images for describing the diffusion reflection and a phase model, based on differential pathlength factor calculation<sup>1-3</sup>.

**Results:** In the proposed research four mice topically treated by different gels: NPs only, complex of NPs with drug, the complex with additional enzyme, and enzyme only. The results showed that the technique could profile the permeation of the NPs, observe the effect of the NPs as nanocarriers for the drug, and the effect of the enzyme on the NPs penetration.

**Conclusions:** The IMOPE technique has the capability to detect the presence of NPs in different skin layers as a change of the optical properties when tailored for the optical properties range of the biological sample and the NPs.

### References:

- 1 Shapira, C. et al. Noninvasive Nanodiamond Skin Permeation Profiling Using a Phase Analysis Method: Ex Vivo Experiments. *ACS nano* (2022).
- 2 Shapira, C., Yariv, I., Ankri, R., Duadi, H. & Fixler, D. Effect of optical magnification on the detection of the reduced scattering coefficient in the blue regime: theory and experiments. *Optics Express* 29, 22228-22239 (2021).
- 3 Yariv, I., Shapira, C., Duadi, H. & Fixler, D. Media characterization under scattering conditions by nanophotonics iterative multiplane spectroscopy measurements. *ACS omega* 4, 14301-14306 (2019).



Rosh Electroptics LTD Proudly Represent:

# THORLABS



Optics ■ Imaging Systems ■ Sensors & Cameras ■ Calibration Systems ■ Laser & Light Sources Spectroscopy ■ Motion Systems ■ Quantum Optics ■ THz ■ Fiber Optics ■ Laser Safety Equipment

**Learn more on our website!**

For expert technical assistance and more information, contact us +972-9-8627401  
info@roshelop.co.il ■ www.roshelop.co.il ■ Follow us



## OPTICAL ENGINEERING Session

### Oral Presentations Abstracts:

#### Designing Zoom Lenses from Scratch: using the varifocal differential equation

Mr. Alon Geller

*Light Engineering*

##### Abstract:

One of the challenges of lens design is finding an appropriate starting design. This is particularly true of zoom lenses, where requirements for total length, element diameters, zoom range, focus range, field of view, and relative aperture compete when choosing an initial layout. Through a series of papers in the 90s, ChunKan (1992, 1995) and Yeh, Shiue, & Lu (1995,1996) show how to use differential equations to solve for the paraxial layout. Used properly, this technique prevents lens groups from colliding, and results in smooth cam curves. In a short presentation, I will describe how a zoom system is set up using first order (Gaussian) optics, describe the boundary conditions and limitations, and show how to solve for the initial paraxial design.

#### Using fluorescence for laser beam alignment and measurements

Mr. Arie Amitzi

*QCC Hazorea Calibration Technologies*

##### Authors:

Arie Amitzi and Doron Peled

QCC Hazorea Calibration Technologies

##### Abstract:

Using fluorescence for laser beam alignment and measurements

**Objectives:** In some cases, those who perform open laser beam alignment need to meet the following criteria:

1. Class 3B or Class 4 visible or invisible laser.
2. Beam Irradiance vs spot shape: round, elliptical or any other shape.
3. Ability to see and align different laser spot shapes, depending on their irradiance.
4. Ability to perform the procedure accurately within a short time.

During the procedure they must work in a Laser Controlled Area and wear Laser Protective Eyewear.

Problems: Most common laser accidents occur during open beam alignment and they are caused by:

1. Unanticipated eye exposure during laser beam alignment.
2. Fatigue, leading to carelessness or inappropriate shortcuts.

**Methods:** We applied the hierarchy of safety controls and eliminated risks by using a reliable laser safety enclosure with a special optical device. Instead of performing open beam mode alignment and measurements, or using an expensive beam profiler, we used a special opaque window with proper reticles and attenuators. This opaque window contains a proper fluorescent coating sensor that emits clear visible light when illuminated by a Visible and Nonvisible (UV or IR) laser beam.

This solution can only be used when the optical device has a proper damage threshold and creates a proper fluorescence contrast above the threshold limit.

**Results:** This new approach makes it possible to perform laser beam alignments and beam measurements with no eye risk, increased accuracy, and reduced duration.

**Conclusions:** Applying this innovative approach makes it possible to perform complicated laser beam alignment and spot shape measurement more easily, without the need to wear laser protective eyewear, and yields more accurate results in less time, which means that the machine is disabled for a shorter duration.



## In-situ optical surface reconstruction of liquid mirrors in microgravity experiments

Mr. Omer Luria

*Technion – Israel Institute of Technology*

### Authors:

Omer Luria, Khaled Gommed, Mor Elgarisi, Israel Gabay, Jonathan Ericson, Valeri Frumkin, Alexey Razin, Daniel Widerker, Ruslan Belikov, Jay Bookbinder, Vivek Dwivedi, Howard Cannon, Edward Balaban, and Moran Bercovici

### Abstract:

From imaging planets to gathering spectra of distant stars, space telescopes are humanity's main instruments for space exploration. All existing telescopes, including those which are still under development, are manufactured on earth using conventional techniques (lapping and polishing) and launched into orbit. This sets a barrier on the possible aperture of space telescopes, as the payload must fit into the launcher. This limitation is a significant obstacle in improving imaging resolution and contrast, and the main reason why the 'holy grail' in astronomy – direct imaging of exoplanets – remains out of reach.

The Fluidic Telescope (FLUTE) project proposes to overcome launch constraints through in-space fabrication of large liquid mirrors. In the absence of external forces, liquid interfaces naturally take the shape of optically smooth spherical surfaces. Liquids are also compact and can be easily packaged to any launchable shape. FLUTE thus aims to deploy a space telescope with a 50-m diameter liquid mirror – an order of magnitude larger than the state-of-the-art.

In our recent parabolic flight experiments we have demonstrated the creation of liquid mirrors under microgravity using a gallium alloy and an ionic liquid – two materials which are compatible with space conditions and are candidates for FLUTE.

In this talk we will first present the hardware developed to shape the liquids into concave spherical mirrors under microgravity, addressing several unique challenges introduced by the properties of these liquids and the flight conditions. We will then present the hardware and algorithm we developed for real-time reconstruction of the surfaces of the mirrors from Shack-Hartmann wavefront sensing data, without the need for a reference surface. The system was proven to be operational in microgravity conditions and will serve as the basis for future space experiments in more controlled microgravity conditions.

## Fluidic approach to corrective eyewear manufacturing

Mr. Mor Elgarisi

*Technion, Israel*

### Authors:

Mor Elgarisi<sup>1</sup>, Omer Luria<sup>1</sup>, Yotam Katzman<sup>1</sup>, Daniel Widerker<sup>1</sup>, Valeri Frumkin<sup>1,2</sup>, Moran Bercovici<sup>1,3</sup>

<sup>1</sup> faculty of mechanical engineering, technion – israel institute of technology, haifa, Israel

<sup>2</sup> Current affiliation: Department of Mechanical Engineering, Boston University, Boston, MA, USA

<sup>3</sup> Current affiliation: Department of Materials, ETH Zürich, Switzerland.

### Abstract:

In the developed world, we take corrective eyeglasses for granted. Owing to the outstanding accessibility to corrective eyeglasses, we often forget that they are in fact medical devices that treat an otherwise severe medical condition. Unfortunately, this is not the case for over 1 billion individuals in developing regions who suffer from vision impairment yet lack access to corrective eyewear. This problem has been highlighted over and over again by the global medical community and the economic community. Their conclusion remains consistent – despite progress in diagnostics using mobile devices, the prescription itself is useless unless an actual pair of eyeglasses can be manufactured. However, this problem has been in a deadlock for decades, as existing manufacturing technologies (machining/polishing, molding) are simply incompatible with the limited resources and the lack of required infrastructure in low-income areas. At the same time, existing additive manufacturing technologies cannot meet the surface quality requirements of ophthalmic applications.

In this work, we present a novel additive manufacturing technology for ophthalmic manufacturing that creates high-quality ophthalmic lenses with any spherical or cylindrical prescription. The approach is based on utilizing surface tension to drive a volume of liquid polymer under neutral buoyancy toward a desired minimum energy state that corresponds to a lens geometry. We developed a theoretical model that relates simple and tunable geometrical parameters to the optical powers of the lens itself, and developed a tabletop device that consumes less than 25W of power, generates no waste, and enables the fabrication of high-quality ophthalmic meniscus lenses without any machining or polishing steps, all within minutes. We show successful fabrication of more than 100 lenses with a wide range of spherical and cylindrical diopters, with a surface roughness of 1 nm (an order of magnitude better than spectacle polishing) and excellent agreement with our mathematical model.

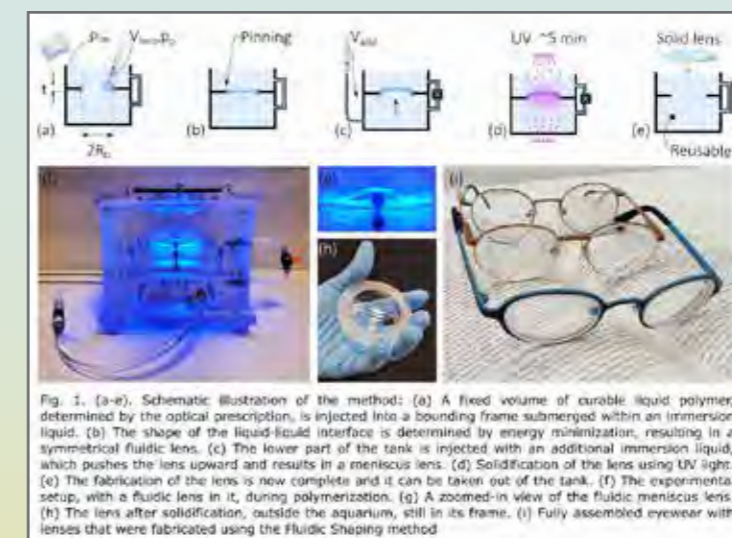


Fig. 1. (a-e), Schematic illustration of the method: (a) A fixed volume of curable liquid polymer, determined by the optical prescription, is injected into a bounding frame submerged within an immersion liquid. (b) The shape of the liquid-liquid interface is determined by energy minimization, resulting in a symmetrical fluidic lens. (c) The lower part of the tank is injected with an additional immersion liquid, which pushes the lens upward and results in a meniscus lens. (d) Solidification of the lens using UV light. (e) The fabrication of the lens is now complete and it can be taken out of the tank. (f) The experimental setup, with a fluidic lens in it, during polymerization. (g) A zoomed-in view of the fluidic meniscus lens. (h) The lens after solidification, outside the aquarium, still in its frame. (i) Fully assembled eyewear with lenses that were fabricated using the fluidic Shaping method.

### 3D-printed coupling aids for efficiently interfacing silicon chip to rectangular core fiber

Mr. David Halfon

Hebrew University of Jerusalem

#### Authors:

David Halfon, Ksenia Shukhin, Aleksei Kukin and Dan M. Marom

#### Abstract:

Optical fibers transmit many data communication signals encoded over wavelengths (i.e., Wavelength Division Multiplexing). Yet today's single mode fiber (SMF) infrastructure is quickly nearing its capacity limit. Alternatively, spatial multiplexing encodes multiple data streams onto different spatial modes within multimode fiber (MMF).

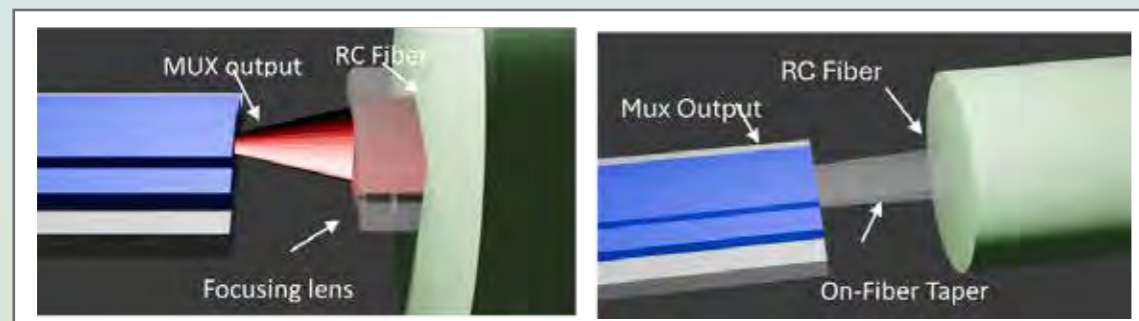
We are exploring rectangular core fibers (RCF) for simplified, high-capacity mode division multiplexed (MDM) optical communications. Unlike traditional circular core MMF, RCF have well-spaced propagation constants for their spatial modes, reducing crosstalk between multimode channels.

To efficiently use RCF for MDM, we designed a silicon chip spatial mode multiplexer that supports both polarizations thanks to 3  $\mu\text{m}$  thick silicon waveguide technology. However, the output facet (37.5  $\mu\text{m}$  wide and 3  $\mu\text{m}$  high) suffers from vertical mode mismatch to the RCF (33  $\mu\text{m} \times 6.2 \mu\text{m}$ ) and contributes 3 dB loss across the fiber's four spatial modes. To improve coupling efficiency, we developed two multimode coupling enhancement solutions based on 3D printing: a cylindrical lens and an adiabatic taper.

The cylindrical lens is printed directly on the RCF facet and at a working distance of 9.1  $\mu\text{m}$  achieves coupling losses between -1.08 dB and -1.43 dB without contributing to crosstalk in FDTD simulations.

The on-fiber taper, also printed on the RCF facet, demonstrated coupling losses between -0.29 dB and -0.56 dB, also without inducing crosstalk at nearly contact conditions in simulation.

These designs significantly enhance coupling efficiency in RCF-based MDM systems, advancing the development of high-capacity optical communication networks to meet future data demands.



### All-optical, computation-free time-multiplexing super-resolved imaging based on speckle illumination

Mr. Ariel Ashkenazy

Bar-Ilan University

#### Authors:

Ariel Ashkenazy, Faculty of Engineering and the Institute of Nanotechnology and Advanced Materials, Bar-Ilan University, Ramat Gan 5290002, Israel; Nadav Shabairou, Faculty of Engineering and the Institute of Nanotechnology and Advanced Materials, Bar-Ilan University, Ramat Gan 5290002, Israel; André Stefanov, Institute of Applied Physics, University of Bern, 3012 Bern, Switzerland; Peng Gao, School of Physics, Xidian University, Xi'an, 710071, China; Dror Fixler, Faculty of Engineering and the Institute of Nanotechnology and Advanced Materials, Bar-Ilan University, Ramat Gan 5290002, Israel; Eliahu Cohen, Faculty of Engineering and the Institute of Nanotechnology and Advanced Materials, Bar-Ilan University, Ramat Gan 5290002, Israel; Zeev Zalevsky, Faculty of Engineering and the Institute of Nanotechnology and Advanced Materials, Bar-Ilan University, Ramat Gan 5290002, Israel

#### Abstract:

**Objectives:** To develop a super-resolution (SR) imaging technique that overcomes the diffraction limit without requiring computational post-processing or prior knowledge of illumination patterns, making it suitable for real-time applications.

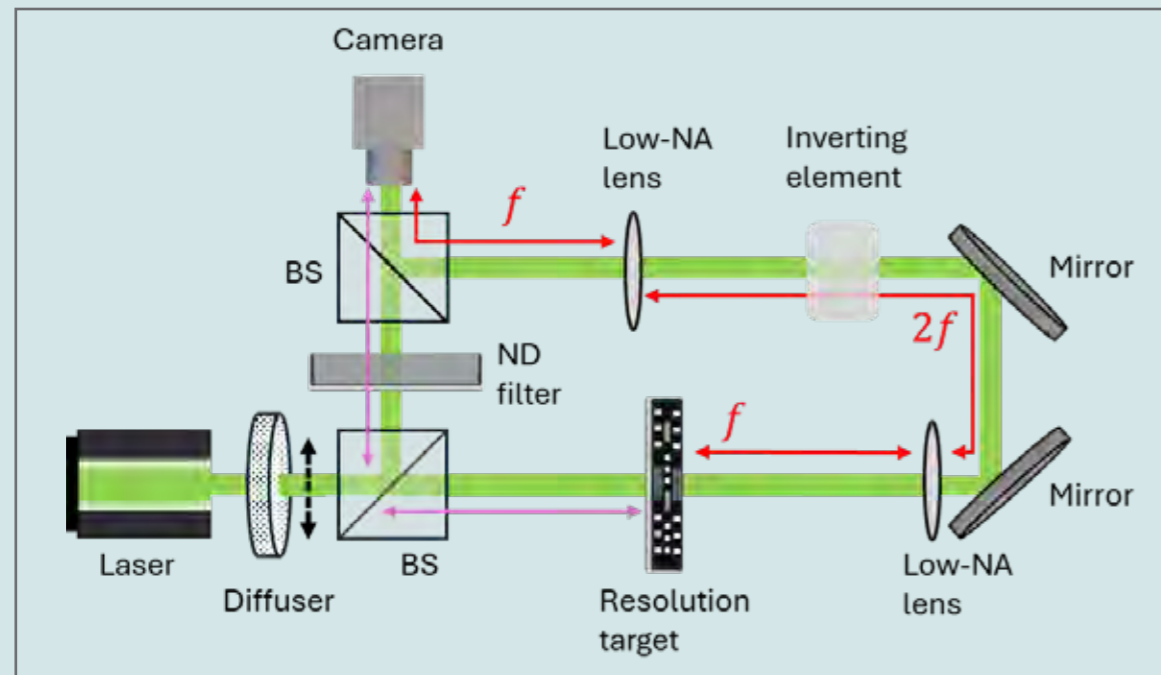
**Methods:** The proposed method employs an all-optical, time-multiplexing scheme. Objects are illuminated with multiple speckle patterns generated by passing a laser through a rotating diffuser. The object image is then optically interfered with the illuminating speckle pattern, enabling spatial homodyne detection. A theoretical derivation is provided, proving that the camera's integration of the intensity at the output yields a real-time SR image, free of resolution reduction caused by the imaging point-spread function (PSF). The technique was further validated through numerical simulations and experimental demonstrations.

**Results:** Simulations and experimental results demonstrated significant resolution enhancement. In simulations of a 1951 USAF resolution target as the object, the SR image obtained after averaging over 50,000 speckle patterns showed clear resolution improvement compared to low-resolution images obtained under incoherent illumination. The experimental setup successfully replicated these results, showcasing the method's ability to produce SR images in near real-time without computational post-processing.

**Conclusions:** This novel, computation-free near real-time SR imaging approach eliminates the need for complex post-processing or prior knowledge of illuminating patterns. The method's simplicity and effectiveness make it suitable for a variety of real-time applications in fields where rapid, high-resolution imaging is critical.

#### Reference:

A. Ashkenazy et al., All-optical, computation-free time-multiplexing super-resolved imaging based on speckle illumination. *Opt. Lett.* 50, 566–569 (2025).



### E posters Abstracts:

#### Thermal Model of Photopolymerization for Terrestrial and In-Space Fabrication of Optical Elements

Mr. Jonathan Ericson

*Technion-Israel Institute of Technology*

#### Authors:

Jonathan Ericson, Daniel Widerker, Eytan Stibbe, Mor Elgarisi, Yotam Katzman, Omer Luria, Khaled Gommed, Alexey Razin, Israel Gabay, Hanan Abu Hamad, Ester Segal, Yaron Amouyal, Moran Bercovici

#### Abstract:

Photopolymers are increasingly used in optical fabrication, as they allow precise control of polymerization initiation and location, and eliminate the need for on-site homogenous and bubble-free mixing of multiple components. However, photopolymerization reactions are typically highly exothermic, which together with low thermal conductivity may lead to thermal defects and poor optical quality. Above certain temperatures, the chemical stability of photopolymer resins is compromised, resulting in evaporation and surface blistering. These challenges exist in terrestrial fabrication but are particularly important in in-space fabrication where temperature regulation is hindered by the absence of free convection.

The temperature during photopolymerization is affected by a large number of parameters, including material properties, thermal boundary conditions, excitation light propagation, and sample geometry. There is thus a need for a simulation tool capable of predicting the thermal dynamics throughout the photopolymerization process.

We present an experimentally validated numerical model that predicts polymerization states and temperature profiles during fabrication, for defect-free manufacturing in terrestrial and microgravity environments. The model is based on the heat equation, with a heat source term that originates from the photopolymerization reaction, and which depends on the local light intensity. It applies to both terrestrial and microgravity environments, and is applicable to any photopolymer following characterization of the polymer's thermal and optical properties.

We demonstrate the use of the model as a design tool for determining the conditions under which successful, defect-free, polymerization can be achieved in a given environment. Furthermore, we use the model to investigate polymer surface blistering observed during our fluidic lens fabrication on the ISS (Eytan Stibbe, RAKIA mission)(see figure). The model reveals significant heat accumulation in microgravity due to the absence of convection and correctly captures our observations in photopolymerization of VidaRosa and Norland optical adhesives in space.



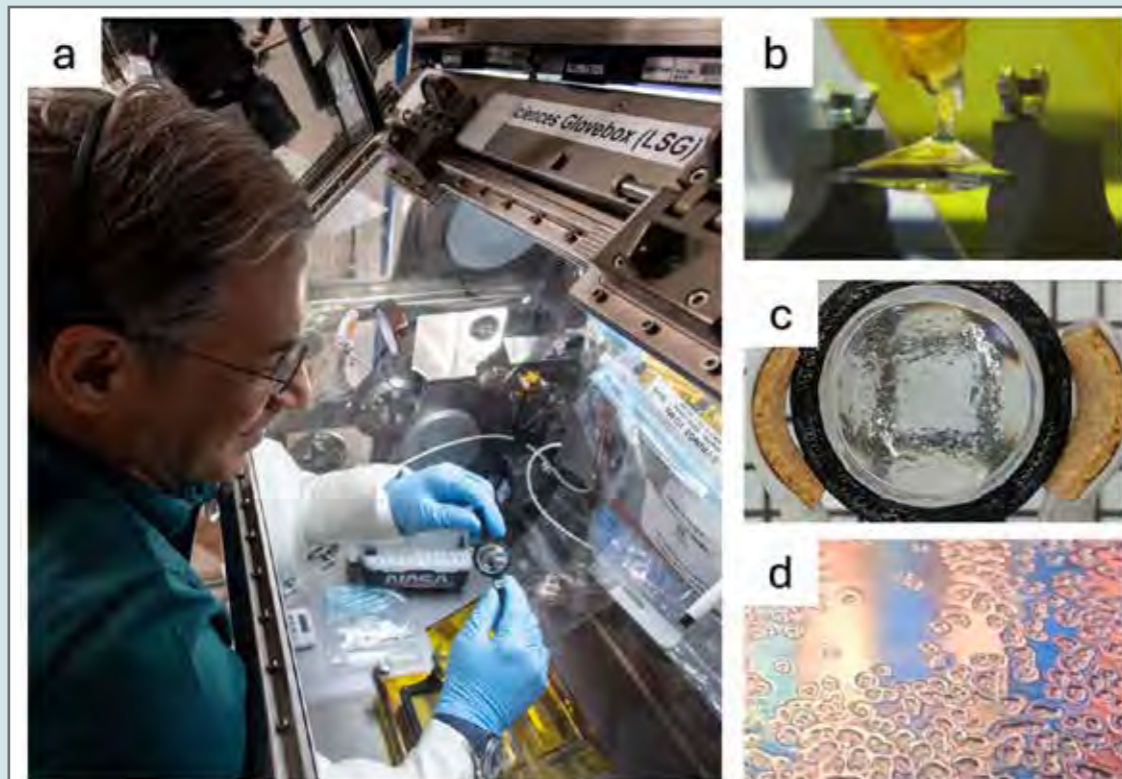


Figure 1. Thermal effects on photopolymerization of lenses fabricated in microgravity. (A-B) Astronaut Eytan Stibbe fabricating lenses on board the ISS using Fluidic Shaping. (C) Blistering on a VidaRosa (acrylate photopolymer) lens produced in space, due to lack of convection. (D) Successful reproduction of the blistering effects in the lab.

## No edging – manufacturing of ophthalmic lenses directly in eyewear rims using Fluidic Shaping

Mr. Yotam Katzman

Technion – Israel Institute of technology

### Authors:

Yotam Katzman, Mor Elgarisi, Amos Hari, Omer Luria, Jonathan Ericson, Valeri Frumkin, Moran Bercovici

### Abstract:

Conventional eyewear lens manufacturing relies on bulk material processing such as machining (grinding and polishing) or molding. In both cases the final step is edging, in which the lens is cut to fit the desired rim. These processes are time-consuming, resource-intensive and generate substantial material waste.

In previous work, our group developed a lens fabrication method called Fluidic Shaping, where a photopolymer is injected into a frame contained in an immersion density-matched liquid, allowing buoyancy forces to negate the effects of gravity. Under these conditions, surface tension drives the liquid interface into its minimum energy state, resulting in a liquid lens that can be solidified by UV curing. We have also shown that by using elliptical frames with varying aspect ratios, any sphero-cylindrical prescription can be readily achieved. However, the edging process – removing the edges of the lens to fit the desired rims, remained thus far unaddressed.

We here introduce an algorithm, which we term the ‘Cookie Cutter’, for the design of varying-edge-height frames that enables the fabrication of lenses directly to the shape of the customer’s rim. By integrating our algorithm with Fluidic Shaping, we offer an end-to-end solution for fabrication ophthalmic lenses, eliminating the need for any mechanical processing, including edging.

The design process relies on two theoretical geometrical objects: a Fluidic Shaping lens based on a standard circular or elliptical frame, and a generalized cylinder whose cross-section corresponds to that of the desired rim. We show theoretically and experimentally that the surface resulting from the subtraction of the cylinder from the lens (hence ‘Cookie Cutter’) defines a new frame whose varying height would guarantee the reconstruction of the lens surface upon injection of the correct volume of liquid. We will show experimental results demonstrating complete eyewear manufacturing using the Cookie Cutter method, together with its optical characterization.

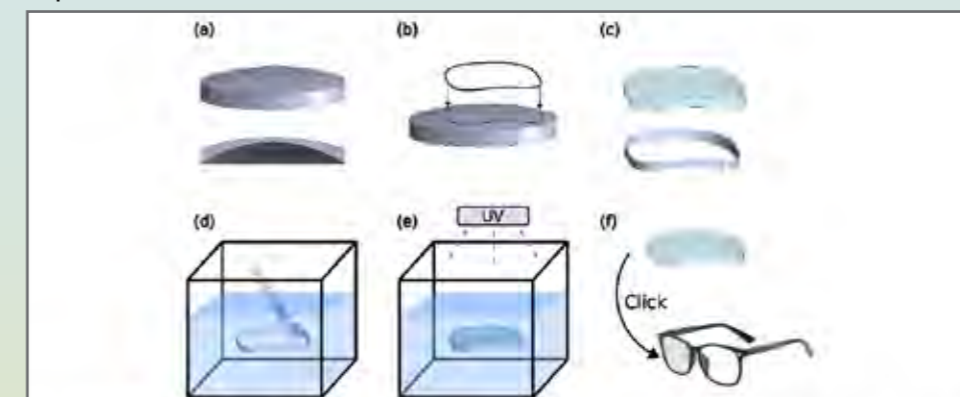


Figure 1: The Cookie Cutter method and fabrication process. (a-c) A new frame is defined by the theoretical intersection of a Fluidic Shaping lens and a generalized cylinder whose cross section corresponds to that of the desired rim. (d-e) The new frame can be used in the Fluidic Shaping approach to create a lens, whose optical properties are identical to the original (theoretical) lens. (f) The resulting lens can be directly inserted into the eyewear rim without the need for further processing.

## Plasma Dispersion Effect induced focusing of 775nm laser beam in silicon

Mr. Asaf Malran

Bar Ilan University

### Authors:

A Malran, A Arcobi, N Shabairou, Z Zalevsky, M Sinvani

### Abstract:

**Objectives:** To achieve super resolution in laser scanning microscopy in silicon by shaping the probe laser beam by a second laser beam induced focusing in the silicon.

**Methods:** We generate an instantaneous lens within a silicon sample using a pump-probe technique. The pump beam has a donut-shaped profile with a wavelength of 775 nm and a pulse duration of 30 ps, while the probe beam follows a Gaussian profile. In previous experiments, we employed a probe beam at 1550 nm; in this study, we explore the use of a shorter wavelength (775 nm). Both beams originate from the same laser source, simultaneously, with some delay time, such that the beam splits into a high-intensity pump and a weaker one for probe beam. The beams are orthogonally polarized to ensure clear distinction.

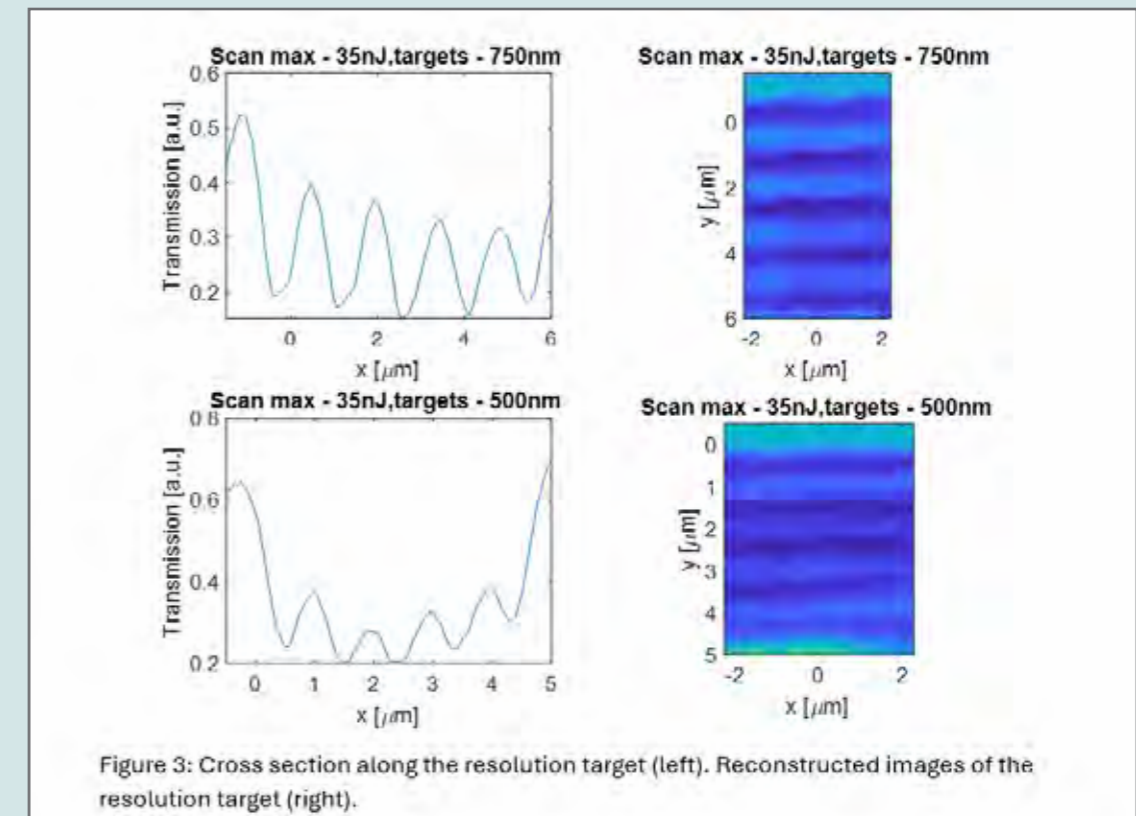
The donut-shaped vortex pump beam induces a spatial distribution of free charge carriers (FCCs) in silicon, mirroring its own shape. Due to the plasma dispersion effect (PDE), this results in a donut-shaped region with a reduced refractive index, forming a gradient-index (GRIN) lens. This GRIN lens focuses the portion of the probe beam that overlaps with it, directing light toward the center of the donut.

**Conclusions:** Our experiment demonstrates that the pump beam effectively reduces the full width at half maximum (FWHM) of the probe beam by forming a GRIN lens within the silicon sample, locally altering its refractive index. The results show a twofold improvement in probe beam narrowing. Future studies will focus on further enhancing this effect by optimizing experimental parameters.

This approach holds significant potential in silicon-based microscopy, offering valuable applications in nanoelectronics, particularly in integrated circuit (IC) failure analysis.

### References:

- 1 Pinhas, H.; Wagner, O.; Danan, Y.; Danino, M.; Zalevsky, Z.; Sinvani, M. Plasma Dispersion Effect Based Super-Resolved Imaging in Silicon. *Opt. Express* 2018, 26 (19), 25370–25380.
- 2 Shabairou, Nadav, et al. "Dynamics of laser-induced tunable focusing in silicon." *Scientific Reports* 12.1 (2022): 6342.
- 3 Shabairou, Nadav, Zeev Zalevsky, and Moshe Sinvani. "Laser Beam Self-Focusing in Silicon at an Absorbed Wavelength by a Vortex Beam in the Same Wavelength." *ACS omega* 9.15 (2024): 16969–16975.





## Direct 3D-Printing of near-index matched diffractive optical elements

Mr. Leonid Leites

Russell Berrie Nanotechnology Institute, Technion–Israel Institute of Technology, Haifa, Israel

### Authors:

Leonid Leites, Reut Orange–Kedem, Ori Cohen and Yoav Shechtman

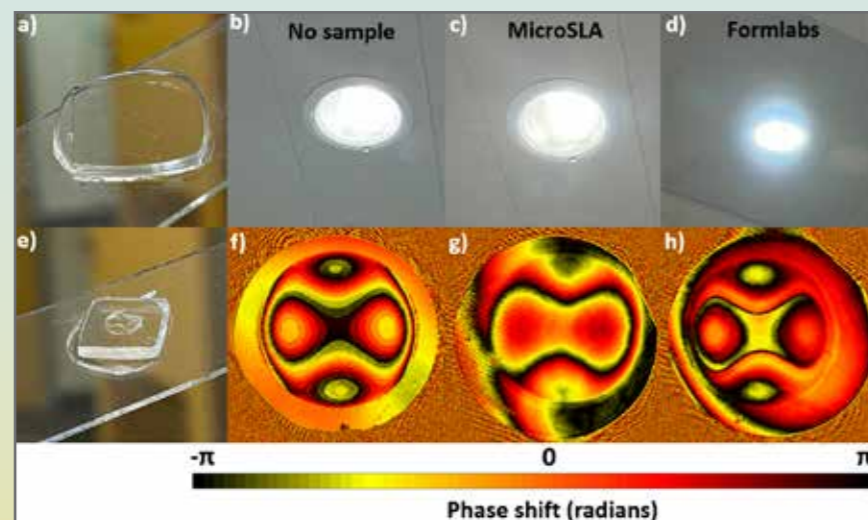
### Abstract:

**Objectives:** This project advances stereolithography-based 3D printing for diffractive optical elements using transparent resins and near-index matching. Traditional methods like photolithography, CNC milling, and microinjection molding are costly and slow. Current 3D-printing techniques often lack the resolution required for high-quality optics or rely on expensive, low-output methods like two-photon polymerization. Previous research implemented index-matching techniques to improve height accuracy and error tolerance in 3D-printed optical elements [R. Orange–Kedem et al., Nat. Commun. 12, 3067 (2021), R. O. Kedem et al., Light Sci. Appl. 12, 222 (2023)]. However, that work focused on molding templates with similar refractive indices, a time-consuming and error-prone process. A direct 3D-printing approach with transparent UV-curing resins could significantly improve the process.

**Methods:** Additive manufacturing with transparent materials for optical applications faces challenges like non-uniform polymerization, leading to sample heterogeneity. Tests on smooth-surfaced transparent samples (Fig. 1a) revealed optical inhomogeneities, such as the “halo” effect (Fig. 1d), caused by resin tank surface interactions; pictures of the light source were taken by attaching samples to a phone camera. A “Tetrapod” phase mask for 3D localization microscopy [Shechtman et al., Nano Lett., 2015, 15, 4194–4199] was also manufactured (Fig. 1e) with the second resin molded above. The refractive index difference was  $\sim 0.009$ .

**Results:** Using smooth, highly transparent FEP films in resin tanks, replaced with each print, improved optical homogeneity (Fig. 1c). The symmetry of the 3D-printed “Tetrapod” phase mask improved by reducing tilt during molding. Phase maps from a Mach–Zehnder interferometer are shown in Fig. 1f (calibration), Fig. 1g (asymmetric), and Fig. 1h (improved symmetry).

**Conclusions:** The proposed approach reduces manufacturing time to  $\sim 1$  hour with minimal human intervention. Further work is needed to address differences between photolithography and 3D printing, including aligning refractive index differences and fine-tuning the UV light source.



## Active metasurface design based on VO2

Mr. Vladimir Kostriukov

Bar-Ilan University

### Authors:

Vladimir Kostriukov, Sukanta Nandi, Omer Levi, Amos Sharoni, Tomer Lewi. From Bar-Ilan University

### Abstract:

**Objectives:** Actively tunable resonators are the holy grail in the field of metasurface, with much interest in LIDAR, adaptive optics, and nano-electro-optic applications. We turn our attention to VO<sub>2</sub> as a candidate for thermally tunable resonators, and not only show they are promising in theory, but also realizable for optical devices in the mid-IR range. The long-term goal for the project is to demonstrate actively tunable metasurfaces with local pixel control for beam steering applications.

**Methods:** Simulations for design optimization are done using Ansys’s Lumerical FDTD. Device fabrication is done on a Sapphire or Quartz substrates, involving e-beam evaporation for Si film deposition and reaction sputtering of VO<sub>2</sub> with a substrate baked at 600°C with Ar:O<sub>2</sub> (26:0.6) atmosphere with a VO<sub>2</sub> target at a deposition rate of 0.11 Å/s. E-beam lithography is employed to imprint a hard-mask pattern, made in reactive sputtering out of AlN, to then etch the resonators using SF<sub>6</sub>:C<sub>4</sub>F<sub>8</sub> (30:15) atmosphere, with an etch rate of 170nm/min, with a hard-mask removal step following.

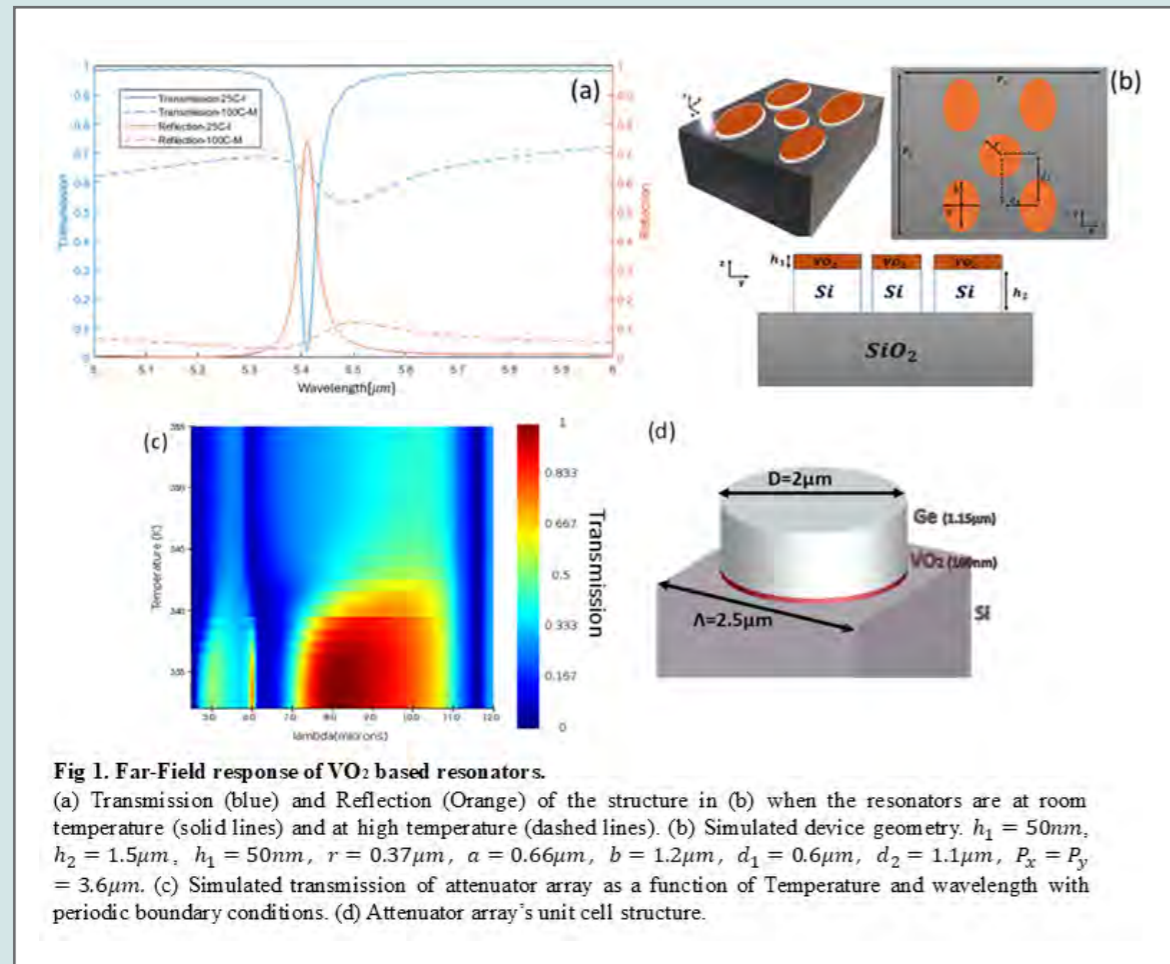
**Results:** We present FDTD results for a switching device of high-Q-factor resonator array with a supercell comprising 4 elliptical and one circular resonators[1]. The device acts as a switchable beam splitter that could outperform a simple static beam splitter. Furthermore, a naïve approach to a cylindrical Ge resonator atop VO<sub>2</sub> and a Si substrate can be used to make a tunable mid-IR spectral filter. Fabrication is currently under-way to optimize the protocols and eventually realize the devices.

**Conclusions:** VO<sub>2</sub> shows a great promise for mid-IR application, specifically for tunable and switchable metasurfaces. Current challenges mostly include the fabrication process, and particularly the etching of the multilayer devices.

### References:

- 1 W. Sun et al., “Potential of high Q dual band Mid-Infrared metasurfaces with Quasi-BIC for refractive index sensing,” Opt Laser Technol, vol. 174, p. 110631, 2024.





איתך לאורך כל הקרוך

## NONLINEAR OPTICS SESSION

### ◆ Invited speakers Abstracts:

#### **Prof. Guy Bartal**

*Faculty of Electrical and Computer Engineering, Technion*

#### **Abstract:**

Near-field microscopy is an essential tool for monitoring evanescent fields associated with both guided modes of photonic integrated circuits and with surface waves on metal-dielectric interfaces and meta-interfaces or polaritons in 2D materials.

While traditional near-field methods rely on scanning and direct perturbation of the near-field at close vicinity to the interface, my group has recently introduced a nonlinear-optical approach to directly observe such waves in real-time and with no perturbation, allowing to monitor the evolution of surface and guided modes and access waves buried under thick transparent layers.

In my talk, I will present our recent advances relying on those new capabilities. Those include active control over near-field patterns such as directing plasmonic focal spot over several microns with 30nm control precision, toggling among multiple values of angular momentum of near-field modes and direct visualization of light inside photonic integrated circuits.

### **Oral presentation Abstracts:**

#### **Kerr frequency comb generation in Saddle-Shape microresonators**

#### **Mr. Yaakov Neustadter**

*Soreq NRC*

#### **Authors:**

Yaakov Neustadter, Soreq NRC, Yavne, Israel; Salman Noach, Jerusalem College of Technology, Jerusalem, Israel; Eyal Yacoby Soreq NRC, Yavne, Israel

#### **Abstracts:**

Frequency comb sources are integral to many applications such as optical sensing, accurate optical clocks, and fundamental research. This work presents, for the first time, a Kerr frequency Comb (KFC) source generated in a high-Q silica Saddle-Shape Microresonator (SSM).

As an optical platform, Whispering Gallery Mode (WGM) microresonators are of great interest for generating KFCs due to their simplicity, small dimensions, and very low power consumption. An SSM is fabricated by welding together two silica microspheres and is coupled to a tapered fiber in the “valley” region between them, displaying a high Q-factor exceeding 108. Through the third order non-linear Kerr effect, a KFC is generated within the microresonator.

A comparison of the frequency comb characteristics is offered between a SSM-based comb and a microsphere-based comb. The repetition rate of a SSM-comb may be significantly smaller than is expected from a comparable microsphere-comb of the same size. The optical mode of WGM microspheres is simulated both analytically and numerically and compared with numerical simulations of the mode volume and distribution for SSM WGMs. The unique geometry of SSMs, as well as the spatial properties of their WGMs, ensure a stable coupling to a tapered fiber, and support packaged WGM-based sensors and light sources. Additionally, a Raman laser source is demonstrated in an SSM, providing further potential for this package as a stable optical source.

Fiber coupled WGM SSMs hold great promise as packaged, mechanically stable, KFC and Raman light sources for laboratory use or out-of-lab applications alike.

## Optically Programable Quasi Phase Matching in Four-Wave Mixing

Dr. Gil Bashan

Tel Aviv University

### Authors:

Gil Bashan, Avishay Eyal, Moshe Tur and Ady Arie. School of Electrical Engineering, Faculty of Engineering, Tel Aviv University, Tel Aviv, Israel

### Abstract:

Quasi-phase matching (QPM) has long been employed as a powerful technique to enhance the efficiency of nonlinear optical processes and control the conversion efficiency spectrum. Traditionally, QPM involves the permanent spatial modulation of linear or nonlinear polarization to achieve results akin to true phase matching. Conventional methods of modulating susceptibility are often impractical in centrosymmetric or anisotropic materials where the dominant nonlinearity is third-order, like standard optical fibers. Optically induced QPM has previously been demonstrated in high-harmonic generation within ionized gases [2], the approach leverages the extreme sensitivity of plasma electrons to field dynamics, a mechanism unavailable in standard nonlinear optical materials. Alternative methods of optically induced QPM reported in the literature exhibit either a lack of constructive buildup of light along the nonlinear medium or limited flexibility, as the nonlinear pattern cannot be easily modified or erased after inscription [3].

In this work, we propose and demonstrate the first efficient, optically controllable QPM within the realm of perturbative nonlinear optics. Through temporal modulation of counter-propagating pump waves, we achieve spatial modulation, equivalent to traditional QPM, along a standard polarization maintaining fiber, resulting in spatiotemporal modulation of the nonlinear polarization in four-wave mixing. Unlike conventional QPM techniques that require permanent modifications to the optical medium, our method leaves the medium unaltered. We demonstrate broadband wavelength conversion over a spectral range of 300nm, including the C-band and L-band of optical telecom (Fig 1(a)), and it is limited only by the lab equipment [4]. We demonstrated a significant conversion efficiency of 5.4%. Experimental results validate the efficacy of our approach, showcasing wavelength tunability and spectrum shape modulation through pump wave modulation (Fig 1(b)) [4]. Beyond classical data processing and fiber sensing applications, optically programmable QPM promises adiabatic control of quantum states and robust frequency conversion.

### References:

- [1] Armstrong, J. A., et al. Interactions between Light Waves in a Nonlinear Dielectric. *Phys. Rev.*, 127(6), 1918–1939 (1962).
- [2] Zhang, X., et al. Quasi-phase-matching and quantum-path control of high harmonic generation using counterpropagating light. *Nature Phys.* 3,270–275 (2007).
- [3] Billat, A. et al. Large second harmonic generation enhancement in Si3N4 waveguides by all-optically induced quasi-phase-matching. *Nature Commun.* 8, 1016 (2017).
- [4] Bashan, G. et al. Optically Programable Quasi Phase Matching in Four-Wave Mixing. Under consideration at *Nature Commun.*

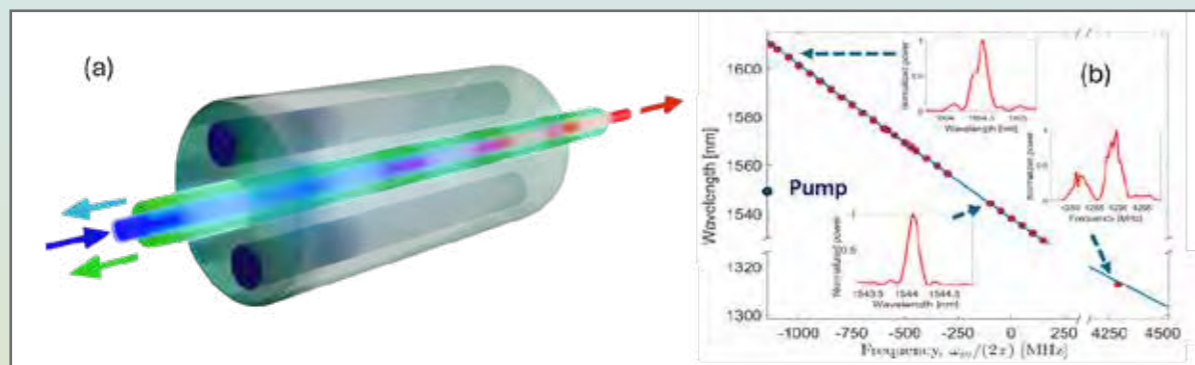


Fig 1. (a) Schematic illustration of Optically Programable QPM [4]. (b) Summary of 27 measurements at different QPM frequencies, demonstrating wavelength tunability of maximum nonlinear coupling. [4].



## Highly-efficient and stable Second Harmonic Generation (SHG) from Para Red Organic Crystals

Mr. Alon Krause

Bar-Ilan University

### Authors:

Alon Krause<sup>1</sup>, Tchiya Zar<sup>1</sup>, Linda Shimon<sup>2</sup>, Martin Oheim<sup>3</sup>, Adi Salomon<sup>1</sup>

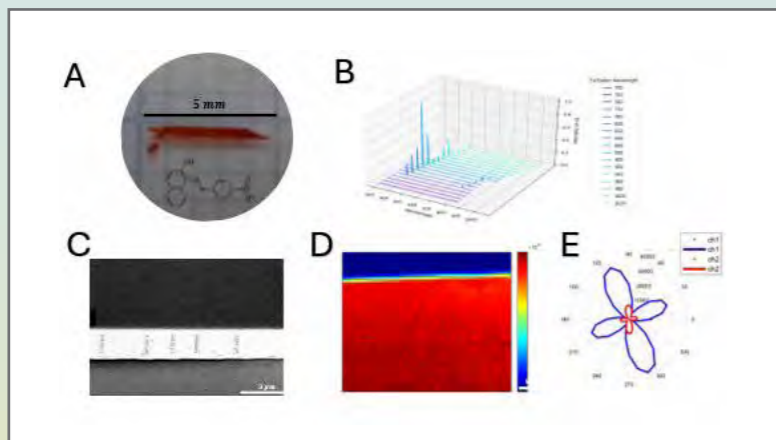
- 1 Institute of Nanotechnology and Advanced Materials (BINA), Bar-Ilan University, Ramat-Gan, 52900, Israel
- 2 Department of Chemical Research Support, The Weizmann Institute of Science, Rehovot, 76100, Israel
- 3 Université Paris Cité, SPPIN (Saint-Pères Paris Institute for the Neurosciences), CNRS UMR 8003, Paris, France

### Abstract:

This work investigates the synthesis and characterization of nonlinear optical organic crystals based on the azo dye Para Red, which possesses a molecular and crystal structure that promote nonlinear activity due to a large conjugated system, donor-acceptor groups, and a non-centrosymmetric crystal group. Those highly stable crystals give rise to both SHG and 2 photon excitation fluorescence.

A novel de-sublimation technique that we developed for the growth of Para Red crystals results in different polymorphs belonging to the symmetry groups  $P_n$  and  $P212121$ , forming needle and thin plates shape. The plates crystals have a millimeter scale with thicknesses between half a micron to two microns. These crystal plates were found to have distinct nonlinear properties, with conversion efficiency of  $1.4 \times 10^{-8}$  and stability of hours under fs laser illumination. These properties are higher than those present in crystals made in conventional evaporation or cooling crystallization.

The crystal structures were determined by using single crystal X-ray diffraction, and the physical dimensions were measured by Optical and Electron Microscopies. The optical activity was examined linearly and nonlinearly using a custom-made scanning SHG setup, and imaging. It is shown that the resulting Para red crystals provide uniform SHG activity, over a wide range of wavelengths, up to 3 times more efficient than industry standard materials such as BBO. These properties make these crystals promising candidates for practical applications in photonic devices, including Terahertz generation.



## Optical nonlinearity of transparent conducting oxides – more metallic than realized

Ms. Naama Harcavi

Ben Gurion University of the Negev

### Authors:

Naama Harcavi (Ben-Gurion University of the Negev, Beer Sheva, Israel), Ieng-Wai Un (South China Normal University, Guangzhou, China) and Yonatan Sivan (Ben-Gurion University of the Negev, Beer Sheva, Israel)

### Abstract:

Transparent conducting oxides (highly-doped semiconductors such as Indium Tin Oxide, Aluminum Zinc Oxide, etc.) exhibit ultrafast optical nonlinearities several orders of magnitude larger than those of noble metals [1,2,3,4,5]. This makes them promising candidates for nonlinear optical materials.

Most early works adopted phenomenological and/or simplistic thermal models. Here, we compare the predictions of our rigorous microscopic adiabatic non-thermal model [6,7] to models used earlier based on the resulting temperature dependence of the Drude model parameters, namely, the plasma frequency and the damping rate.

We find that the effect of the temperature-dependence of the damping rate on the permittivity of ITO is of crucial importance, see Fig.1. Peculiarly, to date, this key insight that has been largely overlooked.

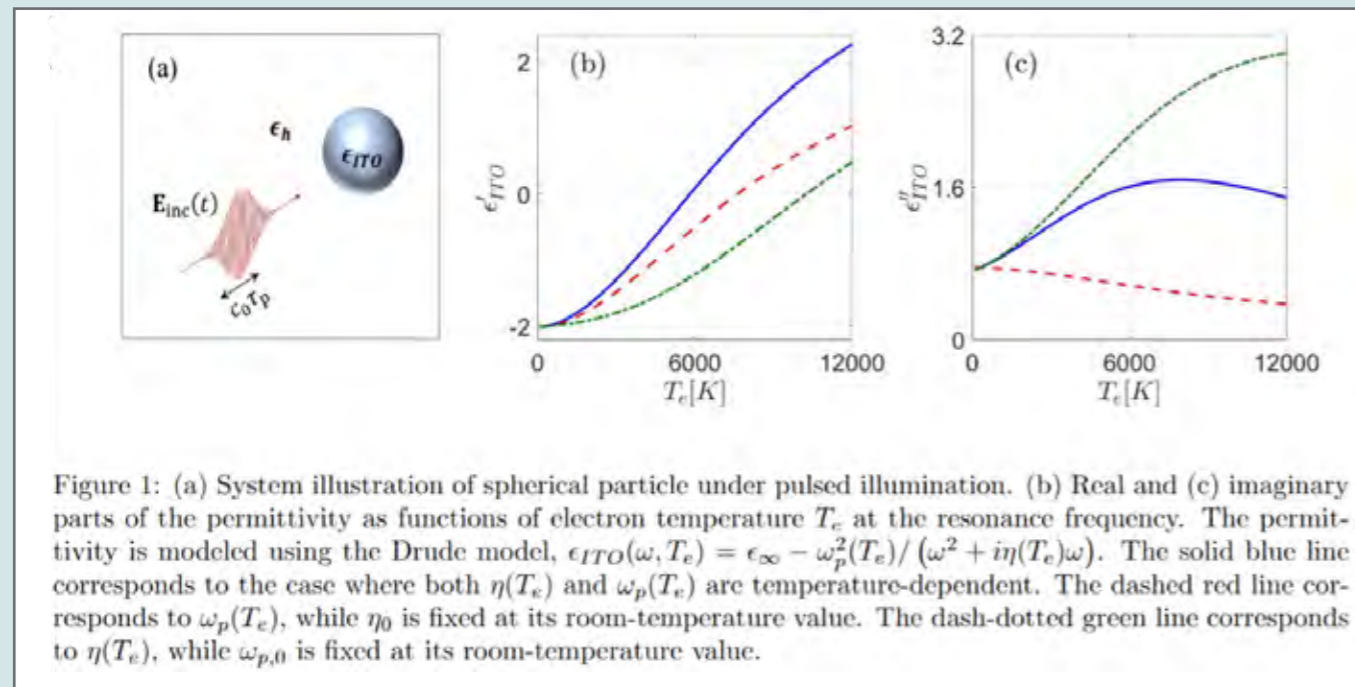
Specifically, the temperature-dependence of the damping rate has two main effects:

1. The real part of the permittivity – the faster collisions associated with the growth of the damping rate upon illumination and consequent heating contribute in a manner both qualitatively and quantitatively comparable to the temperature-dependent plasma frequency. This may explain why this effect was overlooked so far.
2. The Imaginary part of the permittivity – while the plasma frequency decreases with growing temperature, the corresponding increased damping rate is dominant. As a result, our model predicts a qualitatively opposite behavior compared to that assumed so far. Nevertheless, for temperatures higher than  $\sim 7000\text{K}$ , the decreasing plasma frequency becomes dominant. This behavior makes the intensity-dependence of the imaginary part of the ITO permittivity of TCOs reminiscent to that of noble metals.

Importantly, our observations are generic, i.e., they are not sensitive to the exact values of the material parameters, which may vary significantly from one sample to another, as well as from one TCO to another, or from inclusion of more sophisticated models for the collision rates.

### References:

- [1] R. Secondo and J. Khurgin and N. Kinsey. (2020), Opt. Mater. Express, 10:1545–1560.
- [2] J. B. Khurgin and N. Kinsey. (2024), ACS Photonics, 11:2874.
- [3] E. Minerbi, S. Sideris, J.B. Khurgin, & T. Ellenbogen. (2022), Nano Letters, 22, 6194–6199.
- [4] J. Baxter, A. Pérez-Casanova, L. Cortes-Herrera, A. Calà Lesina, I. De Leon., & L. Ramunno. (2023), Advanced Photonics Research, 4.
- [5] M.Z. Alam, S.A. Schulz, J. Upham, I. De Leon, & R.W. Boyd. (2018), Nature Photonics, 12.
- [6] S. Sarkar and I. W. Un and Y. Sivan. (2023), Phys. Rev. Applied, 19:014005.
- [7] I. W. Un and S. Sarkar and Y. Sivan. (2023), Phys. Rev. Applied, 19:044043.



### Strong tunable nonlinearity in atomic vapor induced by an optical frequency comb

Ms. Sutapa Ghosh  
University Of Maryland

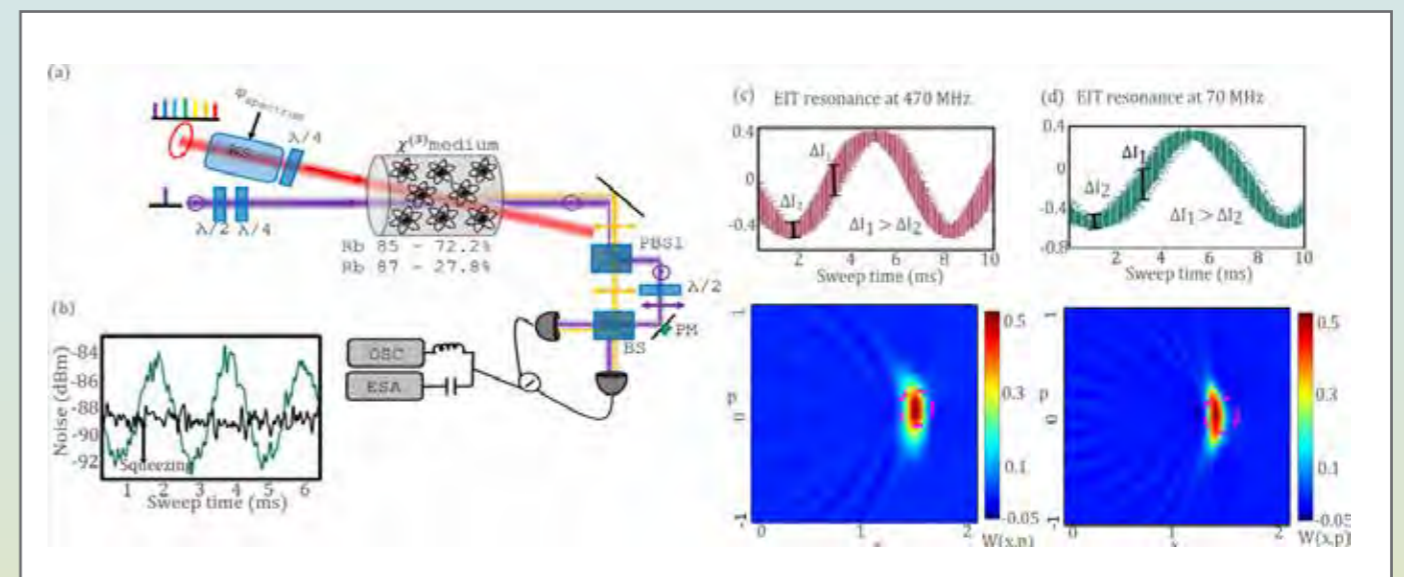
**Authors:**

Sutapa Ghosh, Alexey Gorlach, Chen Mechel, Maria V. Chekhova, Ido Kaminer and Gadi Eisenstein

**Abstract:**

Strong optical nonlinearities are key to a range of optical technologies and to the generation of quantum light states. However, generating strong and tunable nonlinear strength in the optical domain is still challenging. This work demonstrates a giant cross-Kerr optical nonlinearity by driving an atomic vapor by a frequency comb (Fig. 1(a)). The comb-driven-vapor exhibits N-level electromagnetically induced transparency (N-EIT), where thousands of transitions coherently contribute to strengthening the nonlinearity and offer tunability by scanning comb teeth across the atomic spectrum. The third-order nonlinearity induces the self-polarization rotation (SPR) of a co-propagating CW probe for each EIT resonance. The SPR signal is separated from the probe field by a polarizing beam splitter and is characterized by a homodyne system where the strong probe serves as the local oscillator (LO).

The generated light reveals quadrature squeezing of 3.5 dB (Fig. 1 b) and a non-Gaussian Wigner distribution by tuning to different resonance frequencies. Our homodyne measurements characterize the quantum properties of the SPR signal, (Fig. 1(b)), showing maximum squeezing at 200 kHz detection frequency for 85Rb, at a one-photon detuning of 640 MHz. For 87Rb, the obtained squeezing level is around 1.8 dB at a detuning of 470 MHz. To characterize the corresponding states of light, we reconstructed the Wigner function distributions, showing an amplitude-squeezed state (Fig. 1(c)). Around the detuning of 70 MHz, the Wigner function of the quantum state exhibits non-Gaussian crescent (banana) shape (Fig. 1(d)), approximating the cubic-phase state, generated here for the first time without post selection. Such states could be important for various quantum protocols.



## Enhanced Second Harmonic Generation from a Nonlinear Plasmonic Metasurface Coupled to an Optical Waveguide in a LiNbO Thin Film

Mr. Daniil Ansimov

Tel Aviv University, The laboratory of Nanoscale Electro Optics

### Authors:

Daniil Ansimov (Electrical Engineering, Tel Aviv University), Tal Ellenbogen (Tel Aviv University)

### Abstract:

Optical waveguides in thin films of LiNbO<sub>3</sub> on insulator (LNOI) form an emerging platform for nonlinear optics. Here we study the enhancement of second harmonic generation (SHG) by coupling the thin film to a resonant plasmonic metasurface.

The proposed metasurface-waveguide hybrid system consists of a 900 nm thick X-cut LiNbO<sub>3</sub> film on a fused silica substrate. A gold metasurface is placed on the film with nanoantennas oriented along the Z-axis of the LiNbO<sub>3</sub> crystal. This arrangement leverages the highest  $\chi^2$  nonlinear coefficient of the crystal to facilitate coupling to the TE<sub>0</sub> mode and significantly enhances the conversion efficiency.

The gold nanoantennas form a rectangular lattice with a periodicity of  $a_y = 730$  nm and  $a_z = 335$  nm, supporting diffraction only in the Y direction. One lattice period is schematically shown in Figure 1(a). The periodicity is optimized to support a guided mode for the fundamental wave at 1494 nm. The nanoantennas, with dimensions of 120×60×60 nm, are resonant at 900 nm—far from the fundamental harmonic to avoid destructive interference. These dimensions enable achieving a high Q-factor, enhancing SHG efficiency. The system is excited from the metasurface side, and SH is analyzed in transmission and reflection. Figure 1(c) shows the power flow of the generated SH integrated over the substrate for transmitted, and over the excitation port for reflected SH. The final conversion efficiency is given by:

$$\eta = P_{2\omega} / (P_{\omega}^2) = 0.01 \text{ W}^{-1}$$

– more than a 5000 fold enhancement over the bare thin film.

Future improvements could extend the system's capabilities by introducing spatial patterns to manipulate the accumulative phase, aligning antenna resonances with SH field, utilizing novel resonator designs, breaking the system's symmetry to achieve quasi-bound states in the continuum. These advancements will pave the way for efficient and versatile nonlinear optical devices, contributing to the next generation of photonic technologies.

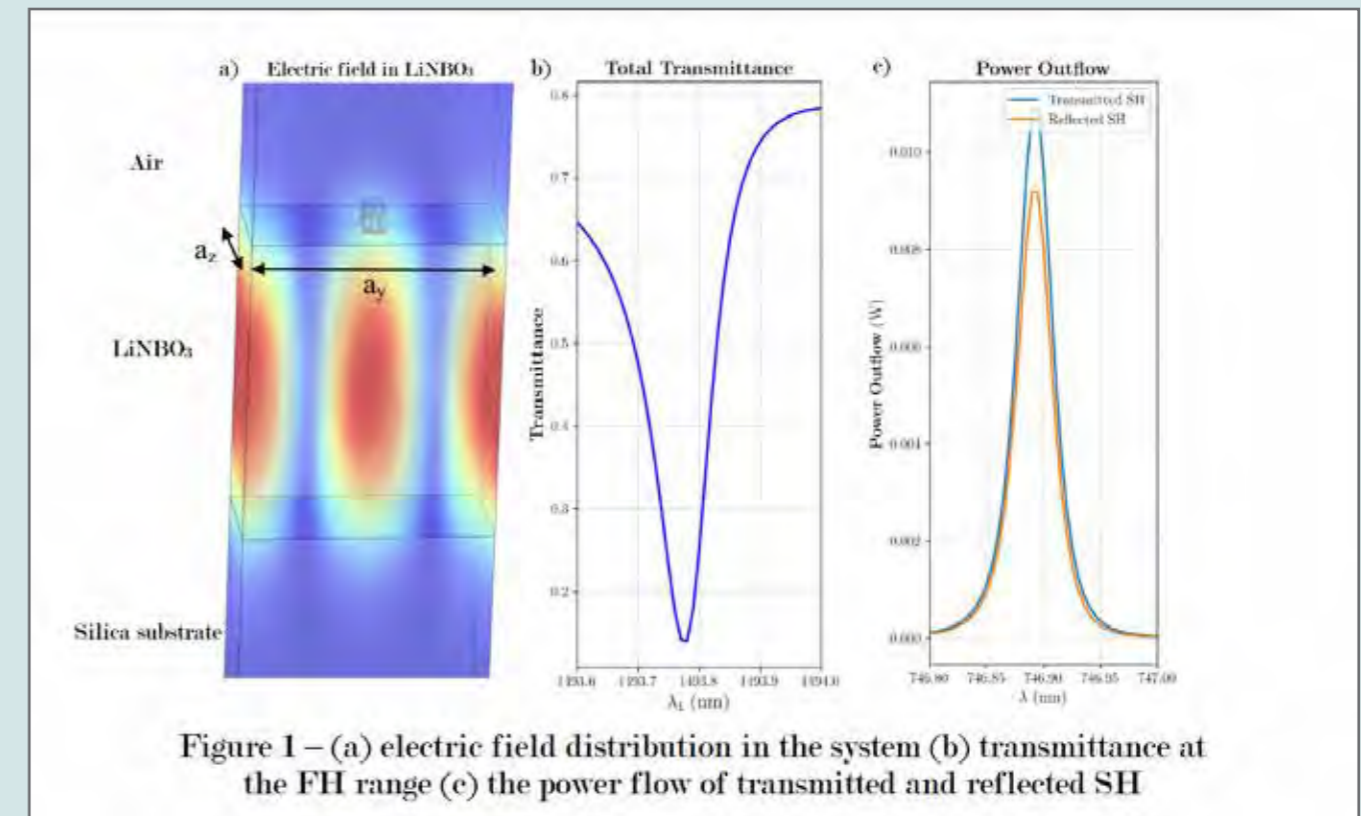


Figure 1 – (a) electric field distribution in the system (b) transmittance at the FH range (c) the power flow of transmitted and reflected SH



## Momentum Band Gap Engineering Using Noncolinear Moving Photonic Time Crystals

Mr. Ohad Segal

Electrical Engineering Department, Physics Department and Solid State Institute, Technion-Israel Institute of Technology, Haifa, Israel

### Authors:

Ohad Segal, Mark Lyubarov, Oded Schiller, Yonatan Plotnik and Mordechai Segev. All **Author**s are affiliated with the physics department, electrical engineering department and solid state institute, Technion-Israel Institute of Technology, Haifa, Israel

### Abstract:

**Objectives:** Momentum band gaps for optical light are a sought-after phenomenon due to their potential for broadband parametric amplification, and enhanced light-matter interactions [1]. These bandgaps originate from interference between time-refracted and time-reflected waves generated from large periodic ultrafast modulation of the refractive index [2]. A promising platform for optical momentum bandgaps are transparent conducting oxides (TCOs) which exhibit refractive index changes on the order of unity within few femtosecond [3].

Here we propose to take advantage of the velocity difference between the refractive index modulation (induced by a modulator pulse) and a probe wave, that occurs due to the chromatic dispersion of TCOs, to engineer momentum gaps and time-reflections.

**Methods:** Using special relativity and conservation laws, we derive the frequency shifts (Fig. 1a) and directional deflection (Fig. 1b) of the time-reflections and refractions from non-colinear propagation between a super-luminal refractive index interface and the optical wavevector of the probe (taking inspiration from [4]). We construct a transfer matrix method (TMM) for analyzing periodic and non-stepwise refractive index changes. Our results are verified using an independent 2+1D FDTD.

**Results:** Our calculations show that generally the transmitted and reflected waves have different frequencies and that the transmission and reflection do not counter-propagate.

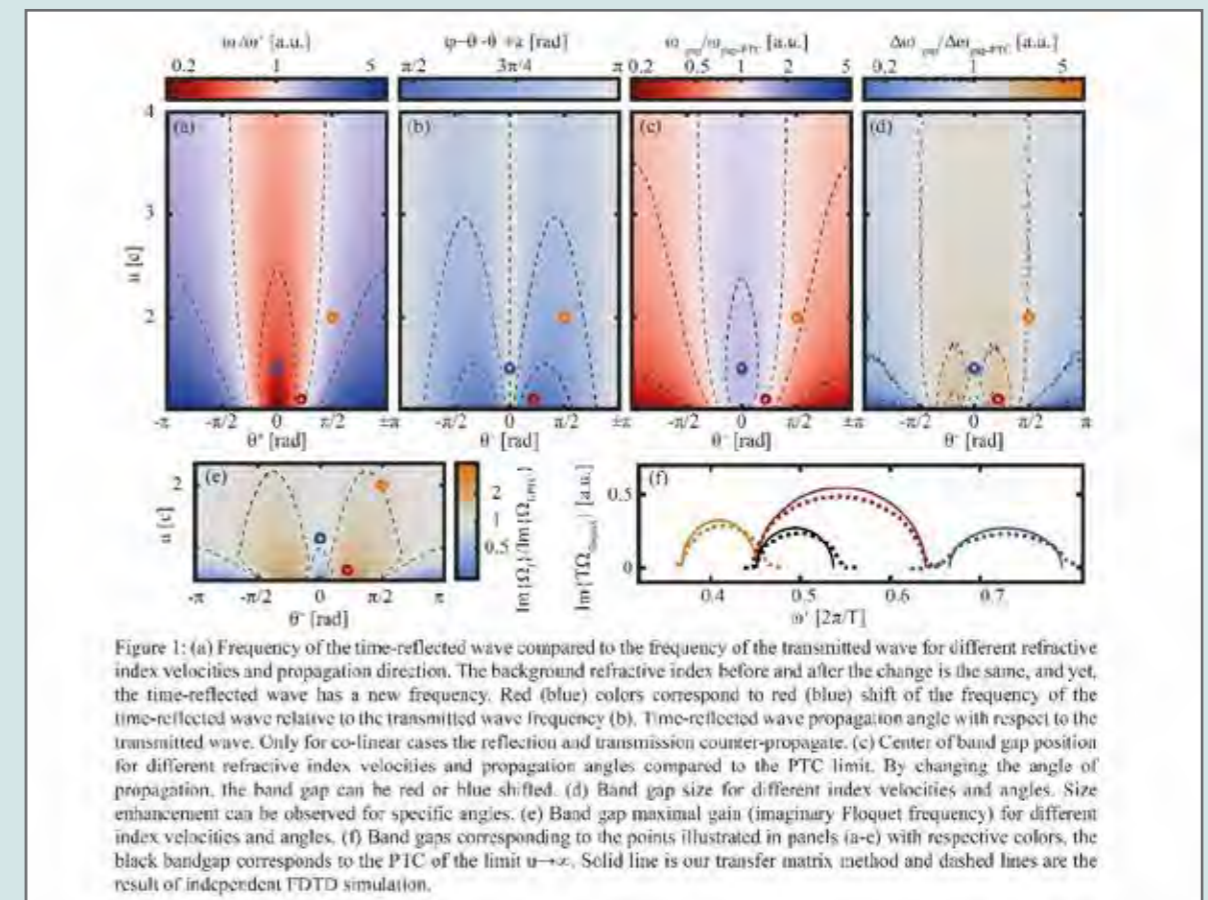
Using our TMM we analyze a periodic index change, which at the limit of infinite velocity describes a PTC with a single momentum gap. We find that the amplified frequency can be engineered by choosing the angle between the refractive index velocity and the optical wavevector.

**Conclusions:** Our results imply that, for our refractive index profile, incident angle of  $\sim \pi/4$  and index velocity approaching  $c$  (red circle in all figure panels) will create the largest momentum gap and maximal gain. Furthermore, in this setup, the time-reflection is redshifted and can be easily distinguished from all other frequencies, while also being deflected to a unique propagation direction. This is an exciting opportunity to create momentum gaps and time-reflections in experiments.

### References:

- [1] M. Lyubarov et al., Science 377, 425 (2022).  
 [2] F. Biancalana et al., Phys. Rev. E 75, 046607 (2007).  
 [3] E. Lustig et al., Nanophotonics 12, 2221 (2023).

- [4] Z.-L. Deck-Léger, A. Akbarzadeh, and C. Caloz, Phys. Rev. B 97, 104305 (2018).



## Kerr Beam Self-Cleaning of multi-millijoule pulses in large mode-area graded index fiber

Mr. Barak Messica

Department of Electrical and Computer Engineering and Solid-State Institute, Technion – Israel Institute of Technology, 32000 Haifa, Israel

### Authors:

Barak Messica and Pavel Sidorenko from the Department of Electrical and Computer Engineering and Solid-State Institute, Technion – Israel Institute of Technology, 32000 Haifa, Israel

### Abstract:

**Background and Objective:** Kerr-induced Beam Self-Cleaning (KBSC) occurs in graded-index multimode fibers (GIMMF) when nonlinear Kerr effects transform a speckle pattern into a stable bell-shaped profile at high power [1]–[3]. KBSC is highly attractive for applications such as high-energy pulse delivery with good beam quality. Here we experimentally demonstrate a KBSC of 10 mJ, 300 ns pulses in 300  $\mu\text{m}$  core graded-index multimode fiber. Our experiments demonstrate for the first time KBSC of multi-millijoules pulses in large mode-area GIMMF opening the door to practical applications.

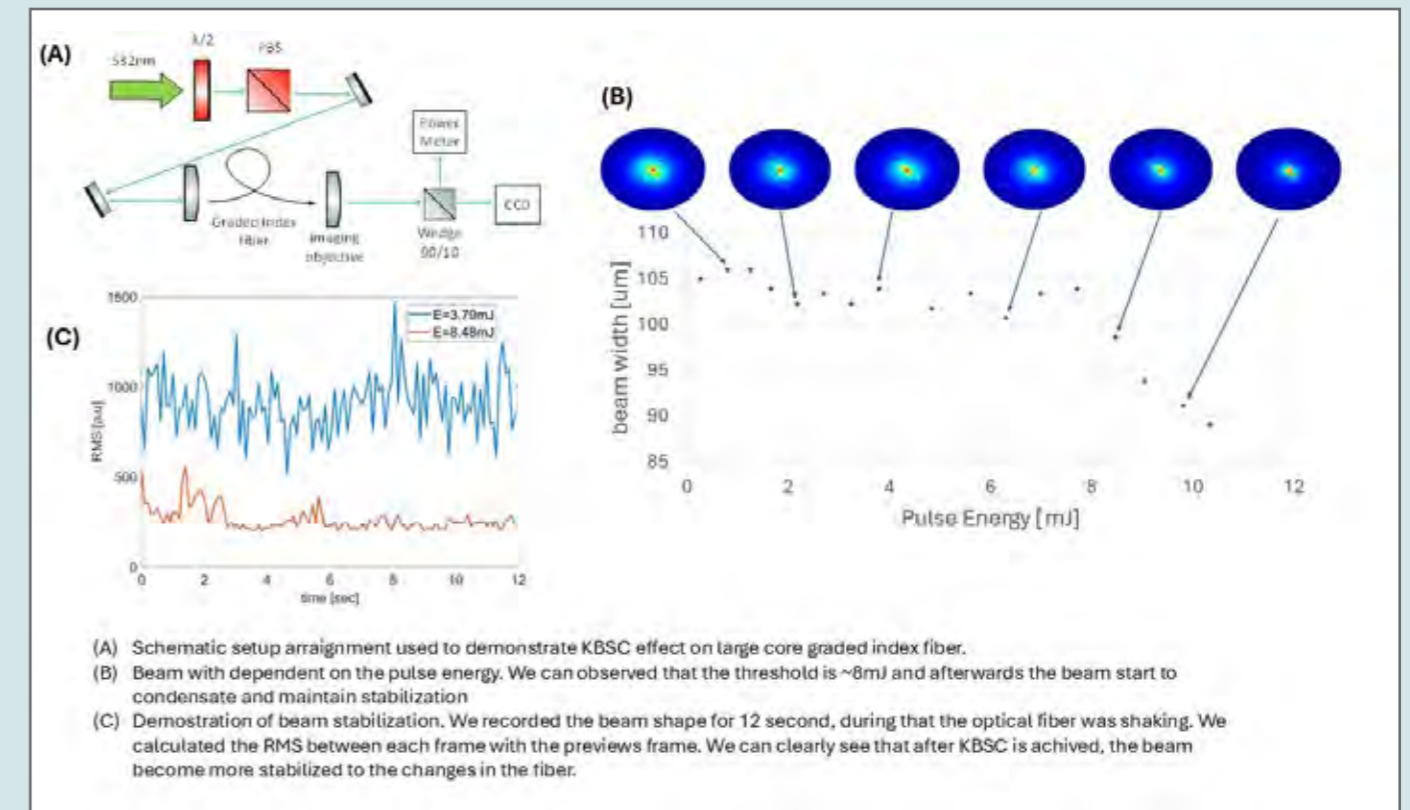
**Method:** Our experimental system is depicted in Fig. 1(a). High-energy laser pulses at 532 nm are coupled into 2.5 meters of 300  $\mu\text{m}$  core GIMMF with 85 % coupling efficiency. The fiber output is imaged on a camera, and pulse energy is measured using a power meter.

**Results:** As the input pulse energy increases (with 85 % coupling efficiency maintained), the output beam diameter from the fiber decreases, as shown in Fig. 1(b). Stimulated Raman Scattering begins to appear at 9.8 mJ causing energy transfer from the pulse to longer wavelengths. To evaluate the environmental stability of the beam's spatial profile at the fiber output, we mechanically perturb the fiber and record the beam profile for 12 seconds. Figure 1(c) shows the Root-Mean-Square-Error of subsequently recorded beam profiles. At low pulse energies, where linear propagation occurs, the beam profile exhibits significant variation (Fig. 1(c) blue curve). As KBSC is observed, these variations are greatly reduced (Fig. 1(c) red curve), demonstrating enhanced environmental stability of the beam.

**Conclusion:** We demonstrate KBSC with record-high pulse energy in an extremely large mode-area fiber. Moreover, we quantify the spatial profile stability of the cleaned beam for the first time. These results pave the way toward stable high-energy pulse delivery with excellent beam quality using the KBSC effect.

### References:

- [1] Krupa, Katarzyna, et al. "Spatial beam self-cleaning in multimode fibres." *Nature photonics* 11.4 (2017): 237–241.
- [2] Wu, Fan O., Absar U. Hassan, and Demetrios N. Christodoulides. "Thermodynamic theory of highly multimoded nonlinear optical systems." *Nature Photonics* 13.11 (2019): 776–782.
- [3] Pourbeyram, Hamed, et al. "Direct observations of thermalization to a Rayleigh-Jeans distribution in multimode optical fibres." *Nature Physics* 18.6 (2022): 685–690.





## Higher dimensional quantum photonics in the frequency domain

Dr. Miri Blau

Columbia University

### Abstract:

Controllable higher-dimensional quantum systems have broad applications including quantum advantage in simulation, quantum metrology, and quantum communication. In my talk I will discuss photons' frequency (energy) degree of freedom (1) for as means to scale up Hilbert space and allow for qudit generation. Highly efficient nonlinear processes are used for mediating single-photon level interactions and creating high dimensional photonic states in a single photon and photon pairs. I will discuss the use of an all-to-all interaction between N photons using Bragg-scattering four-wave mixing (2), and the path to increase the number of energy levels as well as photon number.

Frequency encoded quantum information is a promising path for quantum communication, exploiting the telecom bands (~1300, 1550 nm) opens the way for both free space and optical fiber propagation, based on current and established infrastructure. Encoding information on multiple frequency bins will increase transmission rates and was shown to be more robust to errors. We propose using our established platform to realize quantum key distribution.

### References:

- [1] Stephane Clemmen, Alessandro Farsi, Sven Ramelow, and Alexander L. Gaeta. Ramsey Interference with Single Photons. *Physical Review Letters*, 117(22):223601 (2016)
- [2] Richard Oliver, Miri Blau, Chaitali Joshi, Xingchen Ji, Ricardo Gutierrez-Jauregui, Ana Asenjo-Garcia, Michal Lipson, Alexander L. Gaeta, N-Way Frequency Beamsplitter for Quantum Photonics, arXiv:2405.02453

## Efficient robust spontaneous parametric down-conversion via detuning modulated composite segments designs

Mr. Yuval Rechtes

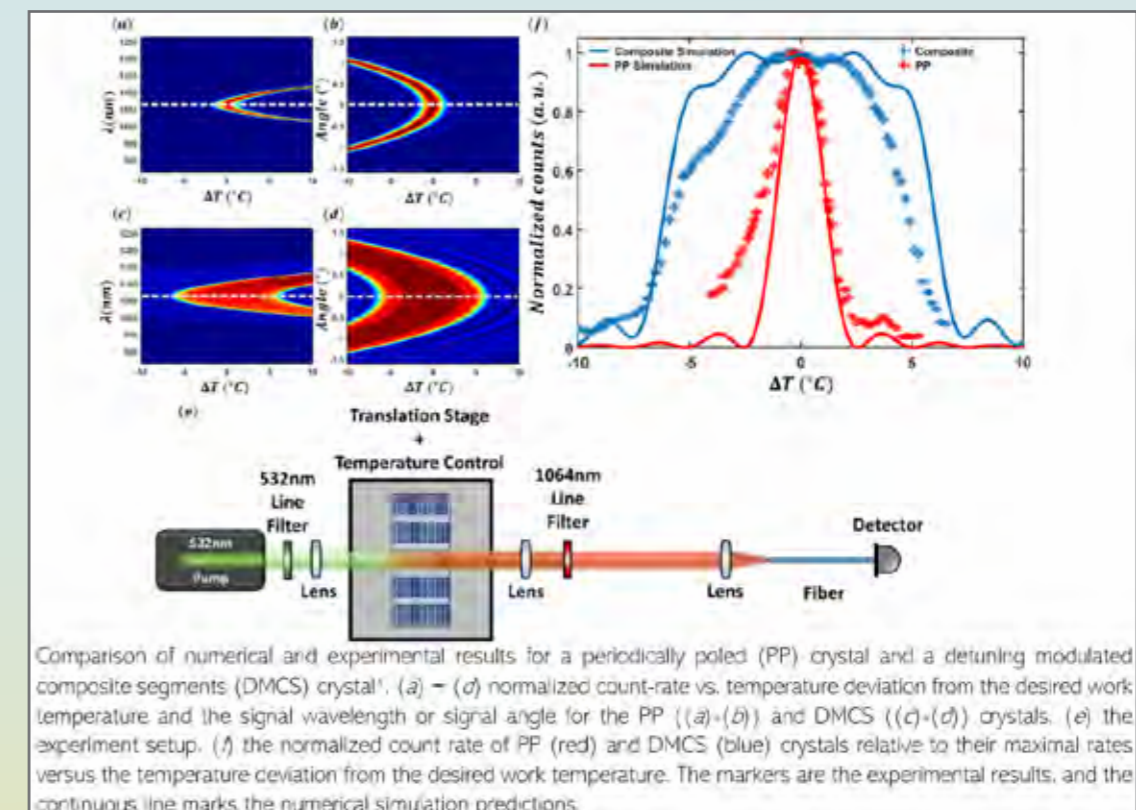
Tel Aviv University

### Authors:

Yuval Rechtes, Muhammad Erew, Ofir Yesharim, Ady Arie, Haim Suchowski  
Tel-Aviv University, Tel Aviv, Israel

### Abstract:

Spontaneous Parametric Down Conversion (SPDC) holds a pivotal role in quantum physics, facilitating the creation of entangled photon pairs [2], heralded single photons and squeezed light, critical resources for many applications in quantum technologies. However, their production is susceptible to physical variations, posing limitations on their robust utility [3]. To overcome these limitations, we introduce a method to significantly enhance the reliability of entangled photon pair generation. Our approach involves introducing a composite design scheme to the SPDC process. The design is based on the development of a theoretical composite segments framework for SU(1,1), offering increased error resilience and robustness of the process. We experimentally demonstrate its practical application by modulating the nonlinear coefficient of a KTP crystal for degenerate 532nm to 1064nm conversion resulting in an effective sevenfold improvement in stability of photon-pair generation and coincidence rate against temperature fluctuations compared to conventional quasi-phase-matching techniques. Furthermore, the presented concept is applicable to other physical systems that exhibit SU(1,1) dynamics. Our methodology can create a leap forward in quantum technologies by significantly enhancing stability and error tolerance, thus paving the way for a new generation of entangled photons sources, holding promise for quantum information processing, communication, and precision measurement applications.





**References:**

- [1] Erew, M., Reches, Y., Yesharim, O., Arie, A. & Suchowski, H. Robust spontaneous parametric down-conversion via detuning modulated composite segments designs.
- [2] Anwar, A., Perumangatt, C., Steinlechner, F., Jennewein, T. & Ling, A. Entangled photon-pair sources based on three-wave mixing in bulk crystals. *Review of Scientific Instruments* 92, 041101 (2021).
- [3] Ling, A., Lamas-Linares, A. & Kurtsiefer, C. Absolute emission rates of spontaneous parametric down-conversion into single transverse Gaussian modes. *Phys Rev A* 77, (2008).

**E Posters Abstracts:****Forward Brillouin Scattering in Few-Mode Fibers****Mr. Elad Layosh***Bar-Ilan University***Authors:**

Elad Layosh, Elad Zehavi, Alon Bernstein, Mirit Hen, Maayan Holsblat, Ori Pearl, and Avi Zadok

**Abstract:**

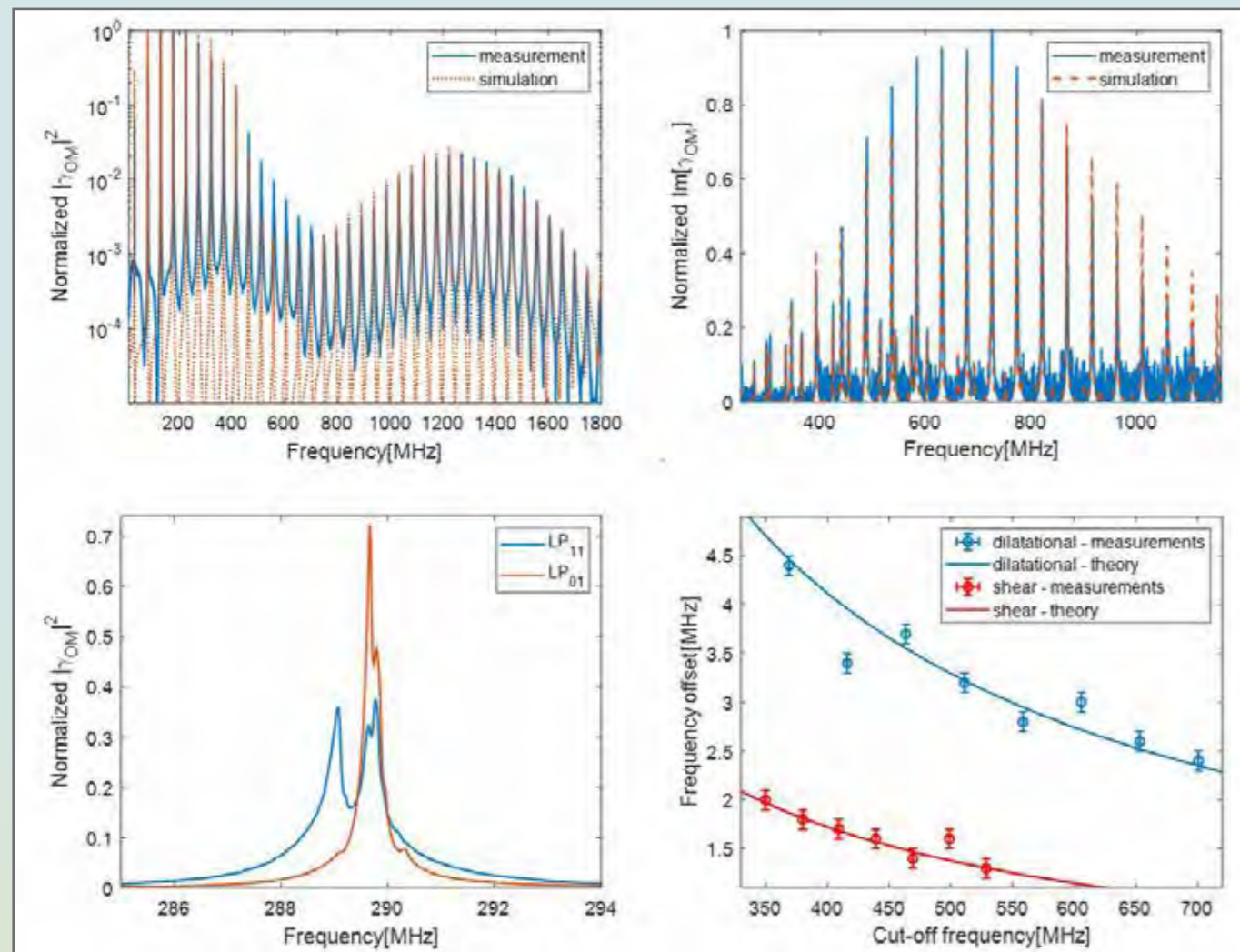
Forward Brillouin scattering is a nonlinear opto-mechanical interaction that couples between co-propagating optical and acoustic waves in a common medium. Two co-propagating pump waves may excite guided acoustic cladding modes through electro-striction. The acoustic modes, in turn, may scatter a third optical probe wave through photo-elasticity. The probe wave may be either phase modulated, polarization rotated, or both. In addition, the two optical pump tones are coupled by the same acoustic waves. The phenomenon has been studied in standard fibers for over 50 years.

Most studies of forward Brillouin scattering in standard fibers were carried out in the single-mode regime, where the two optical fields are guided in the fundamental mode. This restricts the forward Brillouin stimulation for only two specific classes of acoustic cladding modes: purely radial ones, and modes of two-fold azimuthal symmetry. Moreover, the acoustic frequency range is limited up to 600 MHz, and the acoustic modes may be excited only at their cut-off frequencies.

In this work, we extend the study of forward Brillouin scattering to few-mode fibers, through analysis, calculations, and experiments. We observe the Brillouin stimulation of new classes of acoustic cladding modes, with first-order and fourth-order azimuthal symmetries, which are inaccessible in single-mode fibers. The frequencies range of the process is extended to 1.8 GHz. We also report the stimulation of acoustic cladding modes few MHz above their cut-off frequencies, where they are not entirely transverse. The results extend the formulation and scope of fiber opto-mechanics beyond the single-mode regime, and they may find applications in fiber lasers, sensing, and quantum states manipulation.

Figure Text:

Fig. 1. (a): Measured (blue) and calculated (red) normalized spectra of forward Brillouin scattering in a few-mode fiber. The intra-modal process involved two pump waves in the [LP]<sub>02</sub> mode and purely radial acoustic modes. The stimulation of acoustic modes is observed up to 1.8 GHz frequency. The spectrum is markedly different from that of the corresponding process in the fundamental mode. (b): Same as panel (a), for an inter-modal process between one pump wave in the fundamental [LP]<sub>01</sub> mode and another in the [LP]<sub>11</sub> mode group. The process takes place through [TR]<sub>1m</sub> acoustic modes, which cannot be observed in forward Brillouin scattering over single-mode fibers. (c): Magnified view of the measured spectra of intra-modal forward Brillouin scattering. In the orange trace, both pump waves are in the fundamental [LP]<sub>01</sub> mode. The single peak corresponds to a [TR]<sub>2m</sub> acoustic mode. In the blue trace, both pump waves are launched in the [LP]<sub>11</sub> mode group. A second peak is observed 1 MHz below the initial one. That peak corresponds to a [TR]<sub>4m</sub> acoustic mode, which is also inaccessible in single-mode fibers. (d): Circular markers – Differences between the peak frequencies in two spectra of forward Brillouin scattering: inter-modal scattering between one pump wave in the fundamental mode and another in the [LP]<sub>02</sub> mode, and intra-modal scattering in the fundamental [LP]<sub>01</sub> mode. Dilatational (shear) acoustic modes are noted in blue (red). The measurements agree well with theory (solid lines).



## Advancing Temporal Optics into the Quantum Domain

**Prof. Moti Fridman**

*Bar-Ilan University*

### Abstract:

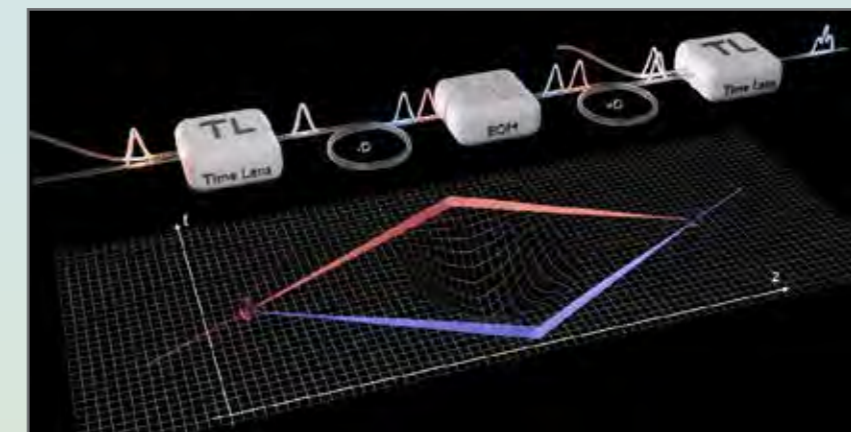
Time-lenses and time-stretch systems enable the measurement of ultrafast phenomena with high temporal resolution and have been employed to study features such as rogue waves and soliton interactions. While previous work has largely focused on classical wave optics, we demonstrate how these advanced temporal techniques can be extended into the quantum regime in three key stages.

First, we utilize temporal-optics devices—time-lenses, time-stretch systems, temporal microscopes, and temporal detectors—to investigate the ultrafast temporal dynamics of quantum phenomena, including photon generation processes, correlated-photon temporal modes, and the evolution of correlations in amplified photons [1].

Second, our time-lenses rely on a four-wave mixing process between a chirped pump wave and an input signal wave. This process inherently produces an output in a squeezed state of light, which we exploit to enhance time-lens sensitivity beyond the shot-noise limit. By arranging two time-lenses in 4f and 8f temporal configurations, we construct temporal interferometers that offer higher temporal resolution and greater sensitivity to ultrafast phase changes than conventional interferometers [2].

Third, by substituting the pump's classical wave with non-classical light, we create non-classical temporal elements. These “non-classical lenses” have no spatial analog and open the door to all-non-classical optical architectures, where both the fields and the optical components are quantum in nature.

In this presentation, we will discuss the theoretical background and experimental realization of all three stages, showcasing how temporal optics can be seamlessly integrated into quantum optics. We will also outline future directions and potential applications of quantum temporal optics in precision measurements, nonlinear photonics, and quantum information processing.



### References:

- [1] S. Meir, A. Klein, H. Duadi, E. Cohen, and M. Fridman, *Opt. Express*, 30(2), 1773 (2022).
- [2] S. Meir, Y. Tamir, H. Duadi, E. Cohen, and M. Fridman, *Phys. Rev. Lett.* 130, 253601 (2023).

## Charac+F8+J8

Dr. Steven Jackel

Tel Aviv University

### Authors:

Steven Jackel (Tel Aviv University, Ramat Aviv, Israel); Ady Arie (Tel Aviv University, Ramat Aviv, Israel)

### Abstract:

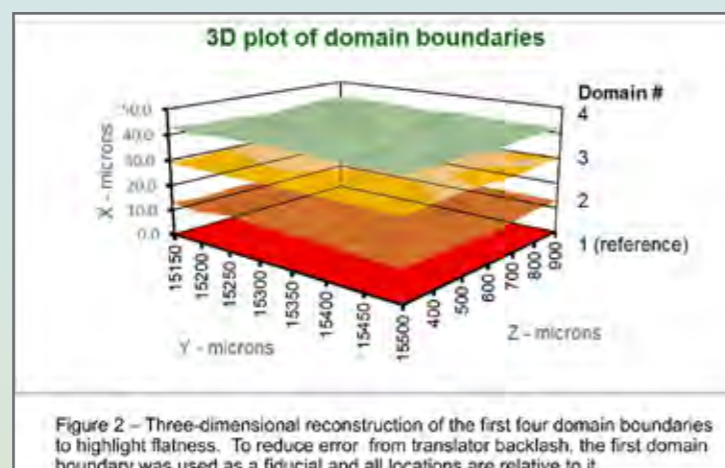
Second harmonic light can be preferentially emitted along domain boundaries within periodically poled crystals (“Cherenkov light”) (1) and/or from interfaces across layered structures (“Bloembergen surface emissions”) (2). These emissions may compliment or interfere with one another in their application.

We report on examination of these emissions from bulk and periodically poled lithium niobate and potassium titanyl phosphate crystals with tightly- focused, 10ns pulses from a 1047nm laser operated at 3kHz. Surface breakdown limited useable average powers to around 35mW. Linear, radial, and azimuthal polarizations were employed.

Light from the focal spot (= 1pixel) within the domain boundary and collected from one lobe within the Cherenkov cone had an average power of up to several 10s of nanowatts. This was sufficient for measurement with a biased Si photodetector or a CMOS camera. By scanning the crystal in three dimensions, a 3D image of the domain boundaries was built up (figure 1).

Positioning the focus on a crystal surface revealed second harmonic propagating parallel to the laser beam. This “0°” harmonic had an average power of several 10s of picoWatt when the crystal was perpendicular to the laser, but increased to nanoWatts when the crystal was rotated to 60–70°. The peak was defined by the balance between a second-order polarizability that increased with angle vs an areal intensity that decreased with angle. Fresnel reflection losses slightly modified the dependence.

Useful interface profiling is limited by the relatively long Rayleigh ranges of the primary and diagnostic lenses. The conjugate application is of more interest i.e., a flat-polished crystal can be scanned through the focus of a test lens to provide a thin source-plane for reimaging with a diagnostic lens (selected only to meet transverse resolution requirements). Sub-Rayleigh range axial beam profiling may, in this way, be achieved.



### References:

1. Cerenkov-Type Second-Harmonic Generation in Two-Dimensional Nonlinear Photonic Structures. S. Saltiel, Y. Sheng, N. Voloch-Bloch, D. Neshev, W. Krolikowski, A. Arie, K. Koynov, and Y. Kivshar. 2009, IEEE J of Quantum Electronics, Vol. 45, pp. 1465–1472.
2. Light Waves at the Boundary of Nonlinear Media. N. Bloembergen, and P. Pershan. 1962, Physical Review, Vol. 128, pp. 606–622.

## Topological synthetic phases in standard optomechanical waveguides

Dr. Arik Bergman

Ariel University

### Authors:

Raphael Chobanyan (Ariel University); Arik Bergman (Ariel University)

### Abstract:

**Objectives:** This work aims to develop an emulator for non-Hermitian lattice models using standard off-the-shelf polarization-maintaining fibers. The emulator is numerically shown to realize several unique features such as the non-Hermitian skin effect and defect-induced localization.

**Methods:** We showcase the proposed emulator by realizing the Su-Schrieffer-Heeger (SSH) dimer chain which is the simplest one-dimensional non-Hermitian lattice model. The lattice sites are composed of discrete frequencies that populate the slow and fast axes of a polarization-maintaining fiber. The alternating hopping amplitudes between adjacent sites are realized by cross-polarization Brillouin-enhanced four-wave-mixing. The dimerization is controlled by the intensities of the counter-propagating pump waves. The increasing wavenumber mismatch across the dimer chain effectively sets the boundaries for the otherwise infinite synthetic lattice. We further show that a PT-symmetric defect state can be formed through backward Brillouin amplification of one of the lattice sites.

**Results:** Through analytical modeling and numerical analysis, we observe the emergence of exponentially localized edge states at the boundaries of the synthetic non-Hermitian SSH lattice. The backward Brillouin gain drives the phase transition of the two-mode defect state, and tips it over to the broken phase regime through the exceptional point singularity. Other characteristic non-Hermitian topological effects such as the breakdown of bulk-boundary correspondence are also observed.

**Conclusions:** The development of a framework for using multimodal light and sound interactions in standard fibers to simulate complex non-Hermitian topological phases represents a significant advancement in the field. Future work will look to study higher-dimensional non-Hermitian systems and explore novel avenues in the non-Hermitian topological band theory using these settings.



## Nonlinear Frequency Conversion and Frequency Combs in Photonic Time-Crystals

Ms. Noa Konforty

Technion– Israel Institute of Technology

### Authors:

Noa Konforty, Moshe-Ishay Cohen, Ohad Segal, Yonatan Plotnik, Mordechai Segev. Solid-State Institute, Technion, Haifa, Israel

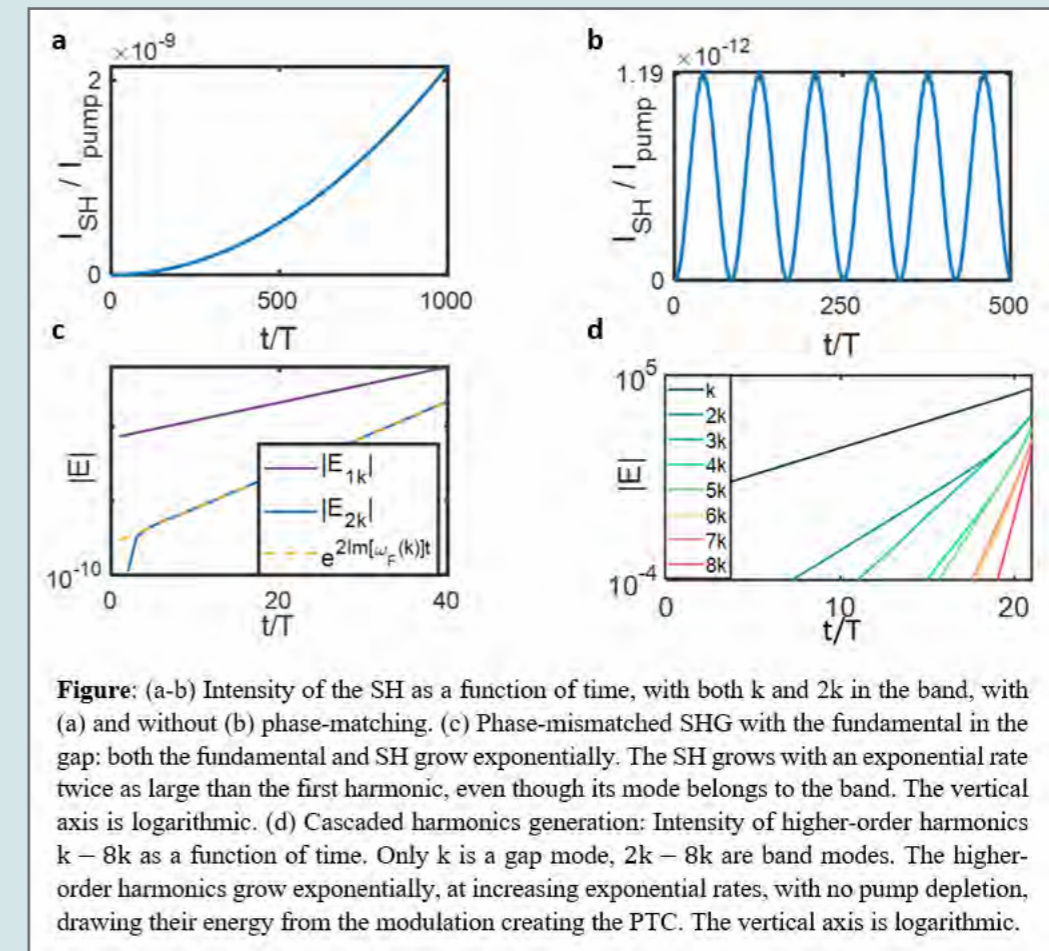
### Abstract:

**Objectives:** Photonic time-crystals (PTCs) are materials with a refractive index that periodically changes in time. PTCs exhibit exponentially growing modes in the momentum bandgap, which arise from the interference between time-refracted and time-reflected waves at the periodic time-interfaces. The momentum bandgap modes contribute to unique light-matter interactions in PTCs. Thus far, light-matter interactions in PTCs were studied mainly in the regime of linear optics. However, the unique dispersion relation and bandgap modes can be utilized to shape nonlinear optical processes in novel ways. In this work we study nonlinear frequency generation processes in photonic time crystals.

**Methods:** We solve analytically the nonlinear wave equation for a PTC with nonlinear susceptibility. We perform numerical simulations of the nonlinear PTC, both in a transfer-matrix and finite-difference time-domain based algorithms.

**Results:** We find solutions for second harmonic generation (SHG) in a nonlinear PTC, identifying the phase-matching conditions of the process. We identify conditions for which the SHG process in a PTC can be enhanced even without phase-matching, drawing energy from the material's modulation. Under these conditions, even if only the fundamental mode is a momentum bandgap mode, the second harmonic will grow with twice the exponential rate of the fundamental. Furthermore, since the process is not depleted, a cascade of higher-order harmonics is generated, each harmonic growing at a stronger exponential rate. This process generates a frequency comb, which can be used to produce ultrashort pulses.

**Conclusions:** In this work we demonstrate how PTCs and time-varying media in general can offer new paradigms for shaping nonlinear frequency conversion processes, and can enable efficient frequency generation in a non-depleted, non-resonant manner, with no phase-matching constraints. Moreover, the cascaded generation of higher-order harmonics can potentially serve as a new process for High Harmonic Generation in solids.



## Direct Comparison Between Bulk and Surface Nonlinearities

Mr. Guy Sayer

Technion – Israel Institute of Technology

### Authors:

Guy Sayer, Matan Iluz, Amit Kam, Guy Bartal. Technion – Israel Institute of Technology. Haifa, Israel

### Abstract:

Nonlinear optics plays a crucial role in modern photonics, often utilizing the nonlinear properties of metals. Most metals are centrosymmetric, meaning their crystal lattices remain invariant under inversion symmetry transformations, which causes their second-order susceptibility to vanish. However, this symmetry is broken at material interfaces, enabling surface nonlinearities alongside the intrinsic third-order susceptibility present in the bulk. Comparing surface and bulk contributions has historically been a significant challenge in nonlinear optics. Here, we employ direct imaging of nanophotonic fields to perform a comparative analysis of the distinct nonlinear mechanisms at gold–air interfaces.

The experimental setup features a nanophotonic gold–air interface where surface plasmon polaritons (SPPs) are excited by a pulsed laser operating at a wavelength of 1560 nm ('signal'). A second pulsed laser beam ('pump'), at 780 nm, is directed onto the sample to overlap with the SPPs, generating two photons through distinct nonlinear processes:

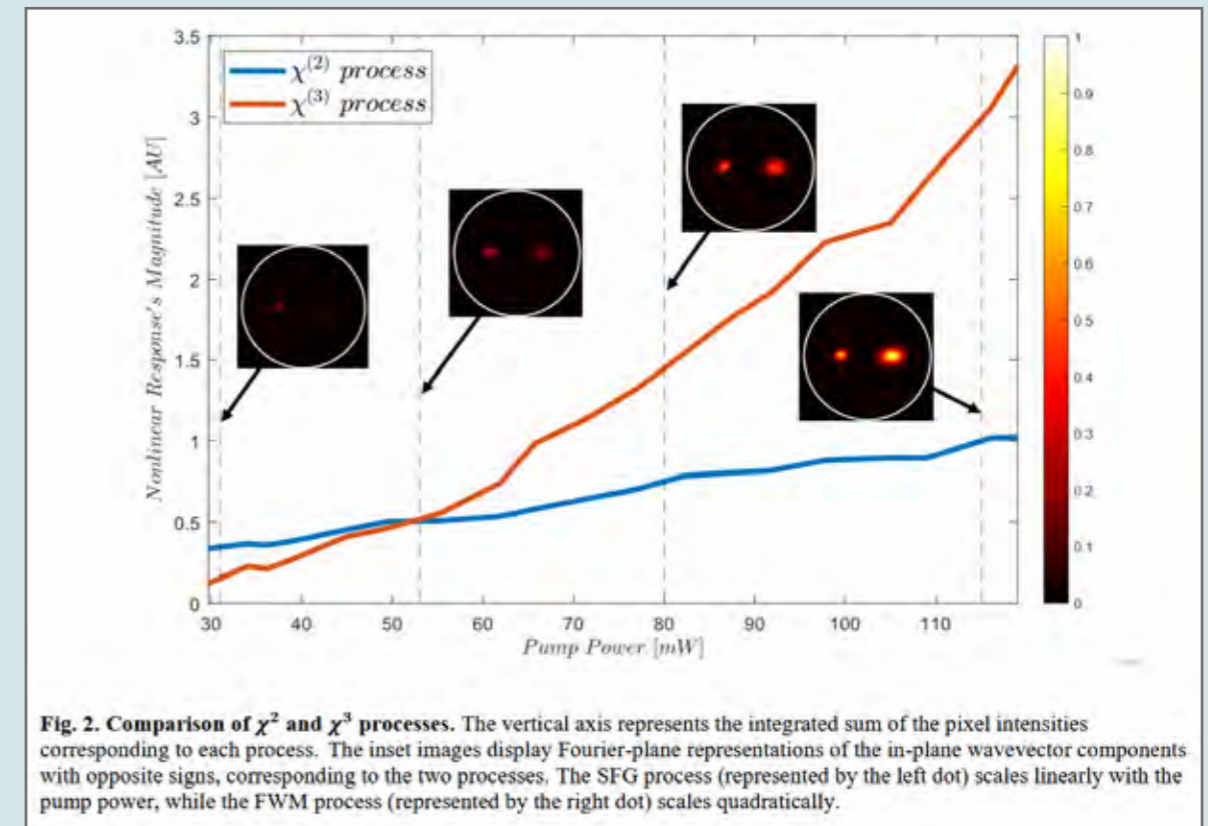
$$\omega_{\text{SFG}} = \omega_{\text{signal}} + \omega_{\text{pump}} \quad (1)$$

$$\omega_{\text{FWM}} = 2\omega_{\text{pump}} - \omega_{\text{signal}} \quad (2)$$

The emitted photons are separated from the pump beam using a dichroic mirror and imaged onto an EMCCD camera at the Fourier plane, mapping the wavevector components of the generated fields. Because the pump frequency is twice the signal frequency, both processes generate nonlinear emissions at the same frequency but with opposite wavevector directions.

The Fourier-space image displays two lobes corresponding to the positive and negative in-plane wavevectors of the plasmonic field. The pump's contribution of two photons to the FWM process and one photon to the SFG process allows the efficiency ratio of the two processes to be controlled by tuning the pump power.

This study demonstrates a direct method for measuring, comparing, and controlling the  $\chi^{(2)}$  surface response and  $\chi^{(3)}$  bulk response by engineering experimental conditions to generate photons with similar frequencies and propagation angles in opposite directions.



## MICRO AND NANO-OPTICS SESSION

### Invited Presentation Abstracts

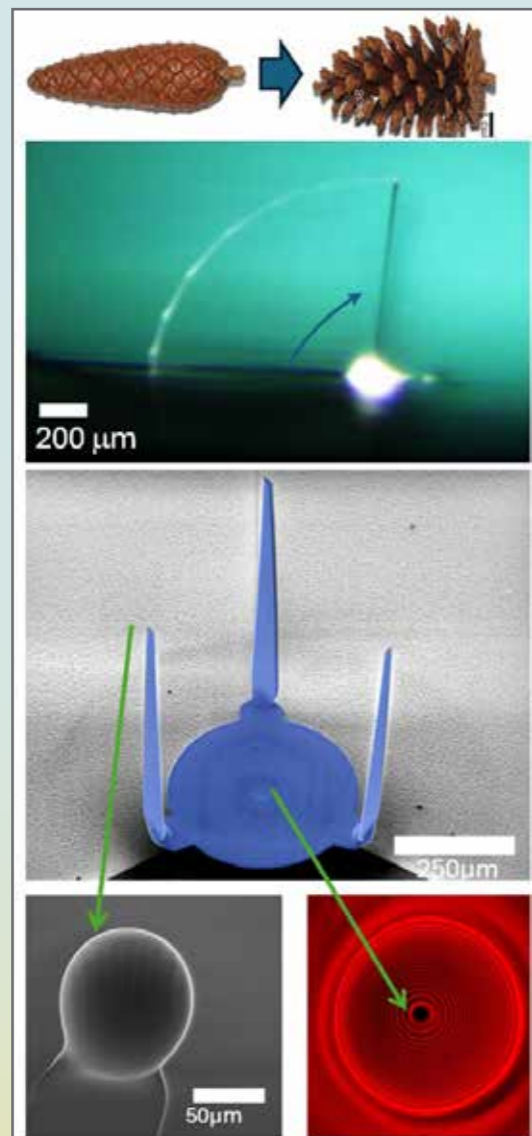
#### On-chip nano-aligned origami at bullet-like, 2000 times the acceleration of gravity

**Prof. Tal Carmon**

*Tel Aviv University*

#### Abstract:

Borrowing hygroscopic principles used in nature for seed-release, we harness surface tension using lasers to melt on-chip SiO<sub>2</sub> sheets, generating snap-motion foldings with nano-resolution alignment, at 19,600 m/s<sup>2</sup> acceleration. Our extremely rapid on-chip folding method might impact 3D-integrated electro-opto-mechanical circuits by allowing 3D nano-alignment capabilities, structural freedom, as well as ultrahigh optomechanical Qs, and size-to-weight ratios. I will also report on a new type of optical vortex allowing droplet carousel where acceleration reaches 1224 times the acceleration of gravity.



#### Mode locking and rogue waves in Q-switched solid-state laser

**Prof. Stanislav Derevyanko**

*Ben Gurion University of the Negev*

#### Authors:

Roza Navitskaya, Ihar Stashkevich ( Faculty of Physics, Belarusian State University, 4 Nezalezhnasti Avenue, Minsk, 220030, Belarus), Alina Karabchevsky and Stanislav Derevyanko ( School of Electrical and Computer Engineering, Ben-Gurion University of the Negev, Beer-Sheva, 8410501, Israel)

#### Abstract:

Spatial and spatio-temporal rogue waves (RWs) are intense “hot spots” that can arise unexpectedly in complex multimode optical systems. Their formation in lasers can be influenced by various factors such as nonlinearity, dispersion, gain, and spatial effects. When nonlinear effects in the laser cavity are minimal, spatial rogue waves can be triggered by the spontaneous phase synchronization of transverse modes with similar frequencies, aided by a spatially anisotropic mode configuration.

Here we describe the creation of spatial rogue waves in an actively Q-switched Nd:YAG laser featuring multiple transverse modes and minimal nonlinear effects within the cavity. Our discussion includes a fundamental theoretical model that successfully replicates the experimental observations of spatial rogue waves in the output Q-switched pulses, attributed to the coherent superposition of transverse modes. The statistical properties of the intensity distribution inside the cavity are influenced by the lasing mode configuration, showing a more pronounced L-shaped distribution in the case of highly anisotropic mode losses and reduced frequency spacing between modes. Conversely, larger frequency spacing between modes leads to mode-locking effects, resulting in periodic dynamics of the transverse beam. These findings suggest that transverse mode-locking and spatial symmetry breaking due to anisotropy in mode configuration are key factors in the emergence of spatial rogue waves in multimode lasers with low nonlinearity.



## Nanometer-scale Phononic Resonators for Far-infrared Radiation

Dr. Itai Epstein

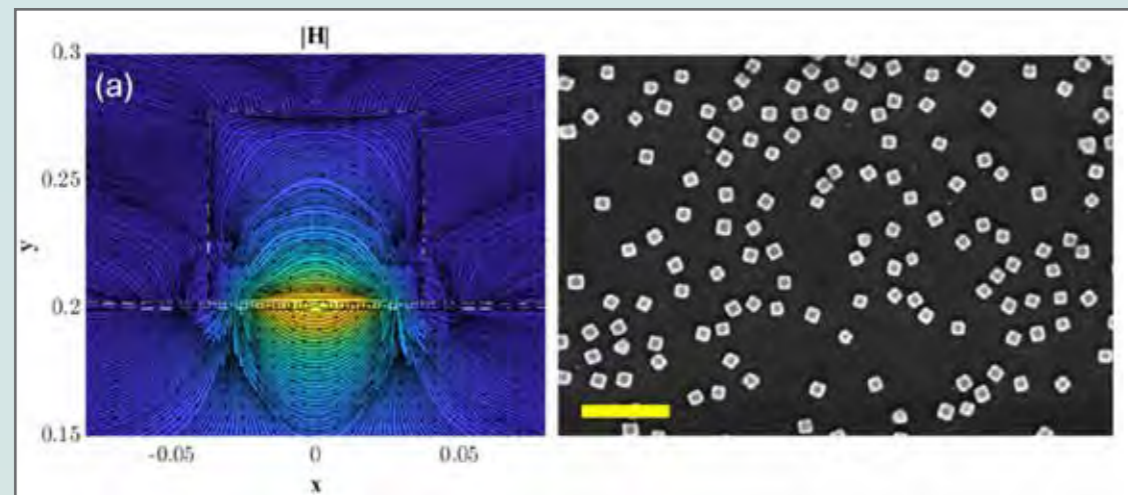
Tel Aviv University

### Authors:

Michael Klein, Itai Epstein

### Abstract:

Long wavelength infrared light introduces hindering challenges in the ability to confine and control such radiation, especially for miniaturized and on-chip applications. In that aspect, acoustic polaritons are highly confined electromagnetic modes that arise from the hybridization of a polariton and its mirror image. Such highly confined modes are usually accompanied by large propagation losses, which reduces their practical utilization in optical devices. However, phonon-polaritons in polar dielectrics offer exceptionally low losses while still maintaining large confinement factors of the optical field. In this work, we present an experimental observation of acoustic phonon polaritons in a system combining optical phonons in silicon-carbide with randomly dispersed, nanometric-size metallic cubes, which act as nanometric resonators for far-infrared light. The method is general and scalable and can be applied to any polar dielectric, covering a wide range of materials and spectral ranges. This new and versatile platform opens up the path for advanced control, manipulation, and sub-diffractive light confinement of optical devices in the long wavelength range.



## Inverse design 50:50 MMI splitters and waveguide couplers having broadband and low loss characteristics

Dr. Aleksei Kukin

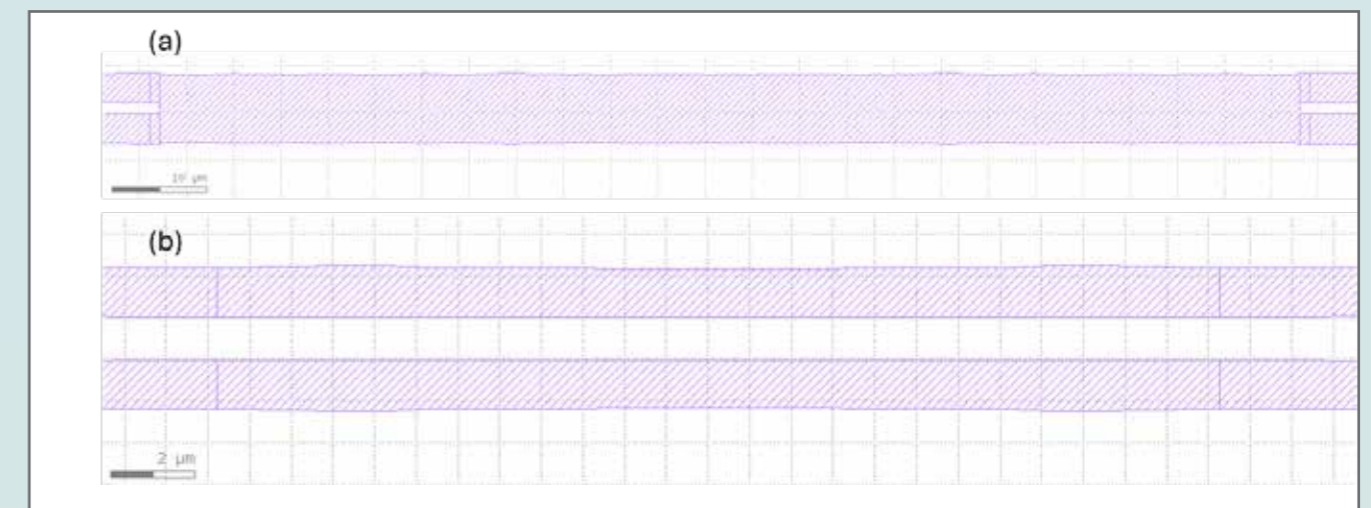
Hebrew University of Jerusalem

### Authors:

Aleksei Kukin, Dan M Marom, Hebrew University of Jerusalem, Jerusalem, Israel

### Abstract:

Our inverse design utilizes silicon nitride waveguides and FDTD simulations controlled by Matlab code, with symmetry constraints to reduce the design space. The shape optimization is based on positioning points (~few tens) connected by a spline curve, with restrictions based on fabrication constraints. The MMI splitter demonstrated symmetrical transmission across both channels within the design wavelength range, with variations in transmission from -3.2 dB to 3 dB. Similarly, the evanescent coupler exhibited crossing transmission curves, with a crossover point near 1550 nm and imbalance values of -2 dB / -4.8 dB at the edges. Both splitters exhibit low excess insertion losses, of less than 0.2 dB.



**Oral Presentation Abstracts:****Ultra-broadband wide-angle anti-reflection scheme utilizing multi-layer resonant metasurfaces****Mr. Yehuda Baum***Tel Aviv University***Authors:**Yehuda Baum<sup>1,4,†</sup>, Dotan Arad<sup>2,†</sup>, Rachel (Gringols) Yarden<sup>2,†</sup>, and Jacob Scheuer<sup>2,3,4</sup>

1 School of Physics and Astronomy, Tel-Aviv University, Tel-Aviv, Israel

2 School of Electrical Engineering, Tel-Aviv University, Tel-Aviv, Israel

3 Center for Light-Matter Interactions, Tel-Aviv University, Tel-Aviv, Israel

4 Center for Nano-Sciences and Nanotechnologies, Tel-Aviv University, Tel-Aviv, Israel †Equal contribution

**Abstract:**

Suppressing reflection at the interface separating media with different optical properties has always been an objective, common to many disciplines involving wave phenomena. This task constitutes an even greater challenge for beams exhibiting complex spatiotemporal profiles as broadband (spectral and spatial) operation is required. Here we present a new approach for obtaining broadband antireflection properties by utilizing nanostructure arrays in a multi-layer metasurface configuration with periodicity in the order of a wavelength. As a concrete example, we show the ability to attain ultra-broadband reflection suppression exceeding  $-30\text{dB}$  in a Silicon-Air interface, over a bandwidth of  $\sim 400\text{nm}$  at telecom wavelengths and an incidence angle of  $\pm 30^\circ$ . This method offers several inherent advantages over moth-eye-like approaches as it allows for a more repetitive fabrication process while facilitating a monolithic, single-material antireflection structure. Furthermore, such AR structures can also be realized using additive manufacturing techniques such as 3D printing and Nano-Imprint Lithography.

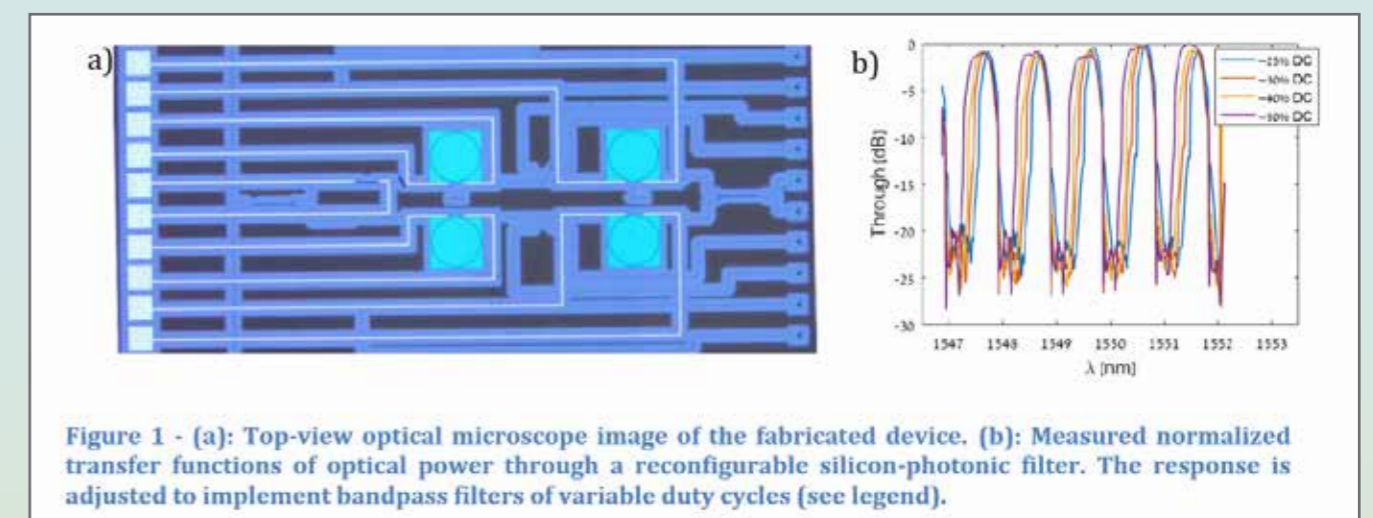
**Highly Reconfigurable Silicon-Photonic Filter Stage****Mr. Matan Slook***Faculty of Electrical and Computer Engineering, the Technion – Israel Institute of Technology***Authors:**

Matan Slook (Technion, Israel), Saawan Kumar Bag (Cielo, Israel), Leroy Dokhanian (Technion, Israel), Shai Ben-Ami (Bar-Ilan University, Israel), Maayan Holsblat (Bar-Ilan University, Israel), and Avi Zadok (Technion, Israel)

**Abstract:**

We present a highly reconfigurable silicon-photonic filter stage incorporating a balanced Mach-Zehnder interferometer (MZI) with two ring resonators integrated into each arm. This configuration allows independent thermo-optic tuning of the optical phase delays in all four rings, as well as the differential phase delay between the two arms of the MZI. Devices were fabricated on a silicon-on-insulator platform using a 220 nm-thick device layer by AMF foundry. The coupling coefficients into the rings were chosen for optimal filter response. Metallic heaters enabled precise control of phase delays, making the device highly versatile.

Experimental results show excellent agreement with theoretical models. Measured transfer functions included sharp bandpass filters with tunable duty cycles (0.25–0.5). Notable achievements include a 0.03 nm transition bandwidth, 20 dB out-of-band rejection, and in-band uniformity of  $\pm 0.2\text{ dB}$ . The filter also achieved a narrow passband with an 8 pm full-width at half-maximum, demonstrating twice the resolution of a single resonator in the same platform, and bandpass filters and narrow passbands down to 1 GHz. These results highlight the potential of reconfigurable silicon-photonic filters for advanced signal processing applications in optical communications and beyond. The demonstrated architecture provides a pathway to dynamic and highly customizable photonic integrated circuits.



## Nature Inspired Design Methodology for a Wide Field of View Achromatic Metalens

**Dr. Jacob Engelberg**

*Hebrew University Jerusalem Israel*

### Authors:

Jacob Engelberg, Ronen Mazurski and Uriel Levi, Hebrew University, Jerusalem, Israel

### Abstract:

**Objective:** The objective of our research is to design a wide field-of-view (FOV) achromatic metalens for the near-infrared (NIR), with parameters relevant to real-world applications, such as a security camera lens. In the design process we point out limiting aberrations, show how to optimize stop position, evaluate performance using accurate performance metrics, and compare to a chromatic metalens. Since it is not possible to achieve diffraction limited performance over the full FOV, we gave preference to the center of the FOV, mimicking the human visual system.

**Methods:** The optimization consisted of two major steps. First is the macro-design of the metalens, where the phase function was optimized for monochromatic illumination at 850nm, at several aperture stop positions, using Zemax. Next comes the nano-design stage, where a nanostructure library of a-Si structures was built using Lumerical FDTD software. A Matlab optimization algorithm was used to select the appropriate nanostructure for each aperture location to achieve an achromatic metalens. A single wavelength dependent phase jump, along the metalens aperture radius, was employed to improve overall performance, giving preference to the center FOV area. Performance was evaluated using an overall performance metric (OPM) [1], thus determining the optimal stop position.

**Results:** A NIR achromatic metalens was designed to operate over a spectral range of 85nm centered on 850nm, with a focal length of 5mm, F/5, and 40° FOV. The OPM was improved by relative amounts ranging from 35% to 95% for different FOVs, compared to a chromatic metalens, with the highest absolute performance occurring on-axis.

**Conclusions:** We presented a design method and rigorous performance analysis of a dispersion engineered achromatic wide-FOV metalens for the NIR, that was designed with parameters relevant to real-world applications, such as a security camera lens. Our results show significant improvement in performance compared to a chromatic metalens.

### References:

[1] J. Engelberg and U. Levy, "Generalized metric for broadband flat lens performance comparison," *Nanophotonics* 11, 3559-3574 (2022).

## Super-resolution Imaging Using Photonic Nanojet through Tapered Optical Fiber

**Ms. Maya Hen Shor Peled**

*Ben Gurion University of the Negev*

### Authors:

M. H. Shor Peled<sup>1</sup> and A. Karabchevsky<sup>1,2\*</sup>

<sup>1</sup> School of Electrical and Computer Engineering, Ben Gurion University of the Negev, Israel

<sup>2</sup> Department of Physics, Lancaster University, LA1 4YB, United Kingdom

\*Corresponding **Author**: alinak@bgu.ac.il

### Abstract:

The resolution limit of conventional optical imaging techniques, imposed by the diffraction of light, restricts the ability to observe nanoscale structures with high precision. This limitation presents significant challenges in understanding biological systems at the nanoscale, which is crucial for gaining insights into disease mechanisms and cellular processes. As a result, there is a growing need for advanced imaging techniques that go beyond the diffraction limit of traditional microscopy [1]. To address this, we utilize the Photonic Nanojet (PNJ) effect, which generates high-intensity, narrow light beams through dielectric structures under plane wave illumination [2].

We demonstrate the resolution of sub-diffraction limit grid lines using a tapered fiber, showcasing its capability in imaging nanoscale structures. Further, we explore the PNJ characteristics by illuminating upright dielectric cylinders with varying diameters (8 to 16 microns). Through experimental imaging and computational simulations, we analyze the full width at half maximum (FWHM) and working distance of the generated PNJ. Our findings indicate that while the FWHM remains relatively constant across different cylinder diameters, the working distance increases with larger diameters. This extended working distance enhances imaging versatility, particularly for applications requiring non-invasive techniques.

By optimizing the fiber diameter to balance resolution and working distance, our approach offers a label-free, sub-diffraction limit imaging solution. This method is particularly advantageous for imaging specimens sensitive to damage from electron microscopy or high-power imaging systems, opening avenues for safer and more effective nanoscale imaging in biological and material sciences.

The research reported in the manuscript was funded by Israel Science Foundation (ISF no. 2598/20).

### References:

[1] Karabchevsky, Alina, et al. "Super-Resolution Imaging and Optomechanical Manipulation Using Optical Nanojet for Nondestructive Single-Cell Research." *Advanced Photonics Research* 3.2 (2022): 2100233.  
[2] Luk'yanchuk, Boris S., et al. "Refractive index less than two: photonic nanojets yesterday, today and tomorrow." *Optical Materials Express* 7.6 (2017): 1820-1847.



## Observation of Localized Resonant Phonon Polaritons in Biaxial $\alpha$ -MoO<sub>3</sub> Nanoparticles

Dr. Asaf Farhi and Dr. Daniel Beitner

### Authors:

Daniel Beitner<sup>1,2,3†</sup>, Asaf Farhi<sup>3†</sup>, Ravindra Kumar Nitharwal<sup>4</sup>, Tejendra Dixit<sup>5</sup>, Tzvia Beitner<sup>1</sup>, Shachar Richter<sup>1,2</sup>, SivaRama Krishnan<sup>4</sup> and Haim Suchowski<sup>2,3</sup>

- 1 Department of Materials Science and Engineering, Faculty of Engineering, Tel Aviv University, Tel Aviv, Israel
- 2 University Centre for Nanoscience and Nanotechnology, Tel Aviv University, Tel Aviv, Israel
- 3 School of Physics and Astronomy, Faculty of Exact Sciences, Tel Aviv University, Tel Aviv, Israel
- 4 Department of Physics, Indian Institute of Technology Madras, Chennai, India
- 5 Department of Electronics and Communication Engineering, Indian Institute of Information Technology Design and Manufacturing (IIITDM), Kancheepuram, India

\*Corresponding Author. Email: Beitner@mail.tau.ac.il

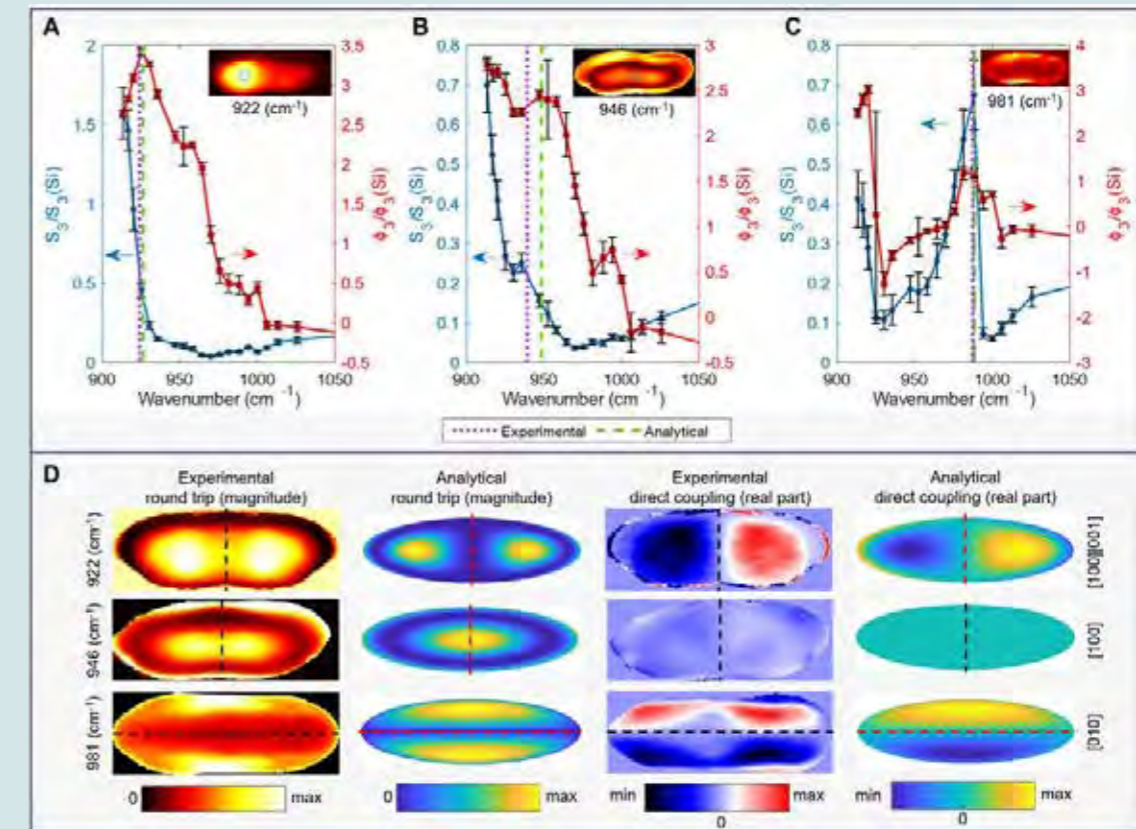
† These Authors contributed equally to this work

### Abstract:

**Goals:** Anisotropic subwavelength particles combine the strong response and tunability of nanostructures with the exotic properties of anisotropic materials, leading to numerous potential applications in photonics, biomedicine, and magnetism. Furthermore, anisotropic particles are ubiquitous in naturally occurring and artificial systems such as ice and dust grains, liquid crystal droplets, and ferromagnetic particles, and they may correspond to atoms in magnetic fields and anisotropic molecules. However, modes and resonances have so far been observed only for uniaxial particles and eigenmode analysis of anisotropic particles has been very limited, hindering their understanding and broad applicability. We aim to bridge these experimental and theoretical gaps by synthesizing biaxial particles, probing their modes and resonances, and deriving an analytical theory for the modes and resonance conditions of anisotropic particles.

**Methods+Results:** Here we synthesize biaxial  $\alpha$ -MoO<sub>3</sub> particles using a novel technique of femtosecond-pulse laser ablation. We then observe for the first time the fundamental and high-order modes of biaxial particles using hyperspectral near-field imaging in the midIR. Finally, we analytically derive the quasiolelectrostatic eigenmodes and eigenpermittivity relations of anisotropic spheres and ellipsoids. We show that anisotropic particles exhibit novel radiation patterns. In addition, we identify axial-eigenpermittivity sum rules, resulting in resonance splitting in uniaxial and biaxial particles and eigenvalue degeneracy in uniaxial spheres.

**Conclusions:** Our findings reveal the physics of polaritons in biaxial subwavelength particles for both the first and higher-order modes. Our study parallels the shift in isotropic plasmon-polariton research towards nanostructure resonators in the visible and infrared, which enabled manipulation of the spectral response in unprecedented manners. Our results pave the way for a new generation of directional and multispectral detectors and biomarkers in unexplored spectral regions and apply to additional fields of physics such as magnetism, heat conduction, and potentially atomic and molecular physics.



## Negative Index makes a Perfect Time Lens

Mr. Oded Schiller

Technion – Israel Institute of Technology

### Authors:

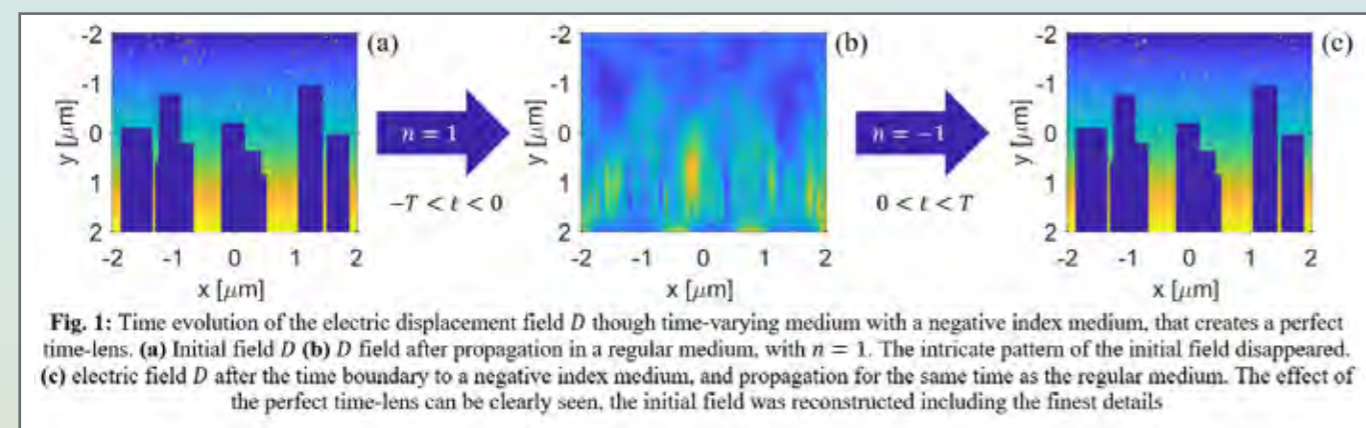
Oded Schiller, Yonatan Plotnik and Mordechai Segev – Technion – Israel Institute of Technology, Haifa, Israel

### Abstract:

**Objectives:** Negative index materials have amazing optical properties. Negative index materials can be used as a perfect lens, a material that unlike a traditional lens images both the propagating and evanescent waves. This property can be used to brake the diffraction limit, and creates a sub wavelength imaging. Following the discovery of the perfect lens property huge community of people tried to create a metamaterial with an effective negative index. A negative index material was observed experimentally both in microwave and the optical frequencies. We set on finding the effects of incorporating negative index materials into a rapidly changing time varying medium. The field of time varying medium is receiving a lot of attention in recent years mainly because of the advances in the experimental ability to change the refractive index of materials in time scales of a single cycle.

**Results:** We find that when the refractive index has an abrupt transition in time from  $n_1=n$  to  $n_2=-n$  the wave traveling in the medium experience perfect phase conjugation. Using this fact, we show that this material acts as a perfect time lens, a material that reverse the time evolution of the EM fields perfectly. Meaning that in order to image the fields at time  $t=-T$  one needs to abruptly change the refractive index from  $n_1=1$  to  $n_2=-1$  at time  $t=0$  and let the fields propagate until  $t=T$ . Notice the difference to the spatial case. in the temporal case the reconstruction is of the fields in the past, and not in a different spatial position.

**Conclusions:** This work shows the potential that a time varying medium hold for imaging, an application that was not thought of up until now. We show this by finding that a negative index material modulated in time can be used as a perfect time lens.



## Total Angular momentum as a Pathway to Entangle Surface-Plasmon Polaritons

Mr. Amit Kam

Technion – Israel Institute of Technology

### Authors:

Amit Kam, Shai Tsesses, Yigal Ilin, Kobi Cohen, Yaakov Lumer, Lior Fridman, Stav Lotan, Anatoly Patsyk, Liat Nemirovsky-Levy, Meir Orenstein, Mordechai Segev and Guy Bartal

### Abstract:

Nanoscale quantum optics offers a promising platform for quantum information applications due to its compact size, minimal losses, compatibility with on-chip technologies, and operation at room temperature. [1-4].

In the vein, single photons encode quantum information across various degrees of freedom, including spin and orbital angular momentum (OAM). However, In the near field regime as in nanophotonic systems the spin and OAM are inseparable and cannot serve as good quantum numbers such that only the total angular momentum (TAM) of the mode could serve as a good quantum number.[4-6]

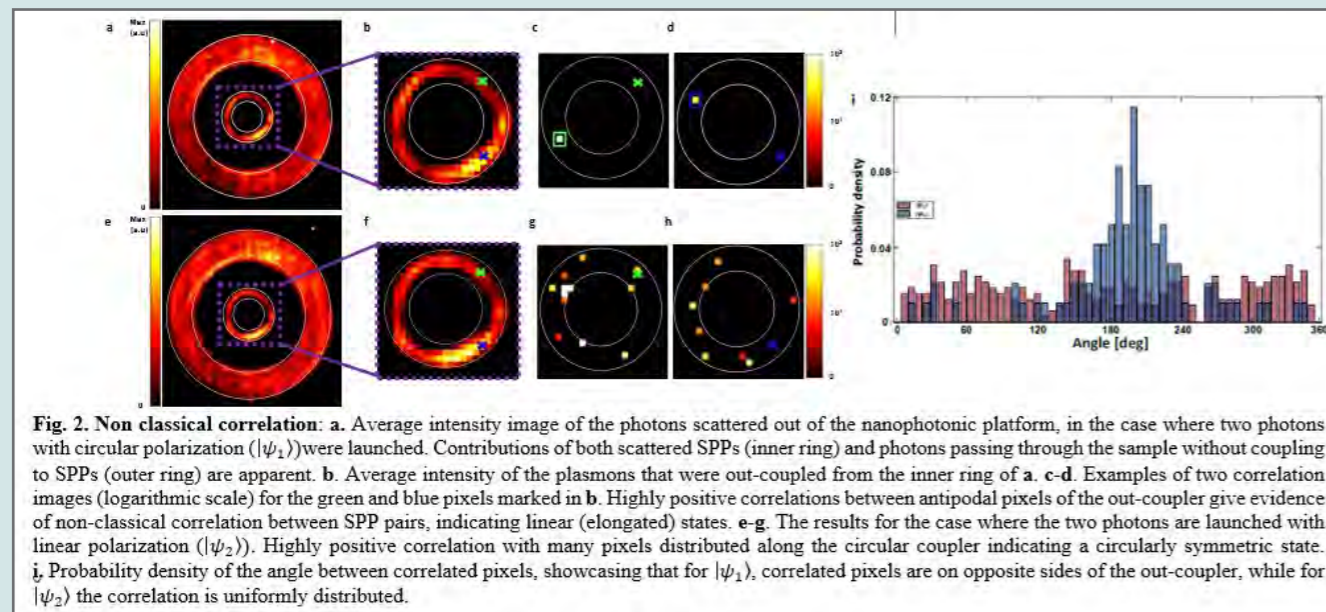
Using a nanophotonic platform comprising a gold-air interface with Archimedean spiral gratings, we coupled photon pairs from spontaneous parametric down-conversion into surface-plasmon polaritons (SPPs). This process entangles photon pairs in the TAM basis, enabling unique quantum correlations. Two input states, defined by different polarization products, were converted into TAM-based entangled states. The resulting entangled-state in the mode basis are either  $|\psi_1\rangle = 1/\sqrt{2} [ |2_{(J_0+J_2)}, 0_{(J_0-J_2)}\rangle + |0_{(J_0+J_2)}, 2_{(J_0-J_2)}\rangle ]$  or  $|\psi_2\rangle = 1/\sqrt{2} [ |2_{(J_0)}, 0_{(J_2)}\rangle - |0_{(J_0)}, 2_{(J_2)}\rangle ]$ , where  $J_0, J_2$  are the total angular momentum, carrying 0 or 2 quanta of total angular momentum[6-7].

We out-couple the entangled plasmonic state with a circular-coupling slit that retains their angular momentum, at a rate of  $\sim 250$  SPPs per second, and image the outgoing photons onto an EMCCD camera. We calculate the correlation between the signal in different pixels of the image by using the cross-correlation algorithm:  $\Gamma_{ij} = 1/N \sum_t x_i^t \cdot x_j^t - 1/(N-1) \sum_t x_i^t \cdot x_j^{(t+1)}$  Where  $x_i^t$  is the intensity value of pixel  $i$  in frame  $t$ , and  $N$  is the number of frames.[8]

The results showed high correlations between opposite sides of the out-coupling structure for  $|\psi_1\rangle$  state and uniform correlations across the out-coupler for the  $|\psi_2\rangle$ . These findings align with theoretical predictions of TAM-entangled SPPs.

In conclusion, We demonstrated the first experimental observation of non-classical correlations between single nanophotonic modes carrying TAM, providing a pathway for on-chip quantum information processing in higher-dimensional Hilbert spaces.





#### References:

- [1] J. Wang et al, Nat. Photon. 14, 273 (2020).
- [2] A. Mair et al, Nature 412, 313 (2001).
- [3] J. T. Barreiro et al, Phys Rev Lett 95, 260501 (2005).
- [4] A. Altewischer et al, Nature 418, 304 (2002).
- [5] Y. Gorotetsky et al, Phys. Rev. Lett. 101, 043903 (2008).
- [6] S. Fakonas James, et al, New Journal of Physics 17, 023002 (2015).
- [7] A. Kam et al, CLEO Fundamental Science FF2C. 5 (2023).
- [8] H. Defienne, et al, Physical review letters 120, 203604 (2018).

#### E Posters Abstracts:

##### Observation of spectrally continuous resonance enhancement by mode coalescence

Mr. Nitzan Shani

Tel Aviv University

#### Authors:

Nitzan Shani, Amit Shakya, Fan Cheng, Vladimir Shuvayev, Lev Deych, and Tal Carmon

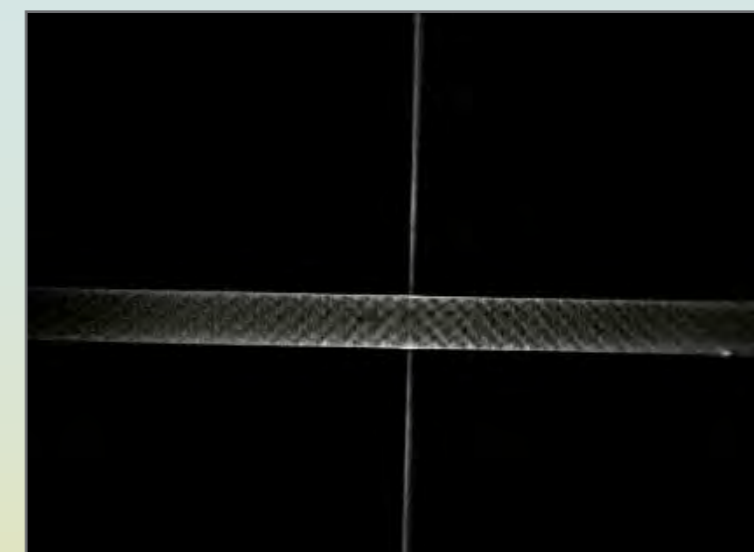
#### Abstract:

The ability to excite several cavity modes with degenerate and continuous frequencies would allow resonantly enhancing fundamental interactions between incoherent light and matter, as well as applications ranging from supercontinuum micro-emitters to perfect absorbers of white light.

However, crossings between levels—that is, degeneracies in resonance frequencies—were considered sets of singular coincidences due to the nature of spectral resonances to intersect at a point upon tuning a parameter.

Here, by making cylindrical microcavities axially semi-continuous, we demonstrate, for the first time, hosting several modes that continuously cover the entire spectrum. We film movies of this continuum using a fluorescent spatial mode-mapping technique, revealing a variety of evolving mode structures while simultaneously monitoring their spectral transmission. As different resonances join here to co-host light; we name this phenomenon – “mode coalescence.”

Mode coalescence might impact engineering applications such as supercontinuum emitters by transforming them from pulsed operation to continuous in-time [CW] and also from tabletop devices to microscales. From a broader fundamental perspective, mode coalescence is relevant for all waves in nature (e.g., sound, matter waves, and quantum probability densities) and might impact fundamental studies in wave-matter interaction, applications in perfect absorption of earthquakes, and energy harnessing from sea waves.





## Spectrally and spatially analyzing soft resonators

Mr. Fan Cheng

Tel Aviv University

### Authors:

Fan Cheng<sup>1</sup>, Vladimir Shuvayev<sup>2</sup>, Amit Kumar Shakya<sup>1</sup>, Mark Douvidzon<sup>3</sup>, Lev Deych<sup>4</sup> and tal carmon<sup>1,\*</sup>

1 School of Electrical Engineering, Tel Aviv University, Tel Aviv 6997801, Israel

2 Physics Department, Queens College of CUNY, Flushing, Queens, New York 11367, USA

3 Solid State Institute, Technion-Israel Institute of Technology, Haifa 3200003, Israel

4 The Graduate Center of CUNY, 365 5th Ave., New York, New York 10016, USA

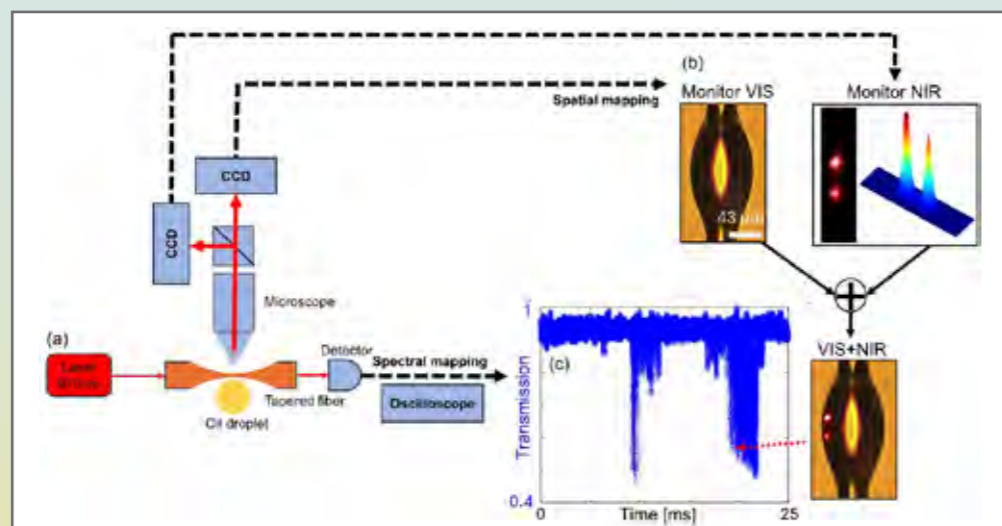
### Abstract:

**Objectives:** We constructed ultra-high-Q opto-capillary resonators capable of facilitating energy exchange between optical waves and capillary waves. By operating on the blue or red side of the optical resonance, optical excitation or cooling of capillary oscillations can be achieved, respectively.

**Methods:** In our experimental setup, illustrated in Fig. 1 (a), a 970 nm laser is directed into a tapered optical fiber, with the fiber's output signal detected by a photodetector. Another tapered fiber tip is dipped in a small amount of silicone oil, which acts as an optical resonator. This fiber tip is mounted vertically on a translation stage, enabling precise adjustment in the relative position between the tapered fiber and the oil droplet. Surface tension and gravity facilitate stable attachment of a single silicone oil droplet to the fiber tip, as shown in Fig. 1(b), ensuring an untouched regime between the tapered fiber and the droplet. The transmission spectrum of the tapered fiber serves as a spectral mapping of the resonator's characteristics, depicted in Fig. 1(c). To spatially map the resonator modes, we employed a microscope system and a near-infrared (NIR) camera, capturing mode dynamics originating from back reflection, as shown in Fig. 1(b). The optical mode displayed in Fig. 1(b) correlates with the transmission gaps observed in Fig. 1(c), indicating via a red arrow.

**Results:** Bidirectional laser wavelength scanning reveals distinct transmission characteristics. When the wavelength decreases, the transmission spectrum is narrower compared to when the wavelength increases. The theoretical results demonstrate an agreement with the experimental observations.

**Conclusions:** We achieved optical excitation and cooling of capillary oscillations on the blue and red sides of the optical resonance.



## Plasmonic Enhancement of Surface Acoustic Wave – Photonic Integrated Devices in Silicon

Mr. Leroy Dokhanian

Faculty of Electrical and Computer Engineering and Solid State Institute, Technion – Israel Institute of Technology

### Authors:

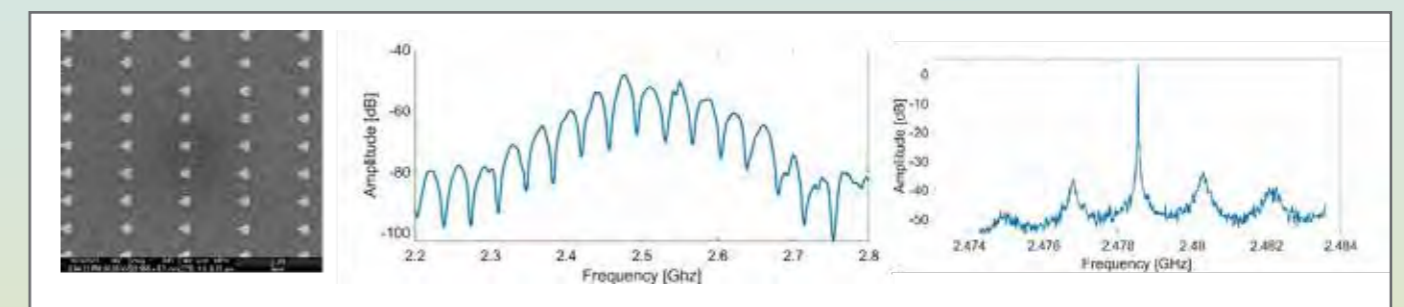
Leroy Dokhanian, Saawan Kumar Bag, Mirit Hen, Inbar Shafir, Matan Slook, Shai Ben-Ami and Avi Zadok

### Abstract:

Surface acoustic wave (SAW) devices have been an anchor of analog electronics for decades. SAW devices have been traditionally implemented over piezoelectric substrates and via electronic interfaces. In recent years, our group has introduced SAWs to standard silicon photonic circuits [1]. The acoustic waves are stimulated via thermo-elastic actuation: the absorption of modulated pump light in periodic metallic gratings and their subsequent thermal expansion and contraction [2]. The resulting strain pattern launches SAWs towards photonic circuit elements [2]. Radio-frequency information is retrieved in the optical domain via photo-elastic modulation of a probe wave within the silicon photonic circuit [1]. This technology enables true time delays, up to 200 ns on-chip, within less than a millimeter. The concept was also used in microwave-photonic filters, thin-film analysis, and opto-mechanical oscillators. However, the intrinsic inefficiency of thermo-elastic actuation results in substantial losses of radio-frequency power, by 65–70 dB [1].

This work introduces a 20 dB improvement of power transmission through the SAW-photonic devices based on plasmonic enhancement of the thermo-elastic actuation mechanism. The uniform stripes of the metallic gratings are replaced with unit cells optimized for surface plasmon resonance at 1550 nm [3] (Fig. 1, left). Figure 1(center) presents the measured transfer function of a SAW-photonic microwave filter, demonstrating transmission losses of only 48 dB. Figure 1(right) presents the output spectrum of an opto-mechanical oscillator based on the same device, exhibiting oscillations at 2.479 GHz with a sidemode suppression ratio of 39 dB, a 33 dB enhancement over previous designs using uniform grating stripes.

Fig. 1: (left) Scanning electron microscope image of part of a metallic grating, comprised of unit cells designed for plasmonic-enhanced absorption. (center): Measured transfer function of electrical power through a SAW-photonic microwave filter. (right): Radio-frequency power spectrum of an electro-mechanical SAW-photonic oscillators at 2.479 GHz.



## Accurate Modeling of Directional Couplers with Oxide Cladding: Bridging Simulation and Experiment

Mr. Yuval Warshavsky

Tel Aviv University

### Authors:

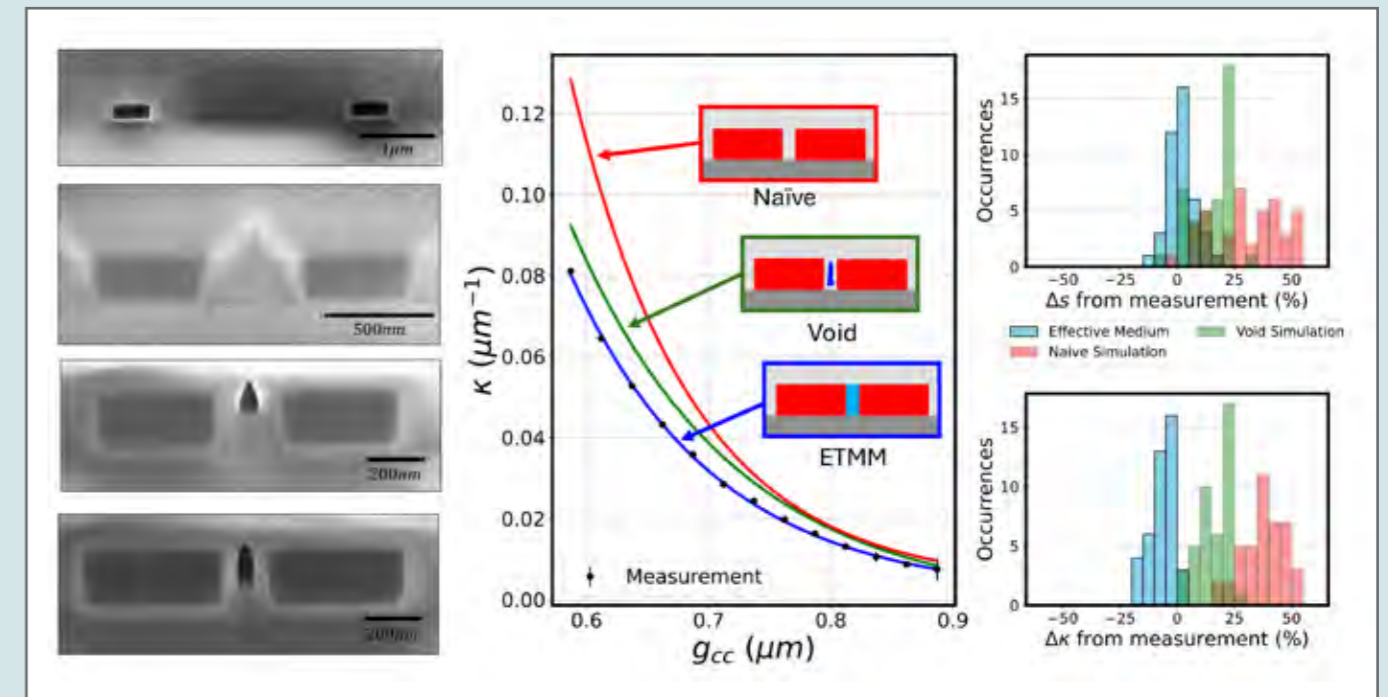
Yuval Warshavsky, Tel Aviv University, Tel Aviv, Israel Yehonathan Drori, Quantum Pulse Ltd., Tel Aviv, Israel Jonatan Piasetzky, Tel Aviv University, Tel Aviv, Israel Amit Rotem, Quantum Pulse Ltd., Tel Aviv, Israel Ofer Shapiro, Quantum Pulse Ltd., Tel Aviv, Israel Yaron Oz, Tel Aviv University, Tel Aviv, Israel Haim Suchowski, Tel Aviv University, Tel Aviv, Israel

### Abstract:

Directional couplers (DCs) are fundamental building blocks of photonic integrated circuits (PICs), playing a crucial role in applications such as power splitting, interference control, and quantum gate implementation. Despite their importance, significant discrepancies between simulated and experimental performances often hinder reliable operation. These discrepancies arise primarily from unknown fabrication-induced density variations and voids in oxide cladding, which are not accounted for in conventional simulation models. In this study, we present the Effective Trench Medium Model (ETMM), a novel approach that accurately predicts DC behavior by incorporating these previously overlooked cladding inhomogeneities. Our work combines experimental optical characterization, scanning electron microscopy (SEM), and advanced numerical simulations to systematically analyze the impact of cladding density variations. SEM imaging revealed that voids enlarge as the wall-to-wall gap between waveguides decreases, significantly affecting the coupling coefficient and SU(2) symmetry parameters. By modeling these effects, the ETMM achieves unprecedented accuracy, reducing coupling prediction errors from 45% in conventional simulations to less than 1.4%. This improvement translates to precise control over coupling coefficients and oscillation frequencies, critical for applications in quantum information processing and optimization-based PIC design.

Furthermore, we validated ETMM across a range of devices with varying geometries, demonstrating its robustness and scalability. The insights provided by this model not only enhance the reliability of PIC simulations but also pave the way for designing compact, high-performance photonic devices. This advancement is particularly significant for applications in quantum information processing, where fault-tolerant operation requires sub-percent accuracy in device behavior.

In conclusion, the ETMM represents a transformative step toward bridging the gap between simulation and experiment in PICs. By enabling reliable and efficient device fabrication, it sets the stage for the next generation of scalable and high-precision photonic technologies.



## Angle Limiting Non-Local Metasurfaces For the NIR

**Mrs. Shany Z. Cohen**

*Bar Ilan University*

### Authors:

Shany Z. Cohen, Vladimir Kostriukov, Sukanta Nandi and Tomer Lewi

### Abstract:

**Conclusions:** The presented non-local metasurface design demonstrates effective polarization-independent angular filtering capabilities, offering an alternative approach to conventional local metasurfaces. The experimental results suggest that non-local interactions can be effectively utilized for angular manipulation of electromagnetic waves. This approach may be applicable to various optical systems requiring precise angular control, including free-space optical communications and imaging applications. Further investigation of bandwidth limitations and scaling to other wavelength ranges would be beneficial for practical implementation of this technology.

## Spatio-Temporal Near-Field Nanospectroscopy of PbTe Mie-Resonators

**Dr. Sukanta Nandi**

*Faculty of Engineering and Institute of Nanotechnology and Advanced Materials, Bar-Ilan University, Ramat Gan- 5290002, Israel*

### Authors:

Sukanta Nandi<sup>#,1,2</sup>, and Tomer Lewi<sup>\*1,2</sup>

1 Faculty of Engineering, Bar-Ilan University, Ramat Gan- 5290002, Israel

2 Institute of Nanotechnology and Advanced Materials, Bar-Ilan University, Ramat Gan- 5290002, Israel

Contact Emails: #sukanta.nandi@biu.ac.il, \*tomer.lewi@biu.ac.il

### Abstract:

**Introduction and Background:** Lead chalcogenides are promising for nanophotonics due to their high refractive indices, mid-infrared (MIR) transparency, and exceptional thermo-optic coefficients. This work reports the hydrothermal synthesis and MIR resonant properties of lead telluride (PbTe) hoppercubes (HCs) in the near-field, both in the spatial and temporal domains.

**Objectives:** Investigate Mie-resonant properties of PbTe HCs and then employ scattering-type scanning near-field optical microscopy (s-SNOM) coupled with pump-probe spectroscopy to study the spatially varying scattered signals, and to investigate the ultrafast tunability and carrier dynamics.

**Methods:** Far-field reflection Fourier transform infrared spectroscopy (FTIR) was conducted with an FTIR spectrometer coupled to an IR microscope. Spatio-temporal near-field nanospectroscopy was performed using s-SNOM with pump-probe spectroscopy, employing a pulsed 780 nm beam ( $\approx 91$  fs) for pumping and a broadband MIR laser (4.5–15  $\mu\text{m}$ ) for probing.

**Results:** Far-field spectroscopy of HC resonators revealed subwavelength confinement with a unit cell size of  $\approx \lambda/6$ , highlighting their ultracompact nature. s-SNOM measurements showed edge signals up to five times stronger than the center ( $\approx 600$ – $700$  nm apart), indicating enhanced absorption at the HC centers. Nano-FTIR hyperspectral scans mapped near-field amplitude and phase, capturing higher-order modes with Q-factors close to 100 [1]. Near-field pump-probe nanospectroscopy further revealed ultrafast carrier dynamics and active tunability, evidenced by modulated and shifted spectra under optical pumping, unlike the negligible response in bulk PbTe crystals.

**Conclusions:** MIR high-index PbTe HC structures with subwavelength confinement and open-face voids offer potential for biosensing, nanoscale optical trapping, and ultracompact nanophotonic devices. s-SNOM analysis further reveals local optical properties, enabling advanced functionalities such as quantum sensing and nonlinear light-matter interactions.

### References:

[1] S. Nandi, T. Shimoni, E. Yitzchaik, and T. Lewi, *Adv. Optical Mater.* 12(25), 2400646 (2024)



## 7-Source × 6-Mode Micro-Scale Photonic Lantern Spatial Multiplexer 3D-Printed on Multi-Mode VCSEL Array

Mr. Yoav Dana

Hebrew University of Jerusalem

### Authors:

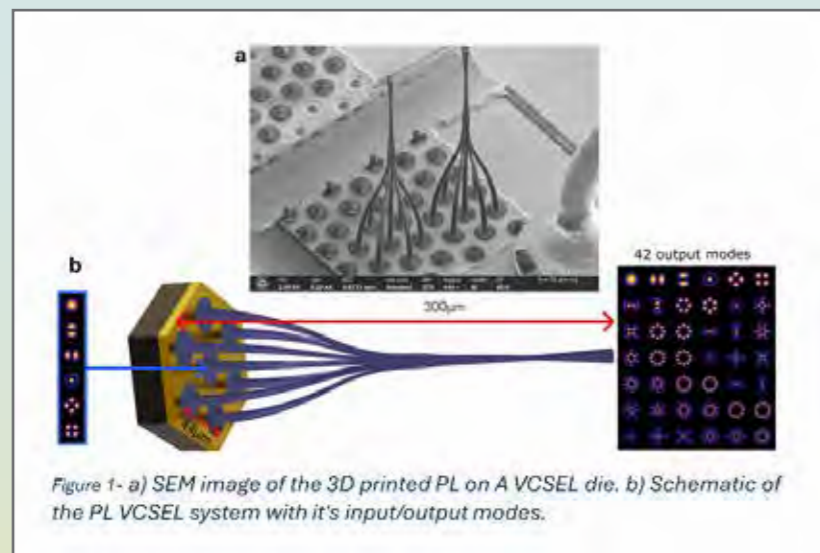
Ksenia Shukhin, Aleksei Kukin, Yehudit Garcia, Dan Marom

### Abstract:

Photonic lanterns (PLs) are spatial multiplexers which are used in high-capacity mode-division-multiplexed (MDM) optical communication networks and free-space optical systems. They efficiently convert between a multi-mode (MM) optical waveguide and a discrete array of single-mode (SM) waveguides through an adiabatic spatial transition. PLs have traditionally been fabricated using fiber fusion and direct laser writing in glass, typically resulting in millimeter-scale devices, or 3D nano-printing with polymer core/air cladding waveguides, leading to micro-scale PL.

This work demonstrates a PL, converting MM inputs from seven sources—each supporting six spatial modes—into a 42-mode output waveguide. Unlike traditional spatial multiplexers designed for SM input sources, this PL accommodates multimode inputs. Its design was optimized using genetic algorithms and FDTD simulations, alongside an insertion loss (IL) estimation method that reduced transfer matrix calculations from 42 to only 2 simulations per iteration. We fabricated the PL using 3D nano-printing and characterized it using off-axis digital holography, with all 42 guided modes injected via spatial light modulator-generated patterns. A low IL of  $-1.6$  dB was achieved.

Further, the PL was integrated with a multi-mode VCSEL array through direct printing onto the VCSEL die, enabling a compact and efficient spatial multiplexing setup. The optical transmission loss was measured below  $-1.5$  dB, with excess coupling efficiency into a 42-mode fiber estimated below  $-1.5$  dB. These results were validated through complex electric field measurements using self-interference and spatial filtering techniques at the VCSEL-integrated PL output.



## Self-assembled colloidal photonic structures for Next generation X-ray detectors

Dr. Rotem Strassberg

Technion – Israel Institute of Technology

### Authors:

Rotem Strassberg<sup>1,2</sup>, Akihiro Nakanishi<sup>3</sup>, Betty Shamaev<sup>1</sup>, Shaul Katznelson<sup>2</sup>, Roman Schuetz<sup>2</sup>, Georgy Dosovitskiy<sup>2</sup>, Shai Levy<sup>1</sup>, Orr Be'er<sup>1</sup>, Saar Shaek<sup>1</sup>, Tomoya Onoe<sup>4</sup>, Taiki Maekawa<sup>4</sup>, Rino Hayakawa<sup>4</sup>, Kazuma Tsuji<sup>4</sup>, Kei-ichiro Murai<sup>3,4</sup>, Toshihiro Moriga<sup>3,4</sup> and Yehonadav Bekenstein<sup>1,2</sup>

<sup>1</sup> Department of Materials Science and Engineering, Technion – Israel Institute of Technology, 32000 Haifa, Israel

<sup>2</sup> The Solid State Institute, Technion – Israel Institute of Technology, 32000 Haifa, Israel

<sup>3</sup> Department of Chemical Science and Technology, Graduate School of Advanced Technology and Science, Tokushima University, 2-1 Minami-Josanjima, Tokushima, 770-8506, Japan

<sup>4</sup> Department of Applied Chemistry, Graduate School of Science and Technology for Innovation, Tokushima University, 2-1 Minami-Josanjima, Tokushima, 770-8506, Japan

### Abstract:

High-energy radiation detection is being revolutionized by integrating photonic elements into scintillators, transforming the field of scintillating materials [P.Singh et al., ACS Nano. 18, 14029–14049 (2024)]. In this study, we propose a scalable and cost-effective method to achieve tunable emission across the visible spectrum by colloidal self-assembly of photonic crystals on scintillator surfaces. We demonstrate this concept, for  $\text{Eu}^{3+}/\text{Tb}^{3+}$ -doped Gd and Ta oxides. Widely available and affordable colloidal nanospheres of  $\text{SiO}_2$  or PMMA are self-assembled on the scintillators forming photonic crystal layers. The size of the nanospheres, which determines the photonic band gap, is carefully optimized to match the desired emission lines of  $\text{Eu}^{3+}/\text{Tb}^{3+}$ . The resulting structures are homogeneous and closed-packed  $\text{SiO}_2$  or PMMA nanosphere coatings with a clear photonic bandgap in the visible range. Under X-ray excitation, the scintillators covered with our photonic layers, exhibit enhanced light extraction in the direction perpendicular to their surface, compared to isotropic emission in the bare scintillators without the photonic layers. Such scintillation directionality combined with a proper photodetector will result in higher efficiency of the overall detection system. Moreover, X-ray imaging analysis demonstrates an enhancement of 25% in system resolution of the scintillator supplemented with photonic layers compared to unmodified scintillators. We envision that the versatility of our approach allows compatibility with various scintillators and colloidal nanocrystals, offering a cost-effective and scalable solution for industries requiring high-resolution imaging and high-performance detection systems.

## Phonon Polariton Resonators for long wavelength Radiation

Mr. Michael Klein

Tel Aviv University

### Authors:

Michael Klein, Tel Aviv University, Tel Aviv, Israel; Jean-Paul Hugonin, Université Paris-Saclay, Palaiseau, France; Itai Epstein, Tel Aviv University, Tel Aviv, Israel

### Abstract:

Acoustic polaritons are highly confined electromagnetic modes that arise from the hybridization of a surface polariton and its mirror image. While these modes offer high optical field confinement, they are typically hindered by significant propagation losses, which reduce their practical utilization in optical devices. In this context, surface-phonon-polaritons (SPhPs), i.e. propagating electromagnetic modes resulting from the coupling between phonons and photons, offer exceptionally low losses while maintaining large confinement factors of the optical field. However, their acoustic equivalent, the acoustic-phonon-polaritons (APhPs), has not been experimentally documented until now.

In this work, we present an experimental observation of APhPs using a novel system incorporating a silicon-carbide (SiC) substrate with randomly distributed silver nanocubes. These combined SiC-nanocube structures function as single, nanometer-scale APhP resonators that are efficiently excited from the far field. We show that these resonators are able to confine far-IR radiation with mode volume confinement factors up to  $9 \times 10^{-7}$ , and that the response frequency can be controlled and manipulated by dependency on the nanocube size.

The method is general and scalable and can be applied to any polar dielectric, covering a wide range of materials and spectral ranges. This new and versatile platform may open the path for advanced control, manipulation, and sub-diffractive light confinement of optical devices in the long wavelength range.

## Fabrication of microlens array by polymerization shrinkage

Mr. Ofek Efraim

Technion- Israel Institute of Technology

### Authors:

Ofek Efraim, Omer Luria, Valeri Frumkin, Moran Bercovici

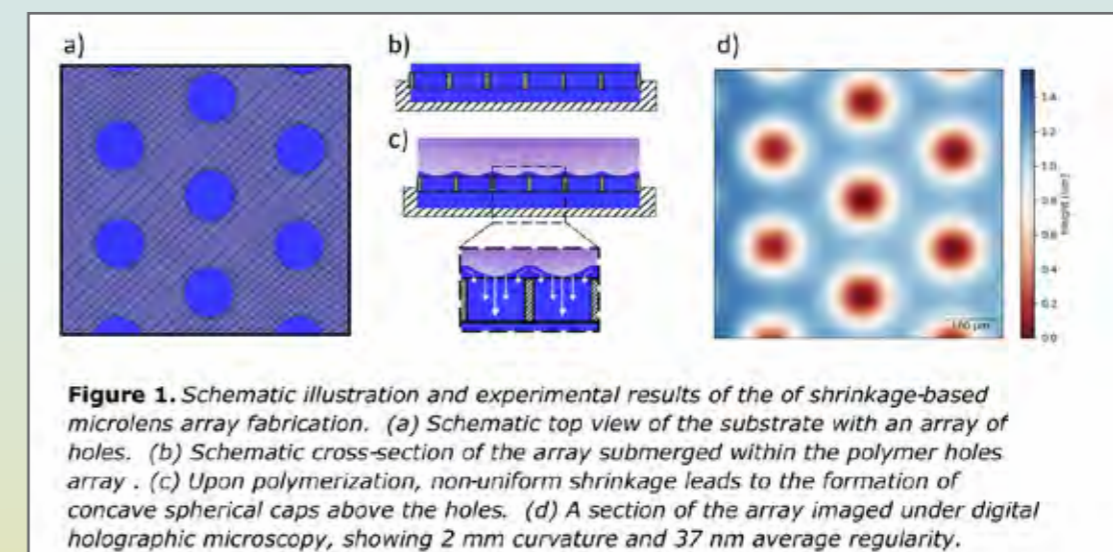
### Abstract:

Microlens arrays have diverse applications in imaging(1), illumination(2,3), sensing(4), and communication(5). However, their optical specifications pose significant manufacturing challenges. Beyond the demands for a specific numerical aperture (NA), smoothness, and shape regularity of individual lenslets, array fabrication requires high uniformity across thousands of lenslets.

Current methods fall into two categories: direct methods relying on surface tension phenomena (e.g., thermal reflow, etching assisted by thermal reflow, and inkjet deposition) and indirect methods using molds created via single-point diamond turning or reactive ion etching(6). Direct methods typically provide high surface quality for an individual lenslet, but the reliance on surface chemistry to control wetting properties limits their NA range and uniformity(6). Mold-based approaches are faster and less sensitive to surface chemistry but existing methods result in lower surface quality(3). Furthermore, high precision molds are expensive and become cost-effective only for large-scale manufacturing.

We here present a novel approach for fabrication of high quality microlens array molds that leverages the interplay of surface tension and polymer shrinkage in thin liquid films. We utilize a solid substrate containing an array of through-holes submerged in a liquid polymer such that the holes are entirely filled and a thin uniform film forms on its upper surface. Upon polymerization, the interplay between polymerization rate, volumetric shrinkage, and flow rates results in an array of smooth localized spherical deformations.

We investigate the degrees of freedom of the method and the range of lenslets that can be produced, and demonstrate the creation of a staggered array of 100  $\mu\text{m}$  diameter lenslets with a radius of curvature of 2mm. We achieve an average regularity of 37 nm RMS across 449 lenslets, with a surface roughness of < 1nm. The entire process requires minutes to complete and can be useful both for prototyping and mass manufacturing applications.



**References:**

1. Hu, X. et al. Measurement Technologies of Light Field Camera: An Overview. *Sensors* 23, 6812 (2023).
2. Zimmermann, M., Lindlein, N., Voelkel, R. & Weible, K. J. Microlens laser beam homogenizer: from theory to application. in *Laser Beam Shaping VIII* vol. 6663 9–21 (SPIE, 2007).
3. Li, L. & Yi, A. Y. Design and fabrication of a freeform microlens array for uniform beam shaping. *Microsyst Technol* 17, 1713–1720 (2011).
4. Zhou, W., Raasch, T. W. & Yi, A. Y. Design, fabrication, and testing of a Shack–Hartmann sensor with an automatic registration feature. *Appl Opt* 55, 7892–7899 (2016).
5. Edwards, C. A., Presby, H. M. & Dragone, C. Ideal microlenses for laser to fiber coupling. *Journal of Lightwave Technology* 11, 252–257 (1993).
6. Ottevaere, H. et al. Comparing glass and plastic refractive microlenses fabricated with different technologies. *J. Opt. A: Pure Appl. Opt.* 8, S407 (2006).

**Nanoscale MOS Capacitors Applications in Photonics****Dr. Avi Karsenty**

*Jerusalem College of Technology (JCT), JCT Nanotechnology Center for Research and Education, Advanced Laboratory of Electro-Optics (ALEO)*

**Authors:**

Matan Levi<sup>1,2</sup>, Avraham Chelly<sup>3,4</sup>, Avi Karsenty<sup>1,2,\*</sup>

1 Advanced Laboratory of Electro-Optics, Jerusalem College of Technology, Jerusalem, Israel

2 Nanotechnology Center for Research & Education, Jerusalem College of Technology, Jerusalem, Israel

3 Faculty of Engineering, Bar-Ilan University, Ramat Gan, 5290002, Israel

4 Nanotechnology Center, Bar-Ilan University, Ramat Gan, 5290002, Israel

\* Corresponding **Author**, E-mail: karsenty@jct.ac.il

**Abstract:**

**Objectives:** This research numerically explores the applications and future prospects of micro and nanoscale MOS capacitors toward integration in photonic systems using traditional CMOS technology. Components like these have emerged as versatile building blocks for photonic systems, enabling a wide range of applications, from optical modulators to sensors, with low cost, high performance, and energy efficiency.

**Methods:** Simulations were performed for illumination and dark conditions on two capacitors, termed NANOCAP and MICROCAP, using COMSOL Multiphysics®.

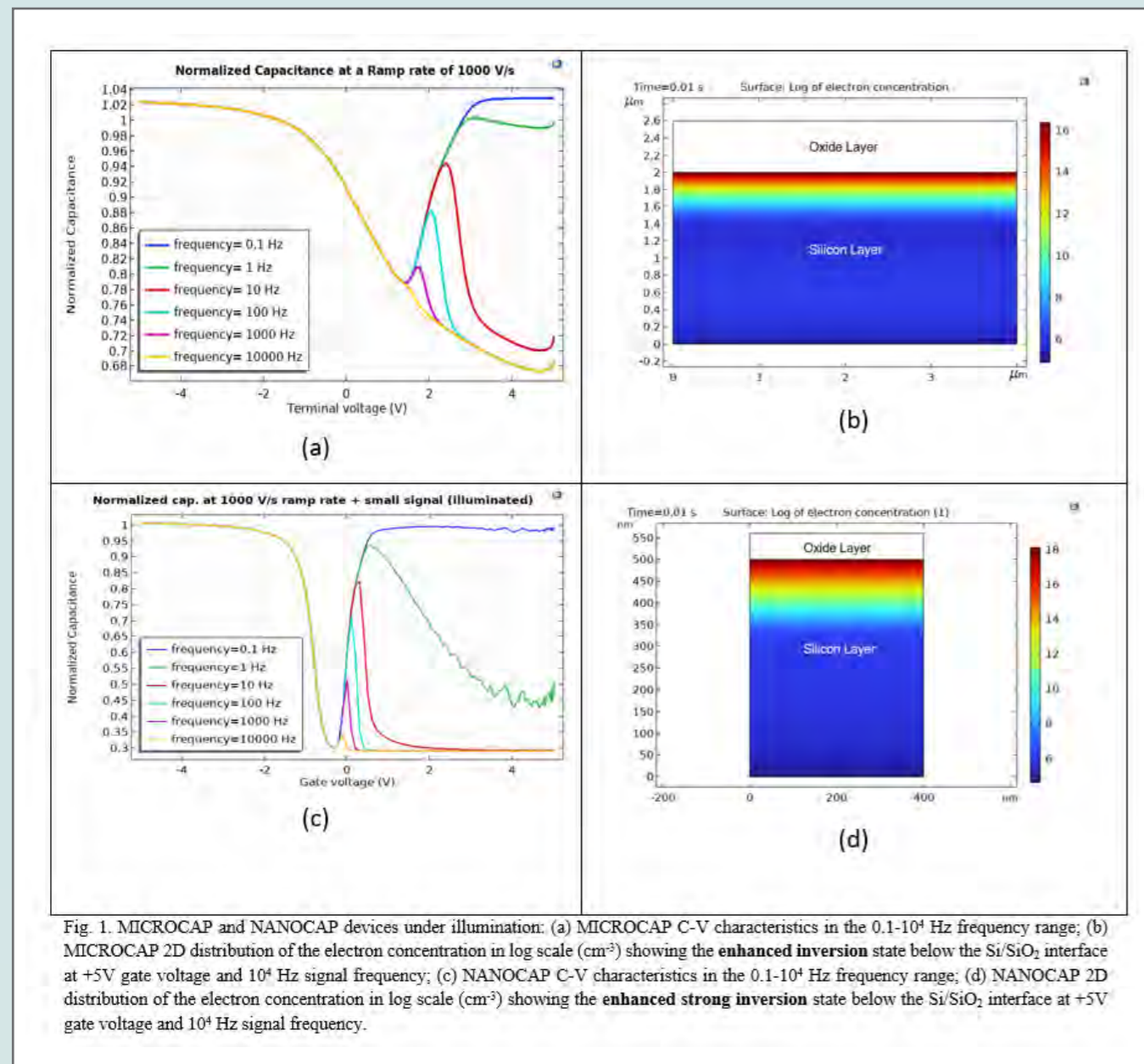
**Results:** Under illumination, NANOCAP achieves semi-equilibrium of the enhanced inversion layer at a higher frequency and lower gate voltage than MICROCAP. This difference, which can be advantageous for light sensitivity, is related to the stronger electric field in NANOCAP's thinner oxide layer, which attracts more minority carriers per unit area to the silicon-oxide/silicon interface for a given positive voltage. Indeed, since the electric field needs to be established across both the oxide and the depletion region, thinner oxide contributes to a larger overall depletion width.

**Conclusions:** Our numerical simulations of external illumination's influence on NANOCAP's C-V characteristic demonstrate the possibility of transforming a passive MOS capacitor into an active photonic device without changing its structure. While the photo-generation effects enhanced the inversion effect of the MOS capacitor, shrinking the device in the nanoscale dimensions leads to a significant enhancement of the inversion effect and to a decrease of the transit time. NANOCAP seems to be a promising device for electro-optical active demodulation.

**References:**

1. A. Karsenty, "Overcoming Silicon Limitations in Nanophotonic Devices by Geometrical Innovation: Review (Invited Article)," *IEEE Photonics Journal*, vol. 15, no. 4, pp. 1–19, 2023.
2. A. Bennett, et al., "Fast Optoelectronic Responsivity of metal-oxide-semiconductor nanostructures," *Journal of Nanophotonics*, vol. 10, no. 3, p. 036001, 2016.





## Engineering a multilayer structure for nanoscintillator with enhanced absorption and fast light emission

Dr. Georgy Dosovitskiy

*Technion- Israel Institute of Technology*

### Authors:

Orr Be'er, Avner Shultzman, Rotem Strassberg, Georgy Dosovitskiy, Noam Veber, Roman Schutz, Charles Roques-Carnes, Ido Kaminer, and Yehonadav Bekenstein

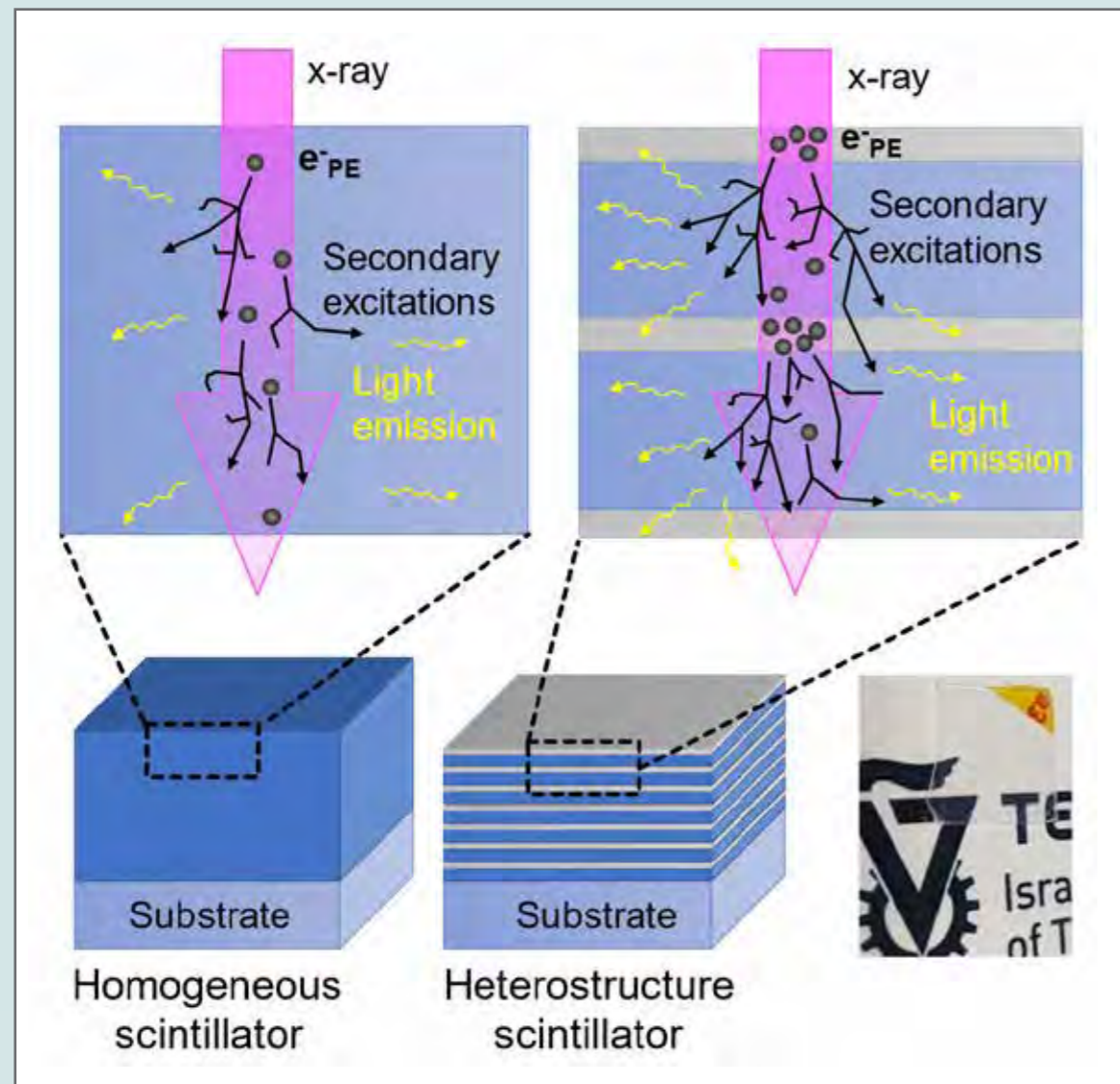
### Abstract:

**Objectives:** Short emission rise and decay times are among the most sought-after properties in modern scintillators, demanded for advanced diagnostic techniques. Plastic scintillators boast fast emission with decay times down to 2 ns, but suffer from low stopping power towards X-rays because of their low density and atomic numbers, which limits their detection efficiency. We overcome this limitation by creating a heterostructure scintillator of alternating nanometric layers, combining fast light-emitting polymer scintillator layers and transparent stopping layers with increased radiation attenuation factor.

**Methods:** We spin-coat multilayer structures consisting of emitting layers of EJ-296 scintillator and stopping layers of PVA-TiO<sub>x</sub>H cross-linked polymer with thicknesses of hundreds of nanometers and measure their light emission under X-ray excitation in spectroscopic and imaging modalities. We also use Monte Carlo modeling (Geant 4) and develop a theoretical framework for layer architecture optimization.

**Results:** A stopping layer thickness has the optimal value to maximize the light output of the hybrid material, reflecting the balance between the fraction of the X-rays stopped by the material, and the fraction of their energy deposited in the emitting layers. The result agrees with Geant 4 modeling. Ti loading has an upper limit, above which particulate inclusions form in the stopping layers, deteriorating the material's transparency. The hybrid sample with a thickness of 6 μm demonstrated the same value of an edge spread function as a homogeneous scintillator layer of equal thickness and light output equal to a 10 μm homogeneous sample, providing significant gain to MTF and DQE. Optimization using the developed theoretical framework has shown that gradually decreasing stopping layer thicknesses provides the optimal light yield.

**Conclusions:** This design increases light yield by up to 1.5 times and enhances imaging resolution by a factor of 2 compared to homogeneous polymer scintillators, due to the ability to use thinner samples.



## Spectroscopy Measurements of hBN-Encapsulated TMD Monolayers from Room to Cryogenic Temperatures

Mr. Matan Meshulam

Tel-Aviv University

### Authors:

Matan Meshulam, Itai Epstein

### Abstract:

Monolayer transition metal dichalcogenides (TMDs) exhibit a set of unique properties that allow them to support robust excitons in the visible to near-infrared (NIR) spectral range. Reduced dielectric screening due to the 2D nature of the monolayers lead to enhanced Coulomb interactions, which results in high exciton binding energies, placing the excitonic energy level well within the electronic bandgap. Also, when reduced from multilayer to monolayer form, TMDs undergo a transition from an indirect to a direct band structure, which enhances exciton formation. Together, these factors make excitons the dominant contributors to the optical response of 2D TMDs.

These pronounced excitonic effects enable diverse optoelectronic and photonic applications, including excitonic photodetectors, light-emitting diodes (LEDs), tuneable and flexible optoelectronic devices, and single-photon emitters. To achieve a more detailed characterization of the optical and physical properties of these excitons, measurements on high-quality samples are essential for accurately extracting these quantities.

In contrast to previous works, which have been limited to either a single TMD, or non-encapsulated monolayers, this work presents a comprehensive spectroscopic study of all four common TMDs, using high-quality crystals encapsulated in hexagonal boron nitride (hBN) across a wide temperature range, helping to display a complete picture of the excitonic properties in TMDs in high quality samples, and extracts from them physical properties such as the exciton dielectric functions and their decay lifetimes.



## Orbit-Orbit Photonics: Harnessing Vortex-Trajectory Interactions for Light Manipulation

Dr. Raghvendra P. Chaudhary

Ben-Gurion University of the Negev

### Authors:

Raghvendra P. Chaudhary and Nir Shitrit, School of Electrical and Computer Engineering, Ben-Gurion University of the Negev, Be'er Sheva 8410501, Israel

### Abstract:

**Introduction:** Light can carry three types of angular momenta: a spin angular momentum, an intrinsic orbital angular momentum (OAM), and an extrinsic OAM. The interplay between these momenta yields the spin-orbit interaction (SOI) of light, in which the spin (circular polarization) controls the spatial degrees of freedom of light: either the extrinsic OAM (trajectory) or the intrinsic OAM (vortex). While the SOI of light has been studied extensively, the interaction between the intrinsic OAM and the extrinsic OAM—the orbit-orbit interaction (OOI) of light—has remained elusive. In this interplay, helical phase fronts of vortices control the trajectory of light. Strikingly, the OOI of light significantly enhances the toolbox available for controlling light by leveraging the manifold OAM states for vortex-controlled light manipulation, in contrast to SOI-based light manipulation, exploiting the binary polarization helicity.

**Objectives:** We report the OOI of light in a plasmonic ellipse cavity, whose unique geometry facilitates the OOI when a vortex is considered in one of the foci of the ellipse. Here, the OOI is achieved by the interplay between the vortex of the source and the ellipse-induced transverse shift of the source beam, positioned at one of focal points.

**Methods:** We performed numerical simulations to calculate the electromagnetic near fields of the plasmonic ellipse cavity for observing the vortex-dependent shifts manifesting the OOI.

**Results:** The OOI of light in the plasmonic ellipse cavity induces transverse vortex-dependent shifts—shifts depending on both the vortex helicity and strength—at the second focal point (Fig. 1). Moreover, we demonstrated information processing via on-chip OAM demultiplexing based on the OOI.

**Conclusions:** By utilizing the multiple OAM states as a new degree of freedom in light manipulation, the OOI offers great potential for OAM-supported applications, including high-bandwidth optical communications, enhanced resolution in imaging and microscopy, and many more.

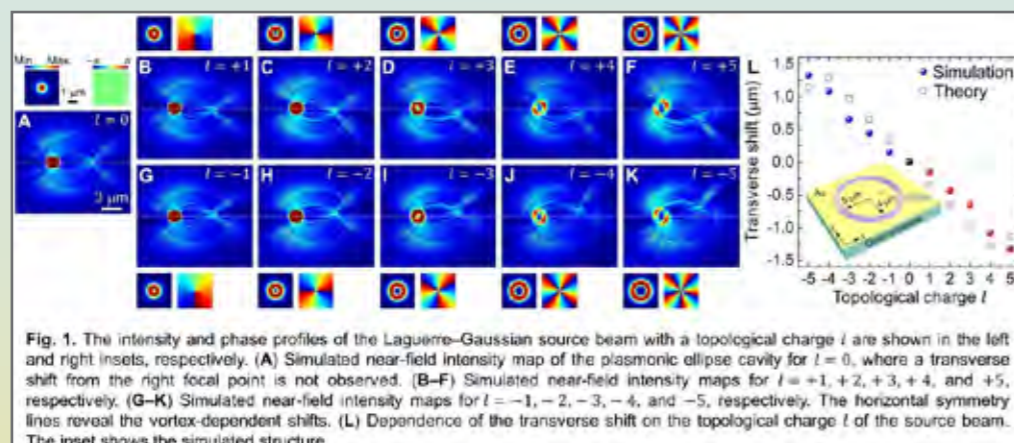


Fig. 1. The intensity and phase profiles of the Laguerre-Gaussian source beam with a topological charge  $l$  are shown in the left and right insets, respectively. (A) Simulated near-field intensity map of the plasmonic ellipse cavity for  $l = 0$ , where a transverse shift from the right focal point is not observed. (B-F) Simulated near-field intensity maps for  $l = +1, +2, +3, +4$ , and  $+5$ , respectively. (G-K) Simulated near-field intensity maps for  $l = -1, -2, -3, -4$ , and  $-5$ , respectively. The horizontal symmetry lines reveal the vortex-dependent shifts. (L) Dependence of the transverse shift on the topological charge  $l$  of the source beam. The inset shows the simulated structure.

## Overcoming the Uniformity Defects in Two-Dimensional Beam Multipliers via Dammann Metasurfaces

Dr. Raghvendra P. Chaudhary

Ben-Gurion University of the Negev

### Authors:

Raghvendra P. Chaudhary, Rinat Gutin, Avraham Reiner, and Nir Shitrit, School of Electrical and Computer Engineering, Ben-Gurion University of the Negev, Be'er Sheva 8410501, Israel

### Abstract:

**Introduction:** By providing unprecedented and simultaneous control over the fundamental properties of light—phase, amplitude, and polarization—metasurfaces revolutionize optical designs by realizing virtually flat, ultrathin, and lightweight optics that replaces bulky optical elements. Strikingly, metasurfaces can outperform their bulk counterparts. One such example is binary phase  $(0, \pi)$  Dammann gratings (DGs)—beam multipliers dividing an input beam into multiple output beams with equal power. DGs are manifested by multiple carefully designed transition points within the grating period, obtained by selectively etching the grating material to a thickness corresponding to a  $\pi$  phase shift. However, two-dimensional (2D) DG structures suffer from a significant reduction of the uniformity; moreover, the mechanism for the uniformity defects in 2D DG diffraction patterns has remained elusive.

**Objectives:** As the structure realization for a target phase, we report Dammann metasurfaces (DMs) based on the geometric phase which outperform DGs by overcoming the uniformity defects in 2D DG diffraction patterns via a highly precise phase imprint.

**Methods:** We theoretically and numerically studied 2D DGs and DMs generating 5-by-5 diffraction orders by calculating their far-field patterns and quantifying the uniformity among the diffraction orders (Fig. 1). Moreover, we quantified the mismatch between the target and imprinted phases via the root-mean-square error (RMSE).

**Results:** We showed that 2D DMs exhibit high uniformity, in contrast to DGs. The RMSEs for DMs exhibit lower values compared to DGs revealing the highly precise phase imprint of metasurfaces based on the geometric phase as the structure realization for a target phase profile. These observations reveal the one-to-one correspondence between the defective phase imprint differing from the target phase and the uniformity defects in the far-field patterns of beam multipliers.

**Conclusions:** This study reveals that metasurfaces can outperform their bulk optics counterparts while facilitating flat, ultrathin, and lightweight optics for wavefront molding at will.



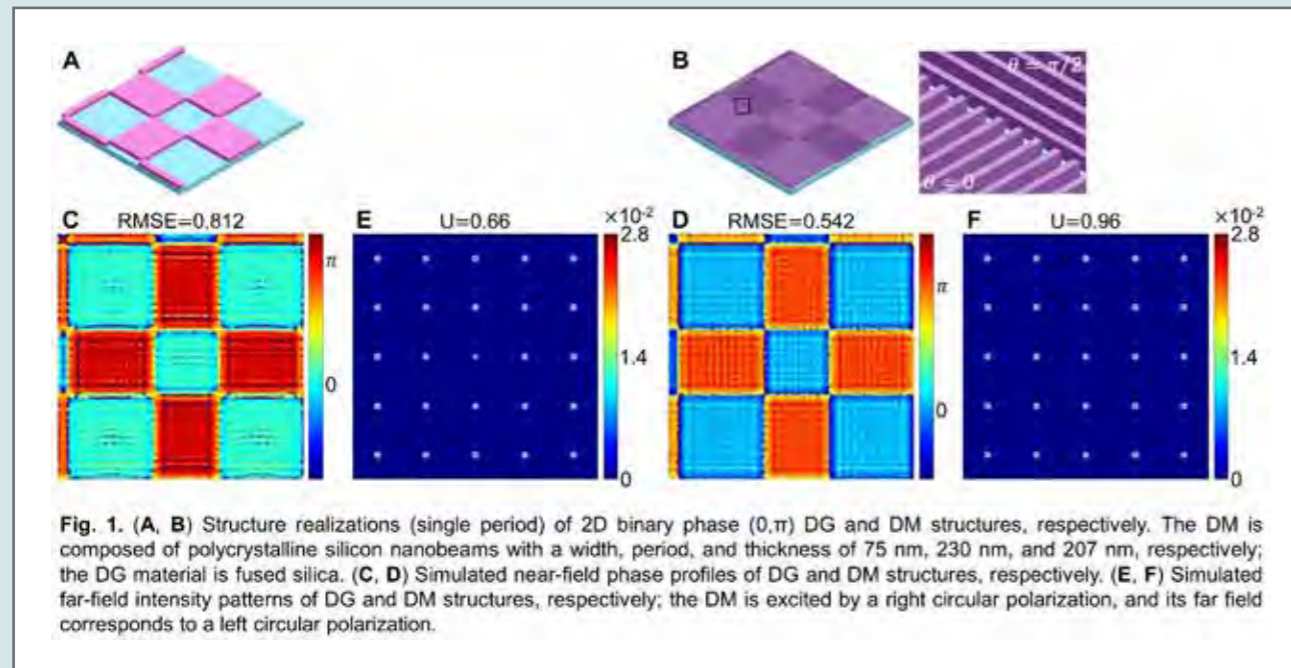


**Fig. 1.** (A, B) Structure realizations (single period) of 2D binary phase  $(0, \pi)$  DG and DM structures, respectively. The DM is composed of polycrystalline silicon nanobeams with a width, period, and thickness of 75 nm, 230 nm, and 207 nm, respectively; the DG material is fused silica. (C, D) Simulated near-field phase profiles of DG and DM structures, respectively. (E, F) Simulated far-field intensity patterns of DG and DM structures, respectively; the DM is excited by a right circular polarization, and its far field corresponds to a left circular polarization.

## Squeezing Free Space with Nonlocal Metasurfaces: Towards a Millimeter-Scale Squeezed Length

Dr. Imon Kalyan

Ben-Gurion University of the Negev

### Authors:

Imon Kalyan and Nir Shitrit, School of Electrical and Computer Engineering, Ben-Gurion University of the Negev, Be'er Sheva 8410501, Israel

### Abstract:

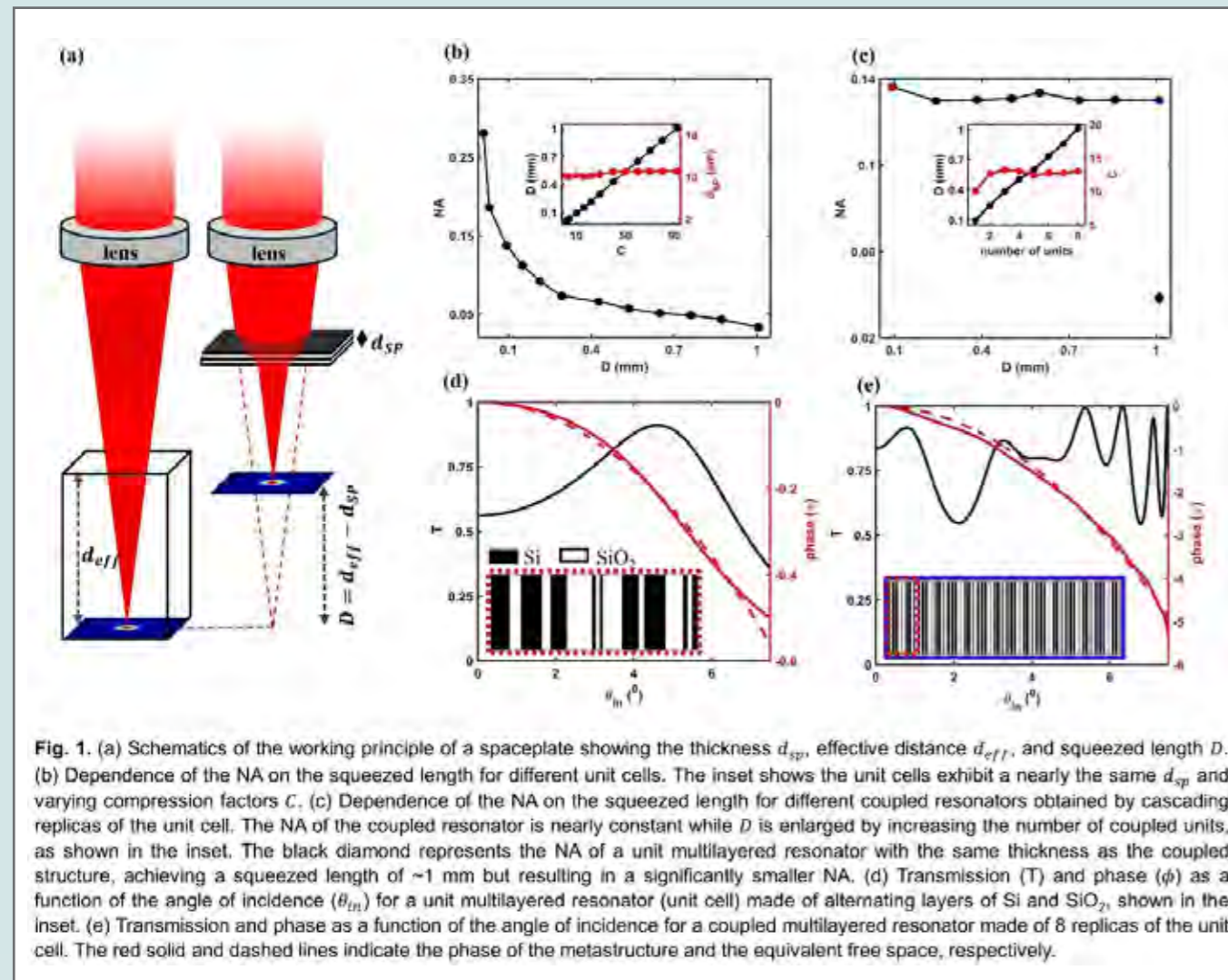
**Introduction:** Free space is an essential part of most optical systems and usually constitutes a great portion of the system volume. A truly miniaturized imaging system needs not only compact flat lenses (metalenses) but also compressed free space. Unlike conventional optics, free space relies on a momentum-dependent transfer function (i.e., a transfer function depending on the angle of incidence). Spaceplates, based on nonlocal metasurfaces, address this challenge by simulating free-space propagation through a momentum-dependent transfer function, thereby reducing the free-space length, as schematically depicted in Fig. 1a. However, their design is constrained by a compromise between the squeezed length and numerical aperture (NA), as demonstrated in Fig 1b, which limits their practical application.

**Objectives:** This study introduces a practical design for a spaceplate based on a nonlocal metasurface of coupled resonators, achieving a significant squeezed length—nearly 1 mm—with a practical NA.

**Methods:** We utilized an optimization-based inverse design technique, relying on the transfer matrix method, to develop a high-performance multilayered spaceplates with an optimized and moderate compression ratio—maintaining the NA within the required limit. Moreover, the trade-off between the squeezed length and NA is mitigated through the proper coupling of multiple copies of this optimized resonator, as shown in Fig 1c.

**Results:** The proposed spaceplate, designed for the mid-infrared region, utilizes alternating multilayers of silicon and silicon dioxide with optimized thicknesses (Figs. 1d and 1e). The optimized design achieves a squeezed length of 1 mm while maintaining a NA of 0.13.

**Conclusions:** A multilayered single resonator shows a high-quality spaceplate with a significant compression factor, while the meticulous coupling of highly efficient single-mode resonators facilitates the realization of substantial squeezed length—without compromising the NA. These advancements open new possibilities for miniaturizing optical systems by squeezing free space with nonlocal flat optics towards ultrathin imaging systems.



## Spatially Single-Cycle Polaritons in 2D Materials

Mr. Tomer Bucher

Technion-Israel Institute of Technology

### Authors:

A. Niedermayr<sup>1†</sup>, T. Bucher<sup>1†</sup>, X. Shi<sup>1†</sup>, Y. Fridman<sup>1</sup>, H. Nahari<sup>1</sup>, R. Dahan<sup>1</sup>, R. Ruimy<sup>1</sup>, E. Janzen<sup>2</sup>, J. H. Edgar<sup>2</sup>, F. H. L. Koppens<sup>3,4</sup>, H. H. Sheinfux<sup>5</sup>, I. Kaminer<sup>1\*</sup> 1. Andrea & Erna Viterbi Dep. of ECE., Technion-Israel Institute of Technology, Haifa, Israel. 2. Tim Taylor Dep. of Chemical Eng., Kansas State Uni., Manhattan, KS, USA. 3. ICFO-Inst. de Ciencies Fotoniques, The Barcelona Inst. of Sci. & Tech., Castelldefels, Spain. 4. ICREA-Institucio Catalana de Recerca i Estudis Avanats, Barcelona, Spain. 5. Department of Physics, Bar Ilan University, Ramat-Gan, Israel. † equal contributors \*kaminer@technion.ac.il

### Abstract:

Single-cycle pulses—compact waveforms confined to a single oscillation period—are a well-established concept in ultrafast optics [1], widely used in applications ranging from high-resolution spectroscopy [2] to precision control of wave-matter interactions [3]. However, extending this idea into the spatial domain, creating oscillations within a spatial sub-period without the use of an ultrawide pulse bandwidth, introduces a new and intriguing paradigm for highly tuneable localized wave phenomena.

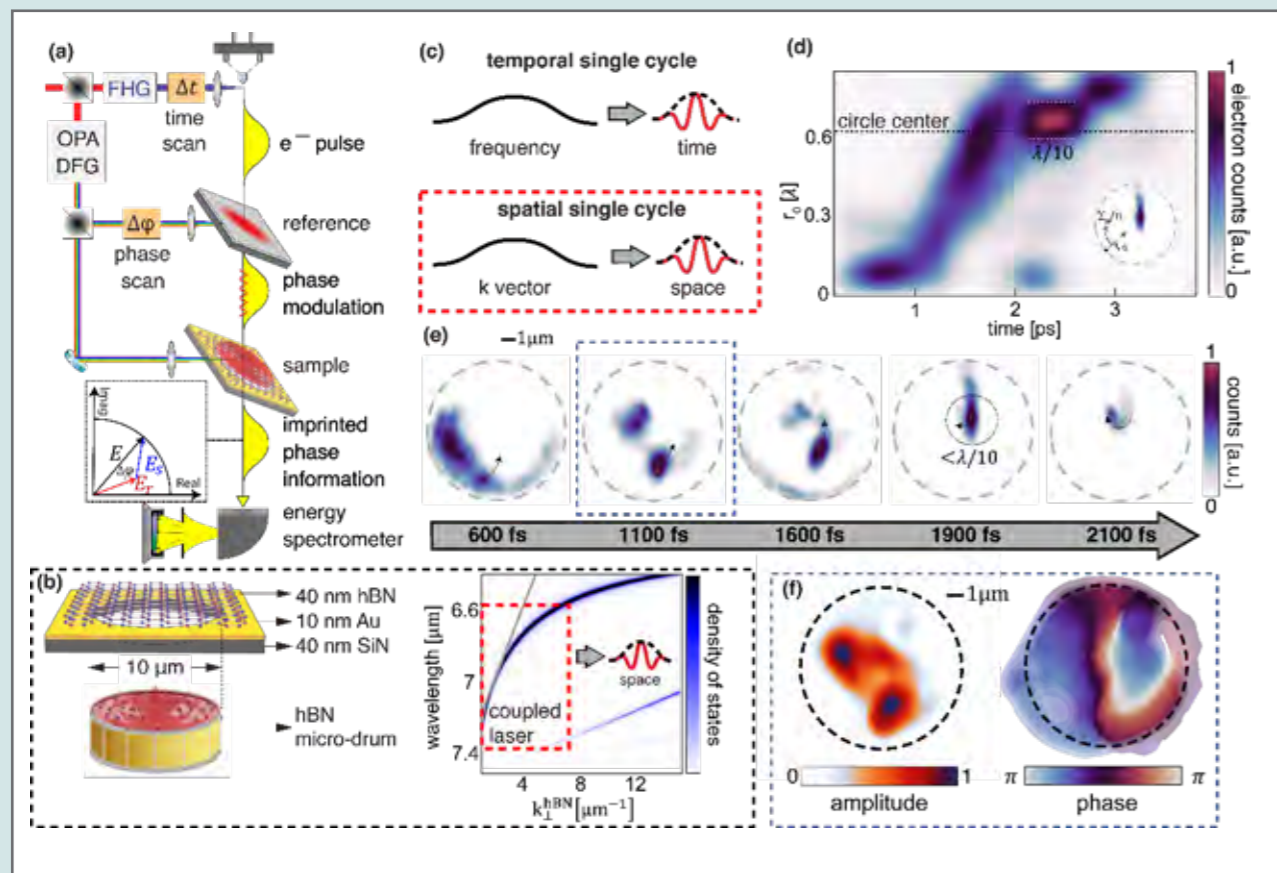
In this work, we report the observation of spatial sub-cycle polaritons. We use a time- and phase-resolved ultrafast electron microscope (Fig.(a)) [4,5] to image the phonon polariton (PhP) near-field in a hexagonal boron nitride (hBN) (Fig.(b)). We demonstrate spatially localized waveforms with sub-wavelength profiles, showing both their group dynamics and their sub-cycle behaviour, which reveals the single-cycle nature of the pulse.

Incident multi-cycle pulses couple into the hBN membrane from its edges, creating a sub-cycle PhP wavepacket by leveraging the relatively flat PhP dispersion. The dispersion translates the narrow frequency bandwidth of the incident pulse ( $\sim 7$  THz @  $7 \mu\text{m}$ , i.e.,  $\sim 16\%$  of the bandwidth) to a broad wavevector  $k_{\parallel}$  hBN bandwidth (near 100%), creating the sub-cycle feature (Fig.(b)). Generating such spatially single-cycle pulses with narrow frequency bandwidth is inherently easier than creating the extremely broad spectra of temporally single-cycle pulses (Fig.(c)). Reaching Sub-cycle compression in space while retaining a multi-cycle temporal envelope enables extended time dynamics and the formation of small-scale spatial features that persist over longer durations—facilitating novel experiments and intriguing applications of exotic polaritons.

### References:

- [1] B. Thomas, and F. Krausz, *Reviews of Modern Physics*.72, (2000):545.
- [2] A. Uzan, et al., *Nature Photonics* 14, (2020):188–194.
- [3] E. Goulielmakis, et al., *Science* 320, (2008):1614–1617.
- [4] T. Bucher, et al., *Science Advances* 9, (2023):eadi5729.
- [5] T. Bucher, et al., *Nature Photonics* 18, (2024):809–815.





## Near-infrared Absorption Enhancement of Reflective Aluminum Gratings

Dr. Roy Avrahamy

Ben-Gurion University of the Negev

### Authors:

Roy Avrahamy<sup>1</sup>, Dror Cohen<sup>2</sup>, Benny Milgrom<sup>3</sup>, Ben Amir<sup>2</sup>, Daniel Belker<sup>1</sup>, Asi Solodar<sup>4</sup>, Erez Golan<sup>4</sup>, Oren Sadot<sup>2</sup>, and Amiel A. Ishaaya<sup>1</sup>

1 School of Electrical and Computer Engineering, Ben-Gurion University of the Negev, P.O.B 653, Beer-Sheva 8410501, Israel

2 Department of Mechanical Engineering, Ben-Gurion University of the Negev, P.O.B 653, Beer-Sheva 8410501, Israel

3 School of Electrical Engineering, Jerusalem College of Technology, P.O.B 16031, Jerusalem 9372115, Israel

4 Nano-fabrication center Ilse Katz Institute for Nanoscale Science and Technology, Ben-Gurion University of the Negev, P.O.B 653, Beer-Sheva 8410501, Israel

### Abstract:

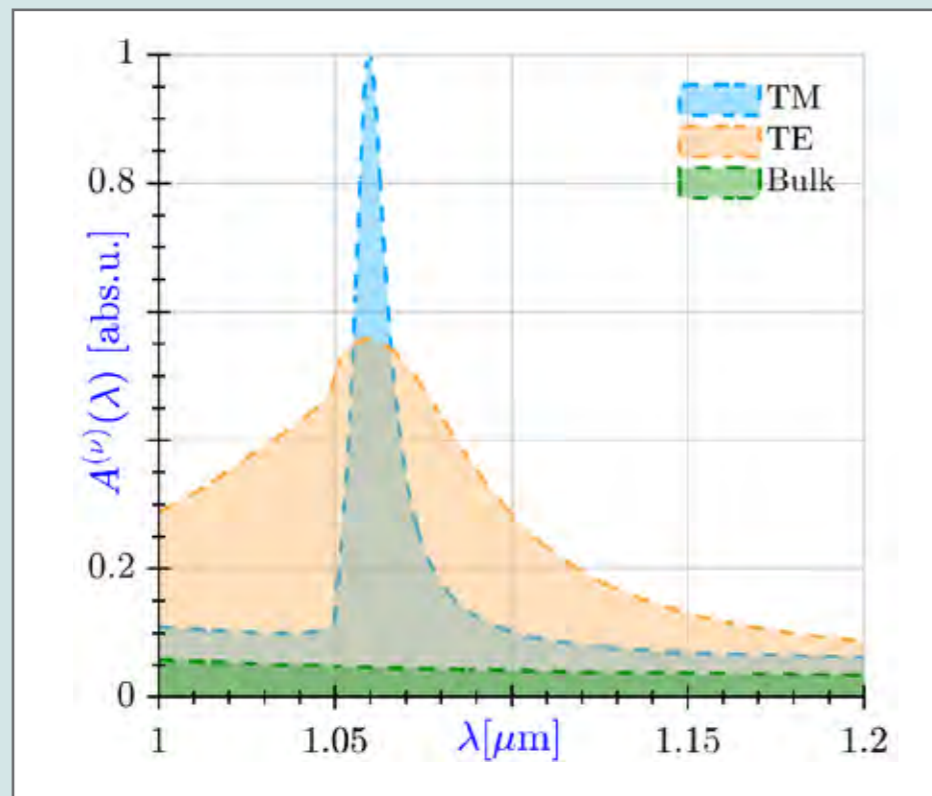
Aluminium (Al) is the most prevalent metal, and due to its many benefits, Al and its alloys are essential for almost every industry, e.g., transportation, packaging, construction, electricity, machinery, etc. In the past decade, high-power fiber lasers with superior beam quality have become accessible and affordable. They are used in many applications, such as material processing, wireless power transfer, laser guidance and designation, satellite optical communication, and defense-related laser systems. Owing to their superior performance, Ytterbium (Yb)-doped fiber lasers, centered around 1.06  $\mu\text{m}$ , dominate the high-power market nowadays. Motivated by the above, we focus on enhancing the absorption of optically thick bulk Al around  $\lambda_0 = 1.065 \mu\text{m}$  solely by periodically corrugating its surface [1].

We fabricated a relatively large area (1 cm x 1 cm) sample of a design, optimized for unpolarized operation (Fig. 1), and comprehensively characterized its spectral and single-frequency polarized absorption of near-to-normal Gaussian-beam incidence. The spectral absorption was derived from reflection measurements using a super continuous laser source and a spectrum analyzer. The single-frequency absorption was measured both optically, and thermally using an in-house linearly polarized Yb-doped photonic crystal fiber laser source, with  $\lambda_0 = 1065 \text{ nm}$  and  $\text{FWHM} \sim 0.2 \text{ nm}$  operated in continuous wave mode. In the thermal experiments, the absorption was numerically derived from the EM-induced heating of the sample, measured using thermocouples. Taking into account a scattered reflection pattern that was carefully investigated, the optical and thermal measurements agreed well with the simulations of the fabricated design. The fabricated design showed experimentally more than 9.5- and 6-fold absorption enhancement over bulk Al in S- and P-polarization, respectively. The Al prevalence and progress and wide distribution of optical sources, mainly fiber-based, around 1.06  $\mu\text{m}$ , promote the proposed designs as promising candidates for many applications.

### References:

[1] R. Avrahamy, D. Cohen, B. Milgrom, B. Amir, D. Belker, A. Solodar, E. Golan, O. Sadot, A. A. Ishaaya, "Comprehensive optical and thermal investigation of optimal near-infrared absorption enhancement of nano-patterned aluminum," *Optics & Laser Technology* 175, 110871 (2024).





## Phonon-Polaritons in h-BN

**Dr. Ori Avayu**

*Tel Aviv University*

### Authors:

Ori Avayu, Michael Klein, Matan Meshulam, Itai Epstein, Tel Aviv University

### Abstract:

We demonstrate the properties of Phonon Polaritons, by launching confined Phonon polaritons in low dimensional van der Waals (vdW) heterostructure, composed of nanometric-size cubes, on top of h-BN flakes. The cubes act as a mid-IR antenna, launching highly confined electromagnetic modes carrying large momentum.

## Exploring confinement factor in waveguides for greenhouse gas sensing

Mr. Uzziel Sheintop

*School of Electrical and Computer Engineering, Ben-Gurion University of the Negev, Beer-Sheva, Israel*

### Authors:

Uzziel Sheintop<sup>1,\*</sup>, Alina Karabchevsky<sup>1</sup>

<sup>1</sup> School of Electrical and Computer Engineering, Ben-Gurion University of the Negev, Beer-Sheva, Israel

### Abstract:

**Introduction:** The near-infrared (NIR) region provides high availability, deep tissue penetration, and cost-effectiveness, making it ideal for applications in medical imaging, telecommunications, and environmental monitoring. Here, we numerically investigate an optimized waveguide structure for gas sensing by maximizing the confinement factor and managing bending losses for an extended interaction length. This approach achieves high sensitivity, minimizes structural losses, and enables real-time monitoring and quality control across multiple industries, including food, pharmaceuticals, agriculture, and environmental surveillance.

**Background:** Spectral fingerprints offer a highly reliable means of molecular identification, surpassing other methods due to their inherent specificity. A molecule's total energy can be partitioned into electronic, vibrational, rotational, and translational components. When illuminated with infrared (IR) radiation, its atoms begin to vibrate, generating distinct optical signatures <sup>1</sup>. Optical waveguides have become a promising platform in diverse sensing applications thanks to their substantial evanescent field, compactness, and configurability <sup>2</sup>. The confinement factor serves as a critical parameter for evaluating waveguide efficiency in fingerprint identification <sup>3</sup>. In addition, careful investigation of bending losses is essential for attaining a longer interaction length with the analyte while minimizing structural losses, thereby enhancing overall sensing performance.

**Objectives:** We have numerically investigated the ability of the planar waveguide to confine a mode and to enhance the evanescent interaction with an analyte for different waveguide architectures, and for wavelengths known for their molecule absorption lines of greenhouse gases.

**Methods:** By numerically solving Maxwell's equations, we investigated various waveguide designs to clarify how the confinement factor influences sensitivity to analytes. In parallel, we analyzed waveguide bending losses to optimize overall sensing performance and ensure robust device operation.

**Results:** We have found that planar waveguides have different confinement factors which depend on the waveguide's parameters such as depth, width, materials; wavelength; architecture.

**Conclusions:** Emerging spectroscopic strategies can be extended to detect and identify analytes and examine their interactions with light in a chip-scale, label-free format, thereby expanding the functionality of chemical and biological monitoring.

### References:

Novikova, A., Katiyi, A., Sheintop, U., Zhang, M., Wang, P., Karabchevsky, A., 2023. Hollow-Micropillared Glass Fabricated on Hollow Joe Pye Weed-Inspired Tubes for Detecting Molecular Signatures, *Advanced Materials Technologies*, 9(2), 2301245.

Karabchevsky, A., Sheintop, U., Katiyi, A., 2022. Overtone Spectroscopy for Sensing – Recent Advances and Perspectives, *ACS Sensors*, 7(10), 2797–2803.

G.J. Veldhuis; O. Parriaux; H.J.W.M. Hoekstra; P.V. Lambeck, 2005. Sensitivity enhancement in evanescent optical waveguide sensors, *Journal of Lightwave Technology*, 18 (5), 677 – 682

## LASERS AND APPLICATIONS SESSION

### Oral Presentation Abstracts:

#### Algorithmically Measuring the Spectrally Resolved Wavefront of an Ultrashort Laser

Mr. Aaron Liberman

*Weizmann Institute of Science*

#### Authors:

Slava Smartsev, LOA, CNRS, Ecole Polytechnique, ENSTA Paris, Institut Polytechnique de Paris, Palaiseau, France; Aaron Liberman, Weizmann Institute of Science, Rehovot, Israel; Igor A. Andriyash, LOA, CNRS, Ecole Polytechnique, ENSTA Paris, Institut Polytechnique de Paris, Palaiseau, France; Antoine Cavagna, LOA, CNRS, Ecole Polytechnique, ENSTA Paris, Institut Polytechnique de Paris, Palaiseau, France; Alessandro Flacco, LOA, CNRS, Ecole Polytechnique, ENSTA Paris, Institut Polytechnique de Paris, Palaiseau, France; Camilla Giaccaglia, LOA, CNRS, Ecole Polytechnique, ENSTA Paris, Institut Polytechnique de Paris, Palaiseau, France; Jaismeen Kaur, LOA, CNRS, Ecole Polytechnique, ENSTA Paris, Institut Polytechnique de Paris, Palaiseau, France; Josephine Monzac, LOA, CNRS, Ecole Polytechnique, ENSTA Paris, Institut Polytechnique de Paris, Palaiseau, France; Sheroy Tata, Weizmann Institute of Science, Rehovot, Israel; Aline Vernier, LOA, CNRS, Ecole Polytechnique, ENSTA Paris, Institut Polytechnique de Paris, Palaiseau, France; Victor Malka, Weizmann Institute of Science, Rehovot, Israel; Rodrigo Lopez-Martens, LOA, CNRS, Ecole Polytechnique, ENSTA Paris, Institut Polytechnique de Paris, Palaiseau, France; Jerome Faure, LOA, CNRS, Ecole Polytechnique, ENSTA Paris, Institut Polytechnique de Paris, Palaiseau, France

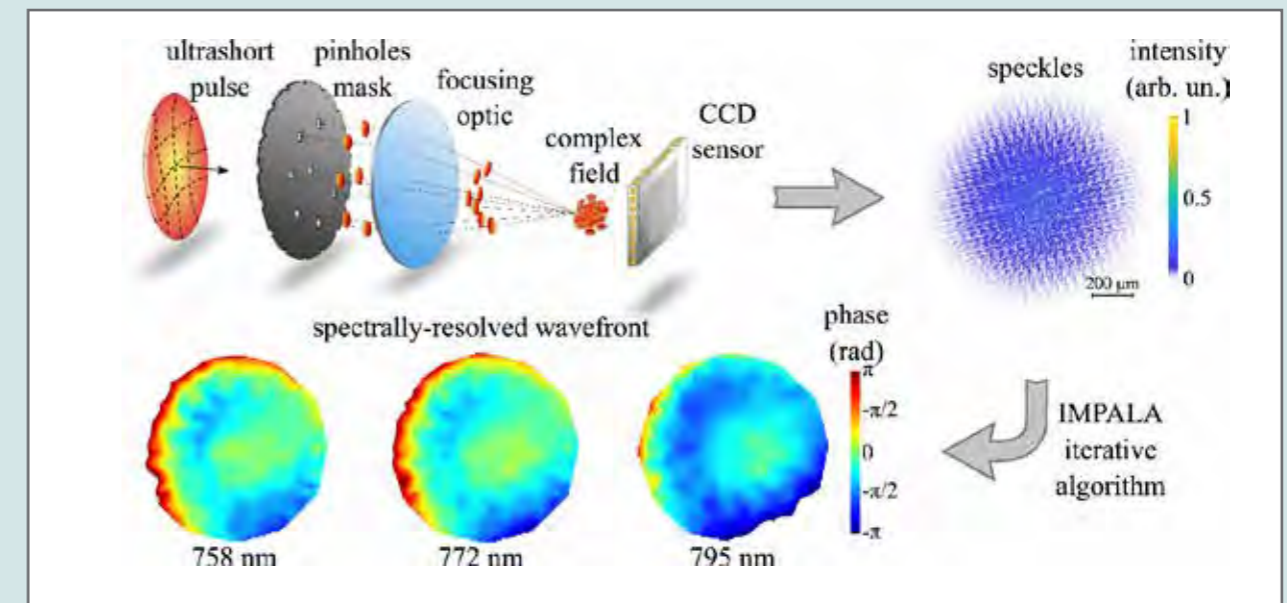
#### Abstract:

We introduce a novel and experimentally simple method for measuring the multispectral wavefronts of ultrashort laser pulses in a single shot. IMPALA, or Iterative Multispectral Phase Analysis for LASers, is based on the linear far-field interferometry of multiple beamlets. This minimally intrusive method relies on placing a mask with specially arranged pinholes in the beam path before the focusing optic and retrieving the spectrally resolved laser wavefront from the speckle pattern produced at focus using a special retrieval algorithm.

The novelty of IMPALA lies in its approach. Rather than using cumbersome and expensive optics to experimentally separate the wavefronts for different frequencies, IMPALA relies on algorithmic separation of this information. Thus, our method is remarkably straightforward because the only non-standard optical element it requires is a pinhole mask placed before the focusing optics used in the experiment.

We conducted a proof-of-principle experiment using Ti:Sapphire 30 fs laser pulses with manually introduced spatio-temporal couplings. We accurately retrieved chromatic aberrations, such as pulse-front tilt (PFT) of a misaligned compressor, pulse-front curvature (PFC), and higher-order aberrations introduced by a spherical lens.

IMPALA is easily scalable to different beam sizes, focal lengths of the optics, and spectral bandwidths. By combining scalability, a simple setup, low cost, and single-shot compatibility with sufficient spatial and spectral resolution for many applications, IMPALA could allow spatio-spectral beam reconstruction to become a standard diagnostic in high-power laser systems.





## M2-meter for live laser beam diagnostics in the VIS and SWIR

Mr. Refael Porcar

*Imagine Optic*

### Authors:

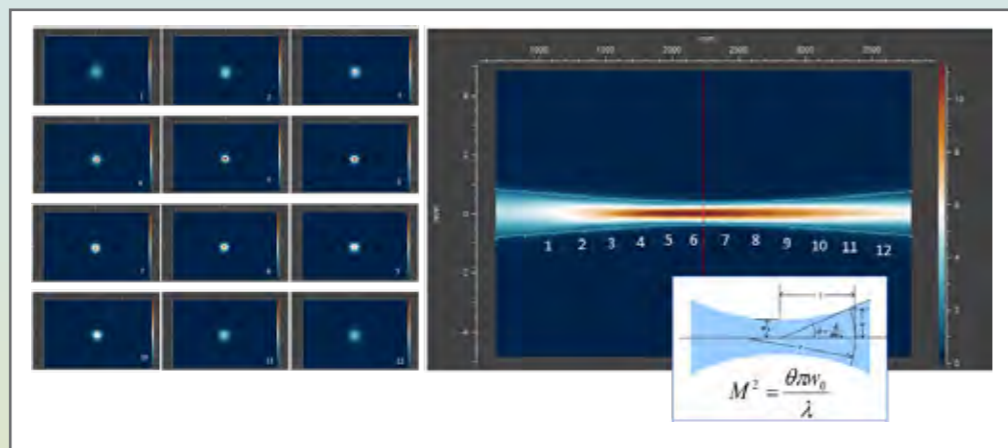
Diego Ormaechea, Cynthia Ibrahim, Audrey Le Lay, Xavier Levecq and Rafael Porcar. Imagine Optic, 18, rue Charles de Gaulle, 91400 Orsay, France

### Abstract:

For the diagnostic of laser beams, the M Squared (M2) is a widely adopted parameter, as it provides information on laser beam quality by comparing the divergence and waist size of its beam to a perfect Gaussian beam. The M2 parameter is usually measured with large bench-based instruments featuring a camera that is translated to several longitudinal positions along the laser caustic. The M2 is then fitted from the different intensity frames acquired. This process is therefore tedious, as it requires to align the bench, to adapt the optical setup to the properties and caustic of the laser beam and last, to perform the multiple translations to acquire the signal. The time required to complete the acquisition cycle can also make them incompatible with dynamic effects.

Imagine Optic has proposed a different approach for visible and SWIR lasers where we measure both the intensity and the phase of the laser at the same time and in one single position, thus enabling all the different observation frames required by ISO 11146 to be calculated at once, and then compute the M Squared parameter. The method has the advantage of being very fast (measurement cycle from  $\mu\text{s}$  to ms duration), easy to implement (no alignment or translation required) and perfectly suited for the characterization of pulsed lasers and dynamics effects. In addition, the absence of translation stage makes the system compact, perfect for on-site maintenance or characterization of lasers embedded in machines.

Through our work, we comment on the principle and implementation of such an approach and present the test and validation of the method, with results for different types of lasers in the visible and SWIR wavelengths for the first time, as well as comparisons with standard traditional M Squared benches.



## Widely tunable, pulsed Tm:YAP laser, based on an Active / Passive Q switch with Yag etalons

Prof. Salman Noach

*Jerusalem College of Technology*

### Authors:

Yaakov Neustadter, Gad Horwitz, Uzziel Sheintop, Eytan Perez, Rotem Nahear, Neria Suliman and Salman Noach

### Abstract:

A wide range of applications in the  $2\mu\text{m}$  spectral regime require a variety of laser system specifications such as pulse energy, pulse durations, peak power and repetition rate. Wavelength tunability can be an advantage in some laser systems but essential in others. While there are many reports of tunable CW lasers, options for pulsed mode lasers are very limited and generally display low performance. Here in demonstration of two configurations of pulsed, tunable, Q-switched, Tm:Yap lasers, developed in our lab are presented. In both cases, the tunability was achieved utilizing one or two YAG etalons in the laser cavity.

The first design used an acousto-optic modulator as an active Q-switch, achieved a combination of high-pulsed energies up to 2.3 mJ and tunability between 1926 – 1961 nm, with a narrow bandwidth of 0.15 nm FWHM and a pulse duration of 30 ns at 1 kHz repetition rate.

The second design demonstrates for the first time wide tunability using a passive Q-switch element in the cavity. In this setup wavelength tunability ranging from 1911 – 1952 nm was achieved, with maximal energy per pulse of 1.42 mJ, pulse durations of 26–36 ns at maximal repetition rate of 3 kHz.

The simultaneous combination of these lasers features in the same cavity; tunability range, narrow bandwidth, output power, pulse durations and repetition rate make these lasers a promising tool in the fields of biomedical, sensing, and material processing applications.

## Noise Suppression in Gain-Managed Nonlinear Amplifiers

Mr. Nitzan Haviv

Department of Physics and Solid-State Institute, Technion

### Authors:

Nitzan Haviv, Technion, Haifa, Israel; Yariv Shamir, Soreq NRC, Yavne, Israel; Michael Kruger, Technion, Haifa, Israel; Pavel Sidorenko, Technion, Haifa, Israel

### Abstract:

**Objectives:** The study investigates the Relative Intensity Noise (RIN) characteristics in a Gain-Managed Nonlinear (GMN) Yb fiber amplifier. We explore noise suppression mechanisms and their connection to gain and nonlinear effects, focusing on a potential nonlinear attractor that influences pulse evolution in the GMN amplification regime [1].

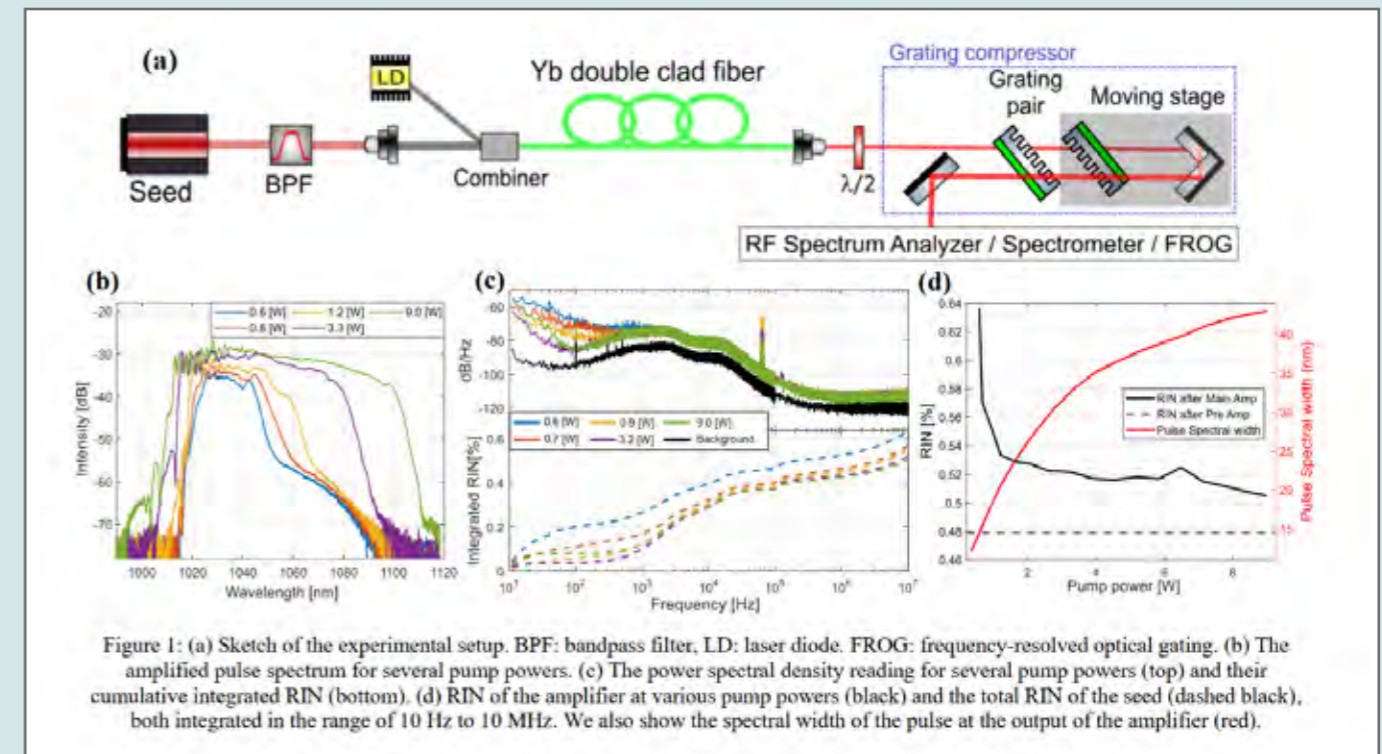
**Methods:** In the experiment, we use a commercial ultrafast oscillator, operating at 80 MHz repetition rate, to seed the GMN amplifier. The amplifier is built with 2.5 meters of double-clad 5/125 PM Yb fiber and is co-pumped by a 976 nm diode. RIN measurements, performed using a high-speed photodiode and RF spectrum analyzer, covered a frequency range from 10 Hz to 10 MHz. Spectral and temporal characteristics of amplified pulses were analyzed at varying pump powers.

**Results:** Key findings reveal RIN suppression with increased pump power and nonlinear effects, contrary to assumptions that higher gain and spectral broadening will lead to noise increase due to various noise coupling mechanisms [2]. The RIN decreased from 0.64% at 0.57 W to 0.51% at 9 W pump power. At maximum power, the pulse had an energy of 40 nJ and was compressed to 45 fs using a grating pair. An inverse correlation is observed between integrated RIN and spectral width, with RIN decreasing as spectral width increases.

**Conclusions:** In conclusion, this study examined the RIN in a gain-managed nonlinear Yb fiber amplifier, showing that increasing gain and nonlinear effects suppress noise. GMN amplifiers excel in producing low-noise, high-energy, sub-50 fs pulses at high repetition rates, making them ideal for ultra-low noise amplification and mode-locked laser noise reduction. The findings suggest a stabilizing nonlinear attractor and indicate potential for even greater RIN reduction, possibly below seed source levels.

### References:

- [1] P. Sidorenko, W. Fu, and F. Wise, "Nonlinear ultrafast fiber amplifiers beyond the gain-narrowing limit," *Optica*, vol. 6, no. 10, p. 1328, Oct. 2019.
- [2] Z. Tang et al., "Nonlinear dynamics of relative intensity noise transfer at fiber amplification and supercontinuum generation," *Optics Communications*, vol. 554, p. 130131, Mar. 2024.



## Enhanced Free Space Optical Communication (FSOC) by Coherent Beam Combining with Optical Phased Array Lasers

**Mr. Shmuel Freudenstein**

*Civan Lasers*

### Authors:

Shmuel Freudenstein, Ariel Roizman, Shmuel Stav, Shalom Weinberger, Ran Vered, Eyal Shekel

### Abstract:

Free Space Optical Communication (FSOC) is an emerging technology that offers a range of advantages for secure, high-speed data transmission. Among its benefits are highly secure communication channels, large bandwidth capacities, and the absence of spectrum licensing requirements, making FSO a compelling alternative to traditional radio frequency communication. However, despite its promise, FSO faces several challenges, primarily in ensuring reliable transmission. Atmospheric aberrations and the difficulty in maintaining a precise line-of-sight alignment lead to signal degradation and reduced reliability in the received data.

Current solutions to address these challenges often focus on enhancing the receiver's capability to detect and correct signal distortion. However, these methods have limitations and are dependent on the received signal.

A new approach to overcoming these limitations lies in Dynamic Beam Lasers based on Coherent Beam Combining (CBC) with Optical Phased Array (OPA) technology. By actively correcting the wavefront and steering the laser beam at MHz frequencies, this technology can effectively compensate for atmospheric disturbances and maintain a strong, reliable signal from the transmitter. This dynamic control of the wavefront enhances the overall performance of FSO systems, ensuring more consistent and higher-quality communication.

This technology is derived from advancements in 1-micron high-power lasers, which have reached power outputs as high as 120 kW. These high-power capabilities, combined with the agile beam control enabled by CBC and OPA, offer a significant improvement in the reliability of FSO communication systems.

## LightSolver's all-optical laser-based analog computer

**Dr. Omri Wolf**

*LightSolver LTD*

### Authors:

Omri Wolf, Chene Trodonsky, Tel-Aviv, LightSolver LTD.

### Abstract:

LightSolver develops a cutting-edge optical computing platform, powered by interacting lasers, designed to revolutionize the performance of demanding computational tasks. By utilizing the speed, efficiency and parallel nature of photonics, LightSolver addresses bottlenecks inherent in traditional, silicon-based hardware. The company's innovative technology aims to serve as both an accelerator and enabler for key operations across industries reliant on high-performance computing.



## Development of a 130kW High-Power Fiber Laser System with Enhanced Reliability and Compactness based on CBC technology

**Dr. Yaniv Vidne**

*VP R&D*

### Authors:

Yaniv Vidne, Ran Vered, Eyal Shekel – Civan Lasers

### Abstract:

This **Abstract** presents the development of a 130kW high-power fiber laser system designed for advanced material processing applications. Leveraging Coherent Beam Combining (CBC) and Optical Phased Array (OPA) technologies, the system achieves high power output while maintaining exceptional beam quality. The combination of CBC and improved OPA allows for dynamic beam control, enabling real-time optimization of the melt pool and mitigating processing defects. Furthermore, the system emphasizes reliability, robustness, and compactness through the use of robust components, a carefully engineered architecture, and the incorporation of knowledge gained from the manufacturing of thousands of previous lasers. This 3rd generation system boasts a 74% volume reduction and 73% weight reduction, achieved in part through the integration of laser diode drivers (LDD) directly within the laser amplifier. This compact and robust 130kW laser system provides a versatile platform for advancing material processing technologies and other applications to be seen in the future.

## Femtosecond inscription of fiber Bragg gratings and Fabry-Perot interferometers structures for various applications

**Dr. Aviran Halstuch**

*School of Electrical and Computer Engineering, Ben-Gurion University of the Negev, Beer-Sheva, 8410501, Israel*

### Authors:

Aviran Halstuch, and Amiel A. Ishaaya

### Abstract:

A Fiber Bragg Grating (FBG) is a periodic modulation of the refractive index in the fiber core, typically spanning a few millimeters. FBGs have diverse applications in optical communications, such as wavelength filters and add/drop multiplexers. They are also widely used as temperature and strain sensors in optical fibers and as reflective mirrors in optical fiber lasers. Traditionally, FBGs are inscribed in photosensitive fibers using a UV laser and a phase mask (PM).

Since the early 2000s, femtosecond micromachining in transparent materials has been extensively studied. The high peak power of femtosecond laser pulses enables permanent material modifications with minimal collateral damage and precise spatial control. These modifications include smooth and anisotropic refractive index changes. Inscribing FBGs using a near-infrared (NIR) femtosecond laser, a PM, and a cylindrical lens has proven to be a rapid, robust, and effective approach. This method complements the other flexible direct writing techniques such as the point-by-point, the line-by-line, and the plane-by-plane inscription techniques.

In this work, we present recent advances in FBG inscription techniques using a NIR femtosecond laser and the PM method. We demonstrate the inscription of phase-shifted gratings with controlled transmission peaks, as well as FBGs and FBG arrays in various optical fibers. In addition, we demonstrate how wavelength tuning is achievable even with a uniform phase mask (PM) and how the inscription of two similar FBGs at different spatial locations can lead to Fabry-Pérot interference. The separation between these FBGs determines the fringe visibility and the free spectral range. These gratings have versatile applications, including optical fiber sensing and shaping, motion control in biomedical devices, and emerging fields such as quantum computing and communications.

## Advanced Optical Analysis of Focal-Point Divergence Between Surgical Neodymium-Doped Yttrium Aluminum Garnet (Nd:YAG) and Aiming Beam Lasers

Mr. Ya'akov Mandelbaum

Jerusalem College of Technology (JCT) – Lev Academic Center

### Authors:

Averbukh, Edward, Hadassah University Medical Center, Hebrew University, Jerusalem, Israel; Slushetz, Yaakov, Jerusalem College of Technology–Lev AC, Jerusalem, Israel; Levy, Jaime, Hadassah University Medical Center, Hebrew University, Jerusalem, Israel; Patal, Rani, Hadassah University Medical Center, Hebrew University, Jerusalem, Israel; Mandelbaum, Yaakov, Jerusalem College of Technology–Lev AC, Jerusalem, Israel; Arieli, Yoel, Jerusalem College of Technology–Lev AC, Jerusalem, Israel;

### Abstract:

Ophthalmology Science

Volume 4, Issue 5, September–October 2024, 100512

//doi.org/10.1016/j.xops.2024.100512

**Background:** The 1064 nm Nd:YAG laser that is routinely used in ophthalmology for intraocular surgery is in fact invisible. Typically, a pair of intersecting auxiliary diode-lasers with a visible wavelength of 635 nm, are used for aiming. Ideally their intersection coincides with the waist of the Nd:YAG laser. However, due to dispersion in the ocular tissue – and in the high-power diverging lens placed adjacent to the eye – the differing wavelengths result in progressive deviation between the two focal points. This problem becomes especially significant for posterior segment laser treatments, threatening the success rate and the safety.

**Objectives:** This work set out to evaluate the divergence between the surgical laser and the aiming diode laser beams foci.

**Methods:** Hospital and laboratory studies were performed to characterized the Nidek – YC–1800 Nd:YAG laser apparatus together with the Volk–Goldman Goniofundus lens. A computerized ray-tracing model was then created to simulate optics in the eye and assess the difference between the focal points of the two beams. Analysis of ocular (sphero-)chromatic aberration was key. A calibration calculator was developed for the surgeons' use which computes the focal deviation in each region interior to the eye.

The aforementioned lens's high negative optical power, poses a challenge for common laboratory equipment and commercial devices. A novel method was developed to directly measure the focal length of a highly negative lens; it simultaneously renders the index of refraction.

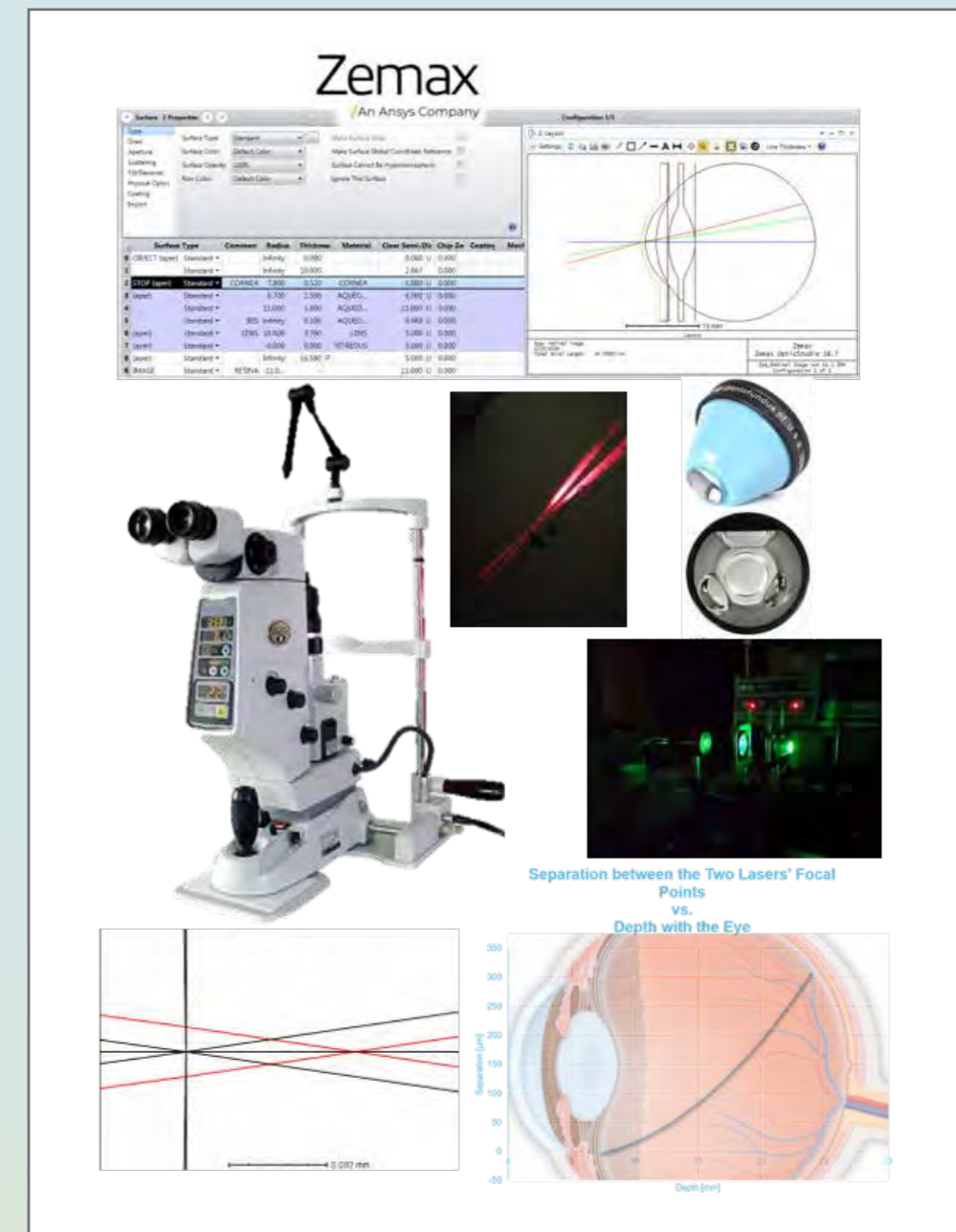
**Results:** Focal points of the two laser beams converge 8 mm behind the cornea. Posterior to this point, the intersection of the diode laser aiming beams lies in front of the focal point of the Nd:YAG treatment laser, with distance between the 2 foci progressively increasing up to 305 microns at 24 mm behind the cornea.

**Conclusions:** To our knowledge this is the first study evaluating the deviation between the target predicted by the guidance beams and the actual focus of the surgical Nd:YAG laser due to chromatic aberration of ocular tissue. These results can be immediately applied in clinical practice to increasing the accuracy and safety of Nd:YAG laser treatment, particularly in the posterior segment.

### References:

Y. Slushetz, R. Patal, Y. Arieli, Y.M. Mandelbaum  
yaaqovm/Advanced-Optical-Analysis-of-Divergence-Between-the-Foci-of-the-Nd-YAG-and-Aiming-Beam-Laser: Additional Material  
Zenodo (2024), 10.5281/zenodo.10832421

//ars.els-cdn.com/content/image/1-s2.0-S2666914524000484-mmc1.pdf



## Lasers Department, Applied Physics Division Soreq NRC

Dr. Yaakov Glick

Lasers Department, Applied Physics Division Soreq NRC

### Authors:

Yaakov Glick, Yoav Sintov, Mirit Rosenfeld and Shaul Pearl  
Soreq NRC, Appl. Phys. Div., Yavne, Israel

### Abstract:

High energy nanosecond pulses, from an all fiber laser/amplifier setup, with good beam quality are hard to obtain simultaneously, but are desirable [1–3]. All-fiber configurations are generally robust in relation to bulk optics configurations, and such lasers can be useful for applications such as material processing.

An all-fiber amplifier at a wavelength of 1061nm was designed and constructed. It produced 41mJ in a 28nsec pulse-length, at a repetition rate of 10kHz with a beam quality of  $M^2=38$ .

To the best of our knowledge, these results are the highest reported pulse energies in an all-fiber laser/amplifier system with a beam quality better than  $M^2=40$ . Cai et al [1] reported 51mJ with a beam quality of  $M^2=54$ , from a 300mm core active fiber, and Dinger et. al [2] reported 150mJ from a 600 mm core fiber. In ref. [2], the beam quality was not reported, however based on the fiber diameter, it can be supposed that it was significantly higher than the values discussed here. Wang et al [3] reported 25mJ from a 100 mm core fiber with a beam quality of  $M^2=8.2$ .

The setup is based on a commercial seeder, which provides 0.95mJ at a repetition rate of 10kHz. This was amplified with an OFS manufactured amplifier, which employs a 200/375 mm (core/clad) Yb doped active fiber. The output fiber of the amplifier has a 300 mm core. The amplifier was pumped with five nLight diodes at 920nm, which could deliver up to a power of ~150W each.

The peak of the spectrum at the output energy of 41mJ was at 1061nm with a FWHM bandwidth of 2.7nm. The output power was as high as 470W. Of this, 410W were average power resulting from the pulsed energy, while 60W was amplified spontaneous emission (ASE) CW power. Fig. 1 shows the pulse energy and the power vs. the input power. Fig. 2 shows the pulse shape of the output and of the seeder.

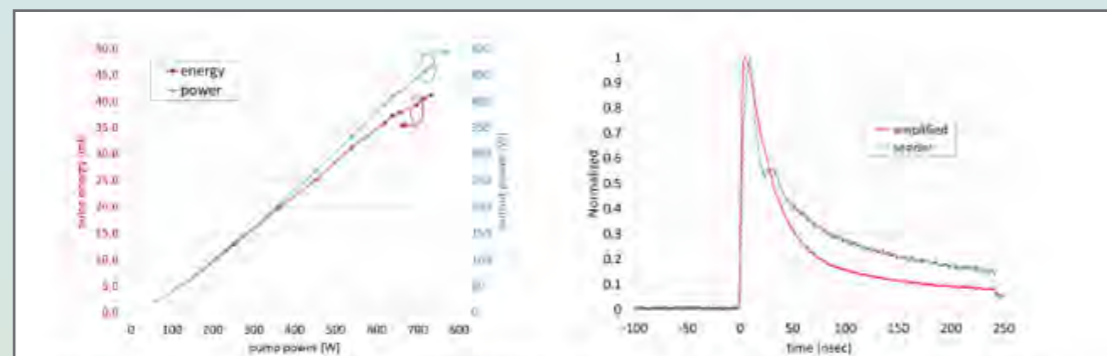


Fig. 1. Output pulse energy and power vs. pump power. Fig. 2. Pulse shape of seeder and after amplification

**Acknowledgement:** The work was partially supported by Elbit systems.

### References.

1. Cai, Y., et al. "High-power Yb-doped and all fiber-based nanosecond MOPA laser." *IEEE Photonics Journal* 14.3 (2022): 1-5.
2. Dinger, R., et al. "Short-pulse MOPA fiber laser with kilowatt average power and multi-megawatt peak power, applying advanced XLMA fiber amplifiers." *Fiber Lasers XIV: Technology and Systems*. Vol. 10083. SPIE, 2017.
3. Wang, S., et al. "All-fiber pulsed laser generation of 25.5 mJ and solution of parasitic oscillation." *Applied Optics* 60.5 (2021): 1117-1120.

## Front-End Bandwidth and Contrast Control for multi Joule Mixed Nd:glass Ultrafast Laser for proton Acceleration

Dr. Yariv Shamir

Soreq NRC

### Authors:

Yariv Shamir<sup>1\*</sup>, Zaharit Refaeli<sup>1</sup>, Marcelo Wyszkin<sup>1</sup>, Moshe Koren<sup>1</sup> and Jonas Kolenda<sup>2</sup>

1 Soreq NRC, Yavne 8180000, Rd 4111, Israel

2 Ekspla, Savanoriu Av. 237, LT-02300, Vilnius, Lithuania

### Abstract:

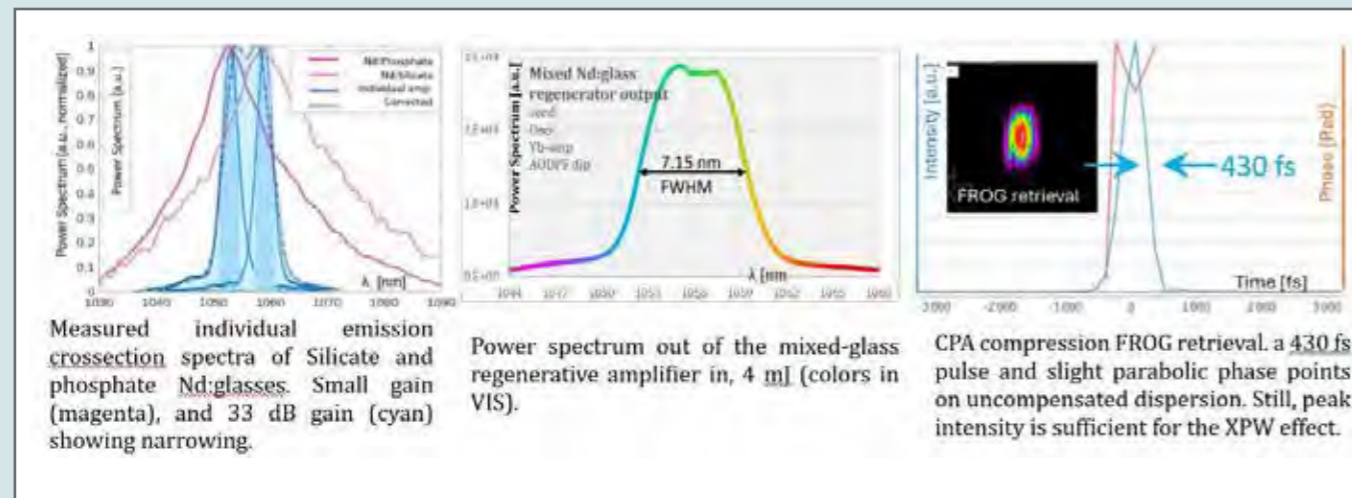
**Background:** A long-standing challenge associated with high energy Neodymium-doped glass (Nd:glass) ultrafast lasers is countering the gain-narrowing trend, compromising chirped-pulse-amplifier (CPA) system's pulse shortening and peak-power potential [1,2]. Capable of tens to kiloJoule energies and intensities exceeding  $10^{19}$  W/cm<sup>2</sup>, ultrashort Nd:glass lasers provide labs approach to hot plasmas, X-ray, and particle or heavy-ions acceleration, with recent worldwide focus on clean nuclear-fusion energy harvesting [3,4].

**Objective:** In this work the establishment few mJ front-end, planned to seed 30-Joule 100-TW double-CPA laser-based proton accelerator for exploring future HB<sup>11</sup> clean-energy harvesting process [5].

**Method:** Fourfold strategy was taken to preserve adequate optical-bandwidth to support short pulses. Firstly, a <100 femtosecond seed was stretched and amplified to ~μJ, maintaining 14-nm linewidth, postponing early-stage narrowing. Next, a specialty designed regenerator-amplifier (Ekspla APL41-REG-1053), hosting two gain-materials with shifted peak emission-crosssections: Silicate-type (peak emission 1060 nm), and Phosphate-type (1053 nm), thus their common spectral gain renders broader than each separately. Additionally, an Acousto-Optic Dispersive Programmable-Filter (AOPDF) was applied with an intentionally perforated spectral-dip introduced to the seed. The latter enforces the common-gain profile to broaden at the expense of the center peak, provided 36 dB amplification (1μJ fiber-amplifier seed to ~4 mJ).

**Results:** While individual-glass amplification narrowed the CPA seed to ~3.3 nm, the mixed-glass regenerator yielded linewidth in excess-of 5 nm, and with the AOPDF, up-to 8.5 nm was measured. These results pointing on potential pulses shorter than 400 and 220 fs, respectively (assuming supergaussian spectrum). The matched stretcher-compressor pair (volume-Bragg-gratings) did not fully compensate for the excess fiber and glass dispersion, this, aided by AOPDF, ~430 fs was measured. focal peak intensity of  $>3.5 \cdot 10^{13}$  W/cm<sup>2</sup> (~150 μm spot-size), more than the required for Cross-Polarization-Wave (XPW) contrast enhancement stage [6]. Preliminary XPW pulses were already produced and filtered by Glan-laser polarizers.





## E Posters Abstracts:

### Head of the Nanotechnology Center for Research and Education, Jerusalem College of Technology, Jerusalem, Israel

Dr. Avi Karsenty

Head of the Nanotechnology Center for Research and Education, Jerusalem College of Technology, Jerusalem, Israel

#### Authots:

Itamar Ganan<sup>1,2</sup>, Michael Bendayan<sup>3</sup>, Avi Karsenty<sup>1,2</sup>

1 Advanced Laboratory of Electro-Optics, Jerusalem College of Technology, Jerusalem, Israel

2 Nanotechnology Center for Research & Education, Jerusalem College of Technology, Jerusalem, Israel

3 Rafael Advanced Defense Systems LTD., Haifa, Israel

#### Abstract:

**Objectives:** We investigated the modification of an Asymmetric Quantum Well's (AQW) electrical features through photonics, looking at the effects on charge distribution and induced electric field due to illumination with a CO<sub>2</sub> laser. This basic component enables photon-electric charge interactions, and our research will expand the ability to integrate photonics into the microelectronics industry.

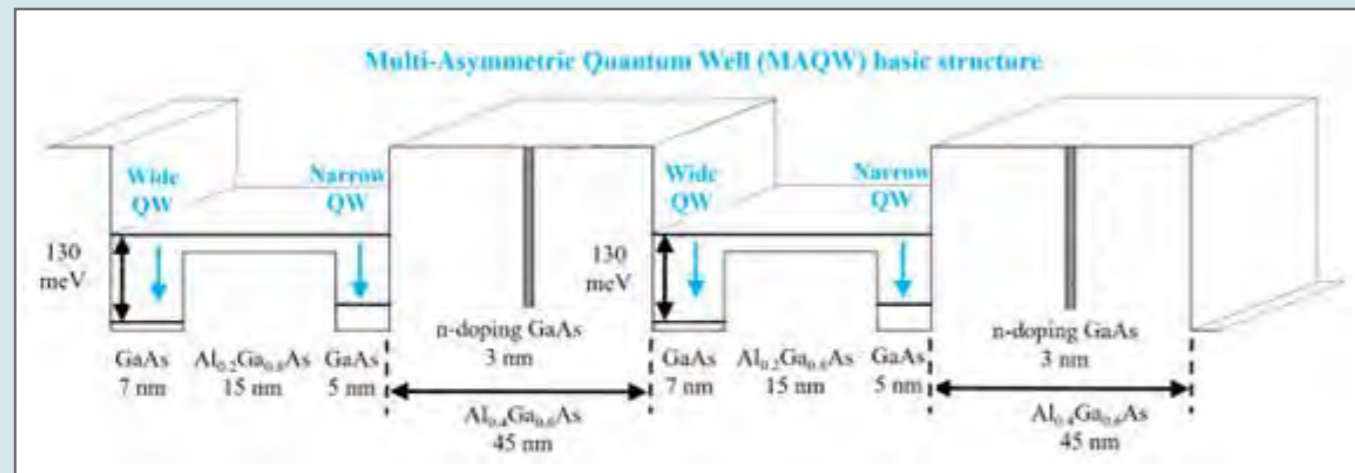
**Methods:** The basic device consists of pairs of wide and narrow GaAs quantum wells separated by a potential barrier, with each pair surrounded in turn by another, higher potential barrier. The barriers consist of Al<sub>x</sub>Ga<sub>(1-x)</sub>As, with  $x=0.2$  and  $x=0.4$  respectively. Electric charge is supplied by a narrow doping region in the high barriers. Through dimensions adjustment, the lowest energy level is placed in the wide well, the second lowest in the narrow well, and the third lowest will be common to the wells and the low barrier. In equilibrium, most of the charges will be at the lowest energy level. Using appropriate wavelength photons, charges are excited to common energy level and then decay to the wide and narrow wells, changing their distribution.

**Results:** Effect evidence has already been observed before [1] and was confirmed by numerical simulations using COMSOL-Multiphysics [2]. Further improvement of the numerical model is necessary to refine its agreement with experimental results and to investigate the activity of the device at room temperature.

**Conclusions:** Research of a basic component is underway in order to model the laser/semiconductor interaction, with the hope of expanding the research to additional materials and increasing the scope of the interaction.

#### References:

- [1] A. Khakshoor, et al., "Doping Modulation of Self-Induced-Electric-Field (SIEF) in Asymmetric GaAs/GaAlAs/GaAs Quantum Wells", Results in Physics 32 (2022), 105093.
- [2] M. Bendayan, et al., "Modulated Photoluminescence Low Temperature Measurements with Controlled Self-Induced-Electric-Field (SIEF) in Asymmetric GaAs/GaAlAs/GaAs Quantum Wells", Journal of Luminescence 250 (2022), 119109.



### VCSELS FOR CHIP SCALE RUBIDIUM BASED ATOMIC CLOCKS

Mr. Inbal R. Marciano

MSc student, Technion

**Authors:**

I. R. Marciano<sup>1</sup>, V. Mikhelashvili<sup>1,2</sup>, L. Gal<sup>1</sup>, A. Willinger<sup>1</sup>, G. Sery<sup>1</sup>, Y. Milyutin<sup>1</sup>, O. Ternyak<sup>1</sup>, A. Shacham<sup>1</sup>, M. Orenstein<sup>1,2</sup> and G. Eisenstein<sup>1,2</sup>. (1) Electrical and Computer Engineering Dept. Technion, Haifa 32000 Israel (2) Russell Berrie Nanotechnology Institute, Technion, Haifa 32000 Israel

**Abstract:**

Chip scale atomic clocks are driven by VCSELS that require a special combination of properties. We report on such VCSELS that exhibit all the required characteristics surpassing all commercially available VCSELS of this kind.

The top emitting VCSEL was designed to have a minimum threshold near 363 K. Spatial mode filtering is determined by a top metal ring electrode and the oxide aperture, both being 5 μm wide. The key characteristics include a negative TO leading to a minimum threshold of 0.6 mA at 363 K (Fig. 1), single mode operation exactly at 795 nm with a 30 dB side mode suppression ratio and a polarization discrimination of 25–27 dB at 2 V and also at 363 K (Fig. 2). Since CSACs use FM spectroscopy techniques for detection of the atomic transition, it is desirable that in these applications that the a parameter should be large. The ± parameter in the present VCSELS is in the range of 8–10. We also studied the correlation between the electrical and optoelectronic characteristics. We found that at moderate bias levels, up to transparency, the current flows in parallel paths along the periphery of the mesa (Fig. 3). The conventional exponential current dependence on voltage changes above transparency to a power law dependence when the diode reaches the so-called high injection regime where  $I=V^m$ . When  $m=2$ , The laser emits spontaneous emission while above threshold  $m=1$ . This leads to a nonlinear contribution to the series resistance which is not considered in common models.

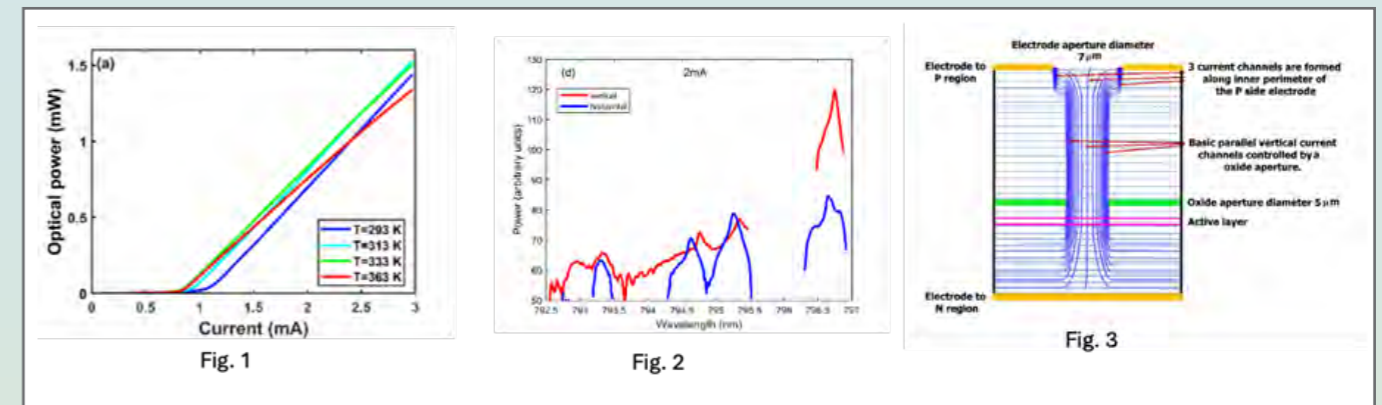


Fig. 1

Fig. 2

Fig. 3

## High-power monolithic Thulium-doped all-fiber MOPA as a pump source for Holmium-doped lasers

Mr. Guy Shafri

*Ben-Gurion Univ. of the Negev Israel*

### Authors:

Guy Shafri, Amiel A. Ishaaya: School of Electrical and Computer Engineering, Ben-Gurion University of the Negev, Beer-Sheva 8410501, Israel; Joris Lousteau: Dipartimento Di Chimica, Materiali e Ingegneria Chimica "Giulio Natta", Politecnico Di Milano, Via Mancinelli 7, Milano, 20131, Italy; Nadia G. Boetti: LINKS Foundation, Via Pier Carlo Boggio 61, 10138, Turin, Italy

### Abstract:

High-power Thulium-doped fiber lasers (TDFL) are well-established fiber lasers operating at 1.95–2.05  $\mu\text{m}$  wavelengths, prized for their eye-safe wavelengths functionality and high efficiency when diode-pumped by 793 nm, which exploits the cross-relaxation process. However, their performance diminishes at wavelengths outside this range. For longer wavelengths, such as 2.1–2.3  $\mu\text{m}$ , Holmium-doped lasers pumped by 1908 nm sources are typically used. Therefore, a TDFL operating at 1931 nm offers an effective balance between the Thulium emission band and the Holmium absorption band, making it a suitable pump source for high-power Holmium-doped lasers.

In this work, we design a 300W continuous-wave (CW) TDFL operating at 1931 nm, employing a master oscillator power amplifier (MOPA) configuration. The master oscillator features a homemade fiber cavity with inscribed fiber Bragg gratings (FBG), including high-reflective FBG (HR-FBG) as the rear mirror and optimized low-reflective FBG (LR-FBG) as an output coupler (OC). In addition, a water container is used in the amplifier stage to immerse the double-clad large mode area Thulium-doped fiber (DC-LMA-TDF) for high-power operation. To explore this high-power pump laser, the laser will be tested as a pump source in a L-shape free-space Holmium-doped rod cavity incorporating one of two rods: the well-established Holmium-doped YAG (Ho:YAG) and a Holmium-doped Germanate glass (Ho:Germanate) developed by Politecnico Di Milano and LINKS Foundation in Turin.

The designed high-power TDFL operates at 1931 nm, offering a promising solution as an effective high-power pump source for Holmium lasers. It is suitable for both CW laser operation and high-peak-power pulsed laser operation. The all-fiber design enhances portability and eliminates the need for realignment. Detailed design and experimental results will be presented, shedding light on the performance and potential of this fiber laser.

## ELECTRO-OPTICS IN INDUSTRY SESSION

### ◆ Invited speakers Abstracts:

## Methods for Protection of Electro-Optical Seeker Heads Against Electro-Magnetic Radio Frequency Interference

Dr. Shay Joseph

*Rafael*

### Authors:

Shay Joseph and Yarden Weber. Rafael, Haifa, Israel

### Abstract:

Electro-optical seeker heads are prone to disruptions due to exposure to electro-magnetic radiation, in the radio frequency range. This is because the transparent window or dome material which protects the seeker head is not only transparent in the relevant optical band but unfortunately also allows a wide portion of potentially damaging radiation inside the seeker, harming the electrical circuit boards and leading to the disruption of the seeker head. The most well-known solution to overcome these disruptions is the application of transparent conductive oxide coatings which are conductive enough but still allow for radiation in the relevant bands to pass through. Unfortunately, the more conductive the coating becomes, the less radiation passes through, especially in the infrared. Another possible solution is the application of conductive meshes. These meshes block radiation passage relative to the area they cover and are highly conductive. There are challenges of applying these meshes particularly on curved surfaces. In this talk, we will discuss several possibilities to increase protection of seeker heads under electro-magnetic interference. First, we will discuss  $\text{In}_x\text{O}_y$  thin films prepared by Direct Current magnetron sputtering and the attempt to improve their infrared transparency while still maintaining the necessary electrical conductivity to allow for sufficient seeker protection. We will show how decreasing oxygen flow during deposition changes the microstructure and relate these changes to the optical and electrical properties of the films. We will also bring examples of the application of metallic meshes onto the surface of optical domes. We will focus on two main techniques: Hydro-printing and direct aerosol printing. We will show that by optimizing both the ink type and print conditions, it is possible to obtain line width of less than 30 microns, very low sheet resistance of 1–5ohms/square and optical transparency over 90% even in the mid and far infrared.



## Femtosecond laser welding of BK7 glass to aluminium alloys for industrial applications

**Dr. Aviran Halstuch**

*School of Electrical and Computer Engineering, Ben-Gurion University of the Negev, Beer-Sheva, 8410501, Israel*

### Authors:

Aviran Halstuch<sup>1</sup>, Rami Cohen<sup>2</sup>, and Amiel A. Ishaaya<sup>1</sup>

<sup>1</sup> School of Electrical and Computer Engineering, Ben-Gurion University of the Negev, Beer-Sheva, 8410501, Israel

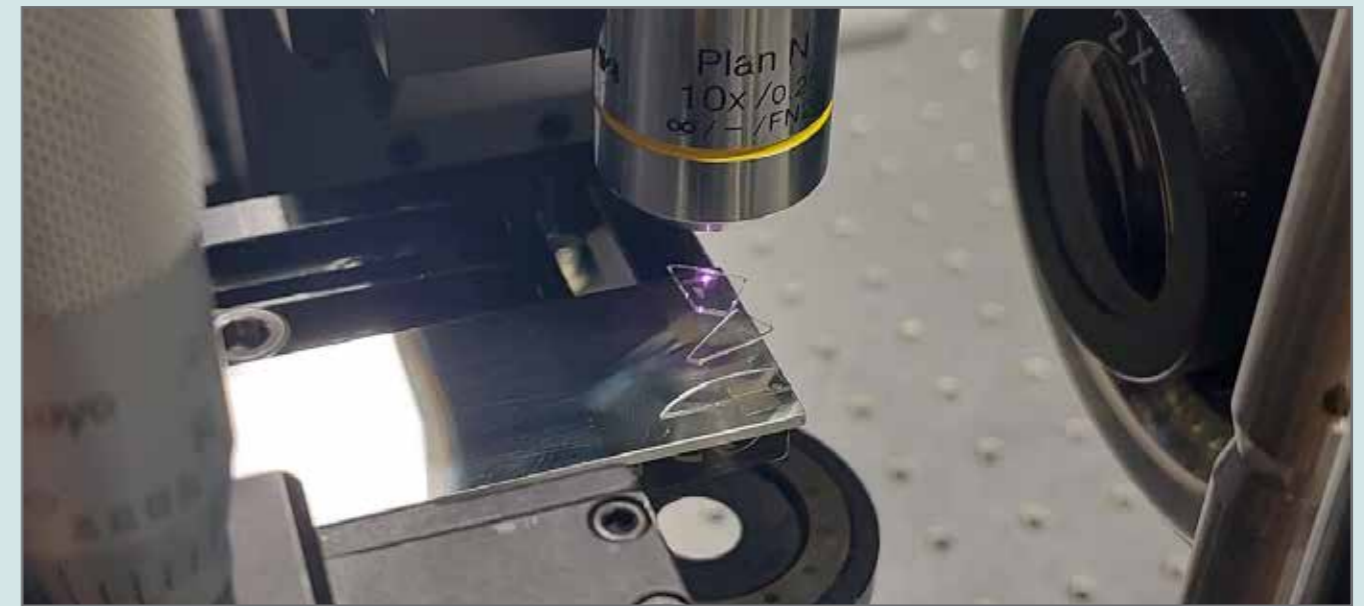
<sup>2</sup> Elbit Systems Electro-Optics ELOP Ltd., Rehovot, Israel

### Abstract:

Joining transparent materials (e.g. glass) and opaque materials (e.g. metals) is a critical manufacturing process across various industries, including medical devices, solar cells, sensors, and particularly remote sensing applications in space. Traditional joining techniques, such as epoxy gluing and anodic or adhesive bonding, face challenges related to defects, aging, and contamination. Epoxy glues, commonly used in space, are prone to outgassing, which can shorten instrument lifetimes and contaminate optical components like windows and lenses.

Ultrafast laser micro-welding has emerged as a promising alternative due to its precision, minimal thermal damage, and speed. This method is especially advantageous for bonding dissimilar materials, where only one material is transparent to the laser wavelength, and it has attracted many research groups (e.g. from NASA, UK, Japan and China). The process benefits from nonlinear absorption in the transparent material, such as glass, and linear absorption in the opaque material, enabling localized heating due to plasma formation at the interface. As the plasma cools down to room temperature, a strong bond forms between the materials.

In this study, we demonstrate the use of an amplified Ti:Sapphire femtosecond laser to weld BK7 glass to aluminum alloys. The laser, focused with a 10X objective, typically delivers  $\sim 30\text{--}50\ \mu\text{J}$  energy pulses at a 1 kHz repetition rate, resulting in low average power of only  $\sim 30\text{--}50\ \text{mW}$ . This ensures negligible heat accumulation. The samples are scanned at speeds of  $\sim 50\text{--}150\ \mu\text{m}/\text{sec}$ , exposing each point along the weld line to several hundred pulses. Initial results show promising bonding quality between the materials. Future work aims to optimize the process by reducing stress and defects, ensuring the optical properties of the glass remain intact. Ultimately, this method seeks to replace epoxy glues in space-based remote sensing applications (and other applications), addressing contamination and durability concerns while enhancing performance and reliability.



## Optical methods for Advanced packaging process control

**Mr. Yuval Ginzberg**

*Nova Ltd.*

### Authors:

Igor Turovets

### Abstract:

Advanced packaging of semiconductor chips is one of the main cornerstones of the AI revolution. In our presentation, we will show the role of optical metrology (interferometry and Raman spectroscopy) in enabling the most critical process steps of high-volume manufacturing and advanced packaging of AI devices.

We will focus on the Through Silicon Via (TSV) process flow, which enables advanced packaging of HBM DRAM, Image sensors, and all 2.5 and 3D chipset-based heterogeneous integration schemes. We will present two methods addressing the key challenges of the TSV process: miniaturization of the TSV dimensions and the stress zone around TSV.

Spectral Interferometry (SI) provides a fast and robust metrology solution for isolated and dense high-aspect ratio features such as TSVs. SI capabilities were demonstrated at the current TSV dimensions and the minimal possible TSV sizes required for future devices. One of the method's benefits is that it does not require modeling and allows direct extraction of the parameters of interest from the measurement signals on the production wafers. Another unique capability of SI was demonstrated when measuring the bottom asymmetry of the TSV with polarization control.

Raman metrology allowed measurement of the stress in Si around TSVs arranged in square arrays with different designs, and processed with different conditions. An accumulation of a tensile stress component was observed between the vias in these arrays in addition to the strong compressive stress expected in close proximity to the TSVs. Since accurate predictions of total stress for large TSV arrays and complicated layer structures are not impossible, access to accurate stress measurements using Raman spectroscopy becomes valuable both for the process development and for in-line monitoring to maximize the usable area for device structures on production wafers.

## Tailoring light-matter interactions for optical wafer inspection

**Dr. Hadar Greener**

*Physicist, Applied Materials*

### Authors:

Hadar Greener, Oded Ovdad, Amir Shoham

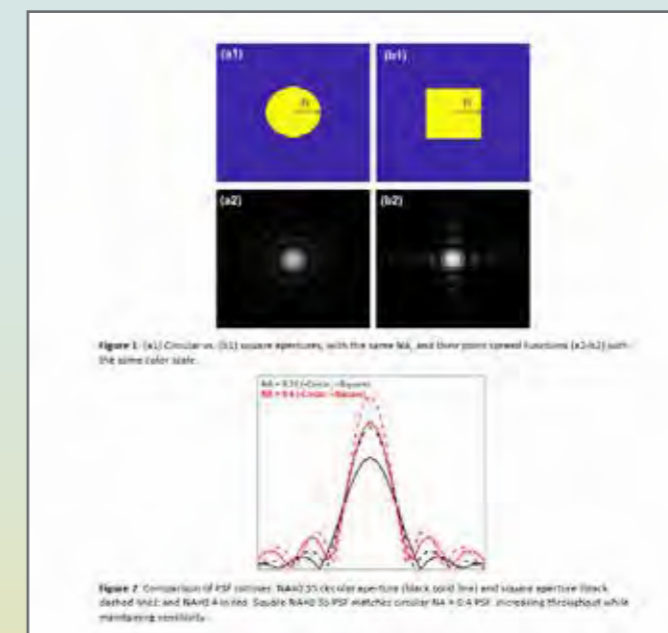
### Abstract:

Emerging semiconductor technologies driven by artificial intelligence, cloud computing and big data demand complex fabrication, that is still in the process development stage. The process yield (percentage of useful devices produced) improvement requires high resolution optical wafer inspection tools, sampling many points in the production line. Economics compel such tools to work very fast, i.e. inspection throughput of many wafers per hour.

Optical wafer inspection technologies have been around for many years, applying wavelengths from infrared, to visible, ultraviolet, and deep ultraviolet. In parallel, semiconductor technologies have matured from the micrometer scale to the nanometer scale, thus optical inspection technologies are struggling to keep up with the resolution challenge. It is crucial for wafer inspection to include novel optical configurations, which push the limits of resolution for enhanced detection of sub-wavelength process defects, while successfully suppressing noise. This requires the tailoring of light-matter interactions at the nanoscale, via optimization of various physical control knobs, such as illumination and collection polarizations, optical transfer functions etc.

Our ever-evolving library of optical configurations are developed in the Physics and Technology groups – from ideation, through CEM (FDTD and FEM), optical design simulations and on-tool proofs of concept, to guiding and verifying field integration on our optical wafer inspection tools.

This talk will include an example of an “out-of-the-box thinking” optical configuration that accelerates throughput while maintaining sensitivity (detectable defect size), without imposing costly requirements on the optics and computation.



## Israeli Free Space Quantum Key Distribution Demonstration

**Dr. Rani Ditcovski**

*Triarii Research*

### Authors:

Rani Ditcovski, Doron Bar-Lev, Patrick Chemla

### Abstract:

In an era of escalating cyber threats and data breaches, traditional encryption methods face unprecedented challenges. The rapid development of quantum computers threatens to break current cryptographic systems, potentially exposing sensitive government, financial, and personal data[1].

We present Israel's first free-space Quantum Key Distribution (QKD) system, designed to provide quantum-safe encryption solutions capable of withstanding both current and future attacks.

The system implements the BB84 protocol, introduced by Bennett and Brassard in 1984[2], using linearly polarized weak coherent states encoded in four predetermined polarization states. We conducted the demonstration across a free-space link under full daylight conditions to simulate real-world implementation challenges.

The system attained key distribution rates of up to 10,000 secure key bits per second over hundred meters range, while maintaining operation in daylight conditions, demonstrating the practical viability of free-space QKD technology.

This demonstration, developed by Elbit Systems' subsidiary Elisra, working alongside with Triarii Research, under the Israeli Innovation Authority's Quantum Communication Initiative, marks a significant milestone in Israeli quantum communication capabilities and proves the feasibility of free-space QKD systems. This project establishes a basis for future quantum-safe encryption implementations in Israel.

### References:

- [1] Tibbetts, J., 2019. Quantum computing and cryptography: Analysis, risks, and recommendations for decisionmakers (No. LLNL-TR-790870). Lawrence Livermore National Lab. (LLNL), Livermore, CA (United States).
- [2] Bennett, C.H. and Brassard, G., 2014. Quantum cryptography: Public key distribution and coin tossing. Theoretical computer science, 560, pp.7-11.

## Dynamic Beam Laser for Welding and Metal Additive Manufacturing: Advancing Fiber Laser Technology through Coherent Beam Combining and Optical Phased Arrays

**Dr. Eyal Shekel**

*Civan Lasers*

### Authors:

Ruben Cesana, Rachel Assa, Yaniv Vidne, Civan Lasers, Jerusalem Israel

### Abstract:

This study highlights the revolutionary capabilities of the Dynamic Beam Laser (DBL), a cutting-edge fiber laser technology leveraging Coherent Beam Combining (CBC) and Optical Phased Array (OPA) [1,2]. By utilizing real-time beam-shaping properties inherent to CBC and OPA, the DBL achieves precise manipulation of energy profiles, enabling unprecedented control over thermal gradients, melt pool dynamics, and solidification processes. This approach aims to enhance material properties, minimize defects, and expand the application potential for welding and metal additive manufacturing (AM).

**Methods:** The DBL technology employs CBC and OPA to generate high-power, single-mode beams with adjustable intensity profiles and spatial energy distribution. Experiments were conducted on crack-sensitive materials and dissimilar alloys to test its ability to adapt beam parameters dynamically—such as phase shifts, energy density, and focal depth—within the melt pool. High-speed imaging and spectral diagnostics captured the influence of these adjustments on thermal behavior, grain structure evolution, and defect formation [3].

**Results:** The DBL demonstrated exceptional beam quality, with long focal lengths and high depth of focus, critical for precise energy delivery in demanding applications. The CBC and OPA-based architecture enabled smooth transitions in thermal gradients, reducing hot cracking and porosity. These innovations facilitated the formation of refined equiaxed grains, improving material strength and durability. Additionally, the DBL's ability to weld thick sections and challenging material combinations positions it as a transformative solution for advanced manufacturing.

### References:

- [1] Shekel E., Vidne Y., Urbach B. 16 kW single mode cw laser with dynamic beam for material processing. SPIE LASE, vol. 11260, SPIE, 2020.
- [2] J. Wagner, et al. Influence of dynamic beam shaping on the geometry of the keyhole during laser beam welding. Procedia CIRP 111 (2022).
- [3] Schwarzkopf, K., et al. Dynamic Beam Shaping in DED-LB/M: In-Process Observations and Adjustable Microstructure. ICALEO (2024).



## Design of reference optical receiver with 50GHz bandwidth for use in high speed fiber optic systems

Mr. Efi rotem

MKS

### Authors:

Efi Rotem, Andrew Davison, Jaesang Oh, Chintang Yen  
MKS Instruments

### Abstract:

**Introduction:** In high data-rate fiber optic communications systems, testing components against established standards is critical for obtaining low error-rate transmission. Such standards typically dictate test system performance for a specific modulation format, e.g., 28 Gbps NRZ or 53 GBd PAM4. This presentation describes the design and performance of a multimode optical-to-electrical converters (OE) for use in 28Gb/s NRZ and up to 112GBd PAM4 testing with controlled performance to 70 GHz. Designing a multimode OE to reach 70 GHz presented both optical and RF challenges. Custom RF amplifier and photodiode were developed for this project.

**Justification:** As data centers require ever-increasing communication bandwidth, bit rates rise and the number of fiber links increases. To accommodate this trend, new test systems are needed that operate at bandwidths near the edge of what is possible. With expertise in optics and RF, and a long history of manufacturing OE's, MKS is well positioned to provide this component.

**Overview of Data & Derived Conclusions:** Noise, gain, linearity and frequency response are the parameters that define the performance of an OE, and since the OE is the front-end of the test system, they determine key system specifications. Measurement results of prototype OE's will be presented.

## Advancements in Miniaturization, Weight Reduction, and Power Optimization for Infrared Imaging Systems by SCD

Dr. Yoram Karni

SCD

### Abstract:

This study focuses on recent advancements developed by SCD to address challenges in infrared (IR) imaging systems, particularly in reducing size, weight, and power consumption (SWaP) while enhancing system performance. The research emphasizes the development of novel technologies and design methodologies, offering a comprehensive approach to next-generation IR imaging.

A primary aspect of this work involves the design and implementation of advanced Readout Integrated Circuits (ROICs) tailored for real-time video processing. These ROICs incorporate algorithms for high-speed detection of short laser pulses and efficient change detection, enabling significant reductions in power consumption at the edge. The work demonstrates how such innovations can provide robust, low-power solutions for applications requiring real-time data processing in compact systems.

Another focus is the development of IR detectors with a 5-micron pixel pitch, representing a significant step forward in spatial resolution and sensitivity. These detectors enhance the system's ability to capture fine details and subtle variations, which are critical for a wide range of applications, including surveillance, navigation, and environmental monitoring.

The study also explores the integration of meta-material technologies to achieve substantial advancements in device miniaturization. By incorporating meta-optical elements into the detector architecture, this research enables reductions in edge unit size and weight while maintaining or improving optical performance. These advancements highlight the potential of meta-materials to redefine the design constraints of traditional optical systems.

The findings presented in this work demonstrate significant progress in addressing the SWaP challenges of IR imaging systems. The integration of advanced ROICs, high-resolution detectors, and meta-material technologies underscores the potential for transformative impacts across various domains, including defense, aerospace, and scientific instrumentation. Future work will focus on refining these technologies and exploring their applications in emerging fields requiring advanced IR imaging capabilities.

## Advancing Photonic and Optic Chip Packaging: Challenges and Technological Solutions

**Dr. Aviv Ronen**

*Beckermus Technologies*

### Abstract:

The ever-increasing demand for compact, high-performance photonic and optic chips is driving transformative changes in the semiconductor industry. As devices become more integrated and functionalities expand, the packaging of photonic and optic chips has emerged as a crucial yet complex challenge. Unlike traditional electronic packaging, photonic systems require precise optical alignment, efficient thermal management, and low optical losses – all while maintaining scalability and cost-effectiveness.

This lecture will provide a comprehensive overview of the critical challenges associated with photonic and optic chip packaging. Key areas of discussion will include the difficulties in achieving high-density integration, managing thermal loads in high-power photonic devices, and ensuring signal integrity across diverse material interfaces. These challenges are amplified by the need to maintain reliability in demanding operational environments, such as those found in telecommunications, data centers, and sensor applications. Innovative technologies and methodologies are paving the way for addressing these issues. The presentation will spotlight recent advancements in hybrid and monolithic integration techniques, automated alignment solutions with sub-micron precision, and the adoption of advanced materials that enhance thermal and mechanical performance. Real-world case studies will illustrate the successful application of these approaches, shedding light on best practices and lessons learned.

Attendees of this lecture will gain valuable insights into the current state of photonic chip packaging, emerging technologies, and future directions for research and development

## E posters Abstracts:

### Enhancing Mind Wandering Detection Through Multimodal Video and Audio Analysis: A Foundation for Neural Photonic Technologies in Education

**Mr. Amir Rabinovich**

*Holon Institute of Technology (HIT)*

### Authors:

Amir Rabinovitch, Eden Ben Baruch, Maor Siton, Nuphar Avital, Menahem Yeari, Dror Malka  
Holon Institute of Technology (HIT), Bar Ilan University

### Abstract:

**Objectives:** Mind wandering is a common phenomenon among schoolchildren and academic students, negatively affecting learning quality and teaching effectiveness. Current methods for detecting mind wandering while reading, such as eye trackers and EDA sensors, are often invasive and focus solely on external facial indicators. This study aims to develop a novel algorithm for detecting mind wandering using a combination of blink ratio, pitch frequency, and reading rate, providing a non-invasive and accessible solution.

**Methods:** The proposed method uses standard computer cameras and microphones to analyze both video and audio data. It integrates image recognition (Viola-Jones model), pitch frequency analysis, and voice activity detection (VAD). An experiment was conducted with ten participants who read aloud a 1,304-word text to validate the algorithm's performance.

**Results:** The algorithm achieved an accuracy of 76% in predicting mind wandering during specific text segments, demonstrating the effectiveness of the approach. The results indicate that non-invasive physiological indicators can reliably detect cognitive disengagement during reading.

**Conclusions:** The study highlights the feasibility of using non-invasive methods to detect mind wandering, with promising results in a controlled setting. This work also opens the door to future advancements, particularly through the integration of photonic technologies like photonic neural networks based on multimode fibers, which can enhance cognitive state detection in large-scale, long-duration scenarios. These innovations offer the potential for improved accuracy, processing speed, and data handling, contributing to seamless integration into educational systems and future research applications.

## ARTIFICIAL INTELLIGENCE IN OPTICS SESSION

### Oral presentation Abstracts:

#### Brightfield to fluorescence microscopy transfer via diffusion models

Mr. Oded rotem

##### Abstract:

**Objectives:** Alternatives and improvements to the current fluorescence microscopy methods is of great interest to the biomedical field. Fluorescence microscopy is often used to drive drug discovery and biological insights of cell level understanding. This bioimaging acquisition microscope is high cost, time consuming and has deformation effects on the specimen.

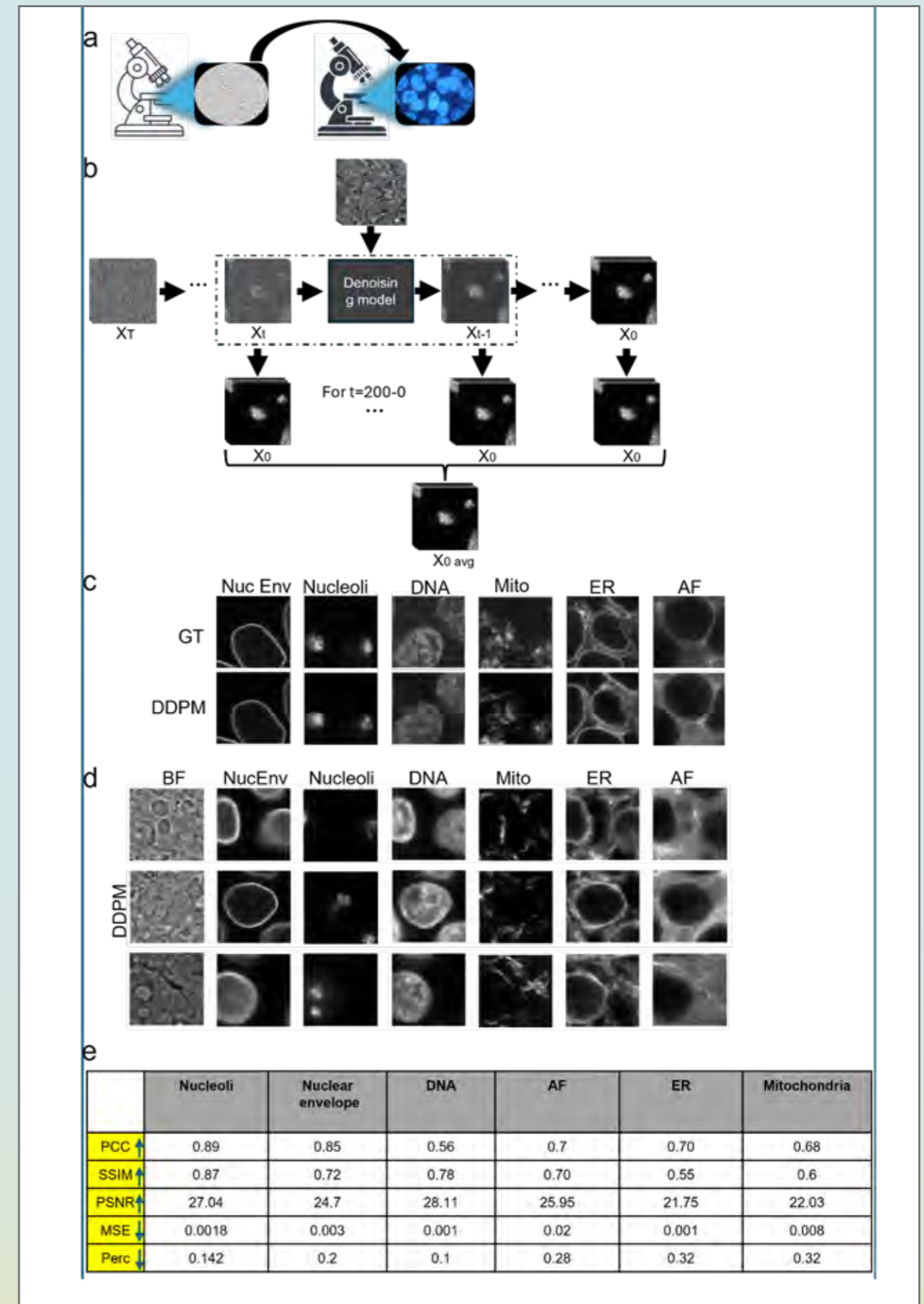
**Methods:** Similar to deep learning super-resolution techniques, image-to-image translation models can be developed for cross-modality problems such as transmitted light to fluorescence microscopy (Figure 1a). This deep learning alternative relies only on transmitted light microscopy which is cheaper and requires no heavy lifting in inference.

In this work we employ the Denoising Diffusion Probabilistic Model (DDPM) paradigm to faithfully predict volumetric fluorescence images of cell substructures from brightfield images. We optimized the DDPM model inference prediction for fluorescence biological images which have high background random noise and a relatively small percentage of foreground which include the regions of interest. This was done by averaging multiple timesteps predictions which can be extracted during inference, resulting in increased SNR (Figure 1b). We train a model for every fluorescence cell substructure from its paired brightfield transmitted microscope.

The DDPM predicted images similarity is compared to the ground truth using several metrics, spanning from spatial, spectral, information theory, deep perception networks as well downstream biological related measurements.

**Results:** We show very positive qualitative (Figure 1c – ground truth compared to DDPM generated images and Figure 1d – Generated images of six cell substructures from a single brightfield image) and quantitative results (Figure 1e) of our microscopic translation model. All cross-modality metrics and measurements show high similarity between ground truth and Diffusion generated predictions on six different substructures of cells.

**Conclusions:** We demonstrate the efficacy of applying SOTA diffusion-based models to synthesize realistic fluorescence microscopy images with high qualitative and quantitative similarity, driving an alternative to high end microscopy optics.





## Optical inference using nonlinear optical diffraction

**Prof. Alon Bahabad**

Tel-Aviv University

### Authors:

Oded Katz, Gilad Robert Barir, Barak Hadad, Daniel Marima and Alon Bahabad  
Tel-Aviv University

### Abstract:

**Objectives:** This study [1] introduces a novel optical inference platform that leverages nonlinear optical diffraction for computational tasks. The primary objective is to achieve efficient, all-optical computing for tasks such as image classification, addressing challenges like the inefficiency of nonlinear optical interactions and the bottleneck associated with hybrid electronic-optical systems.

**Methods:** We employed second-harmonic generation (SHG) in a nonlinear crystal, utilizing spatially modulated optical waveforms and phase-matching conditions to optimize performance. The system was trained using the MNIST handwritten digits dataset. The input data were encoded on a spatial light modulator (SLM), while the system's output was detected through second-harmonic (SH) intensity patterns. The crystal's temperature was fine-tuned as a hyperparameter to maximize computational efficiency by matching the spatial spectral distribution of the input data with the phase-matching curve.

**Results:** The platform demonstrated successful partial classification of handwritten digits while using a meager number of degrees of freedom. Optimal performance was observed slightly below the collinear phase-matching threshold, where spatial mode mixing is most effective. The system's computational operation was found to be significantly enhanced by phase-matching, which increased nonlinear interaction efficiency. The study highlights the scalability potential of the approach, with improvements achievable through additional computational layers and advanced optimization algorithms.

**Conclusions:** This research validates the feasibility of using nonlinear optical diffraction for inference tasks in an all-optical platform. By optimizing phase-matching conditions, the system achieves notable accuracy and efficiency. This work represents a step toward scalable, cost-effective all-optical computing, offering advantages in speed and parallelism compared to hybrid electronic-optical systems. Future efforts will focus on enhancing scalability and incorporating multi-layer architectures to further improve performance.

### References:

[1] Oded Katz et al., Applied Physics Letters, 125, 101105 (2024).

## Deep Phase Coded Image Prior

**Mr. Nimrod Shabtay**

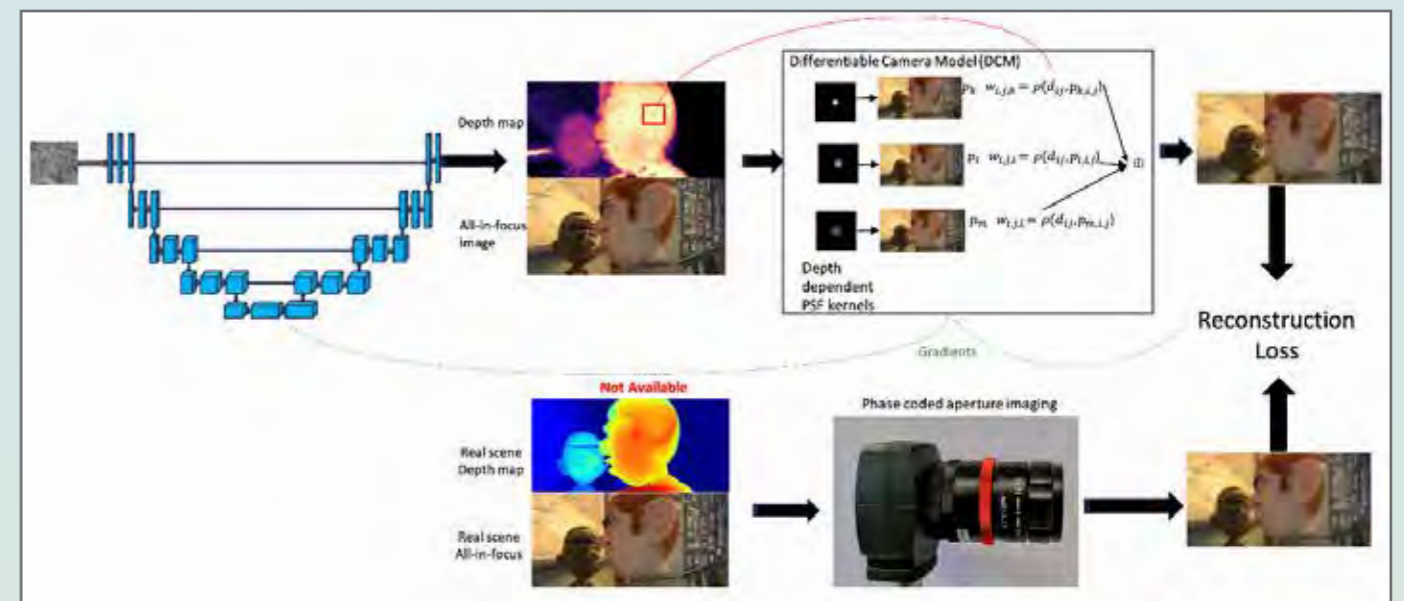
Tel-Aviv University

### Authors:

Nimrod Shabtay, Eli Schwartz and Raja Giryes

### Abstract:

Phase-coded imaging is a computational imaging method designed to tackle tasks such as passive depth estimation and extended depth of field (EDOF) using depth cues inserted during image capture. Most of the current deep learning-based methods for depth estimation or all-in-focus imaging require a training dataset with high-quality depth maps and an optimal focus point at infinity for all-in-focus images. Such datasets are difficult to create, usually synthetic, and require external graphic programs. We propose a new method named "Deep Phase Coded Image Prior" (DPCIP) for jointly recovering the depth map and all-in-focus image from a coded-phase image using solely the captured image and the optical information of the imaging system. Our approach does not depend on any specific dataset and surpasses prior supervised techniques utilizing the same imaging system. This improvement is achieved through the utilization of a problem formulation based on implicit neural representation (INR) and Deep Image Prior (DIP). Due to our zero-shot method, we overcome the barrier of acquiring accurate ground-truth data of depth maps and all-in-focus images for each new phase-coded system introduced. This allows focusing mainly on developing the imaging system, and not on ground-truth data collection.



## Flexible polymeric all-optical logic gates

**Dr. Amir Handelman**

*Holon Institute of Technology*

### Authors:

Amir Handelman  
Holon Institute of Technology, Holon, Israel

### Abstract:

The increased implementation of artificial neural network (ANN) in our daily lives requires non-traditional hardware that supports fast training sessions and is energy efficient. This need has given rise to several technologies especially designed for ANN processors, among them all-optical processors. While most of the photonic ANN architectures proposed to date are based on inorganic materials (especially silicon), using organic and polymeric materials represents a highly attractive alternative given that they are environmentally-friendly and have advantages in terms of biocompatibility, and ease of fabrication at low-costs. The basic building block in modern computing is the logic gate. Even ANN can be composed of logic gate operations. In this lecture, I will present our fast and simple method to construct Y-shaped two-terminal all-optical logic gate, made entirely by Poly(dimethylsiloxane) (PDMS). In addition, I will review the field of all-optical logic gates and discuss its relation to photonic neuromorphic computing. I will also show how we fabricated an ON/OFF switch, (which can also be considered as an all-optical NOT gate) from self-assembled amino-acid microcrystals.

## Coherence Awareness in Diffractive Neural Networks

**Mr. Matan Kleiner**

*Technion- Israel Institute of Technology*

### Authors:

Matan Kleiner, Lior Michaeli, Tomer Michaeli

### Abstract:

**Objectives:** Diffractive neural networks hold great promise for applications requiring intensive computational processing. Considerable attention has focused on diffractive networks for either spatially coherent or spatially incoherent illumination. In this work, we study the effect of the degree of spatial coherence on diffractive networks and propose a general framework for training these networks for any specified degree of spatial and temporal coherence.

**Methods:** We numerically optimize networks for image classification using our proposed framework and thoroughly investigate the dependence of their performance on the illumination's coherence. Our configuration comprises a spatially incoherent, uniformly bright source that illuminates a planar object, which is placed in front of a diffractive network and a detector. We control the spatial coherence level on the object by tuning the object's distance from the light source, using the van Cittert-Zernike theorem. We control the temporal coherence by simulating multiple wavelengths over the desired bandwidth.

**Results:** We show that when the spatial coherence length on the object is comparable to the minimal feature size preserved by the system, neither the incoherent nor the coherent extremes serve as acceptable approximations. This situation applies to autonomous vehicles and smartphones, where the illumination source is located near the camera's entrance pupil and is of similar dimensions.

Our analysis of trained networks indicates that spatial coherence has a significant impact on their performance, especially under a mismatch between the coherence conditions used in training and testing. To overcome this, we introduce the concept of coherence-blind networks and illustrate that this approach leads to enhanced resilience to changes in illumination conditions.

**Conclusions:** Our work provides means for adapting diffractive networks to environmental illumination rather than restricting their use to specialized settings. It constitutes a first step towards understanding the potential and limitations of optical computing under uncontrolled environmental lighting.

## AI-aided rapid cell classification using label-free interferometric imaging flow cytometry

**Ms. Dana Aharoni**

*Department of Biomedical Engineering, Tel Aviv University, Tel Aviv, Israel*

### Authors:

Dana Aharoni, Eden Dotan, Prof. Natan Shaked  
Tel Aviv University, Tel Aviv, Israel

### Abstract:

**Aim:** The goal of this research is to develop an automated cell classification algorithm based directly on off-axis imaging holograms, capable of processing thousands frame per second, as required in imaging flow cytometry.

**Methods:** We process directly the raw interferometric images, instead of quantitative phase images, of blood and cancer cells during rapid flow, to reduce time and computational resources, which is an essential step for real-time imaging flow cytometry. Optical imaging interferometry is used to capture the cells during flow quantitatively via their refractive index, which does not require chemical cell staining. A localization algorithm is applied on the off-axis imaging interferograms to detect cells within the frames, and a convolution neural network (CNN) is used for automatic cell classification. For rapid classification, we design a compact CNN architecture and employ optimization strategies to minimize inference time and model complexity without compromising accuracy.

**Results:** Our technique increases throughput compared to state-of-the-art models, achieving real-time label-free quantitative interferometric cell classification during flow.

**Conclusions:** This cell classification approach demonstrates rapid cell classification. In the future, integrating our model with high-speed cameras is expected to enable real-time implementation with much higher throughputs possible today.

## A one-click software for PSF-engineering-based 3D localization microscopy

**Mr. Dafei Xiao**

*Technion – Israel Institute of Technology*

### Authors:

Dafei Xiao, Yoav Shechtman

### Abstract:

3D localization microscopy by point spread function engineering (PSF) has become a powerful tool for super-resolution imaging of cellular structures. Deep learning has further enhanced this field, offering state-of-the-art algorithms for processing blinking images with densely labeled molecules. However, training these neural networks typically requires the realistic simulation of molecule images, which demands accurate modeling of both PSF and noise—posing a significant barrier for biologists without advanced computational expertise.

To address this challenge, we develop a user-friendly, one-click software tool. This graphical user interface (GUI) accepts optical system parameters, a z-stack of bead images with corresponding axial positions, and experimental images for localization, and outputs a localization list. It integrates phase retrieval, noise parameter determination, training data generation, network training and inference. Specifically, the software employs a scalar model-based phase retrieval method to derive a practical PSF model from the optical parameters and bead images. Then this model is used to guide us to determine noise parameters in experimental blinking images. Using the retrieved noise parameters and PSF model, we generate representative training data for a neural network, localization net—an enhanced version of DeepSTORM3D. Finally, the trained localization net performs inference on experimental data to produce a localization list. Our software bridges the gap between algorithm developers and biologists, enabling accessible and precise 3D localization microscopy without requiring extensive computational expertise.



## Achromatic imaging systems with flat lenses enabled by deep learning

Mr. Roy Maman

*The Hebrew University of Jerusalem*

### Authors:

Roy Maman, Eitan Mualem, Noa Mazurski, Jacob Engelberg and Uriel Levy  
The Hebrew University

### Abstracts:

**Objectives:** One of the major obstacles to the widespread use of meta lenses and other flat lenses in imaging systems, is their inherent chromatic aberrations which make them wavelength dependent. This is a physical limitation that cannot be avoided using hardware only, as the maximal achievable bandwidth is strictly limited by the uncertainty principle.

This work demonstrates a novel method, leveraging deep learning to achieve state-of-the-art, high-quality imaging of wide-field color images, comparable to commercial bulky imaging systems.

**Methods:** A dual-camera system was developed to simultaneously capture chromatic-aberrated images with a flat lens and reference images with a refractive lens. A dataset of outdoor images taken in natural conditions was created. Using this dataset, a deep-learning model based on visual transformer was trained to correct chromatic aberrations. Post-processing involved optical flow alignment to ensure precise matching of aberrated and ground truth images. Quantitative metrics such as PSNR and SSIM were employed to evaluate the reconstruction quality.

**Results:** The trained deep-learning model achieved notable success in correcting chromatic aberrations, producing images of high visual and quantitative quality across the visible spectrum. The average PSNR of the sampled image, relative to the ground truth images exceeded previous approaches by 8 db. The method outperformed existing deblurring techniques, in terms of several image quality metrics, setting a new benchmark for flat lens-based imaging systems.

**Conclusions:** This research presents a breakthrough in using deep learning to mitigate chromatic aberrations in flat lenses, enabling their application in advanced polychromatic imaging systems. The results provide a pathway for the widespread adoption of flat lenses in optical devices, offering advantages in size, cost, and weight reduction. The dataset and methodologies also create opportunities for further advancements in the field.



## E posters Abstracts:

### Attention-Driven Reconstruction of Lensless Polarization Images Using RGB Guidance

Ms. Noa Kraicer

*Giryas Deep Learning Lab, School of Electrical Engineering, Tel Aviv University*

### Authors:

Noa Kraicer, School of Electrical Engineering, Tel Aviv University, Tel Aviv, Israel. Raja Giryas, School of Electrical Engineering, Tel Aviv University, Tel Aviv, Israel.

### Abstract:

**Objectives:** This study introduces a robust approach for reconstructing polarization images from lensless cameras, utilizing attention mechanisms and RGB guidance. Lensless imaging offers compact, cost-effective solutions but poses significant challenges in polarization reconstruction because of limited spatial mapping. Our framework addresses this ill-posed inverse problem by combining baseline lensless polarization reconstruction with high-level features extracted from an RGB image. By leveraging self-attention for intra-domain fusion and cross-attention for inter-domain fusion, we aim to enhance reconstruction quality and establish a generalizable method for accurate polarization imaging under diverse conditions. Ultimately, it fosters advanced lensless imaging applications.

**Methods:** We trained our neural network using the PolarLITIS dataset, containing paired RGB and polarization images. A point spread function (PSF) convolution and a multiplexing polarization mask simulated lensless measurements. We first reconstructed the polarization images using hyperspectral FISTA, generating a baseline. Next, we fed these outputs and their corresponding RGB images into a reconstruction network, which alternately applied self-attention within each modality and cross-attention between modalities to fuse relevant information. To improve guidance, we replaced shallow RGB feature extraction with pretrained DINOv2 embeddings, incorporating semantically richer representations. AdamW optimization with L1 and LPIPS losses stabilized overall training.

**Results:** Our method substantially outperformed baseline reconstructions on the PolarLITIS test set, improving SSIM from 0.63 to 0.76 and PSNR from 21.81 dB to 25.74 dB. We also validated performance on the CEREMA dataset, featuring different RGB cameras and scenes, where SSIM increased from 0.82 to 0.92 and PSNR rose from 28.34 dB to 34.08 dB. These consistent gains highlight our framework's generalizability. Qualitative assessments revealed sharper polarization details and visually pleasing reconstructions across both datasets.

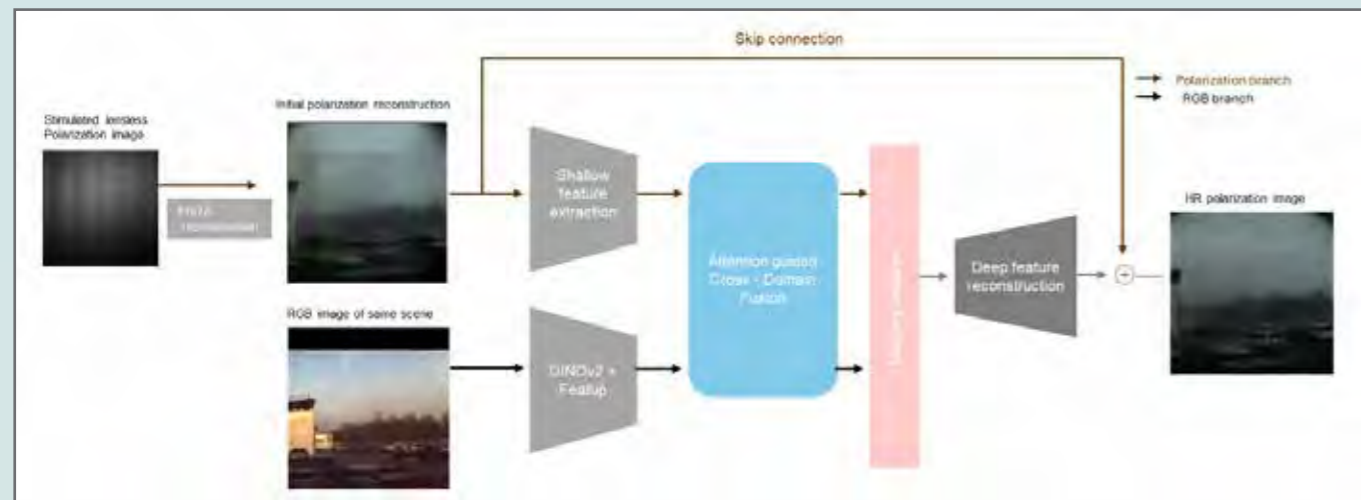
### Conclusion:

**Objectives:** This study introduces a robust approach for reconstructing polarization images from lensless cameras, utilizing attention mechanisms and RGB guidance. Lensless imaging offers compact, cost-effective solutions but poses significant challenges in polarization reconstruction because of limited spatial mapping. Our framework addresses this ill-posed inverse problem by combining baseline lensless polarization reconstruction with high-level features extracted from an RGB image. By leveraging self-attention for intra-domain fusion and cross-attention for inter-domain fusion, we aim to enhance reconstruction quality and establish a generalizable method for accurate polarization imaging under diverse conditions. Ultimately, it fosters advanced lensless imaging applications.

**Methods:** We trained our neural network using the PolarLITIS dataset, containing paired RGB and polarization images. A point spread function (PSF) convolution and a multiplexing polarization mask simulated lensless measurements. We first reconstructed the polarization images using hyperspectral FISTA, generating a baseline. Next, we fed these outputs and their corresponding RGB images into a reconstruction network, which alternately applied self-attention within each modality and cross-attention between modalities to fuse relevant information. To improve guidance, we replaced shallow RGB feature extraction with pretrained DINOv2 embeddings, incorporating semantically richer representations. AdamW optimization with L1 and LPIPS losses stabilized overall training.

**Results:** Our method substantially outperformed baseline reconstructions on the PolarLITIS test set, improving SSIM from 0.63 to 0.76 and PSNR from 21.81 dB to 25.74 dB. We also validated performance on the PolarWeather dataset, featuring different RGB cameras and scenes, where SSIM increased from 0.82 to 0.92 and PSNR rose from 28.34 dB to 34.08 dB. These consistent gains highlight our framework's generalizability. Qualitative assessments revealed sharper polarization details and visually pleasing reconstructions across both datasets.

**Conclusion:** Overall, our novel attention-based method, guided by semantically rich RGB features, offers a promising solution for lensless polarization imaging. These findings suggest potential in biomedical, remote sensing, and industrial surveillance.



## Evaluating Machine Learning Algorithm Efficiency in Embedded Systems for Real-Time Object Detection

**Dr. Yosef Golovachev**

*Jerusalem College of Technology*

### Authors:

Yosef Golovachev, Roni Zukerman and Benny Milgrom

### Abstracts:

Embedded systems have become increasingly popular due to their compact size, affordability, and ability to execute advanced algorithms in real time. Incorporating machine learning algorithms into these systems enhances performance and increases functional efficiency across various applications. However, running machine learning algorithms typically requires substantial processing power and extensive memory, both of which are significantly constrained in embedded systems.

The research aims to adapt the implemented algorithms to appropriate noise conditions, ensuring optimal performance for specific scenarios. The study evaluates YOLO (You Only Look Once) and MobileNet SSD (Single Shot Detection) real-time object detection algorithms, chosen for their distinct architectures, to determine their efficiency under resource-constrained conditions. Common image distortions, such as resolution noise and Gaussian blur, were analyzed separately to assess their impact on neural networks and image processing algorithms.

The experiments revealed distinct strengths of the two algorithms under evaluation. YOLO demonstrated superior accuracy in detecting objects under resolution noise. However, this came at the cost of higher CPU usage, making it less suitable for systems with strict resource limitations. In contrast, MobileNet SSD exhibited better CPU efficiency, maintaining a lower computational footprint while providing reliable performance under Gaussian blur conditions. While YOLO achieved higher detection accuracy overall, MobileNet SSD excelled in real-time execution by maintaining minimal latency and reducing resource strain.

Both YOLO and MobileNet SSD are viable options for object detection in embedded systems, with the choice dependent on the application's specific requirements. YOLO is more suitable for scenarios demanding high detection accuracy, where higher CPU usage can be accommodated. Conversely, MobileNet SSD is ideal for applications requiring stringent real-time performance and CPU efficiency, as it achieves reliable detection with minimal resource consumption. These findings highlight the importance of balancing computational efficiency and detection accuracy in embedded systems.

## All-Optical Inference Engine Based on a Shape-Optimized Multimode Optical Fiber

Mr. Daniel Marima

Tel-Aviv University, Tel-Aviv, Israel

### Authors:

Daniel Marima: Tel-Aviv University, Tel-Aviv, Israel; Barak Hadad: Tel-Aviv University, Tel-Aviv, Israel; Oded Katz: Tel-Aviv University, Tel-Aviv, Israel; Avishay Eyal: Tel-Aviv University, Tel-Aviv, Israel; Alon Bahabad: Tel-Aviv University, Tel-Aviv, Israel

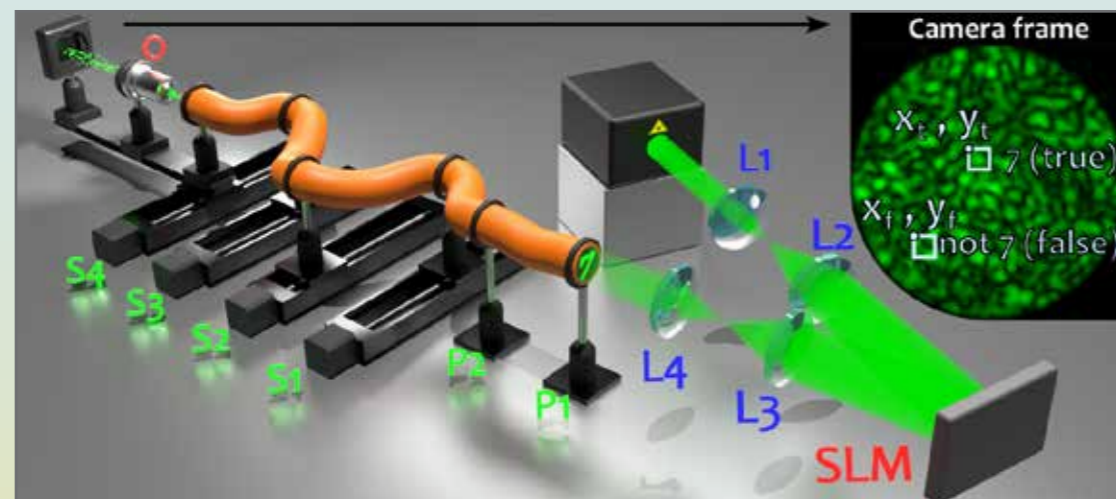
### Abstract:

**Objectives:** Optical computing has been gaining a lot of interest in recent years, as the demand for fast and efficient computing is rapidly increasing. Among the recently researched platforms are multimode optical fibers (MMFs). Most of the platforms that utilize MMFs do not demonstrate an all-optical computation, rather a hybrid combination of optical and electrical computation. The main objective of our work is to enable all-optical computation using an MMF, by optimizing the fiber's shape.

**Methods:** In our experiment, Images of digits from the MNIST dataset are projected into the fiber, and the purpose of the system is to recognize the digits based on light focusing at the output of the fiber according to the projected digit. For this purpose, the fiber is attached to four linear stages, and a genetic algorithm optimizes the shape of the fiber (the positions of the stages) to obtain recognition of the digits. After the training process, recognition of a single digit out of all digits is possible merely by comparing the intensities at two small regions at the output of the fiber, allowing for an all-optical classification.

**Results:** Our system is capable of recognizing images of a single digit out of images of all possible digits. The average classification accuracy is approximately 80%.

**Conclusions:** We presented a proof-of-concept all-optical computation system based on light focusing at the output of an MMF using fiber shape optimization. Aiming to improve the system and make it more applicable, future research may include: adding more control points along the fiber, improving the optimization algorithm, adding non-linearity, and making the system robust to external perturbations (temperature, vibrations, etc.).



## ATOMIC AND QUANTUM OPTICS Session

### Orel presentations Abstracts:

## Massively Multiplexed Wide-field Photon Correlation Sensing

Dr. Shay Elmalem

Department of Physics of Complex Systems, Weizmann Institute of Science

### Authors:

Shay Elmalem (WIS), Gur Lubin (WIS), Michael Wayne (EPFL), Claudio Bruschini (EPFL), Edoardo Charbon (EPFL), Dan Oron (WIS)

### Abstract:

Temporal photon correlations have been a crucial resource for quantum and quantum-enabled optical science for over half a century. However, attaining non-classical information through these correlations has typically been limited to a single point (or at best, a few points) at-a-time. We perform here a massively multiplexed wide-field photon correlation measurement using a large 500×500 single-photon avalanche diode array, the SwissSPAD3. We demonstrate the performance of this apparatus by acquiring wide-field photon correlation measurements of single-photon emitters, and illustrate two applications of the attained quantum information: wide-field emitter counting and quantum-enabled super-resolution imaging (by a factor of  $\sqrt{2}$ ). The considerations and limitations of applying this technique in a practical context are discussed. Ultimately, the realization of massively multiplexed wide-field photon correlation measurements can accelerate quantum sensing protocols and quantum-enabled imaging techniques by orders of magnitude.

The work is presented in parallel as an invited talk in Photonics West 2025:  
[spie.org/photronics-west/presentation/Massively-multiplexed-sensing-of-photon-statistics-with-large-format-SPAD/13392-106](https://spie.org/photronics-west/presentation/Massively-multiplexed-sensing-of-photon-statistics-with-large-format-SPAD/13392-106)

A pre-print on arXiv:  
[arxiv.org/abs/2412.16914](https://arxiv.org/abs/2412.16914)



## Single-photon Raman interaction for realizing the photon-number splitting attack

Mr. Ariel Ashkenazy

Bar-Ilan University

### Authors:

Ariel Ashkenazy, Faculty of Engineering and the Institute of Nanotechnology and Advanced Materials, Bar-Ilan University, Ramat Gan 5290002, Israel; Yuval Idan, Faculty of Engineering and the Institute of Nanotechnology and Advanced Materials, Bar-Ilan University, Ramat Gan 5290002, Israel; Dor Korn, AMOS and Department of Chemical and Biological Physics, Weizmann Institute of Science, Rehovot 76100, Israel; Dror Fixler, Faculty of Engineering and the Institute of Nanotechnology and Advanced Materials, Bar-Ilan University, Ramat Gan 5290002, Israel; Barak Dayan, AMOS and Department of Chemical and Biological Physics, Weizmann Institute of Science, Rehovot 76100, Israel. Quantum Source Labs, Rehovot 7670402, Israel; Eliahu Cohen, Faculty of Engineering and the Institute of Nanotechnology and Advanced Materials, Bar-Ilan University, Ramat Gan 5290002, Israel

### Abstract:

**Objectives:** To propose the implementation of the photon-number-splitting (PNS) attack on quantum key distribution (QKD) protocols leveraging single-photon Raman interaction (SPRINT) within a cavity-enhanced three-level atomic system and assess its feasibility and implications.

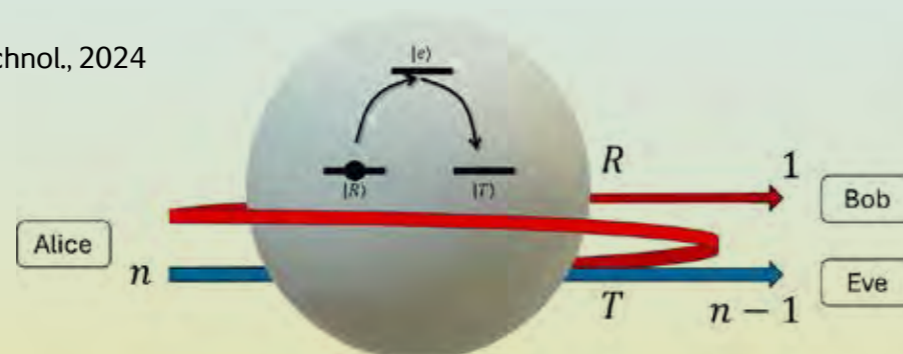
**Methods:** We propose an experimental framework utilizing SPRINT to execute the PNS attack. Analytical derivations and numerical simulations were performed to evaluate the attack's detection statistics for phase-randomized weak-coherent states, the purity of the quantum state post-attack, and the induced coherence changes and quantum bit-error rate (QBER).

**Results:** The proposed framework demonstrates that the PNS attack is feasible with existing technology. Analytical results reveal that the eavesdropper's information gain is not perfect, challenging earlier theoretical assumptions. Furthermore, we show that the attack disrupts the coherence of the quantum state, inducing a non-zero QBER, highlighting the practical effects of PNS on QKD systems.

**Conclusions:** This work establishes the practical realizability of the PNS attack using SPRINT and its limitations in real-world scenarios. The results emphasize the need for advanced QKD protocols, such as the coherent one-way (COW) protocol, to counteract such vulnerabilities. Additionally, the analytical findings provide insights into fundamental questions about single-photon subtraction and quantum information dynamics. If time permits, recent experimental results supporting these theoretical insights will also be discussed, further reinforcing the significance of this research.

### References:

Ashkenazy et al., Adv. Quantum Technol., 2024



## Leveraging Sparsity for Efficient Detection of Entanglement in High

Mr. Stav Lotan

Technion – Israel Institute of Technology

### Authors:

Ronen Talmon Technion Haifa Israel; Guy Bartal Technion Technion Haifa Israel

### Abstract:

Reliable detection and certification of quantum entanglement in high-dimensional systems is vital for quantum technologies. Existing methods use the \$g(2)\$ correlation algorithm, which is computationally expensive and requires extensive data. This research aims to improve the \$g(2)\$ algorithm by leveraging the inherent sparsity in the correlation matrix of entangled quantum data, improving the efficiency and accuracy of entanglement detection.

Here we introduced an optimization framework using L1 regularization to enhance sparsity in the correlation matrix. This technique minimizes the sum of absolute matrix elements, suppressing noise and highlighting significant correlations.

Our objective function is:

$$\hat{\Sigma} = \arg \min_{\Sigma} L(\hat{\Sigma}, \Sigma) = \text{MSE}(\hat{\Sigma} - \Sigma) + \lambda \|\hat{\Sigma}\|_1 \quad (1)$$

where  $\hat{\Sigma}$  is the optimized sample covariance matrix,  $\Sigma$  the sample covariance matrix,  $\lambda$  is a hyperparameter, MSE is the mean square error which is calculated by the L2 norm of a matrix which is  $(\sum_{i,j} |\hat{\Sigma}_{ij} - \Sigma_{ij}|^2)^{1/2}$  and the L1 norm of a matrix is  $\sum_{i,j} |\hat{\Sigma}_{ij}|$ , where  $a_{ij}$  are the matrix elements.

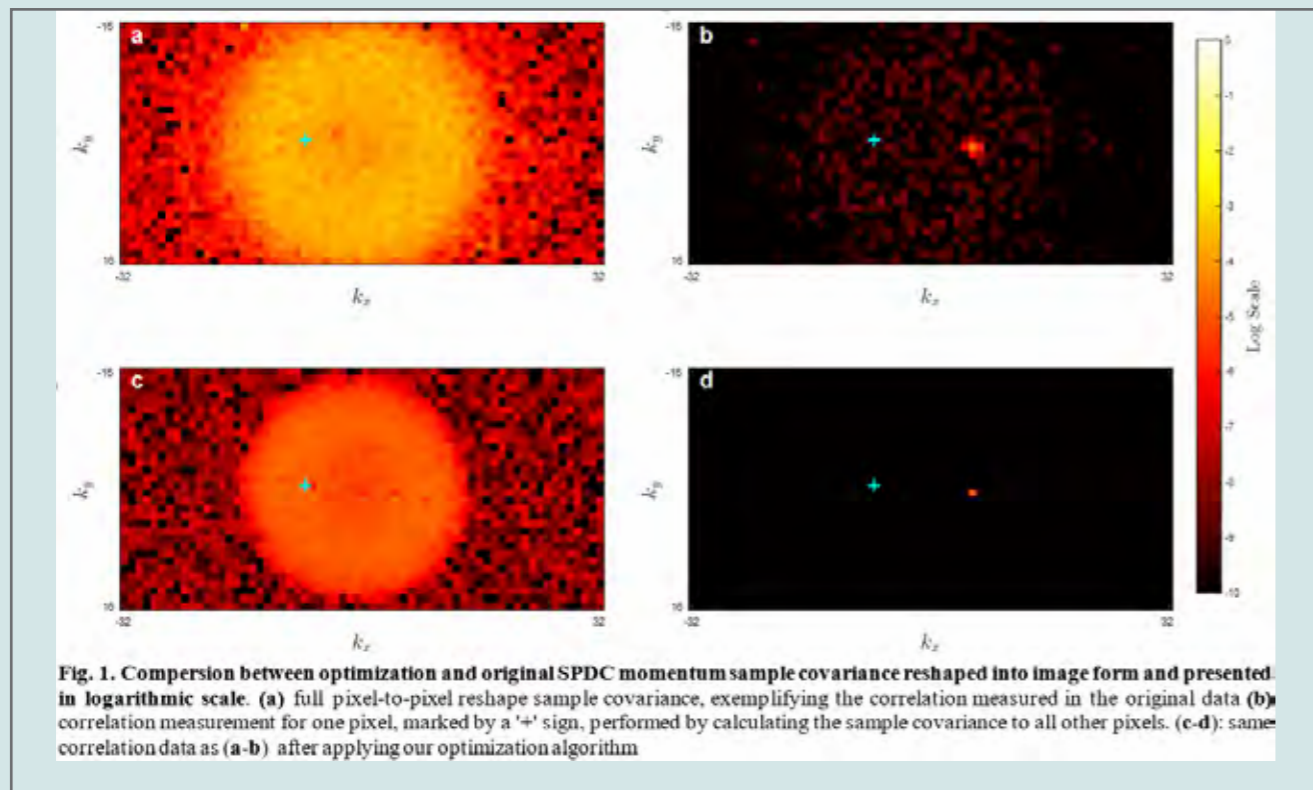
The approach was tested on experimental data from a covariance matrix measurement of SPDC position space using 10 million images from ref [1]. The reconstructed sparse matrices were analyzed using entanglement witness algorithms to estimate the dimensionality of entanglement.

Our sparsity-driven methodology significantly improved the visibility of quantum correlations as shown in the attached image. To further confirm our results, we used an entanglement witness algorithm on the L1-optimized covariance matrices which increased the lower bound on the entanglement dimensionality from 37 to 107 compared to unoptimized matrices.

In conclusion, our approach, combining tools from statistical signal processing techniques with entanglement witness algorithms, revealed significant improvements in the detection of quantum correlations and offers a powerful framework for detecting and certifying quantum entanglement in complex systems.

### References:

[1] B. Ndagano et al, "Imaging and certifying high-dimensional entanglement with a single-photon avalanche diode camera," Npj Quantum Inf. 6, 94 (2020).



### Correlation of Purely Spatial Bell-state Measurements in Event-based Single-Photon Camera

Mr. Gilad Pollack

Tel-Aviv University

**Authors:**

Gilad Pollack, Tel-Aviv University, Tel Aviv Israel. Hadar Aharon, Tel-Aviv University, Tel Aviv Israel. Isaac Reichman, Tel-Aviv University, Tel Aviv Israel. Ofer Kfir, Tel-Aviv University, Tel Aviv Israel.

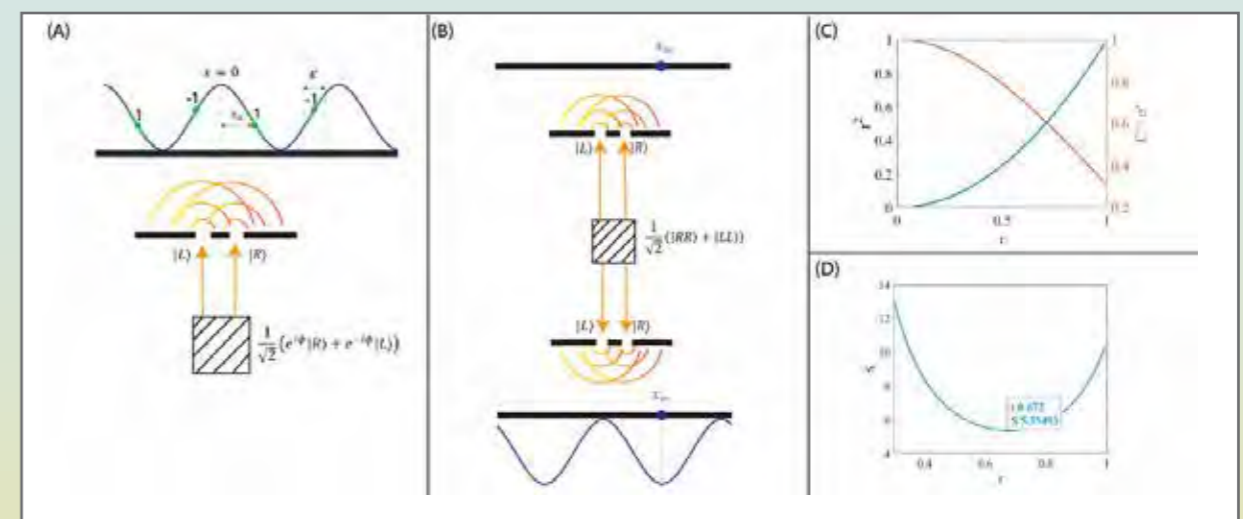
**Abstract:**

The Bell experiment is the undisputed standard for measuring quantum entanglement between pairs of particles. However, experiments so far had only studied pairs of identical particles. When attempting to measure entangled pairs of different particles, such as entangled electron-photon pairs, the existing Bell experiment schemes are insufficient.

We propose a conceptual setup of double-slits and their far-field diffractions, manipulated only by free-space manipulation available for particles, such as deflection (prism) or conversion (lens). In our scheme, Alice and Bob each receive a particle to their (typically opposing) side. Each has a double-slit interferometer as seen in the figure (B). We assume the entangled version of the double slit is manifested in a wave function is  $|\psi\rangle = \frac{1}{\sqrt{2}} (|RR\rangle + |LL\rangle)$ , where R and L represent the right and left slits respectively, the first index represents Alice's side, and the second Bob's. We show that in such a system, a measurement at position  $x_m$  on Alice's far-field results in a distinct phase on the probability pattern Bob's arm. We also show that the basis selection required to conduct a Bell experiment can be implemented by post-selection.

Figure C-D quantifies the correlations in our system in comparison to polarization-based Bell experiments in entangled photons, showing they are of a similar magnitude. The comparison accounts for the continuity of the far-field, in contrast to the two dimensionality of polarization, which creates a tradeoff parameterized by  $r$ . Post-selecting a smaller fraction from the measurements makes them more informative, but reduces their rate. At an optimal post-selection, a diffraction measurement in our scheme requires only  $\sim 5$  times the events of a standard Bell experiment.

We measure this scheme experimentally by recording the interference of entangled photons from an SPDC source on a Timepix3 single-photon camera and present preliminary results.



## Experimental Phase Retrieval of Atomic Matter Waves

Mr. Ron Ziv

Technion – Israel Institute of Technology

### Authors:

Ron Ziv (Technion – Israel Institute of Technology, Haifa, Israel), Sambit Banerjee (Purdue University, West Lafayette, Indiana USA), Hikaru Tamura (Purdue University, West Lafayette, Indiana USA), Yoav Sagi (Technion – Israel Institute of Technology, Haifa, Israel), Chen-Lung Hung (Purdue University, West Lafayette, Indiana USA), and Mordechai Segev (Technion – Israel Institute of Technology, Haifa, Israel)

### Abstract:

Bose-Einstein condensates (BECs) and atomic superfluids are quantum states of matter where particles are trapped and cooled to form a macroscopic population in a single quantum state, resulting in a coherent matter wave. These states are typically studied by imaging particles in-situ or in the “far-field” through time-of-flight (TOF) imaging, which records the atomic density. Alas, as this is a quantum state, it also has a well-defined phase structure, which cannot be resolved by these measurements alone. Phase information is traditionally obtained through interference-based measurements, but such methods are experimentally intricate, destructive, and limited in the information they can provide.

Motivated by these challenges and the growing potential of computational methods, we address the question: can the complete spatial phase and amplitude of a Bose gas be reconstructed from traditional imaging measurements without relying on interferometric techniques or other intricate methods? As we show, this problem relates to the well-known algorithmic phase retrieval challenge in optics but differs in key aspects.

Here, we demonstrate the application of algorithmic phase retrieval to experimental data from a 2D Bose gas for the first time. This approach allows full characterization of the quantum wavefunction of cold atoms using only TOF density measurements. To validate our method, we reconstructed three phase structures imprinted on an atomic cloud: a linear phase gradient, a single vortex, and dipole vortices.

Our results introduce a promising, non-interferometric experimental technique to map the phase structure of quantum wavepackets, overcoming the limitations of traditional interferometric methods. This approach opens new avenues for investigating the spatial phase and amplitude of quantum system, potentially enabling novel probing regimes and offering greater flexibility in existing applications.

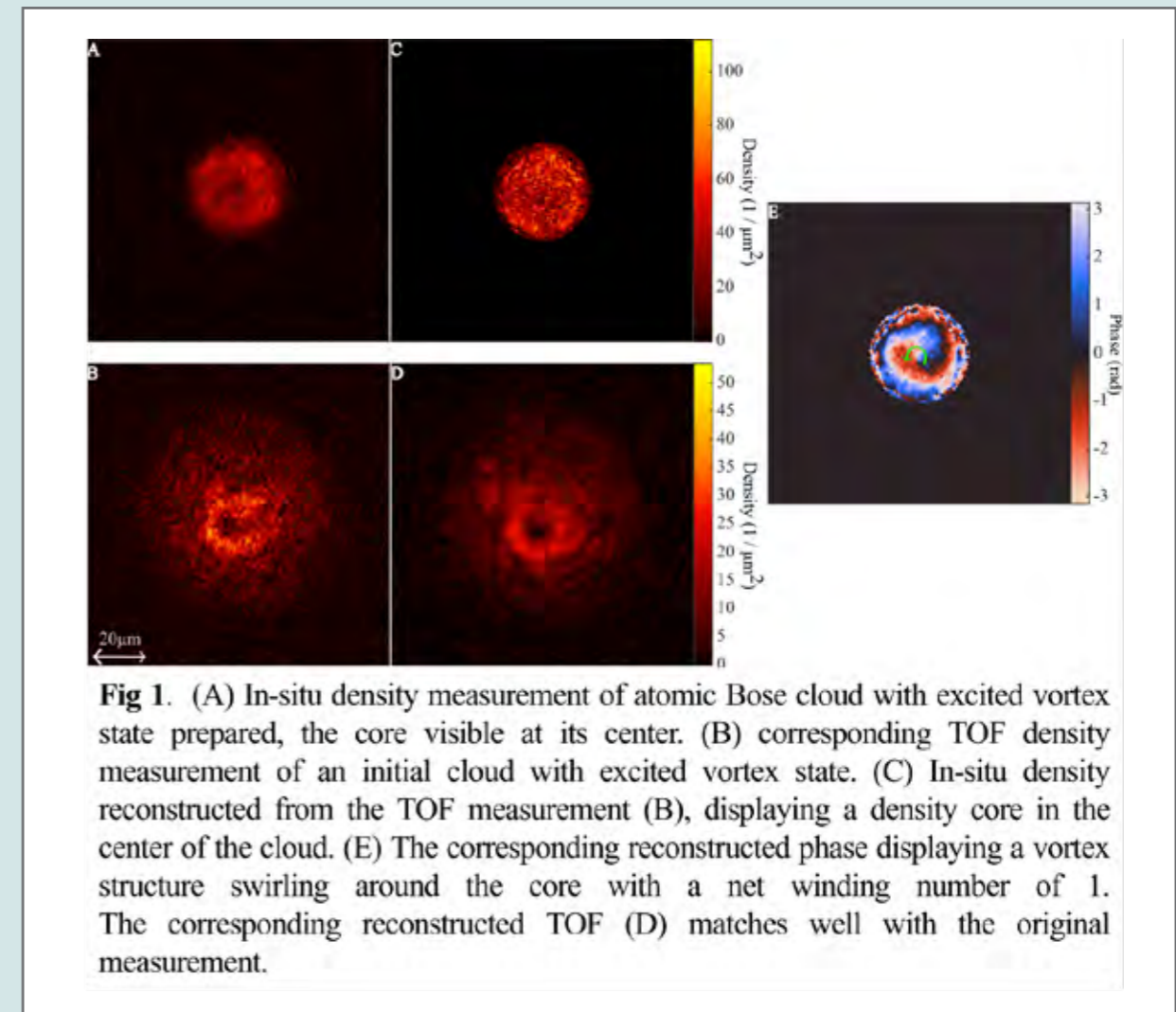


**Fig 1.** (A) In-situ density measurement of atomic Bose cloud with excited vortex state prepared, the core visible at its center. (B) corresponding TOF density measurement of an initial cloud with excited vortex state. (C) In-situ density reconstructed from the TOF measurement (B), displaying a density core in the center of the cloud. (E) The corresponding reconstructed phase displaying a vortex structure swirling around the core with a net winding number of 1. The corresponding reconstructed TOF (D) matches well with the original measurement.



## Superfluorescent Scintillation from Coupled Perovskite Quantum Dots

Mr. Shaul Katznelson

Technion – Israel institute of technology

### Authors:

Shaul Katznelson–Technion–Haifa–Israel, Shai Levy–Technion–Haifa–Israel, Alexey Goralch–Technion–Haifa–Israel, Nathan Regev–Technion–Haifa–Israel, Michael Birk–Technion–Haifa–Israel, Chen Mechel–Technion–Haifa–Israel, Offek Tziperman–Technion–Haifa–Israel, Roman Schuetz–Technion–Haifa–Israel, Rotem Strassberg–Technion–Haifa–Israel, Georgy Dosovitsky–Technion–Haifa–Israel, Charles Roques-Carnes–Stanford–Stanford–USA, Yehonadav Bekenstein–Technion–Haifa–Israel, and Ido Kaminer–Technion–Haifa–Israel

### Abstract:

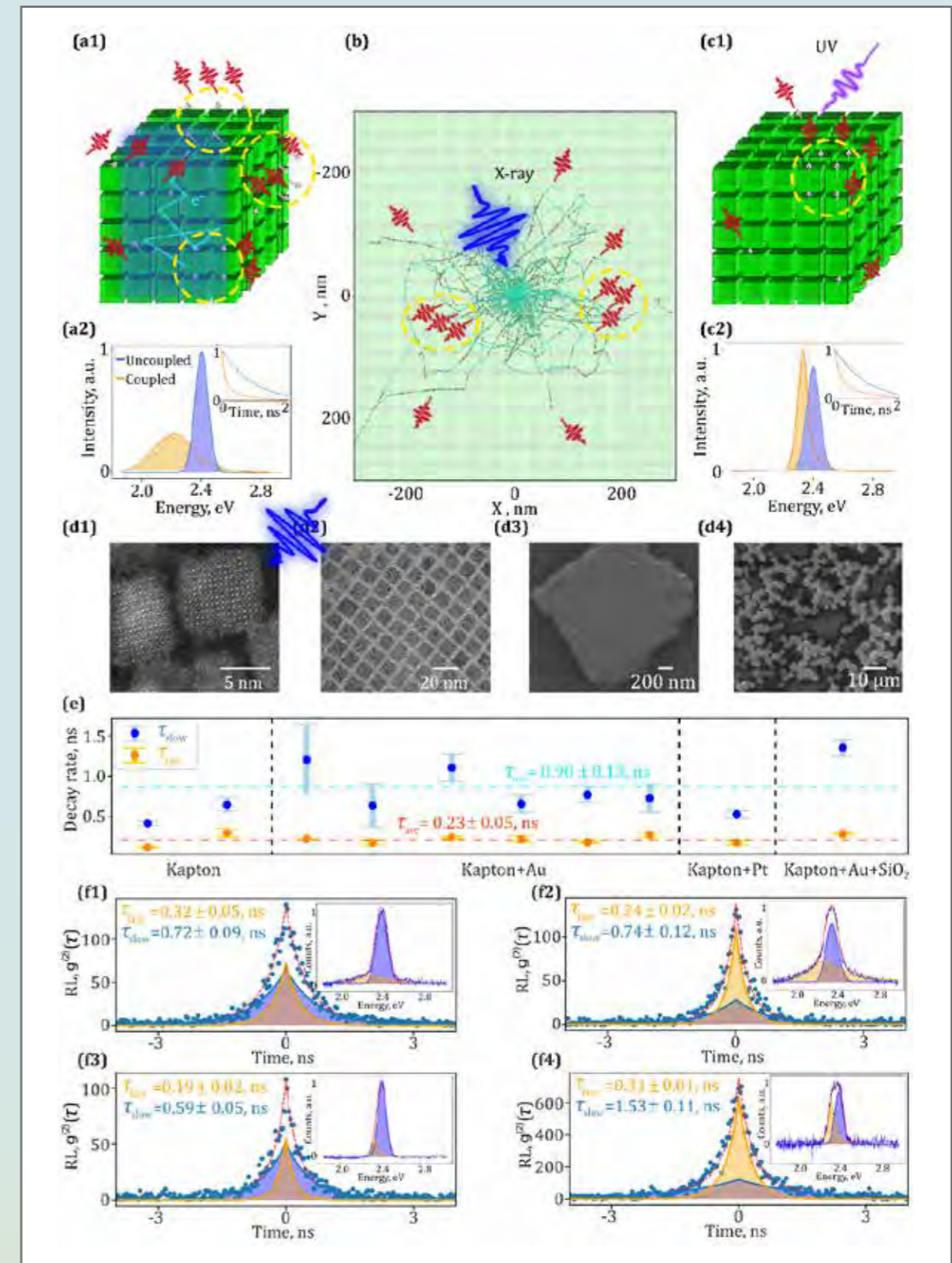
Scintillation, the process of converting high-energy radiation to visible light, is pivotal in applications from medical diagnostics to fundamental science. Despite significant advancements toward faster, more efficient scintillators, there remains a fundamental limit arising from the intrinsic properties of current scintillating materials. The scintillation process culminates in spontaneous emission, which is restricted in its rate by the intrinsic dipole strengths of individual emission centers in the material.

Here, we propose and demonstrate the first superfluorescent scintillator [1] (Fig.a): accelerating the conversion of X-rays to visible light by collective emission from multiple synchronized emitters. Superfluorescent scintillation breaks the fundamental limits on scintillators by using the strong interactions between simultaneously excited coupled perovskite quantum dots (QD). This phenomenon is characterized by a spectral shift and an enhanced rate of emission, reaching average lifetime of 230 ps at 80 K, 14 times faster than their room temperature spontaneous emission. This enhancement is consistent across samples and shown for various substrates, i.e., Kapton, Kapton+Au, Kapton+Pt and Kapton+Au+SiO<sub>2</sub> respectively (Fig.e).

Such QDs (Fig.d) exhibit superfluorescence under UV excitation [2] (Fig.c). However, X-ray superfluorescence is inherently different, as each high-energy photon creates multiple synchronized excitation events, triggered by a photoelectron, resulting in even faster emission rates, a larger spectral shift, and a broader spectrum (Fig.a2,c2). We use a Hanbury-Brown-Twiss (HBT)  $g^{(2)}(\tau)$  setup [3] to analyze the temperature-dependent temporal response of these scintillators (Fig.f1–4). These observations align with our quantum-optical theory explaining both UV- and X-ray-driven effects, supported by Monte Carlo simulations (Fig.b). Superfluorescent scintillators could dramatically improve time-of-flight detector performance, introducing quantum enhancements to scintillation science.

### References:

- [1] Katznelson, S., Levy, S., Goralch, A., Regev, N., et al: arXiv 2412.21101 (2024).
- [2] Rainò, G., et al: Nature 563, 671–675 (2018).
- [3] Katznelson, S., Kasten, N., et al: arXiv 2412.16975 (2024).



## Superradiating Photon Entanglement Source with Multilevel Atoms

Mr. Amir Sivan

Technion – Israel Institute of Technology

### Authors:

Amir Sivan<sup>1,2</sup>, Meir Orenstein<sup>1,2</sup>,

1 Department of Electrical Engineering, Technion, Haifa, Israel

2 Helen Diller Quantum Center, Technion, Haifa, Israel

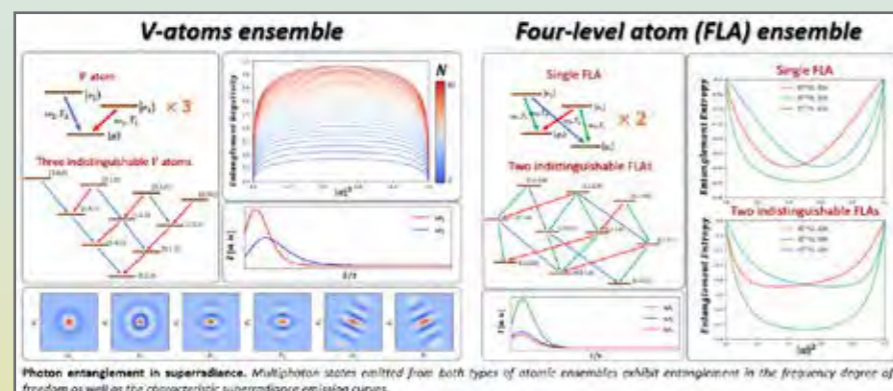
### Abstracts:

**Objectives:** Realization of a source of multiphoton entanglement from an atomic ensemble via a fast and deterministic superradiance process.

**Methods:** We leverage the collective emission phenomenon of superradiance in order to generate multiphoton states entangled in their frequency degree of freedom. The original Dicke superradiance model and its extensions have only dealt with the atomic ensemble entanglement and photonic ensemble-average observables such as intensity and autocorrelation and photonic entanglement have never considered. We achieve our objective by analyzing superradiance from an ensemble of indistinguishable multilevel atoms. We consider two types of atoms – V-atoms and four-level atoms with a partial degeneracy of their radiative transitions. To obtain the quantum properties of the emitted photons we develop a new model based on the Weisskopf–Wigner model of spontaneous emission for generalized Dicke energy ladders. This allows us to calculate the entanglement entropies of the multiphoton states and to analyze their multimodal Wigner distributions.

**Results:** We find that both ensemble types emit multiphoton states which are entangled, emanated via a superradiant processes. The photonic entanglement stems from two mechanisms – (i) excitation of the atomic ensemble into a combination state, (ii) intra-atom degeneracies that induce nonclassical correlations via virtual interatomic transitions – both of which are imprinted onto the emitted multiphoton states, as demonstrated by entanglement entropies and nonclassical correlations seen in the multimodal Wigner distributions. We also dwell on the important property of photonic mode-independent entanglement that manifests in the four-level atom ensembles.

**Conclusions:** We have introduced photon entanglement to superradiance by considering multilevel atoms, thereby creating deterministic, high-yield sources of multiphoton entanglement. The measures of entanglement are highly dependent on the atomic superposition excitation, making this entanglement source controllable. The four-level atoms ensemble has the additional property of emitting multiphoton states with entanglement that does not depend on the measurement basis.



## Prospects of Free-Space Quantum Key Distribution using Spatial Modes of Light: Scaling-up the Dimensionality and the Distance

Dr. Georgi Gary Rozenman

Postdoctoral Associate at the MIT Department of Physics. Group of Wolfgang Ketterle at MIT

### Authors:

Joseph Meyer<sup>1</sup>, Yuval Reches<sup>2</sup>, Georgi Gary Rozenman<sup>1,2,3</sup>, Yaron Oz<sup>2</sup>, Haim Suchowski<sup>2</sup>, and Ady Arie<sup>1</sup>

1 School of Electrical Engineering, Iby and Aladar Fleischman Faculty of Engineering, Tel Aviv University, Tel Aviv 69978, Israel

2 Raymond and Beverly Sackler School of Physics & Astronomy, Faculty of Exact Sciences, Tel Aviv University, Tel Aviv 69978, Israel

3 Research Laboratory of Electronics, MIT-Harvard Center for Ultracold Atoms, Department of Physics, Massachusetts Institute of Technology, Cambridge, MA 02139, USA 02139, USA

### Abstract:

The advancement of Quantum Key Distribution (QKD) is paramount in safeguarding communications against the growing computational power of quantum computers, which threaten classical encryption protocols. This study explores the potential of high-dimensional encoding in QKD using spatial modes of light, providing an innovative alternative to traditional polarization-based systems. Spatial modes, characterized by their spatial distribution patterns, offer the advantage of higher bit-per-photon rates due to their utilization of a high-dimensional Hilbert space. In this work, we implement the BB84 protocol through a classical light analogy, achieving a secure key rate of 1.55 bits per sifted photon in a controlled laboratory setup for dimensions ranging from 2 to 16. We further extend our experiments to an outdoor environment, successfully transmitting QKD signals over distances of up to 90 meters for two-dimensional encoding and 50 meters for four-dimensional encoding.

Our experimental setup employs superpositions of Hermite–Gaussian modes in two mutually unbiased bases for encoding, with holographic modulation of spatial light modulators for efficient mode generation and detection. A comparative analysis of indoor and outdoor results reveals a linear correlation between error rate and dimensionality, attributed to the increasing sensitivity of higher-order modes to alignment and noise.

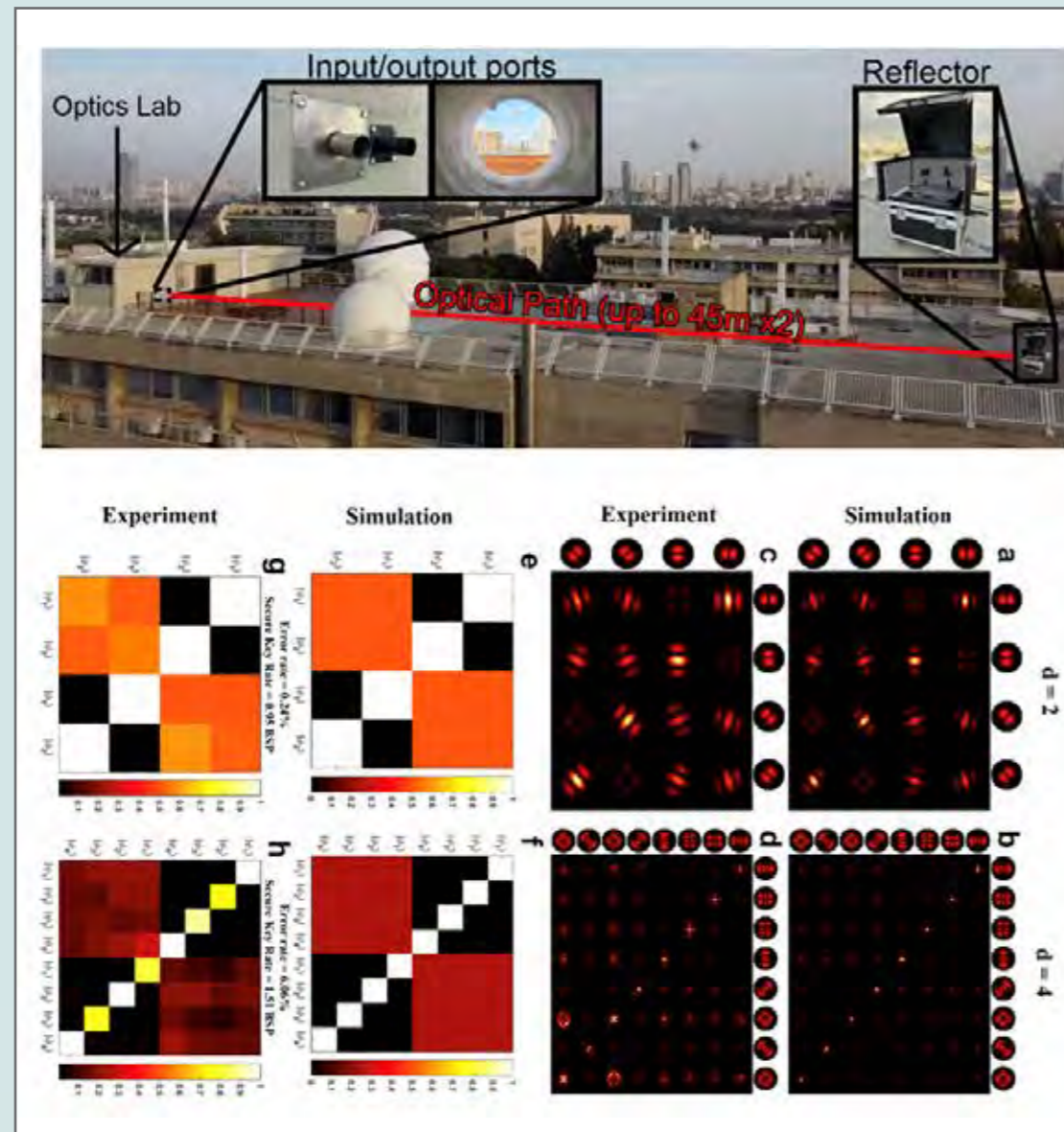
These results demonstrate the feasibility of scaling both dimensionality and distance in free-space QKD while addressing the inherent challenges posed by beam divergence and turbulence in atmospheric channels.

Funding: This work was supported by the Israeli Ministry of Innovation, Science and Technology, grant no. 5349 and by the Tel Aviv University Center for Quantum Science and Technology.

### References:

- [1] Bennett, C. H.; Brassard, G. (1984). "Quantum cryptography: Public key distribution and coin tossing". Proceedings of the International Conference on Computers, Systems & Signal Processing, Bangalore, India. Vol. 1. New York: IEEE. pp. 175–179
- [2] Otte, Eileen, et al. "High-dimensional cryptography with spatial modes of light: tutorial." JOSA B 37.11 (2020): A309–A323.





### E posters Abstracts:

#### Temperature-Dependent Evolution of Photoluminescence - Rate, Coherence, Entropy, and Chemical Potential

Prof. Carmel Rotschild

Technion - IIT

#### Authors:

Carmel Rotschild, Tomer Bar Lev - Technion IIT, Haifa, Israel

#### Abstracts:

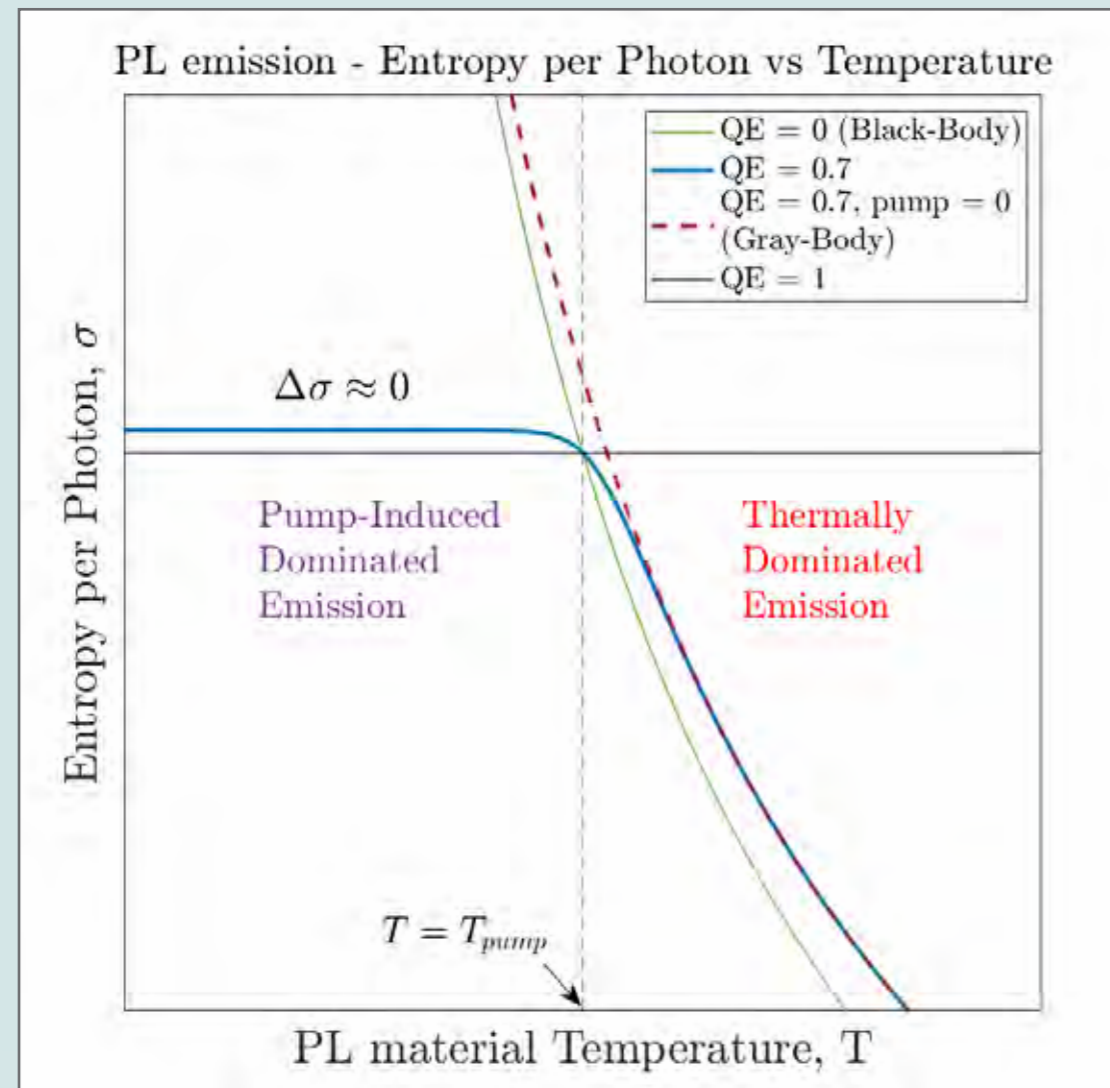
**Objectives:** This study aims to explore the temperature-dependent evolution of photoluminescence (PL), focusing on coherence, entropy, and chemical potential. The work shows how PL transitions from pump-induced emission to thermal characteristics as temperature increases, highlighting the implications for such thermodynamic properties, coherence, and photon statistics. These findings provide a deeper understanding of PL.

**Methods:** The study employs theoretical modeling and analytical derivation of a temperature-controlled bandgap material excited by an optical thermal pump. Building on a previously studied temperature-dependent PL emission, the chemical potential and entropy per photon were calculated. This approach is then extended to continuum energy levels above the bandgap, allowing for the derivation of the coherence length from the emission spectrum. Finally, the photon statistics is analyzed, with the emission statistics shown to depend on temperature.

**Results:** The findings identify a temperature range where the PL emission rate and entropy per photon remain quasi-conserved at lower temperatures, followed by a rapid transition to thermal behavior. At lower temperatures, the chemical potential approaches the photon energy limit ( $h\nu$ ), and as the temperature increases, it drops to zero, indicating thermal equilibrium with the pump. This contrasts the smooth reduction of coherence length with temperature, exhibited by the spectral behavior. At equilibrium, the photon statistics of the PL material and thermal pump exhibit similar statistics. However, thermal equilibrium cannot be reached with a non-thermal optical pump such as a laser.

**Conclusions:** This study provides new insights into the temperature-dependent evolution of PL, bridging pump-induced and thermal emission domains. The findings emphasize the smooth transitions of coherence and photon statistics across the equilibrium temperature compared to the sharp transition of rate, entropy, and chemical potential. These results enhance our understanding of PL processes, with potential technological applications.





## Unique properties of quantum wavefront shaping

Mr. Ronen Shekel

Hebrew University of Jerusalem

### Authors:

Ronen Shekel, Hebrew University of Jerusalem, Jerusalem, Israel; Yaron Bromberg, Hebrew University of Jerusalem, Jerusalem, Israel

### Abstract:

**Introduction and Background:** High-dimensional entangled photon pairs are a vital resource for emerging quantum technologies, such as quantum communications and quantum imaging. However, when propagating through a complex medium such as a turbulent atmosphere or biological tissue - the quantum correlations are scrambled. In recent years, tools from the field of wavefront shaping had been applied to compensate for the scattering.

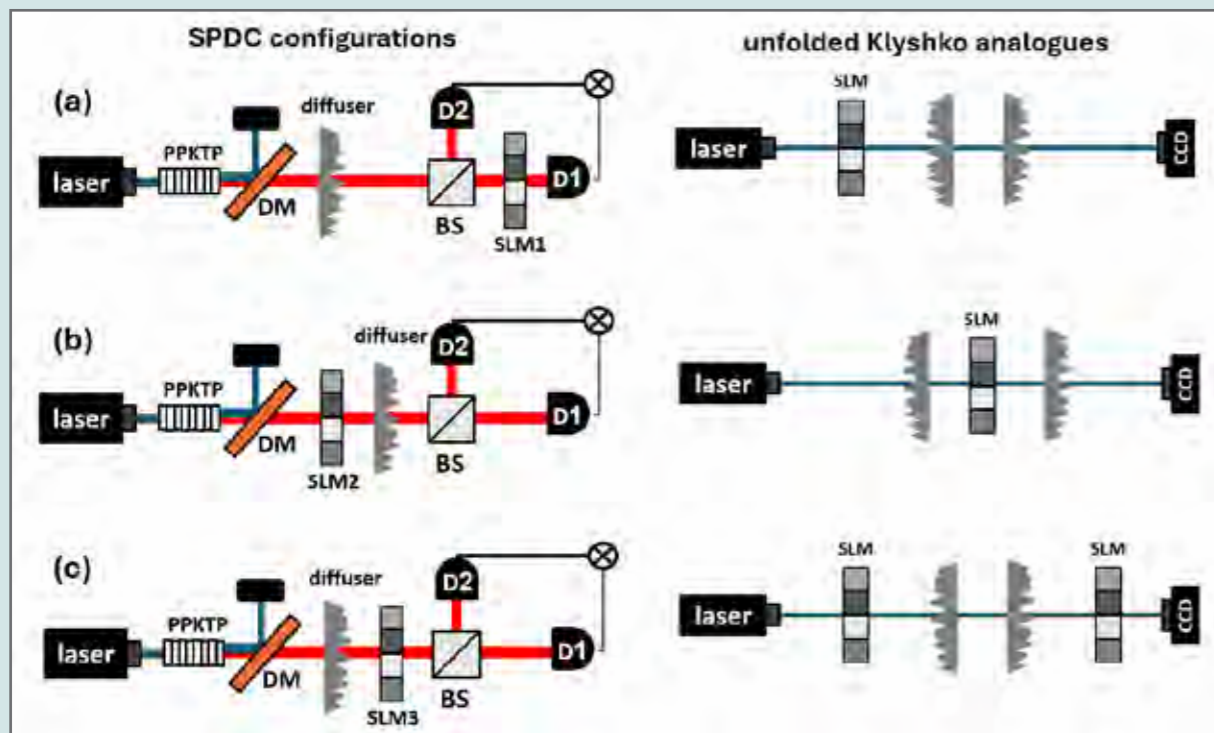
**Objectives and Methods:** In this presentation we show that while the tools of classical wavefront shaping mostly apply in the quantum case, the quantum case has a richer structure. Specifically, we show that in the quantum case the decision whether to shape one or both photons and whether to shape the light before or after the scattering medium has a significant effect on the shaping performance and complexity. We analyze the different configurations using the transmission matrix formalism, and Klyshko's advanced wave picture (see figure). In some cases, we find analytical solutions, while in other cases we solve the problem numerically.

**Results and Conclusions:** We show that: a) Shaping one photon is equivalent to a classical wavefront shaping experiment. b) Shaping both photons, with the SLM before the diffuser will show a reduced enhancement, except for a fully symmetric configuration, where perfect enhancement is achieved. We explain this as a quantum equivalent of optical phase conjugation. c) Shaping both photons with the SLM after the diffuser poses a self-consistent hard optimization problem, with no analytical solution. However, solving the problem numerically we find better enhancement than in the classical case, with a special symmetric configuration that shows perfect enhancement as well. Remarkably, when the scattering is modeled as a Gaussian IID matrix, the achievable power in the optimized mode is found to be larger than the total output energy before the optimization.

We believe this work provides important insights into the foundations of quantum wavefront shaping, as well as providing practical considerations for building such systems.

### References:

[0] Lib, Ohad, and Yaron Bromberg. "Quantum light in complex media and its applications." *Nature Physics* 18.9 (2022): 986-993.



## Tunable Quasi Squeezed Light Generation accompanied by Rabi Oscillations in Artificial Atom Ensembles

Mr. Ori Gabai

Technion – Israel Institute of Technology, Haifa

### Authors:

Ori Gabai, Amnon Willinger, Igor Khanonkin, Vitalii Sichkovskiy, Johann Peter Reithmaier and Gadi Eisenstein

### Abstract:

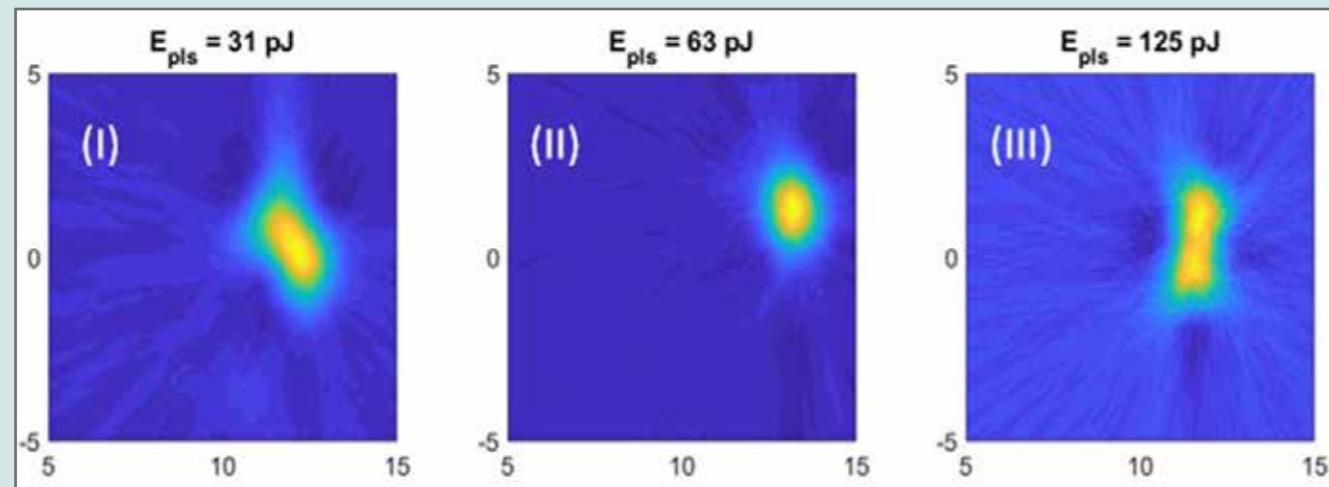
Coherent interactions of short pulses in a room temperature quantum dot (QD) gain medium have been demonstrated for the past decade. Such interactions include Rabi oscillations [1], Ramsey fringes [2], photon echoes and coherent revivals [3]. The experimental tool used in those experiments was X-FROG (Cross-correlation Frequency Resolved Optical Gating), which yielded the complex electric field of the output pulse. Furthermore, a semi classical analysis [1] was developed which describes a classical optical signal interacting with a quantum material. This model confirmed all the X-FROG measurements.

Here we examine the pulses emerging from the QD amplifier using homodyne detection yielding their quantum properties, described by Wigner function distributions. A 100 fs pulse at 1540 nm feeds the QD amplifier and broadens to roughly 1 ps upon propagation along the 1.5 mm long amplifier. A replica of the 100 fs excitation pulse serves as the local oscillator (LO) in the homodyne detection system. Under a 200 mA bias and varying input pulse energies, the homodyne measurements yield a cyclical quasi-squeezing levels dependence on the excitation pulse energy as demonstrated in the Wigner functions shown in Fig. 1.

This cyclical behavior stems from the fact that the QD gain medium undergoes Rabi oscillations [1] so that when in gain, the noise accompanying the signal is squeezed while when it is in absorption or transparency, no squeezing takes place, and the Wigner function is that of a coherent state. It is important to note that the squeezed noise is not sub-shot noise and hence it is termed quasi squeezed. It is reduced though compared to the background noise due to the amplified spontaneous emission emitted by the QD gain medium. Under very intense pulse excitation, the Wigner function becomes non-Gaussian resembling a cubic phase state [4].

### References:

- [1] A. Capua, O. Karni, G. Eisenstein, and J. P. Reithmaier, "Rabi oscillations in a room-temperature quantum dot semiconductor optical amplifier", *Phys. Rev. B* 90, 045305 (2014).
- [2] I. Khanonkin, A. K. Mishr, O. Karni, S. Banyoudeh, F. Schnabel, V. Sichkovskiy, V. Michelashvili, G. Eisenstein, and J. P. Reithmaier, "Ramsey fringes in a room temperature quantum dot semiconductor optical amplifier", *Phys. Rev. B* 97, 241117, (2018).
- [3] I. Khanonkin, O. Eyal, G. Eisenstein, and J. P. Reithmaier, "Room-temperature coherent revival in an ensemble of quantum dots", *Phys. Rev. Research* 3, 033073, (2021).
- [4] T. Tyc and N. Korolkova, "Highly non-gaussian states created via cross-kerr nonlinearity", *New Journal of Physics* 10, 023041 (2008).



## Photonic Entanglement in Synthetic Dimensions of a Single Waveguide

Mr. Amir Sivan

*Technion – Israel Institute of Technology*

### Authors:

Amir Sivan<sup>1,2</sup>, Stav Lotan<sup>1</sup>, Amit Kam<sup>3</sup>, Lior Gal<sup>1</sup>, Guy Bartal<sup>1,2</sup>, Meir Orenstein<sup>1,2</sup>

1 Department of Electrical Engineering, Technion, Haifa, Israel

2 Helen Diller Quantum Center, Technion, Haifa, Israel, 3. Physics Department, Technion, Haifa, Israel

### Abstract:

**Objectives:** Generation of photonic entangled states in a single waveguide using the modal degree of freedom as a synthetic dimension.

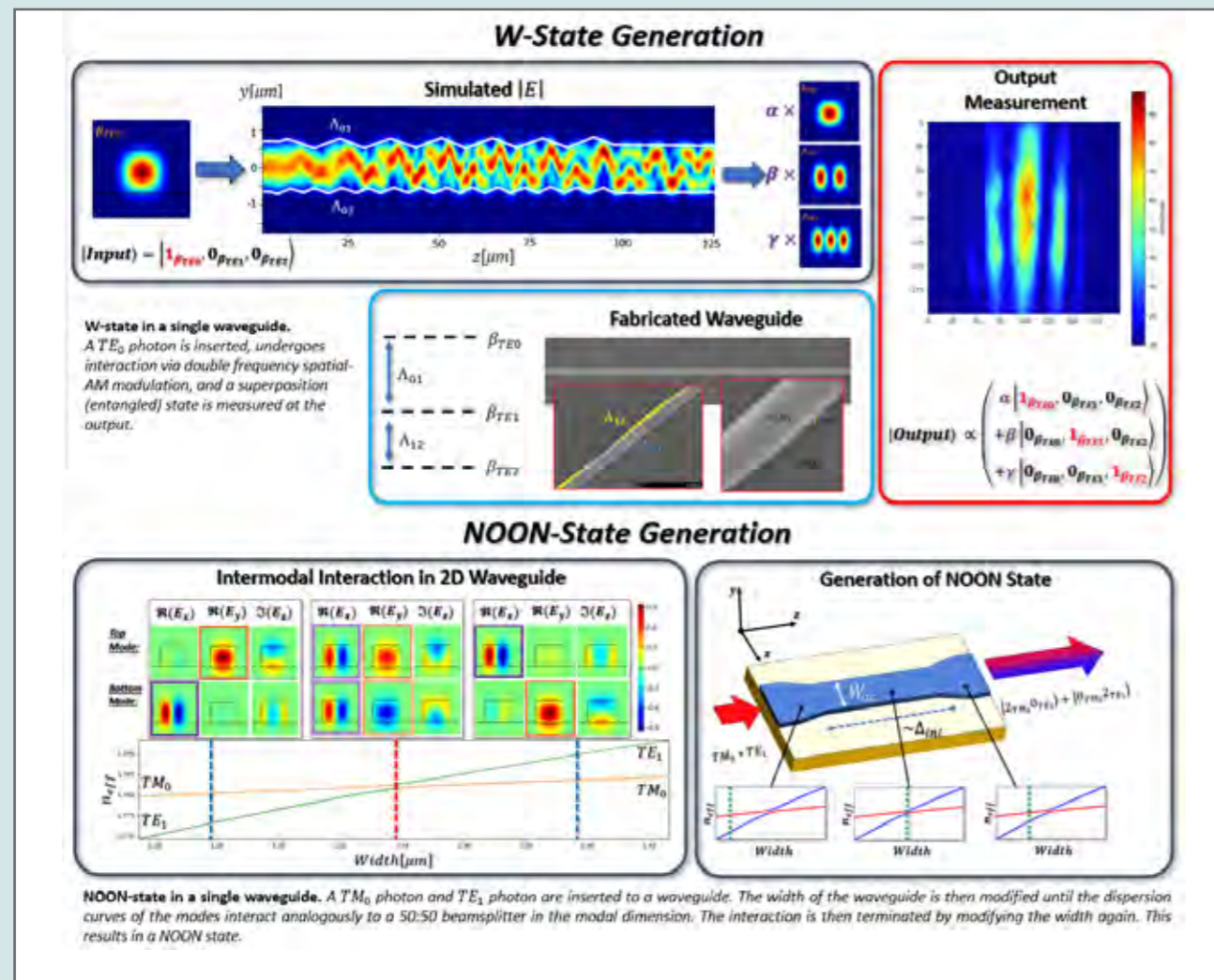
**Methods:** We design the structure of a single SiN waveguide to accommodate interactions between its guided modes. The modal degree of freedom (DoF) therefore acts as a synthetic dimension replacing the spatial DoF, such that a photon inserted into the waveguide will evolve into a multimodal superposition state enabling generation of important entangled states such as NOON and  $W$ . We demonstrate two intermodal interaction mechanisms: (i) spatial AM modulation (ii) interactions of the dispersion curves between the TE and TM modes of the waveguide. In 2D waveguides these modes are not orthogonal and we exploit this to realize a plethora of intermodal interactions by traversing the parameter space, e.g. modifying the waveguide's width to initiate and terminate intermodal interactions as we desire.

**Results:** By employing a double-frequency spatial AM grating along the waveguide, we couple the TE0 mode to the TE1 and TE2 modes and enable generation of a three-modal  $W$ -state from a single photon at a 808[nm] wavelength. Our measurements show the tri-modal superposition state at the output of the waveguide, commensurate with a  $W$ -state when a single photon is inserted.

Measurement of generation of a NOON state by exploiting intersections of dispersion curves of different modes is currently underway. A single TE and a single TM photons are inserted to the waveguide, and are brought to interact at a dispersion curve intersection. Due to the Hong-Ou-Mandel effect, this results in a photonic NOON state at the output.

**Conclusions:** We generate important quantum states in a single waveguide by employing the modal DoF as a synthetic dimension, replacing the spatial dimension. This enables easy and highly scalable implementation of photonic entanglement generators on chip. Additional applications will be discussed.





## Applications of Exceptional Points in NV Centers

Mr. Yonatan Mazor

Hebrew University, Racah Institute of Physics, Jerusalem

### Authors:

Shaked Oz, Hebrew University, Racah Institute of Physics, Jerusalem, Israel. 2. Yonatan Mazor, Hebrew University, Racah Institute of Physics, Jerusalem, Israel. 3. Pavel Peshin, Hebrew University, The Institute of Applied Physics, Jerusalem, Israel. 4. Prof. Nir Bar-Gil, Hebrew University, The Institute of Applied Physics, Jerusalem, Israel. 5. Dr. Adi Pick, Hebrew University, The Institute of Applied Physics, Jerusalem, Israel

### Abstract:

Exceptional points (EPs) are non-Hermitian degeneracies that arise in open systems and have various potential applications [1]. We investigate EPs in nitrogen-vacancy (NV) centers – defects in diamond with excellent optical properties. In this poster, we explore applications of EPs in NV centers for magnetic-field sensing and for topological mode switches. In the parameter space of the driving laser, e.g., Rabi's frequency and detuning, for a 2-level system, EPs form a bowtie, while for 3-level systems, they can also be isolated points.

The EPs are spectral singularities in open quantum systems that exhibit a strong spectral response to perturbations, and have therefore been proposed to be exploited for creating a new generation of sensors [2]. In the first project, we study the role of EPs in achieving sensitivity limits in quantum magnetometry, using Ramsey measurements with NV centers. We explore this question both theoretically and experimentally. We evaluate the quantum Fisher information (QFI) near EPs, to test whether EPs can be utilized to improve the sensitivity of magnetosensors. Our preliminary results show that the QFI is peaked away from EPs. Experimental measurements for mapping the structure of exceptional points, lines, and higher-dimensional surfaces in NV centers are currently in progress.

In the second project, we study topological mode switching around isolated EPs. In the adiabatic limit, properly varying the control fields acting upon the system along a closed loop in the parameter space that encloses an isolated EP, can result in a perfect mode switch [3]. We propose a protocol utilizing special adiabatic loops around EPs to perform a topological mode switch, leveraging the unique properties of EPs. We find that optimal trajectories are ones where the system spends only a small fraction of the time near the EP, where the energy gap is small. Finally, we employ optimal control techniques to refine those processes and enhance robustness.

### References:

- [1] Heiss, W. D. (2012). The physics of exceptional points. *Journal of Physics A: Mathematical and Theoretical*, 45(44), 444016.
- [2] Wiersig, J. (2020). Review of exceptional point-based sensors. *Photonics Research*, 8(9), 1457–1467.
- [3] Pick, A., Silberstein, S., Moiseyev, N., & Bar-Gill, N. (2019). Robust mode conversion in NV centers using exceptional points. *Physical Review Research*, 1(1), 013015.

## Free-Electron Triggered Superfluorescence for Resolving Collective Optical Properties of Quantum Materials

**Dr. Orr Be'er**

*PhD at Bekenstein lab Material science and engineering, Technion*

### Authors:

Orr Be'er<sup>1</sup>, Alexey Gorlach<sup>2</sup>, Alina Nagel<sup>1</sup>, Reut Shechter<sup>1</sup>, Yaniv Kurman<sup>2</sup>, Ido Kaminer<sup>2</sup>, and Yehonadav Bekenstein<sup>1</sup>

<sup>1</sup> Department of Materials Science and Engineering, Technion – Israel Institute of Technology, 3200 Haifa, Israel

<sup>2</sup> Department of Electrical Engineering, Technion – Israel Institute of Technology, 32000 Haifa, Israel

### Abstract:

Long-range coherence and correlations between electrons in solids are fundamental for developing advanced quantum materials and devices (1,2). The concept of correlated spontaneous emission proposed by Dicke (3), lays the groundwork for superradiance and superfluorescence. However, observing these phenomena at nanometer spatial resolution, the scale length for these collective correlations has remained an unresolved challenge (4). This work aims to address this gap by demonstrating free-electron-driven superfluorescence (superfluorescent cathodoluminescence), providing a means to excite and observe electron correlations at nanometer resolution.

To investigate superfluorescence at nanometer scales, flat superlattices of lead halide perovskite quantum dots (5), embedded in a polystyrene matrix were fabricated. The samples were excited using focused short pulses of multiple free electrons in an ultrafast SEM. The electron beam size was varied to explore two distinct emission regimes: at a pulse width of  $\sim 2 \mu\text{m}$ , distant excitations resulted in non-correlated spontaneous emission, while at  $\sim 20 \text{ nm}$ , correlated superfluorescence emerged due to the proximity of the excited quantum dots to an area much smaller than the emitted light wavelength.

The experiments revealed collective ultrafast emission rates exceeding both the intrinsic lifetime and decoherence time of the emitters, confirming the occurrence of superfluorescence. Key signatures included a significant reduction in the quantum dots' emission lifetime and a spectral linewidth narrowed by an order of magnitude. Additionally, a distinct redshift in the emission spectrum was observed, attributed to dipole-dipole interactions between quantum dot excitations. The ability to control the transition between non-correlated and correlated emission regimes demonstrated the feasibility of observing collective phenomena at nanometer scales.

Superfluorescent cathodoluminescence is a novel method to explore coherence and correlations in quantum materials with unprecedented nanometer spatial resolution. The results provide foundational insights that could pave the way for engineering next-generation quantum devices.

### References:

1. Basov, D. N., Averitt, R. D. & Hsieh, Nat. Mater. 16, 1077–1088 (2017).
2. Rainò, G. et al. Nature 563, 671–675 (2018).
3. Dicke, R. H. Phys. Rev. 93, 99 (1954).
4. Gross, M. & Haroche, S. emission. Phys. Rep. 93, 301–396 (1982).
5. Protesescu, L. et al. Nano Lett. 15, 3692–3696 (2015).

## ELECTRO-OPTICS DEVICES SESSION

### ◆ Invited speakers Abstracts:

## Heat Assisted Magnetic Recording – The Path the Ultra-high Volume Co-packaged Optical Integration

**Dr. Richard Pitwon**

### Abstract:

In this talk we introduce Heat Assisted Magnetic Recording (HAMR), which is a disruptive method of increasing storage density on spinning magnetic media in hard disk drives. HAMR requires highly dense integration of a laser, optical waveguide and plasmonic resonator along with other photonic and magnetic components into an area no larger than  $0.3 \text{ mm}^2$  on a rapidly moving recording head. HAMR therefore embodies the most dense heterogenous photonic packaging subsystem ever developed

**Oral presentation Abstracts:****Waveguide Integrated MoS<sub>2</sub>-based Photodetectors in the Shortwave IR****Mr. Eitan Kaminski***Technion – Israel Institute of Technology***Authors:**

Eitan Kaminski, Technion/HUJI, Haifa, Israel. Nathan Suleymanov, Technion, Haifa, Israel. Boris Minkovich, Technion, Haifa, Israel. Anastasios Polymerakis, University of Ioannina, Ioannina, Greece. Elefterios Lidorikis, University of Ioannina, Ioannina, Greece. Ilya Goykhman, The Hebrew University of Jerusalem, Jerusalem, Israel

**Abstract:**

Photodetectors with a broad spectral response, operating at room temperature in the visible and infrared wavelengths, are of major significance in spectroscopy, imaging, and communication [1,2]. Although the traditional crystalline silicon (c-Si) and amorphous silicon (a-Si) technologies have amazingly developed over the years, they have a severe limitation on spectral sensitivity (VIS-to-NIR) and operating wavelength (0.3–1.1 $\mu\text{m}$ ) [3]. Germanium on-Silicon (Ge-on-Si) and other traditional materials, including compound semiconductors HgCdTe, InGaAs, InSb, and type-II superlattices, can cover spectral bands in the infrared but, their technologies are complicated, and they typically face high-cost manufacturing and are not compatible with the standard scalable silicon fabrication facilities [4]. 2D materials integration with SiPh opens an unprecedented opportunity to reach the goal of monolithically integrated broadband photodetectors on-chip.

Here we report the design, fabrication, and characterization of a single-layer MoS<sub>2</sub> (1L-MoS<sub>2</sub>)-based photodetector integrated with silicon-on-insulator (SOI) waveguide, operating at telecom wavelengths (1.5–1.6 $\mu\text{m}$ ). 1L-MoS<sub>2</sub> is a two-dimensional semiconductor with an energy bandgap in the visible wavelengths (1.9eV), therefore it cannot absorb IR radiation directly by the band-to-band absorption [5]. In our design, a metal contact is placed on top of the silicon waveguide and the 1L-MoS<sub>2</sub>, therefore the light absorption takes place at the metal contacts and not in the 2D material itself. Our photodetector operates at zero bias with no dark current. The responsivity of our device can be described by the combined mechanisms of the photo-thermoelectric effect produced by temperature gradient and internal photoemission of the photoexcited electrons at the metal/MoS<sub>2</sub> interface. Our device shows responsivity of 5–10V/W with maximum values of  $\sim 100\text{V/W}$ . Our results pave the way for developing broadband-integrated MoS<sub>2</sub>-based photodetectors from visible to IR.

**References:**

- [1] D. Akinwande et al., *Nature*, vol. 573, 2019.
- [2] N. Ding et al., *Light: Science & Applications*, 11, 2022.
- [3] M. Casalino et al., *Laser & Photonics Reviews*, vol. 10, 2016.
- [4] J. Zha et al., *Adv. Funct. Mater.*, vol.32, 2022.
- [5] A. Splendiani et al., *Nano Letters*, vol. 10, 2010.

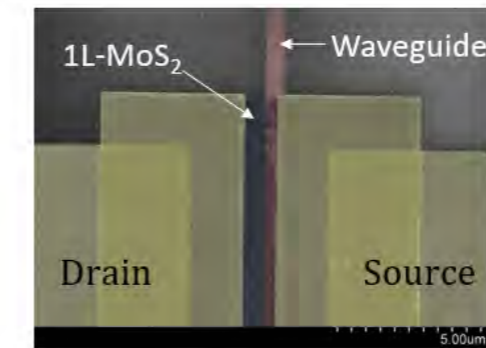


**Figure 1:** Scanning electron micrograph (false-color) of 1L-MoS<sub>2</sub> photodetector integrated with an SOI waveguide.

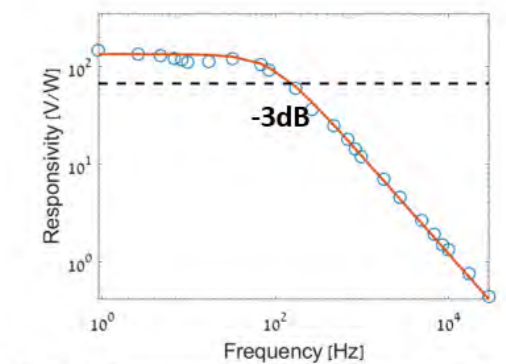


**Figure 2:** Frequency response of the photodetector.



## Electro-optics behind Vaterite-based Drug Delivery

Prof. Pavel Ginzburg

Tel Aviv University

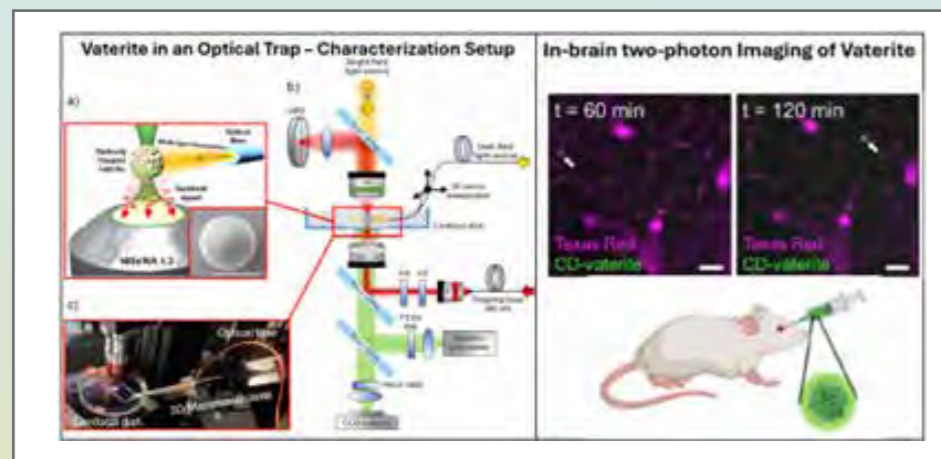
### Authors:

Pavel Ginzburg and Hani Barhom, Andrey Machnev, Andrey Ushkov, Denis Kolchanov, Pavel Bezrukov

### Abstract:

The fast-changing and evolving landscape of biomedical challenges motivates the continuous development of new functional platforms. Implantable devices made from biocompatible materials, capable of responding to optical signals and tailoring propagation of light waves can be employed in health monitoring applications and therapeutics. The incorporation of such elements into living organisms can boost light-tissue interactions and shift conventional approaches towards precision medicine by opening new opportunities in sensing, photothermal therapy, photoacoustic tomography, and bioimaging. One of the grand challenges on those pathways is the miniaturization of biocompatible photonic structures along with providing multiple functionalities, such as monitoring of vital biological processes, light-responsive drug release, or local heating of a nanoscale area with the simultaneous measurement of its temperature.

We demonstrated a new mesoscopic approach to on-demand engineering of electric and magnetic resonances in submicron low-index vaterite spherulites by filling them with gold nano inclusions. This makes it possible to increase the effective permittivity of the structure and provide efficient light trapping. As an example of a potential thermal therapy application, we demonstrate an efficient laser heating of golden spherulites. Both water suspensions and individual spherulites, being illuminated with near-infrared light were investigated via time-resolved fluorometry and fluorescence-lifetime imaging microscopy and demonstrated an efficient local temperature elevation. Also, we have demonstrated a facile synthesis of meta-phenylenediamine CDs exhibiting robust optical fluorescence properties under both single-photon and two-photon absorption regimes. The interaction of the CD-vaterite composites with C6-glioma cells was successfully investigated using one- and two-photon confocal microscopy. This was followed by injection and visualization of CD-vaterite composites in vivo in murine brain blood vessels for the first time. This allows for the tracking of particles in the bloodstream, thereby facilitating investigations involving blood vessels and the blood-brain barrier. Furthermore, with further optimization, this tool can allow real-time study of drug-cell interactions.



## Line-by-line spectral amplitude/phase modulation of an optical frequency comb

Mrs. Vered Riven

The Institute of Applied Physics, The Hebrew University

### Authors:

Vered Riven, Prof. Dan Marom, The Hebrew University

### Abstract:

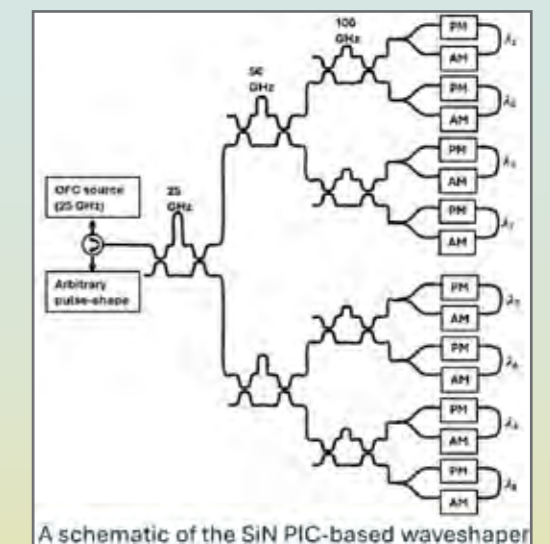
Optical frequency combs (OFC) have revolutionized scientific measurement techniques in the optical and radio frequency domains, owing to their broad spectral coverage, precise spectral position control and coherence across the frequency lines. However, their power per line (or amplitude) is typically not flat and an attenuation per line should be applied for certain applications. Likewise, in pulse shaping applications, we would like to set the spectral amplitude and phase for arbitrary pulse-shape generation, using Fourier synthesis techniques. While an optical waveshaper instrument allows the setting of spectral amplitude and phase, it is designed for continuous spectrum (broadband). For an OFC we only need line-by-line addressing (no bandwidth), which further affords its implementation in compact silicon photonic integrated chip (PIC) form and the platform allows faster modulation rates than achievable in waveshaper instruments.

Our line-by-line spectral amplitude and phase modulator is designed for 25 GHz spaced OFC in the telecom window (1530–1560 nm), with low loss, low crosstalk, high extinction and precise phase setting specification requirements, while being implemented as a PIC. It consists of two main parts: 1) stages of spectral separation by interleavers of different periodicities and 2) phase and amplitude reflection modulators applied to the demultiplexed OFC lines. The OFC traverse the interleavers, its lines are singulated, independently modulated and reflected to the interleavers which recombine the OFC. The spectral separation is achieved using cascaded stages of asymmetric Mach-Zehnder Interferometers (AMZIs), arranged in triplets [1], which provide low-loss and low-crosstalk demultiplexing. Each stage functions as an interleaver with a target spectral periodicity, separating the OFC into individual spectral lines. Each OFC line passes through phase and amplitude modulators, arranged in a reflection geometry.

This optical wave-shaper is designed on a commercial silicon nitride platform, using piezo-electric stress-based phase modulators, providing high-speed, low-loss, and low power consumption.

### References:

[1] T. Akiyama, S. Oda, Y. Nakasha, A. Hayakawa, S. Tanaka, Y. Tanaka, and T. Hoshida, "Cascaded AMZ triplets: a class of demultiplexers having a monitor and control scheme enabling dense WDM on Si nano-waveguide PICs with ultralow crosstalk and high spectral efficiency," *Opt. Express* 29(6), 7966–7985, 2021.



A schematic of the SiN PIC-based waveshaper

**E Posters Abstracts:****Addressing broadening challenges in m-plane GaN two-well terahertz quantum cascade laser****Mrs. Shiran Levy****Authors:**

Shiran Levy, Nathalie Lander Gower, Silvia Piperno, Asaf Albo  
Bar Ilan University, Israel

**Abstract:**

Quantum cascade lasers (QCLs) show great potential at terahertz (THz) frequencies. THz waves are non-ionizing, penetrating materials effectively. Their absorption properties enable high-contrast imaging in medicine, security, astronomy, chemistry, and spectroscopy. However, a compact and efficient THz source is needed to fully harness their potential.

The THz frequency range lies between microwaves and infrared, creating a “Terahertz gap” where neither electronic nor photonic devices operate effectively. QCLs have emerged as a promising solution to bridge this gap through their unique design and operation.

THz QCLs that rely on GaAs as their material system have exhibited a lasing frequency range restricted to 1–5 THz and face a substantial limitation in the frequency spectrum spanning from 5–12 THz. However, THz-QCLs have yet to become commercially viable due to the need for extensive cooling systems, limiting their portability.

Gallium Nitride (GaN) offers a compelling solution. GaN's high longitudinal optical (LO) phonon energy of 92 meV, in contrast to GaAs's 35 meV, enables efficient suppression of thermal back-filling and depopulation of the upper lasing level (ULL) through thermally activated LO-phonon transitions. Moreover, GaN's properties allow to bridge the 6–12 THz frequency gap.

However, experimental demonstrations of THz lasing in GaN-based QCLs are yet to be achieved. The strong electron-LO-Phonon interaction in GaN, addresses challenges and has implications for lifetime and level broadening.

This study investigates the broadening challenge arising from the strong LO phonon coupling strength in GaN. We analyze carrier transport in a practical m-plane GaN two-well THz QCL structure. NEGF technique is employed in a self-consistent manner to analyze gain. Our simulations, indicate that the broadening of laser energy levels caused by phonons is significantly less prominent when compared to other broadening mechanisms. By increasing the doping density, the gain is increased even though the broadening arises from different mechanisms. This research demonstrates the feasibility of achieving lasing at 7.2 THz up to 280 K outperforming traditional GaAs-based QCLs.

**Exploring the Influence of Molecular Beam Epitaxy Growth Properties on the Temperature Performance of Advanced Terahertz Quantum Cascade Lasers****Mrs. Nathalie Lander Gower***Bar Ilan University***Authors:**

Nathalie Lander Gower<sup>1,2</sup>, Shiran Levy<sup>1,2</sup>, Silvia Piperno<sup>1,2</sup>, Sadvikas J. Addamane<sup>3</sup>, Asaf Albo<sup>1,2,a</sup>

1 Faculty of Engineering, Bar-Ilan University, Ramat Gan 5290002, Israel

2 The Institute of Nanotechnology and Advanced Materials, Bar-Ilan University, Ramat Gan 5290002, Israel

3 Center for Integrated Nanotechnologies, Sandia National Laboratories, MS 1303, Albuquerque, New Mexico 87185-1303, USA. a) asafalbo@gmail.com

**Abstract:**

We performed a comparative analysis using non-equilibrium Green's functions (NEGF) on two state-of-the-art two-well (TW) Terahertz Quantum Cascade Lasers (THz QCLs) supporting clean 3-level systems. Both devices, with nearly identical parameters, show NEGF-predicted maximum operating temperatures (T<sub>max</sub>) of ~250 K. However, experimentally, one device achieves a T<sub>max</sub> of ~250 K, while the other reaches only ~134 K. Fabrication and measurements were conducted under identical conditions, verified by reference devices. The key difference lies in the molecular beam epitaxy (MBE) reactors used for growth.

Our NEGF analysis evaluates MBE growth parameters, including aluminum content, growth rate, doping density, background doping, and interface roughness. The results identify in-depth interface roughness as the primary cause of the large performance gap. Simulations indicate both devices exhibit high-quality interfaces, with roughness of approximately an atomic layer for one and a monolayer for the other. Even this small variation significantly affects performance.

Optimizing MBE growth for reproducible, high-performance THz QCLs requires maintaining sharp interfaces. Achieving even sharper interfaces may set new records in T<sub>max</sub>. Graded interfaces, effective for mid-IR QCLs, could be explored for THz QCLs, though tailored studies are essential. Atom probe tomography (APT) is suggested to analyze and improve interface roughness in THz QCLs, as shown for mid-IR QCLs. Further optimization of doping density and profiles could also boost T<sub>max</sub>.

This study clarifies why MIT's high T<sub>max</sub> values (~250 K and ~261 K) have been elusive to others, pinpointing interface roughness as the critical factor. It provides a systematic pathway to enhance temperature performance and addresses challenges in reproducing record T<sub>max</sub> values, contributing both to fundamental understanding and practical advancements in THz QCL technology.

## Electrically Tunable Interband Collective Excitations in Biased Bilayer and Trilayer Graphene

**Mr. Tomer Eini**

*School of Electrical Engineering, Faculty of Engineering, Tel Aviv University, Tel Aviv 6997801, Israel*

### Authors:

\Author{Tomer Eini}\affiliation{School of Electrical Engineering, Faculty of Engineering, Tel Aviv University, Tel Aviv 6997801, Israel} \Author{M. F. C. Martins Quintela}\affiliation{Department of Physics and Physics Center of Minho and Porto Universities (CF-UM-UP), Campus of Gualtar, 4710-057, Braga, Portugal} \affiliation{International Iberian Nanotechnology Laboratory (INL), Av. Mestre José Veiga, 4715-330, Braga, Portugal} \affiliation{Department of Materials and Production, Aalborg University, 9220 Aalborg Øst, Denmark} \affiliation{Departamento de Química, Universidad Autónoma de Madrid, 28049 Madrid, Spain} \affiliation{Condensed Matter Physics Center (IFIMAC), Universidad Autónoma de Madrid, 28049, Madrid, Spain} \Author{J. C. G. Henriques}\affiliation{International Iberian Nanotechnology Laboratory (INL), Av. Mestre José Veiga, 4715-330, Braga, Portugal} \affiliation{Universidade de Santiago de Compostela, 15782 Santiago de Compostela, Spain} \Author{R. M. Ribeiro}\affiliation{International Iberian Nanotechnology Laboratory (INL), Av. Mestre José Veiga, 4715-330, Braga, Portugal} \affiliation{Centro de Física das Universidades do Minho e do Porto (CF-UM-UP) e Departamento de Física, Universidade do Minho, P-4710-057 Braga, Portugal} \Author{Yarden Mazor}\affiliation{School of Electrical Engineering, Faculty of Engineering, Tel Aviv University, Tel Aviv 6997801, Israel} \Author{N. M. R. Peres}\affiliation{International Iberian Nanotechnology Laboratory (INL), Av. Mestre José Veiga, 4715-330, Braga, Portugal} \affiliation{Centro de Física das Universidades do Minho e do Porto (CF-UM-UP) e Departamento de Física, Universidade do Minho, P-4710-057 Braga, Portugal} \affiliation{POLIMA–Center for Polariton-driven Light-Matter Interactions, University of Southern Denmark, Campusvej 55, DK-5230 Odense M, Denmark} \Author{Itai Epstein}\email{itai@tau.ac.il}\affiliation{School of Electrical Engineering, Faculty of Engineering, Tel Aviv University, Tel Aviv 6997801, Israel} \affiliation{Center for Light-Matter Interaction, Tel Aviv University, Tel Aviv 6997801, Israel} \affiliation{QuanTAU, Quantum Science and Technology Center, Tel Aviv University, Tel Aviv 6997801, Israel}

### Abstract:

Collective excitations of charged particles under the influence of an electromagnetic field give rise to a rich variety of hybrid light-matter quasiparticles with unique properties. In metals, intraband collective response manifested by negative permittivity leads to plasmon-polaritons with extreme field confinement, wavelength “squeezing”, and potentially low propagation losses. In contrast, photons in semiconductors commonly couple to interband collective response in the form of exciton-polaritons, which give rise to completely different polaritonic properties, described by a superposition of the photon and exciton and an anti-crossing of the eigenstates. In this work, we identify the existence of plasmon-like collective excitations originating from the interband excitonic response of biased bilayer and trilayer graphene, in the form of graphene-exciton-polaritons (GEPs). We find that GEPs possess electrically tunable polaritonic properties and discover that such excitations follow a universal dispersion law for all surface polaritons in 2D excitonic systems. Accounting for nonlocal corrections to the excitonic response, we find that the GEPs exhibit confinement factors that can exceed those of graphene plasmons, and with moderate losses that would enable their observation in cryo-SNOM experiments. Furthermore, by electrically tuning the excitons’ energy into the Reststrahlen band of the surrounding hexagonal-boron-nitride, we demonstrate that strong coupling between the excitons and hyperbolic

phonon polaritons can be achieved, and well-described by an electromagnetic transmission line model. These predictions of plasmon-like interband collective excitations in biased graphene systems open up new research avenues for tunable plasmonic phenomena based on excitonic systems, and the ability to control and manipulate such phenomena at the atomic scale.



## Discerning Laser Radiation From Ambient Light System

**Mr. Oren Aharon**

*CTO & Founder*

### Authors:

Prof. Eli Cohen, Bar Ilan University, Oren Aharon, Duma Optronics

### Abstract:

**Objectives:** We present a novel system and method designed to precisely differentiate laser radiation from ambient light using a compact and efficient apparatus. This system exploits the unique properties of laser beams, such as their coherence and directionality, in contrast to the incoherent and scattered characteristics of ambient light. Additionally, it enables the measurement of coherence length and wavefront coherence. The system also facilitates advanced calculations and analyses, including the assessment of atmospheric turbulence effects on laser beam propagation.

**Methods:** A well-known double-slit experiment, including a suitable lens and a sensitive CMOS detector, forms the basis of the sensing mechanism, producing distinct interference patterns for laser radiation, while ambient light remains diffusely distributed. Moreover, it allows us to extract information regarding the direction from which the laser is emitted. This apparatus is also robust against the impact of atmospheric turbulence on laser beams and enables to measure the turbulence parameters ( $R_0$ ,  $C_n^2$ ), as well as the resulting coherence length of the incoming beam.

**Results & Conclusions:** The proposed sensor has a dual usage for industrial and military applications, where discerning coherent from incoherent radiation and characterizing it are useful tasks to perform. This revival of the double-slit experiment, resulting from a collaboration between Duma Optronics and Bar-Ilan University, uniquely bridges quantum and classical physics, with down-to-earth applications, enabling advancements across diverse fields.

### References:

Pending Patent – Discerning Laser Radiation From Ambient Light System (App. 18/752,855)

## Built-in Measurement of the “Glass-to-Glass” Latency for Real-time Visual Prostheses

**Dr. Yosef Golovachev**

*Jerusalem College of Technology*

### Authors:

Yosef Golovachev, Ariel Dinner, Baruch Refaelovich, Benny Milgrom

### Abstract:

Visual prosthetics utilize digital photography to enhance human vision, with the rapid processing of visual information providing users with a more natural experience. In this study, we present a simple method for measuring the delay time in visual prosthetic systems, spanning from the moment of real-time image capture, through the communication pathway, to the display of the video on the user's screen. A straightforward technique for measuring delay time can significantly aid system engineers in optimizing performance and preventing inefficiencies. Incorporating built-in measurement capabilities allows for quick and effective latency assessment, simplifying the process for system designers.

In our experiment, we used an Arduino controller with an internal clock of 16 MHz. A light-emitting diode (LED) bulb was connected to an output pin, while a sensitive photodiode was connected to an input pin. It is worth noting that the LDR has a built-in response time of approximately 30 milliseconds, which introduces a delay when calculating results during subsequent interrupts.

The controller was programmed to activate the LED in a 2-second flash cycle, enabling multiple repetitions of the experiment. A camera connected via USB cable recorded the flashing LED and displayed the video on a computer screen, positioned adjacent to the photodiode sensor. The controller measured the elapsed time from when the LED was activated to when the photodiode detected the LED's display on the screen. This process provided a measurement of the delay introduced by the system. For accuracy, we used the controller's internal timer, which offers a resolution of 0.5 milliseconds.

This simple technique not only facilitates the analysis of time delay effects on system performance but also enables the rapid evaluation of modifications to system components, such as the optical system, communication pathway, or user display.

## Advanced Dispatchable Fiber-Optic Biosensor System for Real-Time, On-Site Sediment and Water Toxicity Monitoring: System Optimization (Sundanse)

**Mr. Gal Carmeli**

*Avram and Stella Goldstein-Goren Department of Biotechnology Engineering, Ben Gurion University of the Negev, Be'er-Sheva 84105, Israel*

### Authors:

Gal Carmeli, Abraham A. Paul, Robert S. Marks

### Abstract:

**Objectives:** To develop a second-generation fiber-optic biosensor system for real-time, on-site sediment and water toxicity monitoring that enhances usability, portability, and field readiness while maintaining biological relevance in detecting toxicants.

**Methods:** The upgraded biosensor incorporates bioluminescent bacterial bioreporters immobilized within a calcium alginate matrix on fiber-optic tips. The system quantitatively detects emitted blue light using a photomultiplier tube (PMT). Key design improvements include a lightproof case, an internal power station, and solar panels for sustainable energy. On-site measurements were conducted across potentially contaminated locations in Israel, assessing water and sediment toxicity. Complementary chemical analyses validated the biosensor's results.

**Results:** Preliminary field tests demonstrated the biosensor's capability to detect various toxicants effectively. The enhanced design improved operational efficiency and ease of deployment in field conditions. Comparative analysis with the earlier prototype highlighted notable advancements in usability and portability without compromising sensitivity or accuracy [1–3]. Chemical analysis corroborated the biosensor's findings, confirming its effectiveness as a screening tool.

**Conclusions:** The second-generation fiber-optic biosensor offers a high-throughput, versatile solution for in-situ environmental toxicity screening. Its improved portability and sustainable energy options make it suitable for diverse field applications, bridging the gap between conventional chemical analyses and real-time bioavailability assessment. This innovation marks a significant step towards efficient and accessible environmental monitoring tools.

### References:

- [1] Ivask, A., Green, T., Polyak, B., Mor, A., Kahru, A., Virta, M. and Marks, R. Fibre-optic bacterial biosensors and their application for the analysis of bioavailable Hg and As in soils and sediments from Aznalcollar mining area in Spain. *Biosensors and Bioelectronics*, 22, 7 (2007/02/15/ 2007), 1396–1402.
- [2] Polyak, B., Bassis, E., Novodvoretz, A., Belkin, S. and Marks, R. S. Bioluminescent whole cell optical fiber sensor to genotoxicants: system optimization. *Sensors and Actuators B: Chemical*, 74, 1 (2001/04/15/ 2001), 18–26.
- [3] Polyak, B., Bassis, E., Novodvoretz, A., Belkin, S. and Marks, R. S. Optical fiber bioluminescent whole-cell microbial biosensors to genotoxicants. *Water Science and Technology*, 42, 1–2 (2000), 305–311.

## Vertically Grown Halide Perovskite Heterostructured Lasers the Role of Shape and Interfaces

**Ms. Betty Shamaev**

*Material Science and Engineering Technion*

### Authors:

Prof. Yehonadav Bekenstein, Material Science and Engineering Technion, Haifa, Israel

### Abstract:

Photonics on a chip is critical for the next generation of compact, efficient, and high-performance optical devices. While silicon is the primary material in the semiconductor industry, halide perovskites offer a breakthrough with their exceptional photoluminescence quantum yield, fast carrier lifetimes, and tunable optoelectronic properties. However, vapor-grown halide perovskites are not compatible with standard silicon processes. In this study, we demonstrate halide perovskites grown via CVD, a scalable technique widely used in the semiconductor industry. We show room-temperature, low-threshold lasing from these perovskites, enabling their integration into chip-based photonic systems.

We investigate the impact of micro-wire geometries and interfaces on optical dynamics. By controlling growth and substrate conditions, we achieve two distinct growth modes: in-plane and out-of-plane wires relative to the silicon substrate. The in-plane wires are well-faceted with right-angled rectangular prism cross-sections and grow directly on the substrate. The out-of-plane wires form at a fixed angle relative to the substrate.

Through angle-resolved cathodoluminescence, we determine the growth angle of the out-of-plane wires to be  $57^\circ \pm 3^\circ$ , with the contact surface identified as the  $\{111\}$  CsPbBr<sub>3</sub> plane. While in-plane wires are known to lase, this is the first report of out-of-plane wires exhibiting lasing behavior. We observed high efficiencies and low-threshold lasing for these, highlighting their potential for integrated on-chip optoelectronic applications. We hypothesize that the low strain of the free-standing wires results in high PLQY and efficient lasing compared to those grown parallel to Si.

We also compare the defect and exciton dynamics in both growth modes. The Cs<sub>4</sub>PbBr<sub>6</sub> phase acts as nucleation seeds, influencing the excitonic behavior of CsPbBr<sub>3</sub> wires. Using ultrafast cathodoluminescence microscopy, we explore emission characteristics near interfaces, revealing strong interfacial effects that modulate emission intensity and lifetime.

Our results provide critical insights for designing future halide perovskite-based electro-optical devices and advanced chip-integrated photonics.

## Unveiling Light Dynamics Within Photonic Integrated Circuits

Mr. Matan Iluz

*Technion- Israel institute of technology*

### Authors:

Matan Iluz, Kobi Cohen, Jacob Kheireddine, Yoav Hazan, Amir Rosenthal, Shai Tseses and Guy Bartal

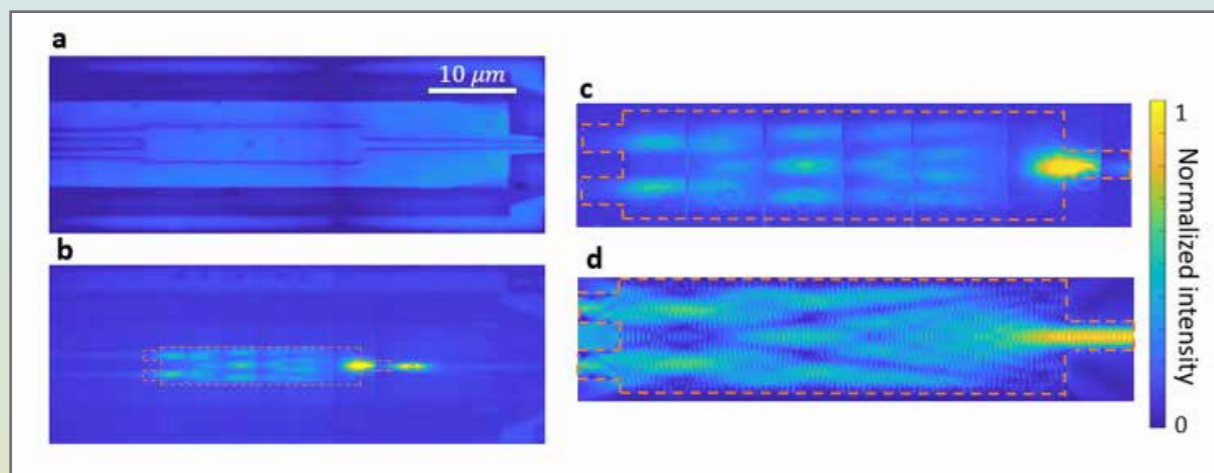
### Abstract:

**Objectives:** This study aims to develop a novel characterization tool for silicon photonic devices. Current lithographic advancements allow precise fabrication, yet there remains a lack of tools for assessing functionality, particularly in the presence of small-scale defects. We aim to visualize light dynamics in photonic components, enabling real-time monitoring of wave propagation, modal analysis, and effective index extraction without introducing defects or fabrication overhead.

**Methods:** We leverage the nonlinear optical process of partially degenerate four-wave mixing (PDFWM) to map guided light in silicon photonic devices. A pump beam, incident on the sample, interacts with a guided signal to generate a nonlinear wave at visible wavelengths. This wave is imaged to capture sub-wavelength details of the guided mode. The spatial frequency distribution is analyzed in the reciprocal (Fourier) plane to extract the mode's effective index and phase velocity. The method is validated on standard waveguides and applied to multimode interferometric (MMI) splitters.

**Results:** Using our approach, we mapped the electric field of a guided mode traveling in a 450 nm-wide, 220 nm-high silicon waveguide. Imaging the device and Fourier planes provided effective index values, revealing the phase accumulation along the propagation direction. For the MMI splitter, we visualized light propagation at different locations, showing the interference evolution and assessing performance metrics like splitting equality and loss distribution.

**Conclusions:** We present a versatile and noninvasive tool for characterizing silicon photonic devices, applicable to waveguides, cavities, modulators, and splitters. By exploiting silicon's intrinsic optical nonlinearity, our method requires no modifications to the devices and supports real-time analysis. This tool holds potential for advancing quality control and design optimization in the semiconductor industry.



## Coupled PT-Symmetric Structure with alternating Gain and Loss: a new route for reconfigurable amplifiers and lasers

Ms. Michal Hazan

*Tel Aviv University*

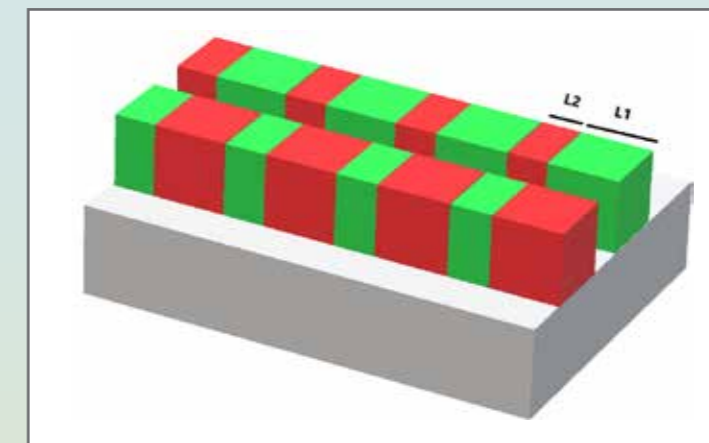
### Authors:

Michal Hazan, Jacob Scheuer

### Abstract:

We propose and study a PT-Symmetric system comprising two coupled waveguides where each waveguide consists of alternating sections exhibiting gain and loss. In contrast to the simple coupled waveguides structure, this scheme exhibits multiple EPs whose number and positions can be tuned and controlled by modifying the structure periodicity and duty cycle. This PT-symmetric architecture allows for better control over the properties of the structure and can pave the way to reconfigurable PT-symmetric optical systems.

The structure consists of two coupled waveguides with coupling coefficient  $\kappa$ , where each waveguide consists of alternating sections having gain and loss. The sections lengths are  $L_1$  and  $L_2$  with gain/loss coefficient  $\gamma$ . Note that the two sections can also exhibit different gain/loss coefficients. To find the eigenmode of this structure we use couple mode theory to obtain a transfer matrix for each section in the unit-cell. These are concatenated to yield the unit-cell transfer matrix,  $M^{\sim}$ , connecting the fields at the unit-cell output to those at the input. For simplicity, it is assumed that the reflection at the interface between gain and loss sections is negligible. Invoking Bloch Theorem, we can find the Bloch phases,  $\beta_{1,2}(L_1+L_2)$  of the structure's Bloch modes which are the solutions of the characteristic equation  $|\mathbf{M}^{\sim} - I e^{i\beta(L_1+L_2)}| = 0$ , where  $I$  is the identity matrix. This is a quadratic equation yielding (in most cases) two phases. The Bloch phase could be either real (indicating propagating modes) or imaginary (indicating exponentially increasing/decreasing waves). Ways of implementation and experimental setup are considered. The inherent flexibility of this structure paves the way to dynamic PT-Symmetric structures exhibiting reconfigurable EP positions and Broken PT-Symmetry regimes, with applications for tunable amplifiers and lasers.





## Near-Field Super-Resolution Enhanced Sensing Method

**Dr. Avi Karsenty**

*Jerusalem College of Technology (JCT), JCT Nanotechnology Center for Research and Education, Advanced Laboratory of Electro-Optics (ALEO)*

### Authors:

Amos Laist<sup>1,2</sup>, Itzhak Desta<sup>1,2</sup>, Jeremy Belhassen<sup>1,2</sup>, Zeev Zalevsky<sup>3,4</sup>, Avi Karsenty<sup>1,2,\*</sup>

- 1 Advanced Laboratory of Electro-Optics, Jerusalem College of Technology, Jerusalem, Israel
  - 2 Nanotechnology Center for Research & Education, Jerusalem College of Technology, Jerusalem, Israel
  - 3 Faculty of Engineering, Bar-Ilan University, Ramat Gan, 5290002, Israel
  - 4 Nanotechnology Center, Bar-Ilan University, Ramat Gan, 5290002, Israel
- \* Corresponding **Author**, E-mail: karsenty@jct.ac.il

### Abstract:

**Objectives:** This research focuses on fabricating, characterizing and measuring the NSOM performances of a dual-mode photodetector-tip with both Atomic Force Microscopy (AFM) and Near-field Scanning Optical Microscopy (NSOM) capabilities.

### Methods:

1. Tip fabrication – Several series of tips were fabricated at the Bar-Ilan Institute of Nanotechnology & Advanced Materials (BINA) and analyzed at ALEO, although the thin-layer deposition process remains challenging.
2. Structural characterization and electro-optical measurements – The characterization phase started with a fabrication process diagnostic to verify the structure's critical dimensions, such as aperture shape and size, to maintain full control in each process step. Next, we characterized the IV profile of the tip using ALEO's probe station and tested the tips.

**Results:** The setup used microprobes connected to a parameter analyzer to apply a voltage sweep on the AFM-NSOM probes. The current variation as a function of the voltage (IV characteristic) was measured. The results expect to match a Schottky diode's IV characteristic.

**Conclusions:** We present a new tip-photodetector device which combines two different types of measurement (AFM-NSOM), enabling complementary and synchronized results in a single scan: topographic and photonic. While the AFM capabilities have been largely developed and studied in previous publications, the NSOM technique still requires advanced measurements in imaging mode, and perhaps electronic additional circuitry. This photodetector-tip, which combine nanophotonics and nanoelectronics principles will serve as a wide-range sensor for synchronized scanning.

### References:

1. M. Karelits et al., "Advanced Surface Probing using Dual-Mode NSOM-AFM Silicon-Based Photo-Sensor," *Nanomaterials*, vol. 9, no. 12, p. 1792, 2019.
2. J. Belhassen, et al., "Nano-Apertures vs. Nano-Barriers: Surface Scanning through Obstacles and Super-Resolution in AFM-NSOM Dual-Mode," *Nano-Structures & Nano-Objects*, vol. 33, p. 100933, 2023.
3. M. Karelits, et al., "Laser beam scanning using near-field scanning optical microscopy nanoscale silicon-based photodetector," *J. of Nanoph.*, vol. 12, no. 3, p. 036002, 2018.

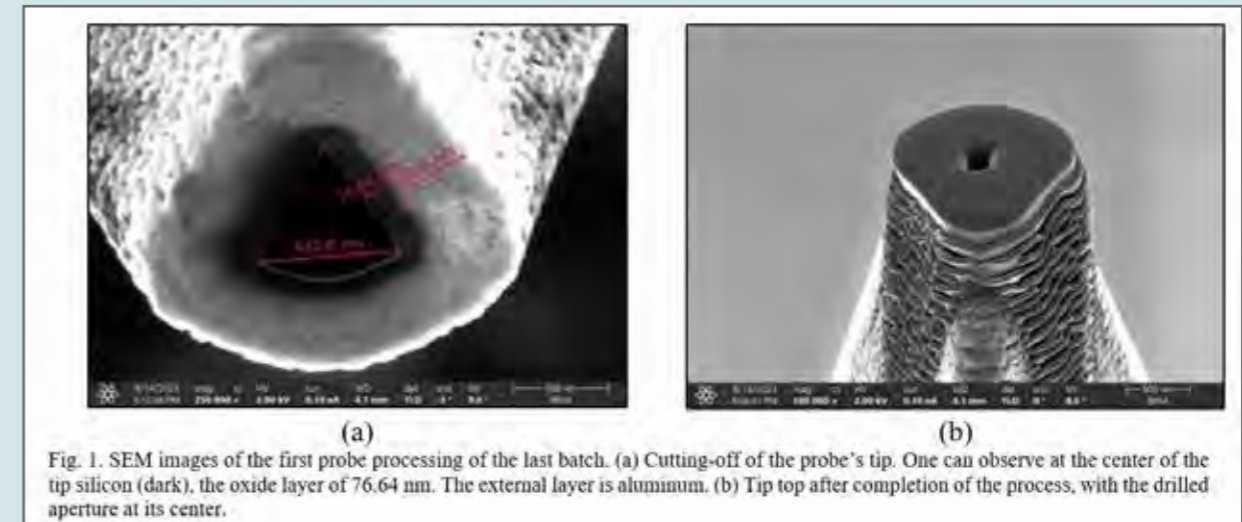


Fig. 1. SEM images of the first probe processing of the last batch. (a) Cutting-off of the probe's tip. One can observe at the center of the tip silicon (dark), the oxide layer of 76.64 nm. The external layer is aluminum. (b) Tip top after completion of the process, with the drilled aperture at its center.

## Hybrid electronic-photonic multi-chip modulator

**Mr. Shalev Haimovich**

*Msc student for electrical engineering*

### Abstract:

Electro-optic modulators are critical components in photonic integrated circuits (PICs), enabling the precise control of light signals for applications ranging from telecommunications to sensing. Their ability to modulate light with high speed and low power consumption makes them indispensable in advancing optical technologies. Co-packaged design, integrating photonic and electronic chips within a single module, offers significant advantages, including reduced latency, improved signal integrity, and enhanced thermal management. This approach streamlines integration, paving the way for compact, efficient, and high-performance optoelectronic systems.

To demonstrate the heterogeneous integration between a photonic integrated circuit (PIC) with nonlinear electrooptic (EO) properties and a CMOS chip, we present the design of a thin-film lithium niobate (LN) PIC. The PIC is specifically designed to interface with a CMOS flip-chip through heterogeneous assembly, forming a multichip module.

The PIC includes an EO phase modulator that leverages the Pockels effect in the LN thin film and employs traveling-wave electrodes to support high-speed modulation. Additionally, the PIC is designed to guide singlemode optical signals, ensuring efficient light propagation. Electrical interconnects are integrated into the PIC, featuring bump pads for connecting the flip-chip and wire-bond pads to interface the multi-chip module with a carrier printed circuit board (PCB). A critical aspect of the design focuses on optimizing the electrical interconnections to ensure impedance matching, minimize signal reflections, and support high-bandwidth operation of the multi-chip module.

This work presents the design and simulation of the integrated photonic and electronic subsystems, including the EO modulator and optimized RF interconnects. The proposed approach enables compact multi-chip modules that support efficient EO modulation and reliable operation.

## In Situ Optimization of an Optoelectronic Reservoir Computer with Digital Delayed Feedback

**Mr. Shadad Watad**

*School of Electrical and Computer Engineering, Ben-Gurion University of the Negev*

### Authors:

Fyodor Morozko, Shadad Watad, Amir Naser, Antonio Cal`a Lesina, Andrey Novitsky, Alina Karabchevsky

### Abstract:

Reservoir computing (RC) is an innovative paradigm in neuromorphic computing that leverages fixed, randomized internal connections to address overfitting challenges. RC has demonstrated remarkable potential for signal processing and pattern recognition tasks, making it highly suitable for hardware implementations across various physical substrates, promising enhanced computational speeds and reduced energy consumption. Despite this, the optimization of RC systems has traditionally relied on simulation-based approaches, limiting the practicality of physical implementations [1].

To overcome these limitations, we introduce an in-situ optimization method for an optoelectronic delay-based RC system with digital delayed feedback. This approach simultaneously optimizes five key parameters: delay-to-clock cycle ratio, input scaling, phase bias, nonlinearity gain, and the regularization parameter used in readout training. The system's performance is benchmarked across three tasks: waveform classification, time series prediction, and speech recognition.

Our experimental results demonstrate state-of-the-art normalized mean squared errors (NMSE) of 0.028, 0.561, and 0.271 for these tasks, outperforming simulation-based optimization in two out of three cases. These findings highlight the critical importance of parameter optimization in enhancing the performance and applicability of physical RC systems. Furthermore, this work validates theoretical predictions about the detrimental effects of delay-to-clock cycle resonances on RC accuracy, offering insights into their mitigation.

This study marks a significant advancement in the field of physical computing, eliminating the reliance on extensive numerical simulations and enabling the practical deployment of RC systems in real-world applications.

The research was supported by the EU ERA-NET DIEGO project Ministry of Energy, Grant No. 221-11-032, and Lower Saxony's Minister of Science and Culture and the Volkswagen Foundation under the program "Zukunft.niedersachsen: Research Cooperation Lower Saxony – Israel" 76251-5615/2023.

## Bistable normally bright smart window with planarly aligned cholesteric liquid crystal

Ms. Niveen Huseen

Ben Gurion university

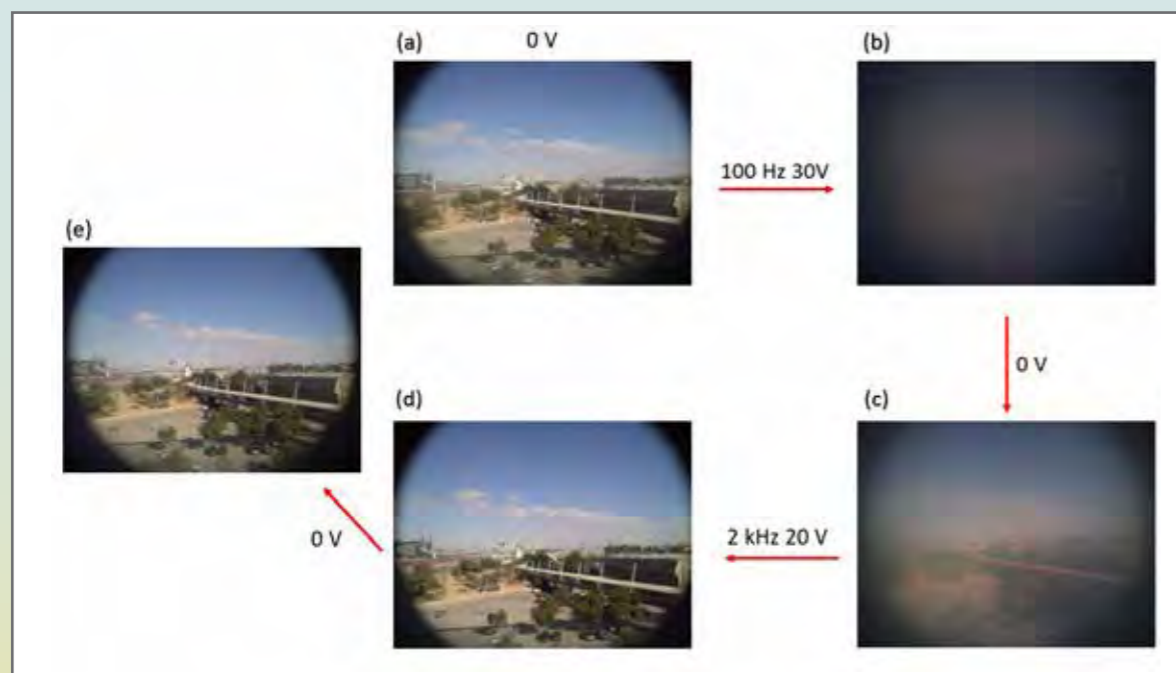
### Authors:

Niveen Huseen and Ibrahim Abdulhalim

### Abstract:

Bistable smart windows have gained significant attention due to their potential for low energy consumption. Unlike traditional liquid crystal (LC) devices, bistable LC devices can maintain two stable states without a continuous power supply. Once the device is set to a stable state, it remains in that state until a specific voltage is applied to change it, meaning it doesn't require ongoing power to maintain its state. This characteristic makes bistable devices particularly advantageous for applications where energy efficiency is a priority, such as smart windows. Cholesteric liquid crystals (CLCs) are especially suited for bistable applications due to their unique structural properties. Bistable CLC based smart windows are usually based on a vertically aligned helix, and the two stable states are the focal conic scattering state and the transparent vertically aligned state. The other possible CLC orientation is to have the helix aligned in the plane of the substrates, which was not reported before as bistable smart window. This planarly aligned helix (PAH) state is achieved using a negative dielectric anisotropy LC (HNG-7156-100), a homeotropic alignment layer, and 10 wt% of the chiral dopant CB15. This combination enables the creation of a bistable smart window that can alternate between transparent and opaque states without the need for a constant voltage. A low-frequency (100 Hz, 30 V) voltage pulse switches the window to an opaque state by inducing ion movement that aligns with the electric field, leading to turbulence and increased light scattering.

Conversely, a high-frequency (2 kHz, 20 V) pulse makes the window transparent again, as the ions limited mobility prevents them from following the field, thus the window will be transparent. The device exhibits a haze of about 5% in the transparent state, which rises to around 80% in the scattering state, yielding a high contrast ratio and effective privacy control.



## Multi-WDM Channel Photonic True Time Delay System

Prof. Dan Marom

Hebrew University of Jerusalem

### Authors:

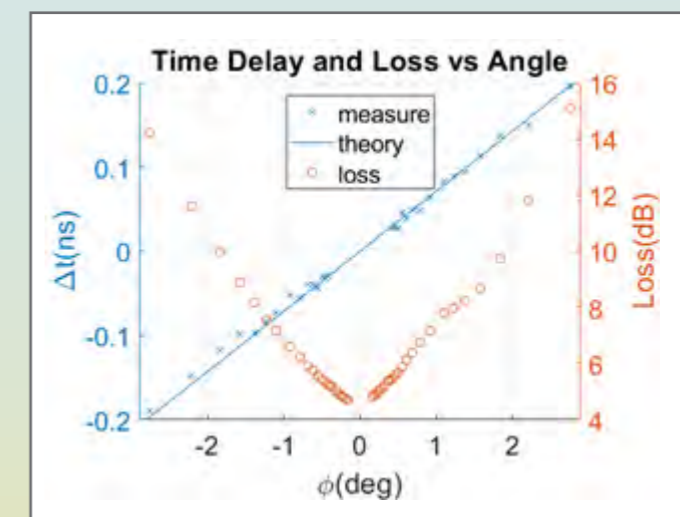
Idan Shefer, Dan M Marom

### Abstract:

Beamforming networks in phased array antennas are essential in radio communication systems, enabling the precise steering of electromagnetic waves for applications such as radar, wireless communication, and optical systems. However, once wider RF bandwidths are utilized – a requirement for target ranging or large bandwidth communication applications – a frequency dependent wavefront is introduced, leading to a spread of the directed beam and temporally distorted pulses in the far field (“squint” phenomenon), causing a loss of spatial and temporal resolution. This can be overcome by adding a frequency-dependent phase delay term to every antenna element, or true time delay (TTD). However, achieving large bandwidth and large delay range with fine resolution, and at low distortion is a formidable task. Photonic TTD (PTTD) systems have been suggested to address this RF challenge.

We realized an optical processor based on free-space optics, capable of continuously varying the temporal delay by beam steering (=varying the path length) of multiple wavelength channels (=number of tracked objects) and many optical ports (=number of antenna elements), implementing a transmitter beamforming network of unprecedented scale. The experimental setup involves key optical components such as diffraction gratings, spatial light modulators (SLMs), and lenses, arranged in a four-path configuration and demonstrating PTTD, as assessed with optical and electrical network analyzers. Our current system, implemented with LCoS SLM, achieves  $\pm 0.19$  ns delay with delay/loss coupling due to pixelation artefacts. We plan next to substitute the SLM with MEMS analog tilting micromirrors, projected to achieve lossless delay and  $\pm 0.6$  ns delay.

The experimental results confirm the feasibility of the proposed PTTD system, achieving accurate beam steering and time delay control within the C-band spectrum. The findings suggest significant potential for integration into modern photonic beamforming networks, paving the way for advancements in high-speed, high-resolution communication technologies.





## ELECTRO-OPTICS IN DEFENSE SESSION

### ◆ Invited speakers Abstracts:

#### Adaptive optics for deep turbulence applications

**Dr. Daniel Golubchik**

*Rafael*

##### Abstract:

Atmospheric turbulence has a profound effect on long range imaging systems, free space optical communication, and directed energy applications, distorting the wave-front of the light and limiting the effective range. For “shallow” turbulence profiles, such as in ground to space or ground to air applications, most of the distortion is close to the aperture and can be measured and corrected by well-known adaptive optics techniques. In ground to ground applications, “deep” turbulence is distributed along the optical path, and both measurements and corrections of distortions are challenging.

In the talk, we present measurements and simulations of laser light propagation and correction in deep turbulence regime. We show that turbulence effects mitigation using coherent beam combining, while far from perfect, can significantly improve the flux and stability of the laser light. Yet, in the deep turbulence regime, distortion of both amplitude and phase of the propagated light inhibits the measurements of the wave-front by commonly implemented wave-front sensors, such as Shack-Hartmann.

One of the solutions of the wave-front measurement problem is to use phase diversity. The technique requires simultaneous measurements of a “guide star” with various known spherical distortions. Very good performance and implementation simplicity of the technique comes at the cost of high computational complexity, which until now, prohibited its implementation in real-time applications. To reduce the computational complexity, we propose a physics-informed neural network (PINN) architecture for wave-front sensing. The proposed unsupervised PINN estimates the phase concurrently with the amplitude of the field, considering the physics of image formation. We demonstrate the effectiveness of our approach on simulated data and in table-top experiment.

### Oral Presentations Abstracts:

#### Tuning Event Camera Biases Heuristic for Detection Applications in Staring Scenarios

**Dr. David El-Chai Ben-Ezra**

*Soreq NRC*

##### Authors:

David El-Chai Ben-Ezra, Daniel Brisk

##### Abstract:

**Introduction:** Event camera (EC) is a bio-inspired sensor that pose a paradigm shift in acquisition of visual information. Each pixel of an event camera is asynchronously independent, and responds only when it feels a brightness change. EC comes with some special properties: timestamp in resolution of microseconds, low latency, high dynamic range (over 120 dB), and low power consumption.

Instead of well-known degrees of freedom, such as frame-rate or exposure time, EC comes with a few unintuitive biases that control the generation of the events by the pixels. Tuning these biases properly is a crucial and difficult challenge that one needs to solve prior to any use of the camera for any application.

**Objectives:** In the talk, we are going to introduce a novel approach to the multivariable problem of tuning event camera biases for detection tasks of small objects in staring scenarios.

**Methods:** We will provide a translation of the problem and the biases behavior into mathematical terms, and show an approach for solving the problem in tasks as mentioned above.

**Results:** We will show how the optimal biases depend on the desired detected signal, and that for a certain type of signals, the optimal biases are very different from the default values given by the manufacturer.

**Conclusions:** We will show that solving the tuning biases multivariable problem is a crucial step for exploiting and unlocking event camera’s potential.

## Estimating Probabilities of Cloud-Free Lines-Of-Sight Through the Atmosphere – Lund and Shanklin method revisited

**Dr. Eyal Agassi**

*Independent Consultant*

### Authors:

Eyal Agassi, Tamir Tsadok, Alon Manor

### Abstract:

The probability cloud free of line of sight (PCFLOS) from ground to air and vice versa, is defined as the probability that a specific line of sight is cloud free, at a given time. It is a useful parameter for the operational research of any optical system that requires a free line of sight between two points in order to ensure its proper functionality. A method for the estimation of PCFLOSs as a function of cloud cover, elevation angle, cloud type and climatological statistics was introduced by Lund and Shanklin in the early 1970s. Extended and updated work was carried out through the excellent work of Shields et al. Her work was based on a much larger data set and a high-quality imager. We present two main innovations with respect to previous works. First, we will show that an additional element is missing in Lund's method and that ignoring it might yield inaccuracy in the estimated PCFLOS. Second, we have used an IR whole sky imager for obtaining the data set. Working in the thermal IR band (and especially in the LWIR) offers some benefits over a visible sky camera. It offers immunity against sun reflections, scattering and stray light. It also provides an equal sensitivity for day and night observations and very high sensitivity in detection and segmentation of low altitude clouds due to the high contrast (tens of degrees K) between the clouds and the sky background. A large and high temporal data set enabled us also to derive the persistence of the cloud cover for short periods.

## Pros and cons for Super-Gaussian based CBC

**Dr. Zeev Schiffer**

*Elbit Systems, iSTAR Division-Elop*

### Abstract:

In beam combining systems, such as in the case of Coherent Beam Combining (CBC) for defense applications, the Power In the Bucket (PIB) is typically limited by optical diffraction of transmitted beams. This effect is an inevitable result of the near-field intensity/amplitude distribution of the natural Single-Mode Gaussian-like beams, generated by laser sources. Fiber laser amplifiers which are typically used in CBC applications are no different in this sense. Whereas optimal system performances on Target requires a "flat-top" near-field spatial power distribution, these Gaussian beams are by-definition not flat. Being wave-guide modes, the generated beams typically have a spatial distribution which is characterized by a peak at the center surrounded by a "tail" which holds a considerable portion of the beam total power. In real-life the system finite aperture size constraints the diameter of the transmitted beams where power in the "tail" is truncated. This fact has negative implications both on the produced optical beam quality/PIB and on the aspect of handling this truncated power within the optical head.

To improve PIB beyond Gaussian beams limitation, one is required to re-shape their near-field distribution so that the beam sent through the hard-aperture has a "top-hat" profile. To accommodate for the mentioned constraints and requirements, a special wave-front converter module or a "Super-Gaussian converter" is considered. In this presentation we discuss the theoretical and technical pros and cons of such "Super-Gaussian converter" module and suggest potential promising directions.

## New modeling features in TRM4 version 4

**Dr. Dov Steiner**

*IARD Sensing Solution*

### Authors:

Dov Steiner<sup>1</sup>, Dan Assaban<sup>2</sup>

1 IARD Sensing Solutions Ltd., Kibbutz Yagur, Israel, 30065

2 DDR&D IMOD, Tel-Aviv, Israel

### Abstract:

TRM4 is a model-based tool for the performance assessment of electro-optical systems, offering an effective approach for designing and comparing electro-optical imagers in spectral bands from visible to long-wave IR. TRM4 is primarily used to calculate the range performance based on imaging system parameters and the environmental conditions. A newly developed version, TRM4ver.4, will be released in the middle of 2025. This version will include two main new features: performance modelling of sub-pixel target scenarios and color cameras, along with ground resolved distance calculations (GRD) for aerial sensors as additional output for NIIRS calculations.

For sub-pixel targets, the calculation of the signal-to-noise ratio (SNR) for the additional target signal is presented, considering different target locations with respect to the detector matrix. Best-case and worst-case detection ranges are derived from specified threshold SNRs of detection algorithms. Range performance calculation for sub-pixel targets is applicable to various scenarios, including short-time events, air-air scenarios (with flying targets observed from above) and satellite imaging.

Modeling of color cameras will include range performance of Bayer-filter cameras and 3-chip CCD/CMOS cameras. The spectral response of color camera detectors is specified for RGB channels and range performance is calculated based on the luminance component. The luminance component is obtained from RGB data by a transformation matrix from the camera's raw space to the CIE XYZ color space. The AMOP (Average Modulation at Optimum Phase) calculation, which is used in TRM4 to describe the spatial signal transfer characteristics along the imaging chain, was extended to include sampling by sensors with Bayer filter and bilinear demosaicing method.

## Experimental Approaches to Optical Atmospheric Turbulence Measurements

**Dr. Mara Baraban**

*Rafael Advanced Defense Systems*

### Authors:

Mara Baraban, Yaakov Monsa (Rafael Advanced Defense Systems, Israel)

### Abstract:

In this talk, we present the set-up and initial results from optical atmospheric turbulence experiments in the Israeli desert. The experimental setup includes a scintillometer, USAM, and DIMM with access to additional meteorological measurements including radiosondes from the measurement location. Our objectives are to validate single-point turbulence measurements of the USAM over an extended period of time and in different meteorological conditions, to develop approaches to measure the Cn2 profile as a function of altitude, and to develop modeling capabilities for Cn2 with WRF. Initial results will be presented.



### Overcoming Data Scarcity in Defense AI : Can Physics-based sensor simulation system be a reliable solution ?

Mr. Pierre Noubel  
OKTAL Synthetic Environment

Authors:  
Pierre Noubel, Jean Latger

**Abstract:**  
AI-based computer vision has shown great promise for defense applications, including automatic target detection in missile seeker-heads, electro-optical surveillance, intelligence, countermeasures, and counter-countermeasures. Yet, a key obstacle persists: the scarcity of labeled training data in the defense domain. This challenge is especially acute for specific sensors such as infrared cameras or SAR imagers, where data collection is highly limited.

To address this, physics-based sensor simulation presents an innovative approach by generating synthetic training datasets to complement real-world data. This methodology offers unparalleled advantages:

- Unlimited data generation with balanced datasets
- Automated labeling for faster AI development
- Full control over scene parameters to meet specific use cases

However, significant challenges remain to bridge the reality gap, increase scene variability, and make such tools accessible for non-expert users.

In this presentation, we will explore OKTAL-SE's efforts to overcome these challenges using its SE-WORKBENCH sensor simulation platform. Key achievements include:

- Enhancing material and environmental variability while reducing costs
- Automating the integration of 3D objects for detailed scenes
- Transforming a scientific tool into a turnkey solution for data generation

The SE-WORKBENCH is a physics-based sensor simulation platform developed by OKTAL-SE, a French software company. SE-WORKBENCH creates fully customizable digital twins of the external world, with rendering capabilities in infrared, radar, and GNSS spectrums. It supports the development and evaluation of EO and RF sensor systems for perception, guidance, and navigation.

Recognized globally, SE-WORKBENCH is trusted by MoD, scientific agencies, and defense industries, around the world, including in Israel.

The image displays a grid of logos for various sponsors and partners, organized into four categories:

- Platinum Sponsors:** Elbit Systems, IAI, RAFAEL (Advanced Defense Systems Ltd.), and APPLIED MATERIALS (make possible).
- Gold Sponsors:** Civan Lasers, PROLOG optics, SCD, RQSH (Electronics Ltd.), KAP LABS photonics, and TECHNOLOGY.
- Silver Sponsors:** FG (Fibre Laser Systems Ltd.), bi-POL, EK SMA OPTICS, and Acktar (Advanced Optics).
- Partners:** ZORGO, מכון ויצמן למדע (Weizmann Institute of Science), Bar Ilan University (אוניברסיטת בר-אילן), and IIBR (International Institute for Business Review).

## Exhibitors



## Media Sponsors

